



THE UNIVERSITY OF
WAIKATO
Te Whare Wānanga o Waikato

Research Commons

<http://waikato.researchgateway.ac.nz/>

Research Commons at the University of Waikato

Copyright Statement:

The digital copy of this thesis is protected by the Copyright Act 1994 (New Zealand).

The thesis may be consulted by you, provided you comply with the provisions of the Act and the following conditions of use:

- Any use you make of these documents or images must be for research or private study purposes only, and you may not make them available to any other person.
- Authors control the copyright of their thesis. You will recognise the author's right to be identified as the author of the thesis, and due acknowledgement will be made to the author where appropriate.
- You will obtain the author's permission before publishing any material from the thesis.

CHANGE IN GEOMORPHOLOGY, HYDRODYNAMICS AND SURFICIAL SEDIMENT OF THE TAURANGA ENTRANCE TIDAL DELTA SYSTEM

A thesis
submitted in partial fulfilment
of the requirements for the Degree

of

Master of Science in Earth and Ocean Sciences

at

University of Waikato

by

ADRIAN MARK BRANNIGAN



THE UNIVERSITY OF
WAIKATO
Te Whare Wānanga o Waikato

University of Waikato

2009

ABSTRACT

Historical change in the geomorphology, hydrodynamics, and surficial sediment of the tidal delta system of Tauranga Harbour are investigated with the general aim of analysing

The general aims of this thesis are: firstly to analyse historical changes to inlet delta system geomorphology using historical hydrographic charts, secondly, to conduct hydrodynamic numerical modelling using historical bathymetries to access changes in peak spring flow and potential net tidal sediment transport, and thirdly, to analyse historical changes in surficial sediment and bedforms.

Geomorphic change was investigated through plotting ‘difference in bathymetry’ graphs and conducting cross sections taken from digitised bathymetries obtained from historical hydrographic charts from 1852, 1879, 1901, 1927, 1954 and a modern bathymetry from 2006.

Two-dimensional hydrodynamic numerical modelling was conducted to investigate the changes in peak tidal current flow and potential net sediment transport between 1852 and 2006.

Changes in surficial sediment patterns were determined through completing a side scan sonar survey with associated sediment samples for ground truthing of grain size and underwater videography to gather surficial shell coverage information. This was used to produce a surficial sediment coverage map which was compared to historical studies

Major geomorphological findings include that the shipping channel appears to have induced minor change in the geomorphology of the FTD but such changes are similar to those identified in the historical bathymetries of 1852, 1879, 1901, 1927, 1954 prior to dredging. Significant changes have occurred on the ETD, with the majority of the ETD showing scour of 1 m while the terminal lobe has extended seawards. This is associated with historical (since 1852) narrowing of the inlet from Panepane Point to Mt Maunganui by ~ 900 m.

Hydrodynamic numerical modelling has shown a significant increase in potential net tidal sediment transport in the Cutter Channel due to dredging, while the Maunganui Roads Channel shows a reduction of net potential tidal sediment transport that is associated with the dredging of this channel.

The area surrounding Panepane Point undergoes significant increases and decreases in net potential tidal sediment transport both before and after dredging. Investigation of the surficial sediment patterns over the FTD and ETD from sidescan sonar and bottom samples show that between 1983 and 2007 there has been a northwards extension of the area of major shell (> 50 %) converge in the main ebb channel as well as reduction in major shell converge in flood tidal delta ebb shield region. The Maunganui Roads Channel changes from silty sands to medium and fine sands.

ACKNOWLEDGEMENTS

This research has been funded by the Port of Tauranga. The financial support which has been provided is greatly appreciated.

Thank you to Terry Healy for establishing the study and funding for this thesis as well the support and guidance he has provided

Sincere thanks to Willem De Lange for his helpful advice and direction over the course of the thesis.

I would like to thank Dirk Immenga, Kyle Spiers, Glen Reeves, and Gegar Prasetya for their help with both the field work and assistance with 3DD.

I am grateful to Owen Maynard and Lance Wood for providing me with hydrographic charts and answering various hydrographic queries.

I thank Brad Scarfe, Pauline Assie and Elodie Hubert for their help with ArcGIS and Surfer

I would like to thank Shawn Harrison and the team at ASR who provided support for 3DD over the year.

Thanks to Carol Kohl from LINZ for copying and sending historical hydrographic charts to me and to Scott Preskett for help in assessing the accuracy of the hydrographic charts.

Thank you to Nana Joy for providing a place to stay over the course of the field work.

Thank you to Sydney Wright who has been a valuable person in helping me with various requests

Finally I would like to thank Bryna, Ali, Zoe, Alex , Nicola, and anyone else who I may have missed for their help and support over the year.

TABLE OF CONTENTS

Abstract	i
Acknowledgements	ii
Table of Contents	iii
List of Figures.....	vii
List of Tables.....	xi

Chapter One: Introduction

1.0	Dredging at Port of Tauranga	17
1.1	Study Aims and Objectives	18
1.2	Structure of the Thesis	19

Chapter Two: Previous Studies of Hydrodynamics, Sediment Dynamics and Geomorphology of Tauranga Harbour

2.0	Introduction	22
2.0.1	Physical Setting	22
2.0.2	Previous Investigations of the Tauranga Inlet	22
2.1	Previous Investigations of Harbour Geomorphology	22
2.1.1	Pre Dredging Geomorphic Changes	23
2.1.2	Dahm – Geomorphology	24
2.1.3	Tauranga Harbour Study – Bathymetries	25
2.1.4	Flood tidal delta geomorphology in 1982 to 1995	27
2.1.5	Concluding points on geomorphology	28
2.2	Previous investigations of Tauranga Harbour hydrodynamics	29
2.2.1	Pre-dredging tidal flow changes	29
2.2.2	Tidal Currents	30
2.2.3	Hydrodynamic numerical modelling	30
2.2.4	Hydrodynamic Model Comparison	33
2.2.5	Changes in current regime due to dredging	33
2.2.6	Rerun of System 21 Numerical Model	34
2.2.7	Fluid velocity structure	35
2.2.8	Concluding points on hydrodynamics	36

2.3	Previous Investigations of Tauranga Harbour sediment dynamics	38
2.3.1	Sediment Transport Patterns	38
2.3.2	Sediment Transport Modelling	39
2.3.3	Tauranga Harbour Study – Morphology	40
2.3.4	Wave induced sediment transport	42
2.3.5	Mathew – Sediment Dynamics	42
2.3.6	Kruger (1999) – Grain size patterns	43
2.3.7	Kruger – Surficial Sediment Facies and Transport	43
2.3.8	Shoaling mechanism and sand bypassing	44
2.3.9	Concluding points on sediment dynamics	46
2.4	Discussion	
2.4.1	Comparisons with previous model of tidal inlets	46
2.4.2	Comparison with national and international examples	47
2.5	Conclusions	49

Chapter Three: Geomorphological Variation of Tauranga Tidal Delta System

3.0	Introduction	51
3.1	Bathymetry and Cross Section Models	51
3.1.1	Cross Section	53
3.2	Bathymetry Results	53
3.2.1	Changes in bathymetry of Tauranga Harbour 1954-2006	64
3.2.2	Changes in bathymetry of Tauranga Harbour 1927-1954	64
3.2.3	Changes in bathymetry of Tauranga Harbour 1901-1927	65
3.2.4	Changes in bathymetry of Tauranga Harbour 1879-1901	66
3.2.5	Changes in bathymetry of Tauranga Harbour 1852-1879	66
3.3	Variation of Historical Sequence Results	66
3.3.1	Ebb tidal delta variation in cross section 1852-2006	67
3.3.1.2	Summary of geomorphic change of ebb tidal delta	70
3.3.2	Tidal inlet gorge variation in cross section 1852-2006	71
3.3.2.1	Summary of geomorphic change of tidal inlet gorge	72
3.3.3	Flood tidal delta variation in cross section 1852-2006	73

3.3.3.1	Summary of geomorphic change of flood tidal delta	77
3.3.4	Summary of geomorphic change of the tidal delta system	78
3.4	Discussion	79
3.4.1	Ebb tidal delta	79
3.4.2	Tidal inlet	79
3.4.3	Flood tidal delta	80
3.5	Summary	80

Chapter Four: Hydrodynamic Numerical Modelling of Historical Bathymetries of Tauranga Harbour

4.0	Introduction	82
4.1	Methods	82
4.1.1	The hydrodynamic numerical model	82
4.1.2	Bathymetry	82
4.1.3	Boundary Conditions	83
4.1.4	Calibration	83
4.2	Results	83
4.2.1	Points to note regarding interpretation of results	84
4.3	Comparison of 1954 and 2006 hydrodynamic results	84
4.3.1	Difference in peak ebb flow conditions 1954-2006	85
4.3.2	Difference in peak flood flow conditions 1954-2006	86
4.3.3	2006 Mean Spring Tide Residual Distance Plot	87
4.3.4	Difference in Mean Spring Tide Residual Distance Plot	88
4.4	Comparison of 1927 and 1954 hydrodynamic results	89
4.4.1	Difference in peak ebb flow conditions 1927-1954	89
4.4.2	Difference in peak flood flow conditions 1927-1954	89
4.4.3	Difference in Mean Spring Tide Residual Distance Plot	89
4.5	Comparison of 1901 and 1927 results	90
4.5.1	Difference in peak ebb flow conditions 1901-1927	90
4.5.2	Difference in peak flood flow conditions 1901-1927	90
4.5.3	Difference in Mean Spring Tide Residual Distance Plot	91
4.6	Comparison of 1879 and 1901 results	91
4.6.1	Difference in peak ebb flow conditions 1879-1901	91

4.6.2	Difference in peak flood flow conditions 1879-1901	92
4.6.3	Difference in Mean Spring Tide Residual Distance Plot (1879-1901)	92
4.7	Comparison of 1852 and 1879 results	93
4.7.1	Difference in peak ebb flow conditions 1852-1879	93
4.7.2	Difference in peak flood flow conditions 1852-1879	93
4.7.3	Difference in Mean Spring Tide Residual Distance Plot	94
4.8	Comparison of all Mean Spring Tide Residual Distance Difference	94
4.9	Comparison with historical studies	95
4.10	Summary	96

Chapter Five: Changes in Surficial Sediment, Shell Coverage and Bedforms of the Tidal Delta System

5.0	Introduction	130
5.0.1	Sidescan sonar configuration	131
5.1	Materials and Methods	134
5.1.1	Sidescan sonar survey methodology	134
5.1.2	Sonograph Data Post Processing	135
5.1.3	Ground Truthing	135
5.2	Surficial Sediment Characterisation of the Tidal Delta System	139
5.2.1	Flood Tidal Delta (FTD)	139
5.2.2	Ebb Tidal Delta (ETD)	139
5.3	Comparison with historical surficial sediment studies	143
5.3.1	1983-1984 Tauranga Harbour Study	146
5.3.2	1998 Kruger Study	149
5.4	Bedforms	150
5.5	Comparison with historical bedform studies	153
5.5.1	1983 Tauranga Harbour Study – Bedforms	153
5.5.2	1998 Kruger Study – Bedforms	157
5.6	Conclusions	158

Chapter Six: Summary and Conclusions

6.0 Introduction	160
6.1 Tidal inlet delta system geomorphology	160
6.2 Tidal inlet delta system hydrodynamics	161
6.3. Surficial sediment patterns of the tidal delta system	162
6.4 Implications for Port of Tauranga Ltd.	163
6.5 Suggestions for future research	163

References	165
-------------------------	------------

Appendix	170
-----------------------	------------

LIST OF FIGURES

Chapter One

Figure 1.1. Outline of study area within Tauranga harbour, with inset showing location of Tauranga harbour in relation to the North Island of New Zealand.

Figure 1.2. Map of Tauranga entrance of Tauranga harbour detailing channel names, the area which is dredged and other geographic features (following De Lange, 1988, Mathew, 1997, Kruger, 1999). (Air photo source: Environment Bay of Plenty).

Chapter Two

Figure 2.1. CHECKTOPO plot of bathymetry changes between 1902 and 1927 (Source: Barnett, 1985).

Figure 2.2. Erosion (cross-hatched) and accretion (dotted) exceeding 1 m in the period from 1901-1927 in Tauranga Harbour (Source: Black 1984).

Figure 2.3. The location on blind flood channel on the 2006 bathymetry

Figure 2.4. Vector plot at mean tide at maximum ebb based on System 21 hydrodynamic numerical model (Source: Barnett, 1985).

Figure 2.5. Vector plot at spring tide at maximum flood based on System 21 hydrodynamic numerical model (Source: Barnett, 1985).

Figure 2.6. Locations of current measurement over the flood tidal delta and adjacent region (map created with source data from Mathew, 1997).

Figure 2.7. Map showing Entrance Channel and the areas that required maintenance dredging in 1998. The dash line shows the boundaries of the dredged inlet channel. The inst details the volume of sediment above a chart datum of 14.2 m in each of the areas (source: port of Tauranga 1998 as cited in Kruger 1999).

Figure 2.8. Model of sediment transport patterns for Tauranga Entrance based on tidal streamlines, bedforms, sediment discharge measurements and theoretical calculations (Source: Davis-Colley and Healy, 1978^b).

Figure 2.9. Direction of net, total load sediment circulation in Tauranga Harbour.

Figure 2.10. Major sedimentary features of Tauranga Harbour from the Tauranga Harbour Study (Healy, 1985).

Figure 2.11. The tidal inlets and ebb tidal deltas of Parengarenga (left) and Rangaunu (right) are both adjacent to rocky headlands, which restricts the growth of the ebb tidal delta on that site (Source: Google Earth, 2009).

Figure 2.12. The Teignmouth tidal inlet like the Tauranga entrance is adjacent to a rocky headland, note the large sandbar on ebb tidal delta

Chapter Three

Figure 3.1. Guide to the extent of the charts used to create the bathymetry for hydrodynamic numerical modelling for 1954, 1927, 1901, 1879, 1852.

Fig 3.2. 2006 bathymetry of Tauranga Entrance tidal delta system with depths in metres on the accompanying scale.

Figure 3.3. 1954 bathymetry of Tauranga Entrance tidal delta system with depths in metres on the accompanying scale.

Figure 3.4. 1927 bathymetry of Tauranga Entrance tidal delta system

Figure 3.5. 1901 bathymetry of Tauranga Entrance tidal delta system

Figure 3.6. 1879 bathymetry of Tauranga Entrance tidal delta system

Figure 3.7. 1852 bathymetry of Tauranga Entrance tidal delta system

Figure.3.8 :Bathymetric changes between 2006 and 1954. Blue indicates areas of accretion while red indicates areas of erosion. Scale is set to metres.

Figure.3.9 :Bathymetric changes between 1954 and 1927. Blue indicates areas of accretion while red indicates areas of erosion. Scale is set to metres.

Figure.3.10 :Bathymetric changes between 1927 and 1901. Blue indicates areas of accretion while red indicates areas of erosion. Scale is set to metres.

Figure.3.11 :Bathymetric changes between 1901 and 1879. Blue indicates areas of accretion while red indicates areas of erosion. Scale is set to metres.

Figure.3.12 :Bathymetric changes between 1879 and 1852. Blue indicates areas of accretion while red indicates areas of erosion. Scale is set to metres.

Figure 3.13: Map detailing locations of cross section in tidal delta system, overlaid on the 1954 bathymetry. Black is the ebb tidal delta cross section, red is the tidal inlet gorge cross section and blue is the flood tidal delta cross section

Figure 3.14: Cross sections of Tauranga ebb tidal delta from Matakana Island (A) northwards to the open ocean (B) comparing bathymetries from 1852 – 2006.

Figure 3.15: Cross sections of Tauranga tidal inlet gorge from Mt Maunganui (C) to Matakana Island (D) comparing six bathymetries dated 1852, 1879, 1901, 1927, 1954 and 2006. Note the extensive inlet narrowing (by over 360 m) between 1879 and 2006, and channel deepening from ~ 12m in 1852 to ~ 35m in 1954.

Figure 3.16: Cross sections of Tauranga flood tidal delta from Maunganui Roads Channel (E) to Matakana Island (F) comparing six bathymetries dated 1852, 1879, 1901, 1927, 1954 and 2006

Chapter Four

Figure. 4.1: Mean spring tide peak ebb velocity vector plot 2006 (A), and 1954 (B) (Every third vector is displayed, colour scale maximum set at 2 m/s).

Figure. 4.2: Difference in mean spring tide peak ebb velocity vector plot (2006 – 1954). (Every third vector is displayed, colour scale maximum set at 1m/s).

Figure.4.3: Mean spring tide peak flood velocity vector plot 2006 (A), and 1954 (B) (Every third vector is displayed, colour scale maximum set at 2 m/s).

Figure. 4.4: Difference in mean spring tide peak flood velocity vector plot (2006 – 1954). (Every third vector is displayed, colour scale maximum set at 1m/s).

Figure.4.5: Mean spring tide residual distance vector plot for 2006 (Every third vector is displayed, colour scale maximum set at 10000 m).

Figure. 4.6: Mean spring tide residual distance vector plot for 1954 (Every third vector is displayed, colour scale maximum set at 1000).

Figure. 4.7: Difference in mean spring tide residual distance vector plot (2006 – 1954) (Every third vector is displayed, colour scale maximum set at 1000).

Figure. 4.8: Mean spring tide peak ebb velocity vector plot 1954 (A), and 1927 (B) (Every third vector is displayed, colour scale maximum set at 2 m/s).

Figure. 4.9: Difference in mean spring tide peak ebb velocity vector plot (1954 - 1927). (Every third vector is displayed, colour scale maximum set at 1m/s).

Figure. 4.10: Mean spring tide peak flood velocity vector plot 1954 (A), and 1927 (B) (Every third vector is displayed, colour scale maximum set at 2 m/s).

Figure. 4.11: Difference in mean spring tide peak flood velocity vector plot (1954 - 1927). (Every third vector is displayed, colour scale maximum set at 1m/s)

Figure. 4.12: Mean spring tide residual distance vector plot for 1954 (A) and 1927 (B) (Every third vector is displayed, colour scale maximum set at 10000 m)

Figure. 4.13: Difference in mean spring tide residual distance vector plot (1954 – 1927) (Every third vector is displayed, colour scale maximum set at 1000).

Figure. 4.14: Mean spring tide peak ebb velocity vector plot 1927 (A), and 1901 (B) (Every third vector is displayed, colour scale maximum set at 2 m/s).

Figure.4.15: Difference in mean spring tide peak ebb velocity vector plot (1927 - 1901). (Every third vector is displayed, colour scale maximum set at 1m/s)

Figure. 4.16: Mean spring tide peak flood velocity vector plot 1927 (A), and 1901 (B) (Every third vector is displayed, colour scale maximum set at 2 m/s).

Figure. 4.17: Difference in mean spring tide peak flood velocity vector plot (1927 - 1901). (Every third vector is displayed, colour scale maximum set at 1m/s).

Figure. 4.18: Mean spring tide residual distance vector plot for 1927 (A) and 1901 (B) (Every third vector is displayed, colour scale maximum set at 10000 m).

Figure. 4.19: Difference in mean spring tide residual distance vector plot (1927 - 1901) (Every third vector is displayed, colour scale maximum set at 1000).

Figure. 4.20: Mean spring tide peak ebb velocity vector plot 1901 (A), and 1879 (B) (Every third vector is displayed, colour scale maximum set at 2 m/s).

Figure. 4.21: Difference in mean spring tide peak ebb velocity vector plot (1901 - 1879). (Every third vector is displayed, colour scale maximum set at 1m/s)

Figure. 4.22: Mean spring tide peak flood velocity vector plot 1901 (A), and 1879 (B) (Every third vector is displayed, colour scale maximum set at 2 m/s).

Figure.4.23: Difference in mean spring tide peak flood velocity vector plot (1901 - 1879). (Every third vector is displayed, colour scale maximum set at 1m/s).

Figure. 4.24: Mean spring tide residual distance vector plot for 1901 (A) and 1879 (B) (Every third vector is displayed, colour scale maximum set at 10000 m).

Figure. 4.25: Difference in mean spring tide residual distance vector plot (1879 - 1901) (Every third vector is displayed, colour scale maximum set at 1000).

Figure. 4.26: Mean spring tide peak ebb velocity vector plot 1879 (A), and 1852 (B) (Every third vector is displayed, colour scale maximum set at 2 m/s).

Figure. 4.27: Difference in mean spring tide peak ebb velocity vector plot (1879 - 1852). (Every third vector is displayed, colour scale maximum set at 1m/s).

Figure. 4.28: Mean spring tide peak flood velocity vector plot 1879 (A), and 1852 (B) (Every third vector is displayed, colour scale maximum set at 2 m/s).

Figure. 4.29: Difference in mean spring tide peak flood velocity vector plot (1879 - 1852). (Every third vector is displayed, colour scale maximum set at 1m/s).

Figure. 4.30: Mean spring tide residual distance vector plot for 1879 (A) and 1852 (B) (Every third vector is displayed, colour scale maximum set at 10000 m).

Figure. 4.31: Difference in mean spring tide residual distance vector plot (1879 - 1852) (Every third vector is displayed, colour scale maximum set at 1000)

Figure 4.32: Difference in mean spring tide residual distance plots. (A: 2007 – 1954. B:1954 – 1927. C: 1927 – 1901. D: 1901 – 1879. E: 1879 – 1852).

Chapter Five

Figure 5.1. Diagram showing the tow fish (or tow sled), electromagnetic cable and the vessel which carries the onboard unit. The outside of the swath

covered by the sonar beam is shown in yellow (Source: NOAA, 2002).

Figure 5.2. Schematic diagram showing the horizontal pulse transmitted by the tow fish and the corresponding sonograph image beneath it (Note: In this image high backscatter is shown as light colours and low backscatter is shown as dark colours (Source NOAA, 2007).

Figure 5.3. Sidescan sonography output from surveys conducted at the tidal delta system at the Tauranga entrance of Tauranga Harbour in 2007.

Figure 5.4. Still images taken from underwater video. The image on the left shows an example of 0% shell coverage while the image on the right shows an example of 100% shell coverage.

Figure 5.5. Surficial sediment and shell coverage of the FTD of Tauranga Entrance to Tauranga Harbour in 2007 based on sidescan sonar and sediment sampling.

Figure 5.6. Surficial sediment and shell coverage of the ETD of Tauranga Entrance to Tauranga Harbour in 2007 based on side scan sonar and sediment sampling.

Figure 5.7. 2006 sidescan sonography overlaid with 2006 multibeam bathymetry in order to show the relationship between depth and grain size on the Tauranga Entrance western ETD. Inset at top left shows location within ETD.

Figure 5.8. Comparison of extent of area for the present study with the 1983 Tauranga Harbour Study and 1998 study by Kruger of the tidal inlet delta system sedimentation and morphology.

Figure 5.9. Comparison between 2007 and 1983 surficial sediment on the FTD, with 1983 major shell coverage shown in red hash and 2007 surficial sediment coverage shown in other colours.

Figure 5.10. Comparisons between 2007 and 1983 surficial sediment on the ETD, with 1983 major shell coverage shown in red hash 1983 ignimbrite shown as a speckled unit and 2007 surficial sediment coverage shown in the other colours.

Figure 5.11. Surficial sediment coverage of ebb tidal delta of Tauranga entrance in 1998 produced by Kruger (1999).

Figure 5.12. Sediment ripples. Water flow is from bottom to top and lee sides and spurs are stippled (adapted from Larson et al. 1997; original in Allen, 1968).

Figure 5.13. Plot of mean flow velocity against mean grain size, based on laboratory studies, showing stability phases of subaqueous bed forms (Larson et al. 1997; original in Ashley, 1990).

Figure 5.14. Bedform map of the Tauranga Entrance tidal delta system for 2006 indicating dominant sediment transport pathways. The green vectors indicate the direction and relative magnitude of sediment movement at various locations around the tidal inlet delta. Bedform data was gathered from the sonograph and aerial photograph.

Figure 5.15 Surficial sediment facies of the ETD from the Tauranga Harbour Study (1983-1984) (Source: Healy, 1995).

Figure 5.16. Surficial sediment facies of the ETD from the Tauranga Harbnour Study (1983-1984) (Source: Healy, 1985).

Figure 5.17. Bedform spacing and orientation map. Grey vectors represent direction of motion of tide induced bedforms, and black vectors represent bedform movement due to wave action (Suorce: Kruger, 1999).

LIST OF TABLES

Chapter Five

Table 5.1. Description of units used for the analysis of surficial sediment on the sonograph

1. INTRODUCTION

1.0. DREDGING AT PORT OF TAURANGA

The Port of Tauranga, located within the Tauranga harbour in the North Island of New Zealand (Figure 1) plays an important role in the national economy (Rea and Graham, 1998). It is the largest port in the country, handling some 12.6 million tonnes of cargo, the leading export port in New Zealand and the nation's second largest import port by value.

The accessibility of this nationally important port is aided through dredging which has been conducted at the Tauranga entrance of Tauranga harbour since 1968 when the dredged navigational channels were established in the tidal inlet and delta system (Healy, et al., 1998). In 1991 - 1992 a major capital dredging programme was conducted where the shipping channels were deepened allowing a high water draught of 13.0 m, extracting approximately 5 million m³ of sediment (Mathew, 1997). The entrance channel is currently maintained at a depth of 14.1 m below sea level (Kruger, 2006).

Today there is a variety of different channel types situated in different morphodynamic environments which require regular maintenance dredging. Since the channel deepening of 1991 – 1992 the Entrance Channel on the ebb tidal delta requires dredging rates of 75,000 – 150,000 m³/yr. The Cutter Channel on the flood tidal delta needs 50,000 – 100,000 m³/yr. The Stella Passage, south of the Cutter Channel requires 10,000 m³/yr, and vessel sitting basins require 5,000 – 10,000 m³/yr. An outline of this dredged area is shown in Figure 2. Episodic storms, climatic cycles and dredging plant availability all affect the volume of sand dredged in any one year (Healy *et al.*, 1998).

The ongoing maintenance dredging removes a significant amount of sand from the harbour which could significantly affect surface sediment, geomorphology and current flow. Currently there are plans to deepen the navigation channels to a depth of 18 m (Thompson, G. 2007. pers comm., 19 Nov) which heightens the need to investigate the effects of dredging.

This thesis investigates the effects of dredging on the surficial sediment, geomorphology and historic changes in current flow at the Tauranga entrance of Tauranga harbour and the adjacent ebb and flood tidal delta.

1.1. STUDY AIMS AND OBJECTIVES

The general aims of this study are to analyse:

1. Historical changes to inlet delta system geomorphology based upon analysis of historical bathymetric charts.
3. Historical qualitative hydrological changes in major current flows with the variations arising from the geomorphic evolution based upon historic bathymetric charts.
2. Historical changes in surficial sediment and bedforms

The specific objectives are:

- i) Analyse historical changes in inlet system geomorphology through producing bathymetric change plots and a series of cross sections over bathymetries from 1852, 1864, 1870, 1879, 1901, 1927, 1954 and 2006.
- ii). Conduct hydrodynamic modelling on historical bathymetries (1852, 1864, 1870, 1879, 1901, 1927, 1954 and 2006) in order to quantify major changes in current flow over time in the major channels and over the flood tidal delta.
- iii). Produce a surficial sediment grain size map for ebb tidal delta and channels surrounding flood tidal delta complete with ground truthing using grab samples for sediment grain size and underwater videography for surficial shell coverage.
- iv). Produce a bedform map for ebb tidal delta and channels surrounding flood tidal delta.

v). Analyse historical changes in surficial sediment and bedforms by comparing maps produced in i) and ii) with maps produced in Tauranga Harbour Study (Healy, 1985) and by Kruger (1999).

1.2 STRUCTURE OF THE THESIS

In order to achieve the specific objectives the thesis is structured as follows:

Chapter 2 provides an outline of the physical setting of Tauranga Harbour then reviews previous studies investigating hydrodynamics, sediment dynamics and geomorphology at Tauranga entrance tidal delta system. The chapter then discusses the tidal delta system in relation to previous geomorphological models and compares similar examples of tidal delta systems worldwide.

Chapter 3 analyses historical changes in inlet system geomorphology from 1852 to 2006.

Chapter 4 presents results from hydrodynamic modelling of historical bathymetries.

Chapter 5 presents the surficial sediment grain size map and the bedform map and the methodology employed to produce these maps. The maps are then compared with historical data to assess the long term changes in surficial sediment grain size and bedforms which are occurring in the harbour.

Chapter 6 contains the summary and conclusion of the study, complete with recommendations for further study.



Figure 1.1: Outline of study area within Tauranga harbour, with inset showing location of Tauranga harbour in relation to the North Island of New Zealand.



Figure 1.2: Map of Tauranga entrance of Tauranga harbour detailing channel names, the area which is dredged and other geographic features (following De Lange, 1988, Mathew, 1997, Kruger, 1999). (Air photo source: Environment Bay of Plenty).

2. PREVIOUS STUDIES OF HYDRODYNAMICS, SEDIMENT DYNAMICS AND GEOMORPHOLOGY OF TAURANGA HARBOUR

2.0 INTRODUCTION

This chapter provides a summary of previous research conducted on the Tauranga Entrance tidal delta system. It firstly provides a summary of the physical setting, secondly outlines previous investigations of the Tauranga Entrance tidal delta system geomorphology, hydrodynamics, and sediment dynamics, and thirdly discusses the southern harbour inlet in relation to general geomorphic models. Lastly, it compares other examples of similar delta systems worldwide.

2.0.1 Physical Setting

Tauranga harbour is an estuarine lagoon system enclosed by two barrier tombolos and a barrier island, located on the Bay of Plenty coast on the North Island of New Zealand (Healy et al., 1996, Hume and Herdendorf, 1998). The estuary has an area of 851 km² (Kruger and Healy, 2006) and has two inlets, Katikati at the north-western end and Tauranga at the south-eastern end adjacent to the Mt Maunganui rocky headland and tombolo (Hume and Herdendorf, 1992). The inlets are dominated by tidal currents and at the Tauranga inlet there is a mean tidal range of 1.4 m and a mean annual significant wave height of 0.5 m. The inlet throat is roughly 500 m wide, reaches a depth of approximately 34 m and has a mean depth of 15 m (De Lange, 1991; Kruger and Healy, 2006).

2.0.2 Previous investigations of the Tauranga Inlet

The major investigations into the Tauranga inlet and tidal delta system geomorphology, hydrodynamics and sediment dynamics are as follows:

The Hydraulics Research Station at Wallingford, UK completed reports in 1963 and 1968 which included a historical chart analysis, fieldwork and scale physical hydrodynamic model tests of Tauranga Harbour (Hydraulics Research

Station 1963, 1968). Sediment dynamics of the Tauranga inlet delta system were first investigated by Davies-Colley (1976) with a particular focus on the flood tidal delta.

Dahm (1983) subsequently investigated the geomorphic development, bathymetric stability and sediment dynamics of Tauranga harbour.

The Tauranga Harbour Study began in 1983 and was a major investigation involving hydrographic soundings, tide gauge recordings, current speed profiles, continuous current recordings, drogue tracking, sediment sampling and underwater photography of the harbour bed, suspended sediment sampling, sediment size analysis, side scan sonar and seismic profiling, aerial photography and climate records. The first hydrodynamic numerical modelling and sediment transport modelling of Tauranga Harbour was also completed (Black, 1984; Barnett, 1985; Healy, 1985).

Wave induced sediment transport and a review of previous model studies of Tauranga Harbour were investigated by De Lange (1988) in his thesis on wave climate and sediment transport within Tauranga harbour in the vicinity of Pilot Bay.

Mathew (1997) conducted an analysis of bathymetric survey data, undertook near bottom current measurements, computed bedload and suspended load transport under unidirectional (tidal flow) from theoretical models using near bottom currents and sediment grain size as input parameters. Grain size patterns, fluid velocity structure, surficial sediment facies and transport, and shoaling mechanisms and sand bypassing were investigated by Kruger (1999) and Kruger and Healy (2006).

2.1 PREVIOUS INVESTIGATIONS OF HARBOUR GEOMORPHOLOGY

2.1.1. Pre dredging geomorphic changes

Large changes in bathymetry were shown to have occurred inside and outside the harbour between 1852 (when the first hydrographic survey was conducted) and 1954 (prior to the first dredging by the Port of Tauranga) by the Hydraulics Research Station (1963). Significant changes in the coastline shape at the south-eastern end of Matakana Island, Panepane Point were noted. The

minimum distance between Mt Maunganui and Panepane Point reduced by 38% between 1852 and 1954 due to an over 300 m eastward extension of Panepane Point on Matakana Island, narrowing the inlet channel. The Hydraulics Research Station (1963) commented at the time that this narrowing was continuing but would not hinder shipping.

Furthermore, the Hydraulics Research Station (1963) notes that in 1852 the primary approach to the inner harbour was the Maunganui Roads Channel, while in 1954 the Western Channel was the major approach. There had not been significant deterioration between 1852 and 1954 in the extent of Maunganui Roads Channel, confirming that there was only a small amount of sediment moving in the area. Moreover there has been no obvious change in the Stella Passage between 1852 and 1954 and the entrance bar had remained at a nearly constant depth of approximately 7 m below Tauranga Harbour Board Datum.

2. 1.2.Dahm – Geomorphology

Geomorphic development and bathymetric stability of Tauranga harbour was investigated by Dahm (1983). It was discovered that hydrographic surveys of the harbour conducted between 1852 and 1954 showed large scale bathymetric and shoreline changes, which were related to the development of the Lower Western channel as a discharge passage for flow from the western part of the harbour.

Previous studies by the Hydraulics Research Station (1963) and Davies-Colley (1976) hypothesised these changes were instigated through deepening in the Lower Western Channel area, leading to current flow through the Upper Western Channel to be diverted through this region. Dahm (1983) rejects these explanations and proposes that the development of the Lower Western channel is due to growth of the Centre Bank.

Dahm (1983) proposes that the growth of the Centre Bank flood tidal delta was caused by deposition from decelerating flood currents. This growth has constricted and ultimately closed the historical shallow channel which linked the Upper Western and Otumoetai Channels. This redirected flow resulting in the strengthening of the Lower Western Channel. The growth of the Lower Western Channel evidently resulted in considerable bathymetric and shoreline changes

both outside and inside the harbour entrance, indicating that the flood and ebb tidal regions have a close and complex dynamic interrelationship.

Hydrographic surveys of the Lower Western Channel from 1962 to 1979 showed that bathymetric change was still occurring - indicating that the harbour has not yet achieved a stable bathymetric configuration, in contrast to the conclusion of Davies- Colley (1976) who asserted that the harbour was bathymetrically stable after investigating historical bathymetric and shoreline surveys. The northern flood tidal delta growth is constricting the Lower Western Channel through deposition, redirecting ebb flow from this area. In 1983 there was a trend of northwards diversion of the ebb flow across the Northern Bank but Dahm (1983) notes that in the future it may be possible for diversion over the Centre Bank. Dahm (1983) also proposes that the fundamental cause for historical bathymetric instability leading up to 1983 was the discharge of flood flow into the harbour against the trend of ebb flow from the western part of the harbour – causing a conflict between the pathways of flood and ebb dominated sediment transport.

2.1.3. Tauranga Harbour Study – Bathymetries

Barnett (1985) digitised hydrographic surveys from 1970, 1954, 1927, 1902 and 1852 to give historical models with 75 m grid area in the Tauranga Harbour Study. The changes between successive 75 m grids were plotted to provide a detailed understanding of historical erosion and accretion stages. The comparison illustrated an ongoing narrowing and deepening of the main entrance gorge, constant instability in the Lower Western Channel and accretion in the centre of the harbour. On the ebb tidal delta the north edge of the Matakana Bank has progressively accumulated. The inner bank area has shown less stability with an overall trend of erosion immediately north of the entrance and accretion along the Matakana Island coast.

CHEKTOPO plots demonstrating bathymetric changes from 1852 to 1983 were produced by Barnett (1985) (an example is shown in Fig 2.1), while countoured plots demonstrating bathymetry changes from 1902 to 1983 were produced by Black (1984) (an example is shown in Fig. 2.2).

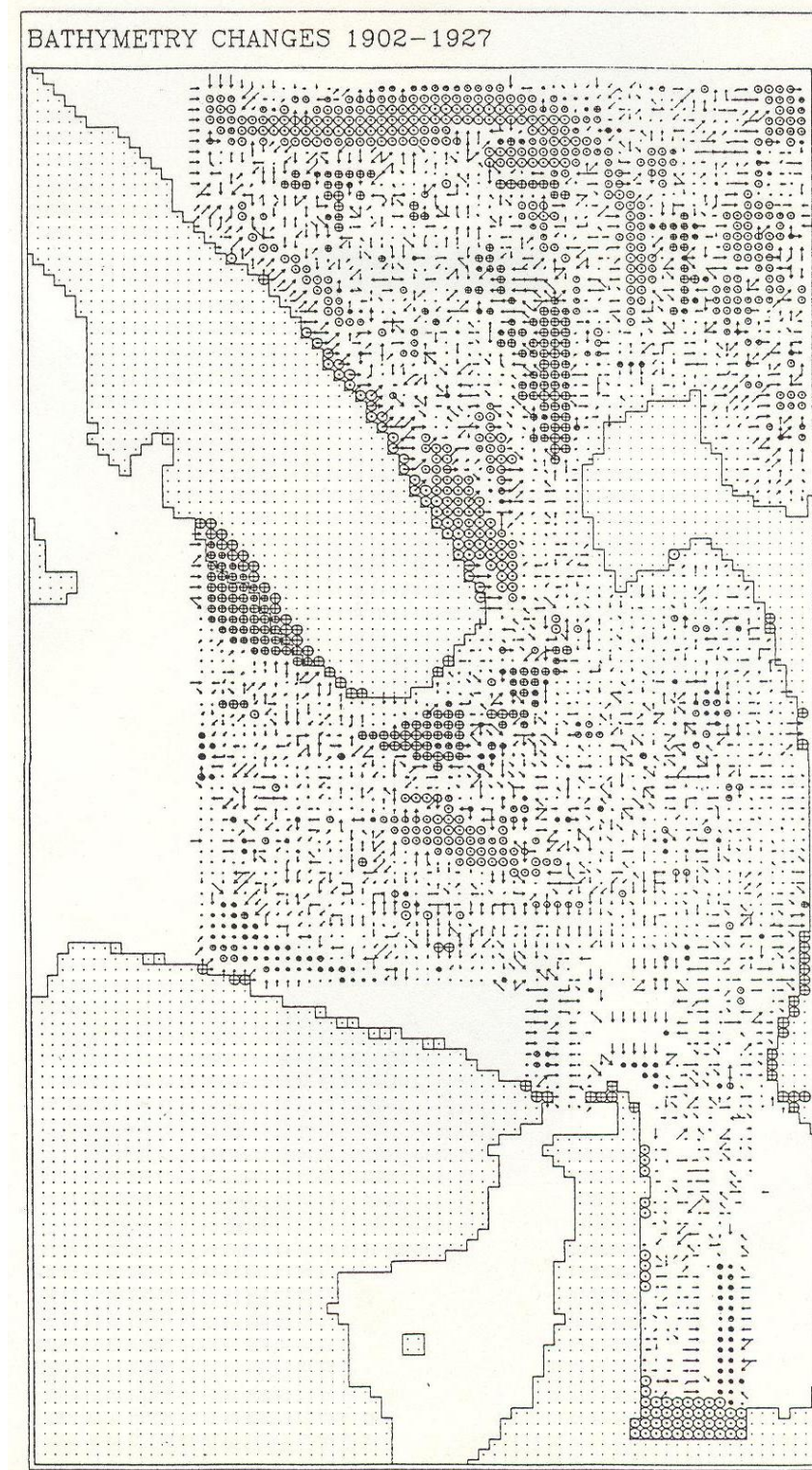


Fig 2.1. CHECKTOPO plot of bathymetry changes between 1902 and 1927
(Source: Barnett, 1985).

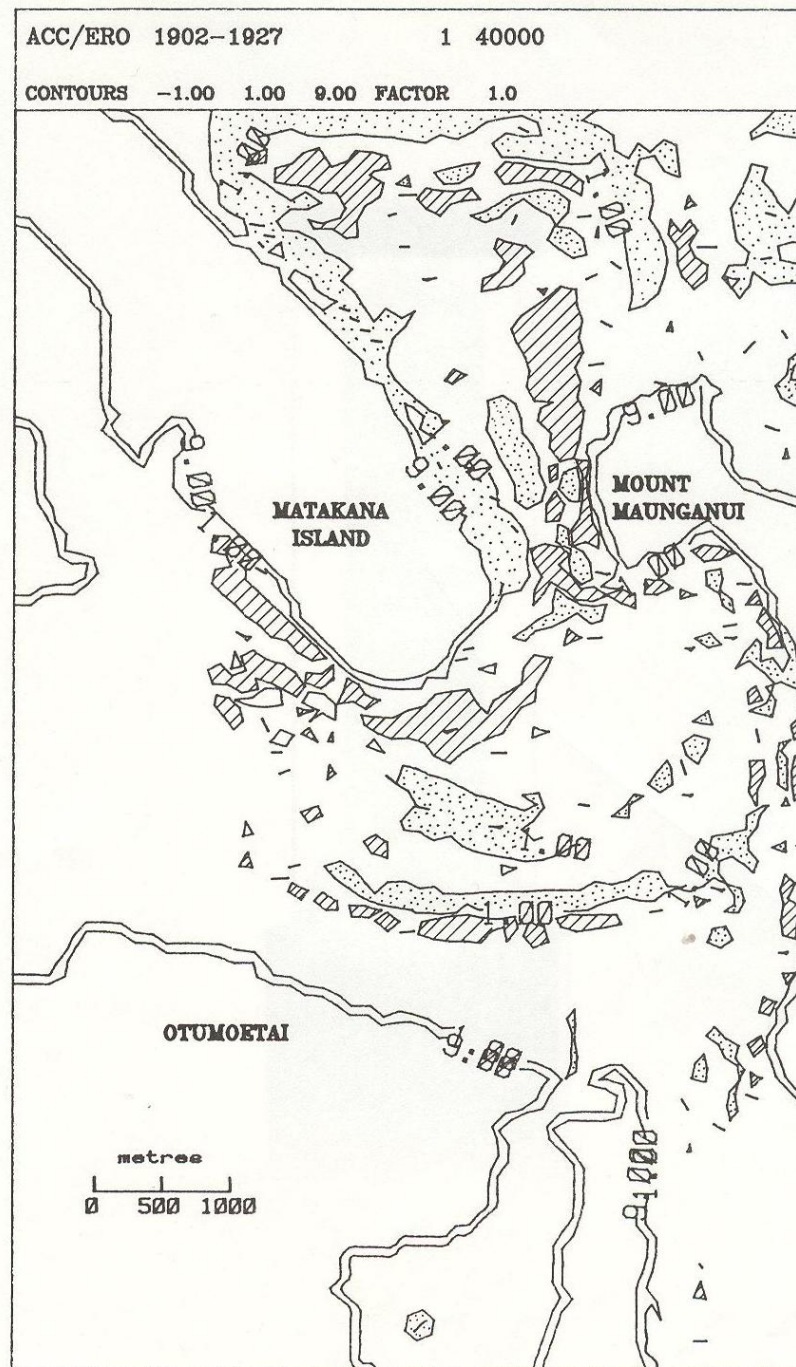


Fig. 2.2. Erosion (cross-hatched) and accretion (dotted) exceeding 1 m in the period from 1901-1927 in Tauranga Harbour (Source: Black, 1984).

2.1.4. Flood tidal delta geomorphology in 1982 to 1983 and 1990 to 1995

Mathew (1997) conducted a detailed analysis of flood tidal delta bathymetric survey data from 1982 to 1983 and 1990 to 1995, with detailed cross sections and volumetric calculations of the flood tidal delta volume. It was demonstrated that there had been considerable changes including:

(a) Sediment deposition in the Lower Western Channel causing it to shoal to less than 5 m (CD) between 1982 to 1989. The channel then opened up again after 1992.

(b) The blind flood channel of the flood tidal delta underwent shoaling of 7 m between 1982 and 1990 as well as shoaling of 3 m at an adjacent location between 1992 and 1994.

(c) Shoaling of 0.5 m occurred on the shallow ebb shield. Apart from these changes, the rest of the flood tidal delta generally remained the same.

An analysis of annual bathymetric surveys and volumetric calculations showed that the ebb tidal delta has generally remained stable between 1989 and 1995. However considerable localised changes are apparent. Sedimentation in the Entrance Channel is particularly noteworthy after dredging, especially on the south eastern side near the C Buoy with dredging having increased to ~110,000 m³, up from a long term average of ~70,000 m³ per year. The proximal blind channel has undergone infilling of 3.5 m from 1989 to 1995, while the distal channel near the terminal lobe has undergone scouring.

Shoreline data analysis of the shore southeast of Matakana Island near the ebb tidal delta shows that the shoreline has not undergone significant changes as a result of the 1991-1992 dredging.

2.1.5. Concluding points on geomorphology

Overall the geomorphologic studies of Tauranga Harbour have identified large morphologic changes prior to dredging between 1852 and 1954 in the harbour particularly around Panepane Point (which has extended over 300 m in this period) and shoaling in the Maunganui Roads Channel, a progressive deepening of the main entrance gorge and accretion on the Centre Bank flood tidal delta. However little change has occurred at the Stella Passage and the terminal lobe Entrance Bar, which has remained at a more or less constant depth for the same time period. Large scale changes in bathymetry of the Lower Western Channels are related to the channel's role as a discharge passage caused by the growth of the Centre Bank flood tidal delta.

The Lower Western Channel has shoaled to less than 5 m below chart datum due to sediment deposition between 1982 and 1989. In 1992 the channel

then opened. The blind flood channel (Fig. 2.3) shoaled 7 m between 1982 and 1990, and this was accompanied by shoaling of 3 m at a nearby area between 1992 and 1994. The ebb shield shoaled by 0.5 m. The rest of the flood tidal delta remained relatively unchanged between 1982 and 1985. The ebb tidal delta essentially remained stable between 1989 and 1995.

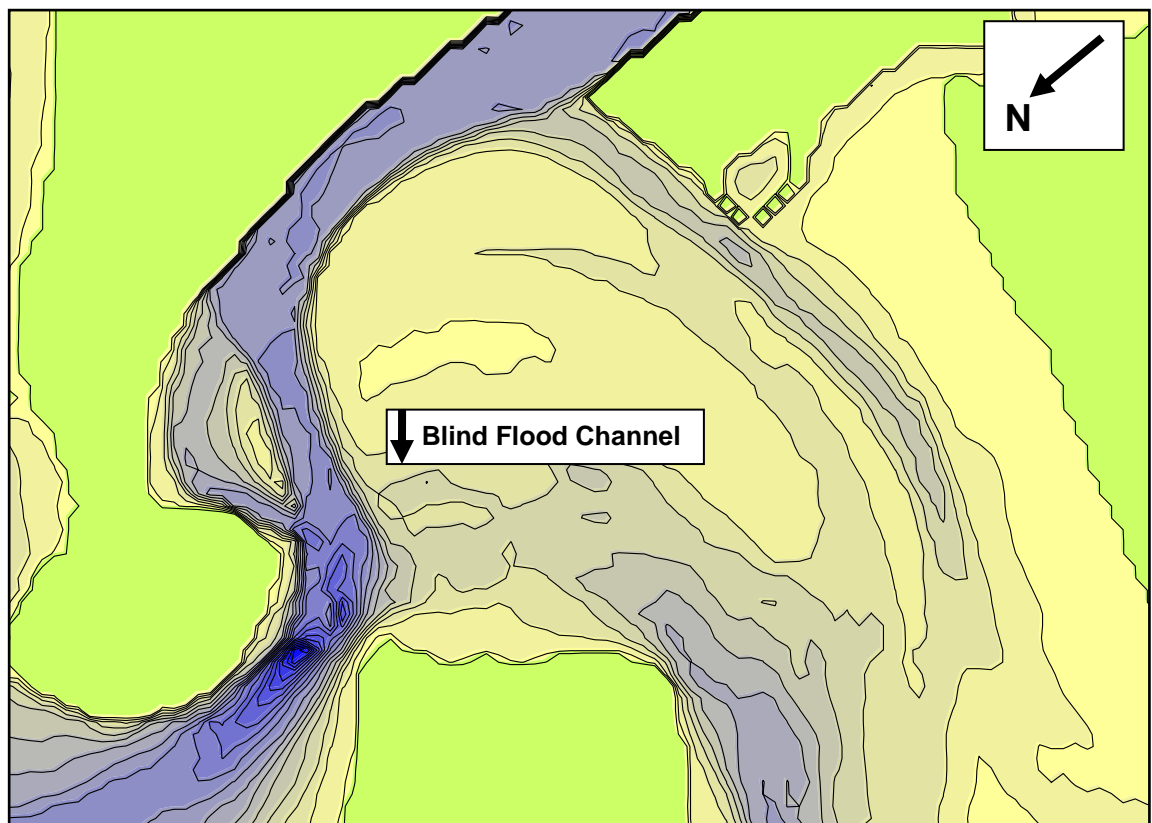


Fig.2.3. The location on blind flood channel on the 2006 bathymetry.

2.2 PREVIOUS INVESTIGATIONS OF TAURANGA HARBOUR HYDRODYNAMICS

2.2.1. Pre-dredging tidal flow changes

The Tauranga Harbour Investigation by the Hydraulic Research Station (1963) notes that in 1852 the Maunganui Channel was the primary channel for the harbour entrance while in 1954 the Western Channel carried a large proportion of the tidal flow into and out of the harbour. This change in dominance of the major tidal channels also been accompanied by shoaling in the channel which joined the Otumoetai and Upper Western Channels. The presence or absence of river inputs

made little difference to the hydrodynamics of the physical model (Hydraulics Research Station, 1963, 1968).

2.2.2. Tidal Currents

Davies-Colley (1978^a) was the first to demonstrate from plotting tidal currents, measured on the flood tidal delta, that the sediment entrainment velocity threshold is exceeded at most stations, including neap tides. This indicated frequent sediment transport in the net direction of dominant tidal currents.

Tidal currents plotted against time from particular oceanographic stations (one in the entrance channel and twelve in the flood tidal delta) by Davies-Colley (1976) indicate a phase relationship with the standard spring curve. The sediment entrainment velocity threshold is exceeded at most stations, including neap tides, indicating frequent sediment transport in the residual direction of dominant tidal currents. Sediments grain size are not graded to peak tidal currents because of the absence of enough coarse grained sediment.

Major current directional asymmetries, associated especially with large eddy systems, are demonstrated by Davies Colley (1976). Peak ebb and flood tidal currents at monitoring stations exhibited velocity asymmetries in both magnitude and direction (Davies-Colley, 1976).

The hydrodynamic investigation of Davies-Colley (1976) suggested that salinity and water temperature did not play a significant role in sediment dynamics of the outer harbour.

2.2.3. Hydrodynamic numerical modelling

The Tauranga Harbour Study (THS) of 1984 used the hydrodynamic numerical model `DHI System 21 with a 300 m grid. The calibrated 300 m grid model was then used to produce tide level boundary condition for a PORT model based on a 75 m square grid, which was developed to study the port area of the harbour (Barnett, 1985). The peak ebb flow patterns from the model (Fig 2.4) demonstrated the spatial extent with strong currents through the harbour entrance and the Lower Western and Cutter Channels, and weaker easterly to northerly currents apparent over the flood tidal delta. The peak flood flow patterns (Fig 2.5)

show strong currents through the entrance with a progressive dispersal of currents over the flood tidal delta. The model output fails to clearly show the eddy present in Pilot Bay during the peak flood tide.

It is important to note that Black (1984), who ran a sediment transport model for Tauranga Harbour raises concerns about the PORT model. Black (1984) notes that the decision to place the open sea boundary in the inlet throat is not ideal for sediment modelling and also raises concerns about the hydraulic interpolation method used to produce velocities on Matakana Bank and in the entrance to Tauranga Harbour.

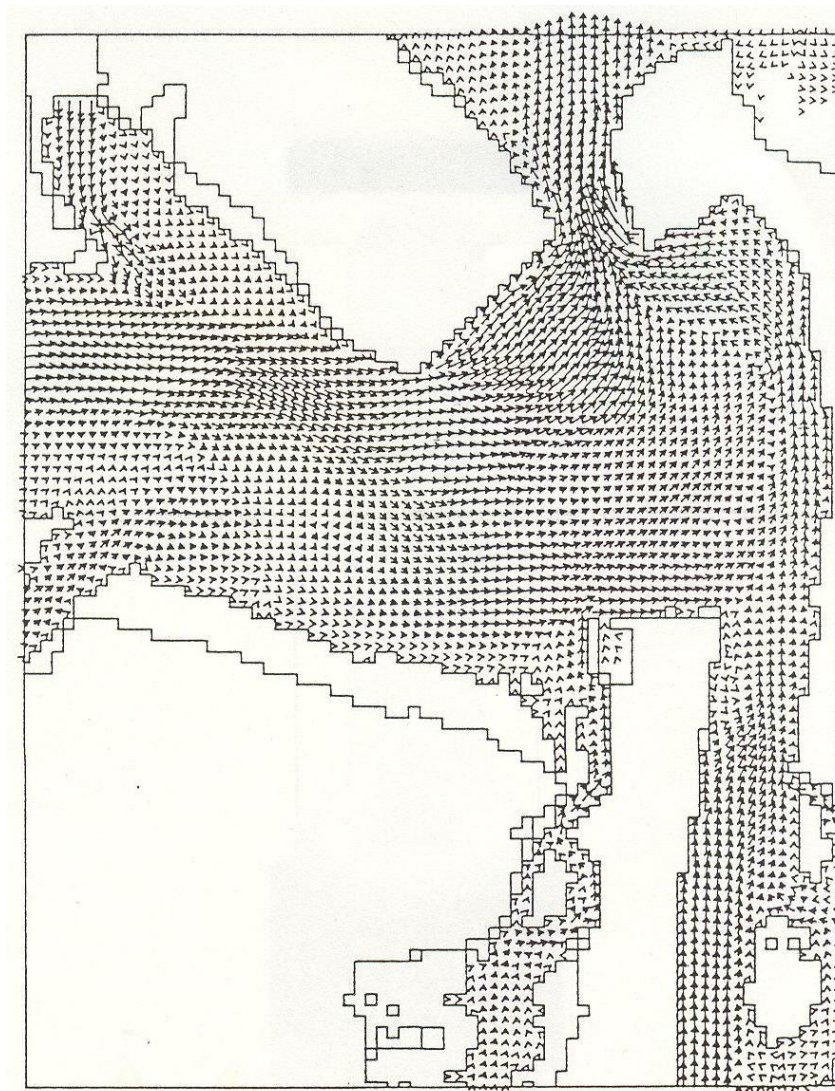


Fig 2.4. Vector plot at mean tide at maximum ebb based on System 21 hydrodynamic numerical model (Source: Barnett, 1985)

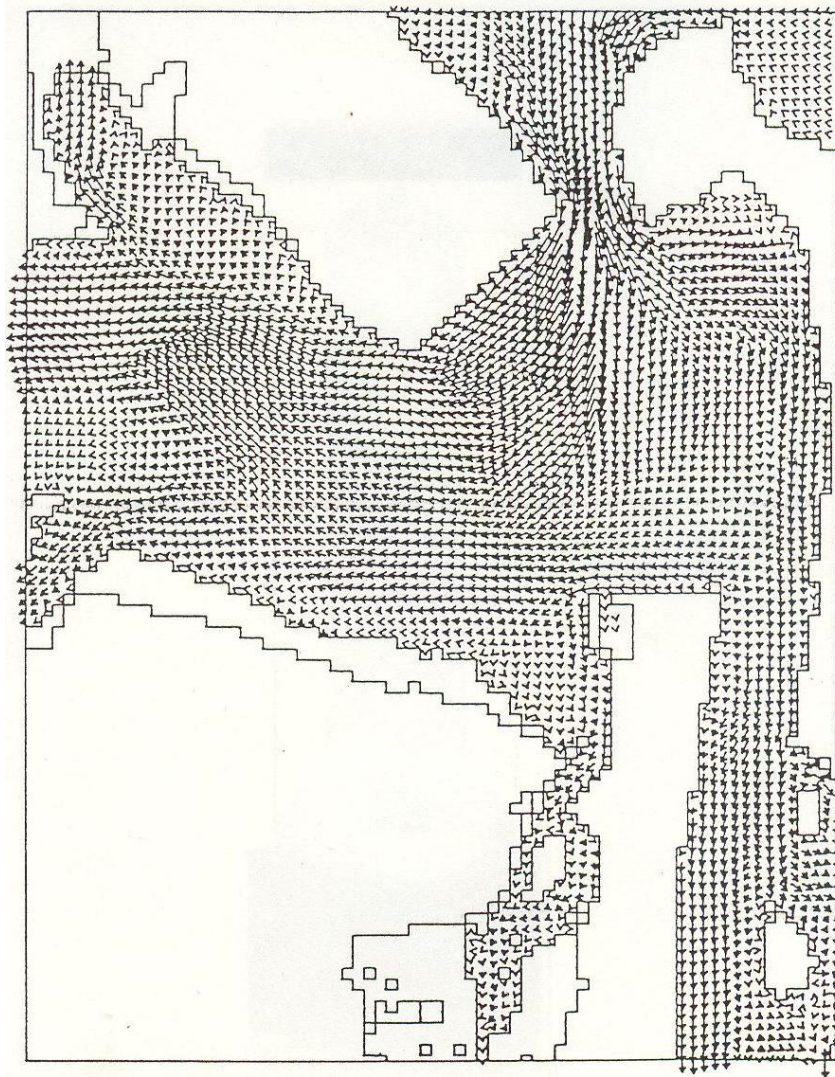


Fig 2.2.5. Vector plot at spring tide at maximum flood based on System 21 hydrodynamic numerical model (Source: Barnett, 1985)

Four historical bathymetries of Tauranga Harbour (1901, 1927, 1954, 1970) were modelled with a grid cell size of 75 m by Black (1984) in order to examine morphological changes. The bathymetric changes, since 1901, predicted by the model included:

- i) the adjustments in the Lower Western Channel
- ii) the narrowing and deepening of the entrance throat
- iii) early sedimentation on the western side of the Centre Bank

Black (1984) concludes that the changes are primarily a tidally induced, natural progression in the harbour as it develops and responds to its own adjustments in bathymetry. However, the model was unable to provide a

satisfactorily prediction of accretive changes to the Matakana coastline on open ocean side of Panepane Point. It was unknown whether this is because the sediment inputs are forced by waves, or whether the uncalibrated models are inadequate in this area.

Black (1984) states that the results further supported the conclusion that the changes immediately prior to 1983 in the Lower Western Channel were primarily natural.

2.2.4. Hydrodynamic Model Comparison

De Lange (1988) measured currents in Pilot Bay and provided a review of the hydrodynamic physical modelling by the Hydraulics Research Station (HRS) (1963), and the hydrodynamic numerical modelling of the Tauranga Harbour Study (THS) (Barnett, 1985).

The general circulation pattern of the Tauranga southern basin was captured by both the physical (HRS) and numerical (THS) hydrodynamic modelling; however the numerical model provides a closer match with current measurements undertaken by De Lange (1988). Both the HRS and THS model capture the ebb dominance of Pilot Bay but neither the HRS nor THS model demonstrate the long duration ebb flows measured by De Lange (1988). The HRS and THS models both show current velocities that are 50 – 75% higher and continued 300 – 500% longer than De Lange's (1988) measured current data. The sediment fluxes through Pilot Bay taken from the THS model are nevertheless similar to results measured by De Lange (1988).

2.2.5. Changes in current regime due to dredging

Changes in the current regime within the harbour due to dredging were investigated by Mathew (1997) through undertaking near bottom current measurements. The Lower Western Channel near Panepane point has experienced a significant increase in tidal current velocity after dredging due to the new hydraulic conditions. The flood velocity has increased in the Cutter Channel region after dredging but no obvious differences were apparent in the ebb

velocity. Tidal flow patterns inside Pilot Bay was shown by the data to be dominated by an eddy which is apparent for the majority of the flood tide.

Mathew (1997) undertook current measurements in six locations in the Lower Western Channel, Cutter Channel, Pilot Bay and the northern part of the flood tidal delta (Fig 2.6). Residual currents were flood directed at all measurement locations apart from Pilot Bay. This implied that cumulative sediment transport was likely to be flood directed in this area.



Fig 2.6. Locations of current measurement over the flood tidal delta and adjacent region (map created with source data from Mathew, 1997)

2.2.6 Rerun of System 21 Numerical Model

Mathew (1997) used the hydrodynamic numerical model System 21 to compare the model predicted changes in the velocity vector and sediment residual current pattern after the major dredging of 1991 – 1992 with the model run using the post dredging (1994) bathymetry and to compare the model results with the measured changes gathered from the bathymetric comparison. The same boundary conditions and model parameters were used by Mathew (1997) as those used in the Tauranga Harbour Study (Barnett, 1985).

Model results were interpreted by Mathew (1997) to have localised decreases in peak ebb and peak flood velocities at the dredged area of the north western end of the Cutter Channel, Tanea Shelf and near Sulphur Point Wharf. However, the velocity vector pattern that was predicted for Otumoetai Channel and Stella Passage is not in agreement with the actual changes. This is because the predictions were based on the dredging of the Otumoetai Channel which did not occur.

Deposition on the eastern end of the flood tidal delta is noted by Mathew (1997) to be consistent with the model finding of an enhanced west to east flow across the flood tidal delta and the possibility of sediment deposition as detailed by Healy et al. (1991).

A comparison of changes interpreted from model results with measured bathymetric changes, shows good resemblance in the majority of the regions.

2.2.7. Fluid velocity structure

The fluid velocity structure was analysed by Kruger (1999) through conducting a 14 hour survey over the Entrance Channel using an acoustic Doppler current profiler (ADP). Residual vector plots of the tidal currents demonstrated that two eddies are present near the inlet: an anticlockwise eddy west of the entrance channel near Panepane Point; and a clockwise eddy east of the inlet approximately 1.6 km north of Mount Maunganui centred on the Entrance Channel. Both eddies showed strong asymmetry, suggesting the bottom topography produces vorticity.

The residual current velocity plot demonstrated that the near-bed currents east of the Entrance Channel are flood dominated, while west of the Entrance Channel the near-bed currents are ebb dominated.

A tidally induced transient eddy can be seen at peak ebb currents about four hours after high water at A Beacon and can be tracked for a further four hours, as the flood currents east of the Entrance Channel sustain the eddy for a portion of the flood cycle.

The tide induced transient eddy pathway is consistent with deposition at dredging area no. 6 (Fig. 2.7) and it is suggested by Kruger (1999) that the horizontal and vertical velocity structure aids the development of a fine sand

sandbank situated in the Entrance Channel which constituted 50% of the dredged sand from the Entrance Channel in 1998.

Kruger (1999) suggests that the spatial control of sediment transport and deposition through the tide induced transient eddy may have increased as a result of the 1992 capital dredging, which increased the channel depth from 12.9 to 14.1 m, by increasing the role of differential bottom friction and water column stretching to total vorticity.

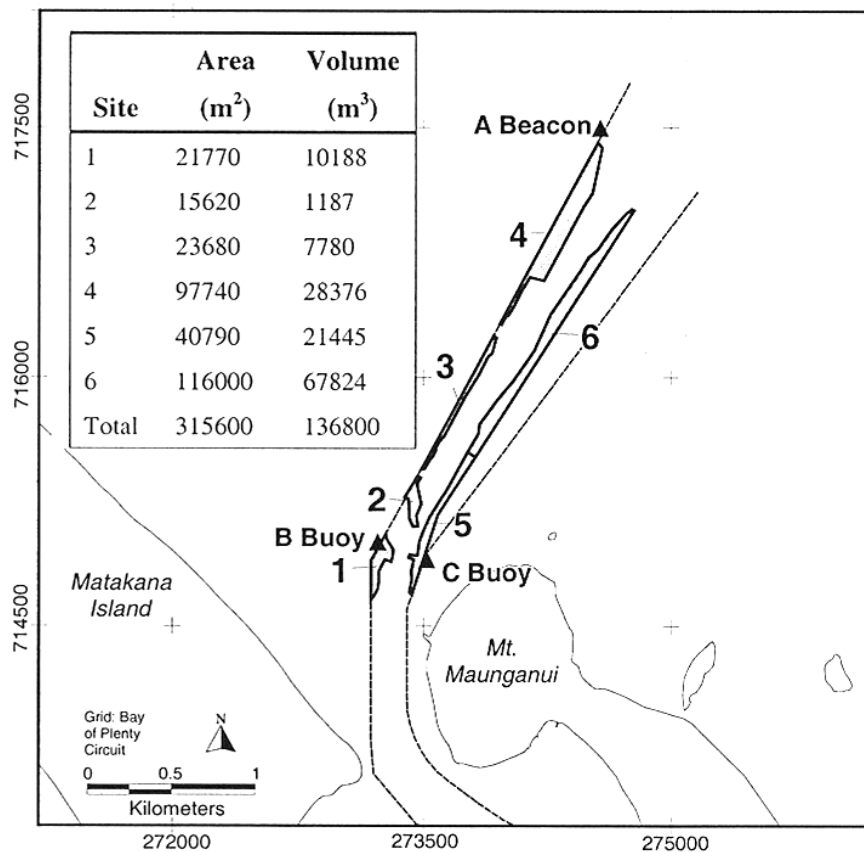


Figure 2.7. Map showing Entrance Channel and the areas that required maintenance dredging in 1998. The dash line shows the boundaries of the dredged inlet channel. The inset details the volume of sediment above a chart datum of 14.2 m in each of the areas (source: Port of Tauranga 1998 as cited in Kruger 1999)

2.2.8. Concluding points on hydrodynamics

An understanding of the hydrodynamics of Tauranga Harbour has been built up over 30 years through the use, initially of physical hydrodynamic models,

and subsequently through numerical hydrodynamic models and accompanying field measurements of current flow at various locations across the ebb and flood tidal delta system. Findings that have particular relevance to the present study are the changes in tidal flow, the dominance of waves and currents in different parts of the delta system, changes in the current regime as a result of dredging, and the measurement of near bottom currents.

A 75 m square grid hydrodynamic numerical model was provided by Barnett (1985) representing current flow across the harbour. From this the general current patterns and sediment flux in Pilot Bay was confirmed by De Lange (1988) as being generally consistent with his measured results. However discrepancies were noted in the magnitude and length of time of peak current velocities. Changes in current regime as a result of dredging were investigated by Mathew (1997) through the measurement of near bottom currents. This showed that the Lower Western Channel had undergone a significant increase in tidal current velocity after dredging while the northern part of the flood tidal delta had experienced an increase in flood velocity. Furthermore an eddy dominates the majority of the flood tide in Pilot Bay while residual currents were flood directed at all measurement sites in the vicinity of the northern part of the flood tidal delta, apart from Pilot Bay. Eddies are present outside of the harbour on the ebb tide – an anticlockwise eddy west of the Entrance Channel near Panepane Point and a clockwise eddy east of the inlet centred on the Entrance Channel. Residual current velocity plots created by Kruger (1999) show that the near bed currents east of the Entrance Channel flood dominated and west of the Entrance Channel are ebb dominated.

In summary, prior to dredging there have been significant changes in tidal flow with the main tidal channel moving from Maunganui Roads Channel to the Lower Western Channel between 1852 and 1954. Considerable changes in the current regime are also apparent post-dredging with an increase in current velocities in the Lower Western Channel, and flood current velocities in the northern part of the flood tidal delta. Tidally induced eddies play a significant role in tidal flow patterns both inside and outside of the harbour entrance.

2.3 PREVIOUS INVESTIGATIONS OF TAURANGA HARBOUR SEDIMENT DYNAMICS

2.3.1. Sediment Transport Patterns

Sediment dynamics of the inlet of Tauranga harbour were first investigated by Davies-Colley (1976). His study examined sediment transport over the ebb and flood tidal delta systems near the inlet entrance with a particular focus on the flood tidal delta. A unified conceptual model of sediment circulation was proposed based on tidal streamlines, bedforms, sediment discharge measurements, and theoretical calculations (Fig 2.8).

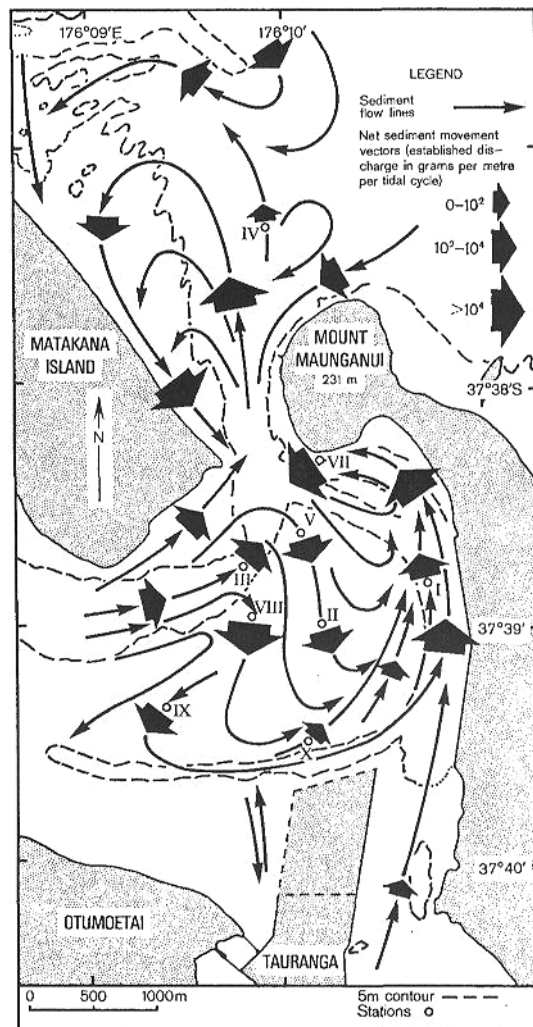


Fig.2.8. Model of sediment transport patterns for Tauranga Entrance based on tidal streamlines, bedforms, sediment discharge measurements and theoretical calculations (source: Davies-Colley and Healy, 1978^b).

Davies-Colley and Healy (1978^b) demonstrated that sediment dynamics are primarily a function of tidal currents, with wave action having a significant effect only in shallow areas. This was achieved through the analysis of tidal current streamlines, the investigation of the alignment and scale of bedforms, and direct estimations of sediment transport rates gathered from bedload monitoring. Time velocity asymmetry of tidal currents is a key process shaping the formation of morphological features at ebb and flood tidal deltas through determining the predominant flow of sediment either into, or out of, the tidal inlet.

Swell waves on the bar of Matakana Bank result in sediment transport in small scale gyres, with landwards movement through wave bores, and seawards movement via ebb tidal currents. Wind waves generally only affect the seabed in shallow areas, less than 1.5 m below chart datum.

A net south-easterly littoral drift was shown to be probable by Davies-Colley (1976) who analysed one year of wave observations, which is consistent with the finding of the Hydraulics Research Station (1963).

2.3.2. Sediment Transport Modelling

Sediment transport numerical modelling was first conducted in Tauranga Harbour by Black (1984) who suggested that the sediment transport patterns of the harbour consisted of two major circulating loops (Fig 2.9). Beginning at Panepane Point, sediment is evidently transported southward and divides into anticlockwise loop over Centre Bank returning through Maunganui Roads and Cutter Channels, and a clockwise loop across the western portion of Centre Bank through the channel which joins Otumoetai and Upper Western Channel and returning through the Lower Western Channel. The second loop apparently transports significantly more sediment than the first, particularly in the Lower Western Channel, where the net eastwards transport rate is about 85,000 – 255,000 m³year⁻¹ which is the difference between sediment transport rates of over one million m³year⁻¹ on both ebb and flood. Therefore, Black (1984) proposed that the dredging required to maintain an artificial channel in this area would likely be large.

Across the western Centre Bank the flood tidal inputs dominate with a net transport southwards of approximately $150,000 \text{ m}^3 \text{ year}^{-1}$, with considerably lower rates elsewhere in the clockwise loop .

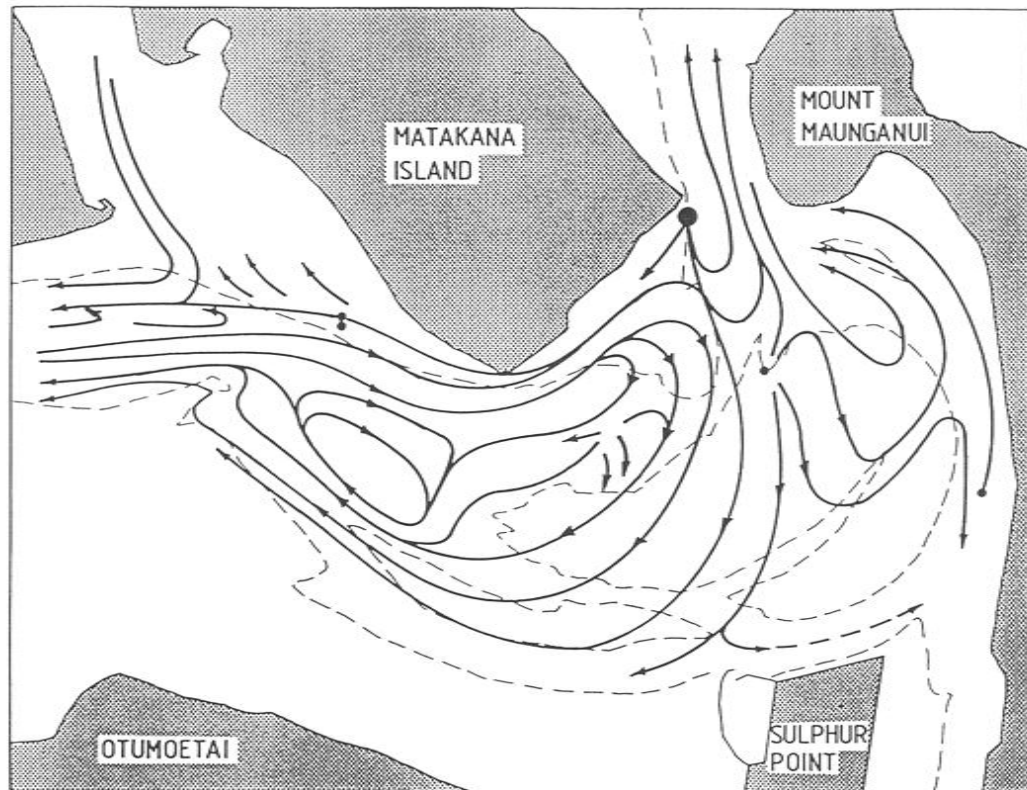


Fig 2.9. Direction of net, total load sediment circulation in Tauranga Harbour.

2.3.3. Tauranga Harbour Study – Morphology

Bottom sediment facies of Tauranga Harbour were interpreted using side scan sonar, echo sounding, hydrographic charts, underwater photographs, diver observations, bottom sediment analysis and aerial photography. Nine major facies units were identified a) shell lag; b) very shelly sands; c) rock outcrop; d) gravel or boulders; e) strongly developed mega ripples; f) poorly developed mega ripples; g) clean sands; h) shelly sands; and j) silty sands. The strongly bedformed areas are indicative of active sediment pathways while the shell lag areas correspond with strong currents and scouring. Figure 2.10 provides a summary of the morphological findings.

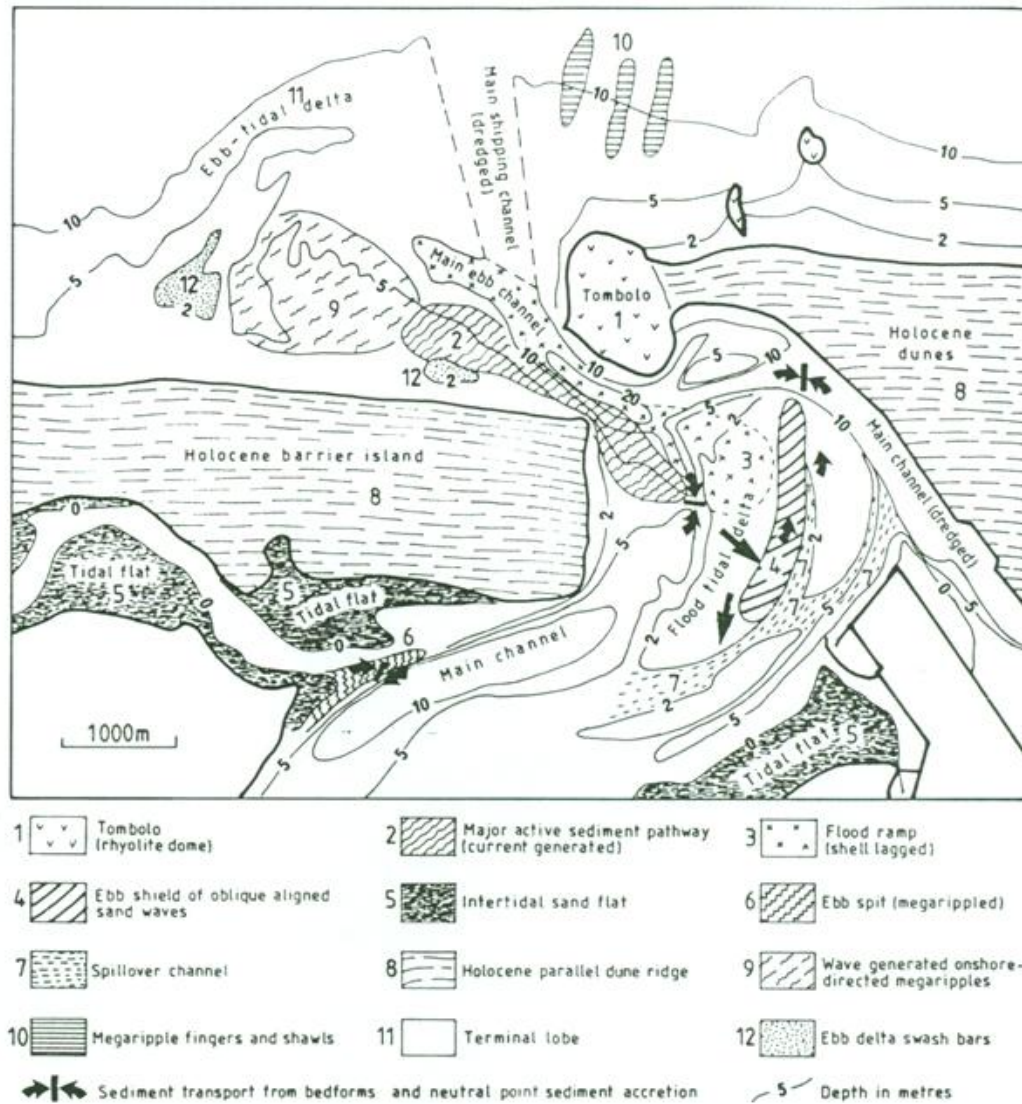


Fig.2.10. Major sedimentary features of Tauranga Harbour from the Tauranga Harbour Study (Healy, 1985).

The hydrodynamic model was compared with the sediment transport pathways inferred from the morphological evidence, and was found to be generally in agreement, apart from the Pilot Bay and the residuals over the ebb shield and adjacent neutral point in the Mt Maunganui Roads Channel (Healy 1985).

Similarly sediment transport modelling provides good agreement with the sea bed morphological features. There is good correlation between bedform patterns identified in the Lower Western Channel and on Matakana Bank.

The sediment re-circulation outside of the tidal inlet is partially driven by waves. Sand transported out onto the Matakana Bank is probably transferred

onshore by wave action and alongshore by the littoral current until it reaches the entrance where accelerating tidal currents act to transfer sediment back into the harbour.

2.3.4. Wave induced sediment transport

High frequency waves in Tauranga Harbour were shown by De Lange (1988) to be able to move sand sized sediment down to a maximum depth of approximately 2 m below the still water level. Consequently wave induced sediment transport is limited to the shallow intertidal zones in the harbour, yet some stirring is present on the shallower parts of the flood tidal delta (Centre Bank) where there is no shell lag.

Wave induced sediment flux is small in the absence of tidal currents, as a result of the low orbital velocities formed by the small short period waves present within the harbour. However, sediment can be entrained by wave action when tidal currents are present as more energy is available to move sediment. When tidal currents and waves are combined the average sediment flux for the intertidal zone within the southern basin of Tauranga Harbour is $\sim 60 \times 10^6 \text{ kgm}^{-2}$ per tidal cycle. It is recognised that this is relatively small compared to current induced sediment fluxes within the harbour, the large area under the action of wave stirring gives an annual sediment flux of $\sim 60,000 \text{ m}^3\text{yr}^{-1}$. This is 1-2 orders of magnitude smaller than the sediment fluxes induced by currents near the harbour entrance and elsewhere in the harbour.

2.3.5. Mathew – Sediment Dynamics

The highest part of the flood tidal delta, the ebb shield, has a series of oblique aligned ebb directed bedforms, indicating asymmetry in tidal wave propagation in these regions. At low spring tide these bedforms are exposed.

The surficial sediment of the flood ramp is comprised of broken shell and coarse sand with a mean grain size of ranging from 0.55 – 0.75 mm ($0.86 - 0.42\Phi$). The surficial sediment of the southern part of the flood tidal delta/ ebb shield is comprised of medium sand, while the Pilot Bay regions are comprised of fine to medium sand.

Bedload and suspended load transport capabilities were calculated through the use of theoretical models employing measured near bottom currents and sediment grain size as input parameters.

The sediment transport rates averaged over a spring neap cycle are greater at the Western Channel sites (Site TGA1, TGA5 and TGA6) (Fig. 2.6) than on the northern part of the flood tidal delta (Site TGA3). The maximum sediment transport has an order of magnitude of 10^{-1} kg/m/s. Pre-dredging transport rates are an order of magnitude less than post dredging rates, evidently due to the increase in current velocity post dredging.

The sediment transport at Site TGA3 occurs mainly as bedload and in a flood phase for a given sediment size. The ebb current velocity at this site only just exceeds the sediment transport threshold for medium sand (0.3m/s).

The flood velocities in the Pilot Bay area (Site TGA2) are too low to transport sediment for the given grain size (fine to medium sand) but the ebb phase has moderate transport. The computations show that there is essentially no suspended load transport for the given grain size.

2.3.6. Kruger (1999) – Grain size patterns

The surficial sediment survey demonstrated that well sorted medium sand was confined to the region of the main ebb jet and flood tidal delta, with a transition to moderately fine sand at the ebb shield. The swash bars on the northwest of the main ebb channel had coarse sand, while the terminal lobe and swash platform had fine sand; with the terminal lobe having sand that was very well to well sorted. Eastwards across the Entrance Channel there was a reduction in mean grain size from medium sand to fine sand. Fine sand in the Entrance Channel was moderately well sorted with a maximum standard deviation of 0.92Φ (Kruger, 1999).

2.3.7. Kruger - Surficial Sediment Facies and Transport.

A sidescan sonar survey was undertaken in order to attempt to identify sediment transport pathways over the ebb tidal delta and within the Entrance Channel.

Four dominant regions were found based upon grain size, water depth, bedform patterns, general hydrodynamic conditions and morphology. The first zone on the outer north-west region of the ETD showed high relief, coarse grained swash bars in a mean water depth of ~ 6.71 m. The second zone on the swash platform west of the ebb channel contained medium mega rippled sand. The third zone in the path of the main ebb jet contained medium sand with small dune bedforms. The fourth zone east of the entrance channel contained featureless fine sand (Kruger and Healy, 2006).

A schematic of sediment transport at the tidal inlet was produced through the mapping of bedforms from the sonograph and SCUBA diver observations. This model is consistent with international literature but different to previous sedimentation models of Tauranga Harbour, as it shows sediment bypassing to the east by crescentic bar migration along the outer edges of the ebb tidal delta. The study suggested that the bar moves easterly at a rate of $\sim 50 \text{ ma}^{-1}$ and is causing the sedimentation on the western edge of the outer part of the Entrance Channel.

2.3.8. Shoaling mechanisms and sand bypassing

Kruger (1999) interpreted that sediment is transported into the ebb tidal delta through the southwards longshore drift along the Matakana Island coastline. Wave and tidal generated currents then transport the sediment over the marginal flood channels and into the main ebb channel. This process results in sedimentation on the eastern side of the main ebb channel north-west of Mt Maunganui, as fine sand is deposited in this area via flood currents.

Strong ebb flow in the inlet may result in the northwards movement of sediment. The mean grain size near the B Bouy is 0.4 mm (medium sand) and peak currents can be as high as 0.75 ms^{-1} in a neap tide and 1.23 ms^{-1} in a spring tide (1 minute average measured at 1.0 m above the bed with an S4 current meter). For a current dominated flow pattern near B Bouy, as in calm conditions with low swell waves, then the stable bedform will be two dimensional straight crested dunes. This was in keeping with SCUBA diver observations and the sonograph imagery. There is a similar situation in dredging areas 1, 2 and the south of C bouy for area no. 5, (Fig. 2.7) as these areas undergo shoaling by the megaripple bedform migration process.

As the ebb jet diverges and slows with increasing distance from the tidal inlet, sediment is deposited. Fine sand that is transferred in suspension near the inlet is deposited near the terminal lobe where the ebb jet reaches the retarding surface waves. There may be an increase in sedimentation as the current field of the ebb jet undergoes a rotational character as a result of eddy formation on the eastern side of the Entrance Channel. The sedimentation on the northern half of dredging area no.5 and the whole of area no. 6 is suggested by Kruger (1999) to be due to the loss of hydraulic gradient enhanced by the vorticity of the tidal induced eddy from the ebb jet.

Currents induced by the tide east of the Entrance Channel are typically small and flood dominated, and generally have insufficient energy to suspend sediment by currents alone. However they are capable of moving sediment suspended by long period waves. Suspended sediment east of the entrance channel is likely to be deposited at area no.6, which is consistent with the results of Mathew (1997).

A well developed swash platform with several coarse sand shoreward migrating swash bars are present on the ebb tidal delta west of the Entrance Channel. Kruger (1999) ascertained that the crescentic bar is moving along the outer edge of the ebb tidal delta at a rate of $\sim 50 \text{ m a}^{-1}$ after re-examining the historical bathymetry analysis of Mathew (1997). The fine sand bar is thought to be formed through the detachment of sediment from the eastern edge of the terminal lobe, and is moving eastwards under the action of refracting wave energy. This leads to the deposition of sediment at the north west end of the Entrance Channel dredging area no. 4.

Kruger's study addresses the causes for sediment deposition in the Entrance Channel, investigating the hydrodynamics related to sediment transport and deposition. The complex morphology of the ebb tidal delta and dredged Entrance Channel produces an environment that gives rise to strong vorticity production mainly due to differential bottom friction. Kruger suggested that a tide-induced eddy determines the location of sediment erosion and deposition causing increased sedimentation of the eastern side of the Entrance Channel. This shoaling is consistent with the location of the tide induced transient eddy, and

accounted for over 50% (~70000 m³) of the dredged volume from the Entrance Channel in 1998.

2.3.9. Concluding points on sediment dynamics

Investigation into the sediment dynamics of the tidal inlet delta system at the entrance to Tauranga Harbour have been conducted since 1976, and have involved the analysis of tidal current streamlines, bedforms, bedload monitoring, sediment transport monitoring, side scan sonar and the measurement of currents. Major findings include that sediment dynamics are primarily a function of tidal current action with wave influences being limited to shallow intertidal zones and shallow parts of the flood tidal delta. Early sediment transport modelling (Black, 1984) suggested that there are two major circulating loops over the flood tidal delta. The first loop began at Panepane Point and transported sediment southwards into an anticlockwise loop over Centre Bank flood tidal delta returning through Maunganui Roads and Cutter Channels. The second loop began at Panepane Point and transported sediment southwards into a clockwise loop over the western side of the Centre Bank flood tidal delta through the channel which joins the Otumoetai and the Upper Western Channels returning through the Lower Western Channel. There is a particularly large amount of sediment transport over the Lower Western Channel which was confirmed by near bottom current measurements. Cresantic bar migration is operating on the outer edges of the ebb tidal delta, longshore sediment transport moves sediment into the ebb tidal delta from the north west while the ebb jet recirculates sediment northwards. Tidally induced eddies encourage sediment transport in and around the entrance channel.

2.4 DISCUSSION

2.4.1 Comparison with previous model of tidal inlets.

The Tauranga tidal inlet delta system shows a relatively good agreement with the general morphological models for tidal inlet delta systems developed by Hayes (1975, 1980), Boothroyd (1985), and Kana (1999), when examined using historical and present bathymetries and aerial photographs.

The ebb tidal delta has a well defined main ebb channel and the terminal lobe. On the western side there is a well defined swash platform and evidence of swash bars. The lack of features on eastern side is thought to be due to the presence of the rocky head land of Mt Maunganui (Hicks and Hume 1996).

On the flood tidal delta there is evidence of a flood ramp, flood channels (the Lower Western Channel, and Pilot Bay prior to the capital dredging of the nearby Cutter Channel, which was originally a blind flood channel) and spill over lobes. Interestingly there is evidence of at least two ebb shields, and a smaller third ebb shield. There is also evidence of small ebb spit (~200 m) on the eastern side of the main ebb shield.

A comparison of the morphological features of the Tauranga Harbour tidal delta system with national and international examples shows some agreement. Essex Bay in north eastern Massachusetts shows reasonable morphological agreement with Tauranga Harbour as it has well developed main ebb channel, terminal lobe, swash platform, swash bar on the ebb tidal delta, and a flood ramp, flood channel, ebb shield and ebb spit. However this delta system is different to Tauranga in its well developed channel margin linear bar, spill over lobe and the development of both sides of the ebb tidal delta (Boothroyd, 1985).

2.4.2 Comparison with national and international examples.

Tauranga harbour is an example of a constricted ebb tidal delta, which occurs at shoreline angles where the body of sand cannot accumulate unrestrained towards the ocean and there is some shelter from waves (in this case provided by the rockyhead land of Mt Maunganui). This results in a delta which is has a low offshore length and is commonly offset between the rocky headland and a sandy barrier which limits the lateral spread of the delta. The length/breadth ratio of the ebb tidal delta is approximately 1:1 which is within the constricted ebb delta limits of 0.6:1.1 to 1.1:1. Other New Zealand examples of constricted deltas are Parengareanga and Rangaunu (Fig 2.11) (Hicks and Hume 1996). Like the Tauranga entrance both of these ebb tidal deltas show limited growth on the headland side.



Fig 2.11: The tidal inlets and ebb tidal deltas of Parengarenga (left) and Rangaunu (right) are both adjacent to rocky headlands, which restricts the growth of the ebb tidal delta on that side. (Source: Google Earth, 2009)

The Tauranga entrance shares some common features with Teignmouth, situated in southwestern England, but has less pronounced short term change. Teignmouth, like the Tauranga entrance, has a rocky headland situated on the south side of the inlet (Van Lacker et al., 2004), and has current speeds of up to 2 ms^{-1} (Medina et al., 2007). Both tidal inlet delta systems require constant dredging in the main channel (Siegle, et al. 2007). The ebb tidal shoals of Teignmouth form a large sandbar system which undergoes cyclic morphological behaviour as shown by modelling and video imagery, which is similar but more pronounced than that of the Tauranga entrance. The sediment transport at Teignmouth, in the deeper regions is dominated by the tide while in shallower areas waves are dominant. The sandbar is suggested to form in the zone between the offshore ebb currents and onshore wave currents due to wave breaking in the region that delimitates the boundary between the channel and the shoal. The opposing flows cause a gyre of sediment transport encouraging deposition in the centre. Consequently the formation of the sandbar is related to high energy wave events. Sandbar movement, after formation, is primarily controlled by waves; with mean onshore flow transporting it onshore, and by ebb tidal currents which move sediment offshore. Therefore when there is low wave energy (eg: in summer months) the developing sandbar may widen in the offshore direction however when there are periods of high wave energy and frequency (eg: winter months) the sandbar

generally develops and is transported in the onshore direction (Siegle, et al. 2004; Siegle, et al. 2007).



Fig 2.12: The Teignmouth tidal inlet like the Tauranga entrance is adjacent to a rocky headland, note the large sandbar on ebb tidal delta.

2.5 CONCLUSIONS

Previous research of the tidal delta system of Tauranga Harbour has demonstrated the following important points:

- The Tauranga tidal inlet delta system has undergone considerable changes in tidal channels and delta system between 1852 and 1954 with predominant tidal flow shifting from the eastern side to the western side of the flood tidal delta. Presently the tide predominantly flows through eastern side through the Cutter Channel. Capital dredging has increased

tidal currents over the Lower Western Channel and the northern part of the flood tidal delta.

- Sediment transport is predominantly controlled by tidal currents with the effects of waves limited to shallow areas. Eddies dominate sediment transport near the Entrance Channel.
- Geomorphically the Lower Western Channel has undergone significant changes since the introduction of capital dredging.
- The Tauranga tidal delta exhibits many of the geomorphic features of general geomorphic models, and shows many of the same features as Essex Bay, Massachusetts.
- As a constricted ebb tidal delta it is similar to the New Zealand examples of Parengareanga and Rangaunu, but does not show as the same large scale short-term changes present in Teignmouth, England.

3. GEOMORPHOLOGICAL VARIATION OF TAURANGA TIDAL DELTA SYSTEM

3.0 INTRODUCTION

The large scale geomorphic of the tidal delta system at the Tauranga Harbour between 1852 and 2006 is examined especially in relation to the effects of dredging. This is undertaken through a comparison of the changes in sequential bathymetries from a bird's eye perspective, followed by cross sections at the locations of continual significant bathymetric change across tidal inlet delta system. The results are then compared with previous studies by Kruger (1999), Healy (1985) and Dahm (1983).

3.1 BATHYMETRY AND CROSS SECTION METHODS

Each of the bathymetries used in this thesis was created using a number of different sources. All of the final grids had the same grid dimensions and grid cell size of 55 m.

The 2006 bathymetry was compiled by Spiers et al. (2009). The data for the shipping channels and tidal delta system came from recent single beam surveys conducted by the Port of Tauranga Ltd. along with recent multibeam surveys from the University of Waikato. The bathymetric data for the remainder of the harbour and the inner shelf was sourced from Environment Bay of Plenty, and consisted of a combination of digitised charts, soundings, and previous model grids (Spiers et al. 2009).

The bathymetries dated 1954, 1927, 1901, 1879 and 1852 were digitised from historical charts using ArcMap Version 9.2. The bathymetries for each year between 1852 and 1954 were created using three different charts (Fig. 3.1). The first chart, a fair sheet for appropriate year (1954, 1927, 1901, 1879 or 1852), covered the tidal delta system and the surrounding channels. Every point from each fair sheet was digitised to help ensure the resulting grid represented 'reality' as accurately as possible, as an accurate bathymetry is necessary for realistic simulation of currents (Black, 2002; Moure et al., 2004). Corrections in the charts, such as the 0.16 foot difference in the 1954 chart, was incorporated into the bathymetric data. The second chart, sounded by the former Bay of Plenty Harbour Board

Engineering Staff in 1960 and 1961, was used for the areas surrounding the first chart up to Omokoroa on the western side, and Matapihi on the eastern side of the harbour. The third chart used was a Royal New Zealand Navy Hydrographic chart of Tauranga Harbour (NZ5411) which covered the remaining areas of the bathymetry – namely, the area offshore from the ebb tidal delta (surveyed in 1960), the southern part of the southern basin (originally surveyed in 1954) and the area west of Omokoroa (originally surveyed in 1961). It is assumed that geomorphic change outside of the tidal delta system and dredged has not been significant. All the bathymetric data (1852 – 2006) was reduced to chart datum and was converted to New Zealand Map Grid. Further details about accuracy of hydrographic charts is found in Appendix 1.

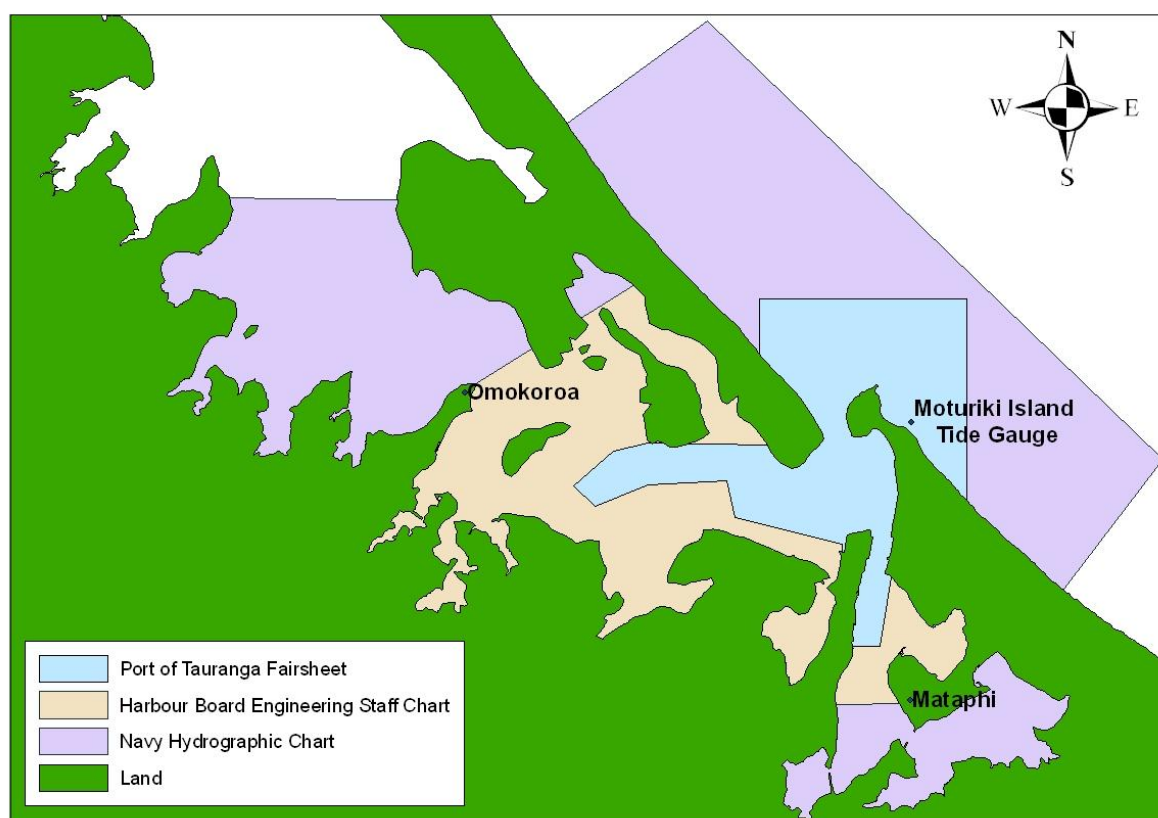


Fig 3.1. Guide to the extent of the charts used to create the bathymetry for hydrodynamic numerical modelling for 1954, 1927, 1901, 1879, 1852.

All the bathymetries were rotated 135° in 3DD and were gridded using Surfer with a search radius of 5000 m to produce a 55 m grid. Smaller search radii were initially used but were found to produce a number of artificial gridding artefacts in the resulting bathymetry and were rejected in favour of the current search radius.

3.1.1 Cross Section

Blanking files were created in the computer software Surfer to ensure that the same profile lines were used in each year (detailed information about the process can be found under the “Creating Cross Section Data” in the Surfer help menu). The resulting cross section text file was then imported into Microsoft Excel where the cross sections were displayed.

3.2 RESULTS

The bathymetric configurations for 1852, 1879, 1901, 1927, 1954 and 2006 is provided in Figures 3.2 – 3.7. All the listed depths in this study are in relation to Port of Tauranga chart datum (e.g. an 11 m depth means 11 m below chart datum).

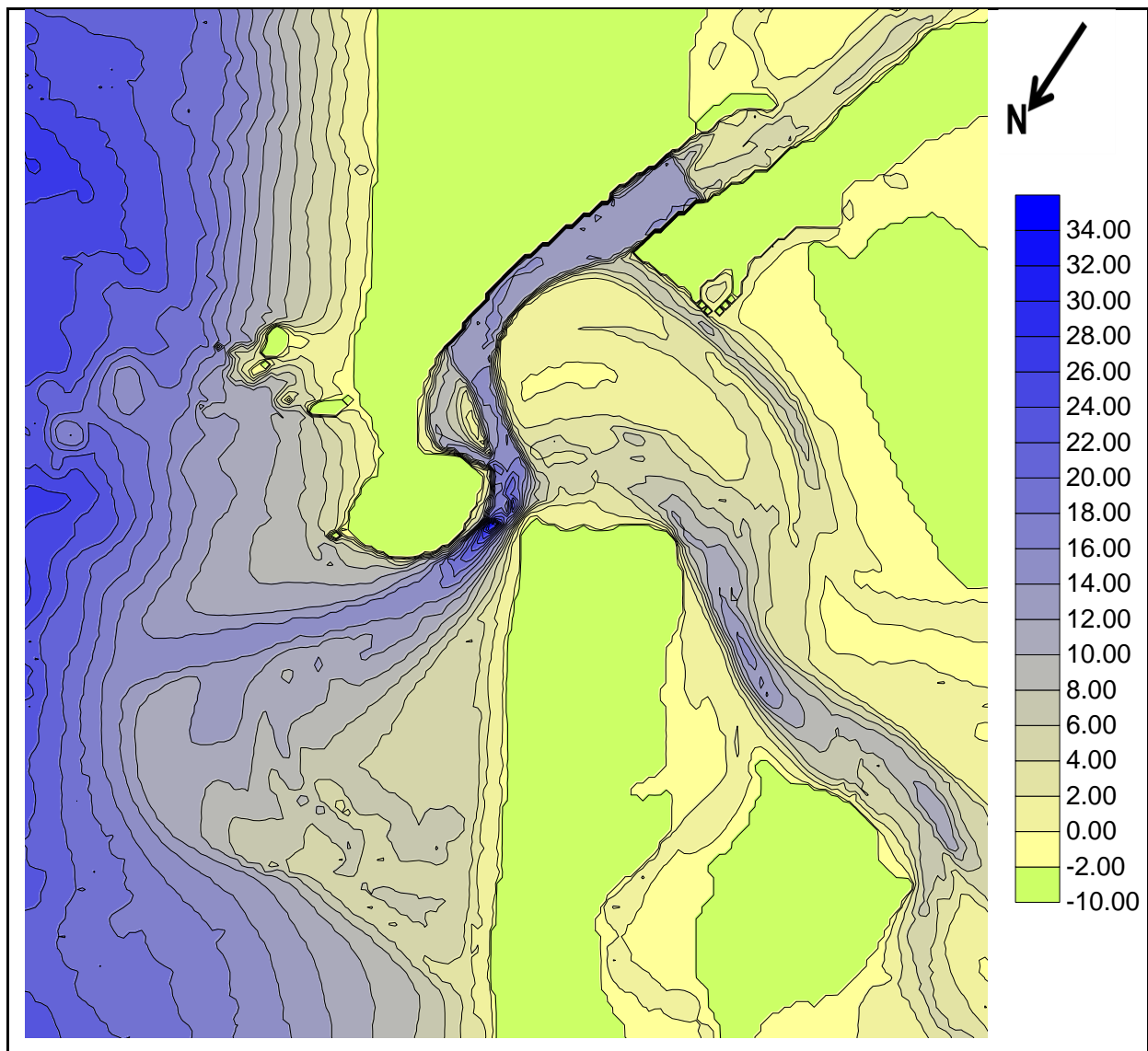


Fig 3.2. 2006 bathymetry of Tauranga Entrance tidal delta system with depths in metres on the accompanying scale.

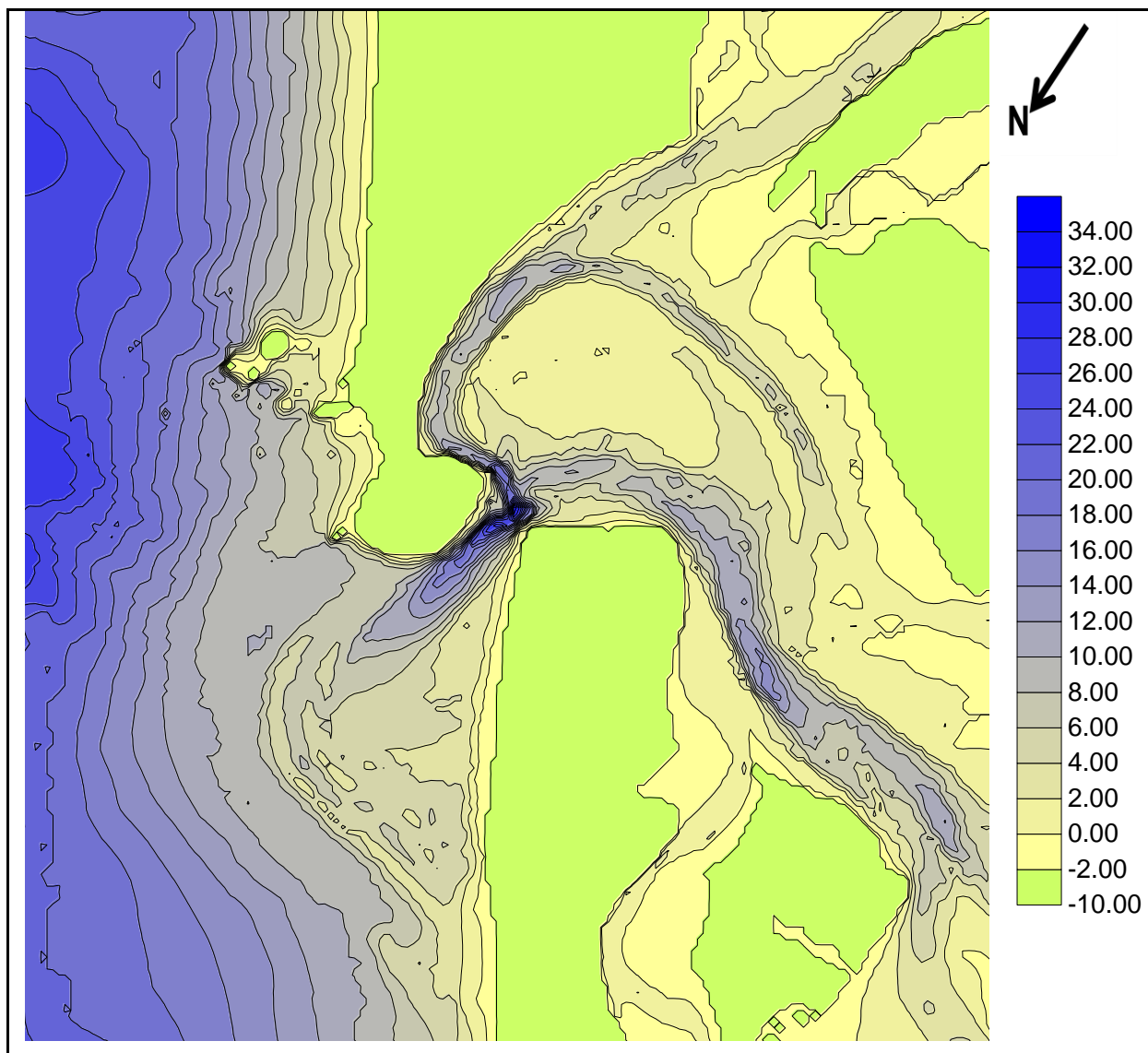


Fig 3.3. 1954 bathymetry of Tauranga Entrance tidal delta system with depths in metres on the accompanying scale.

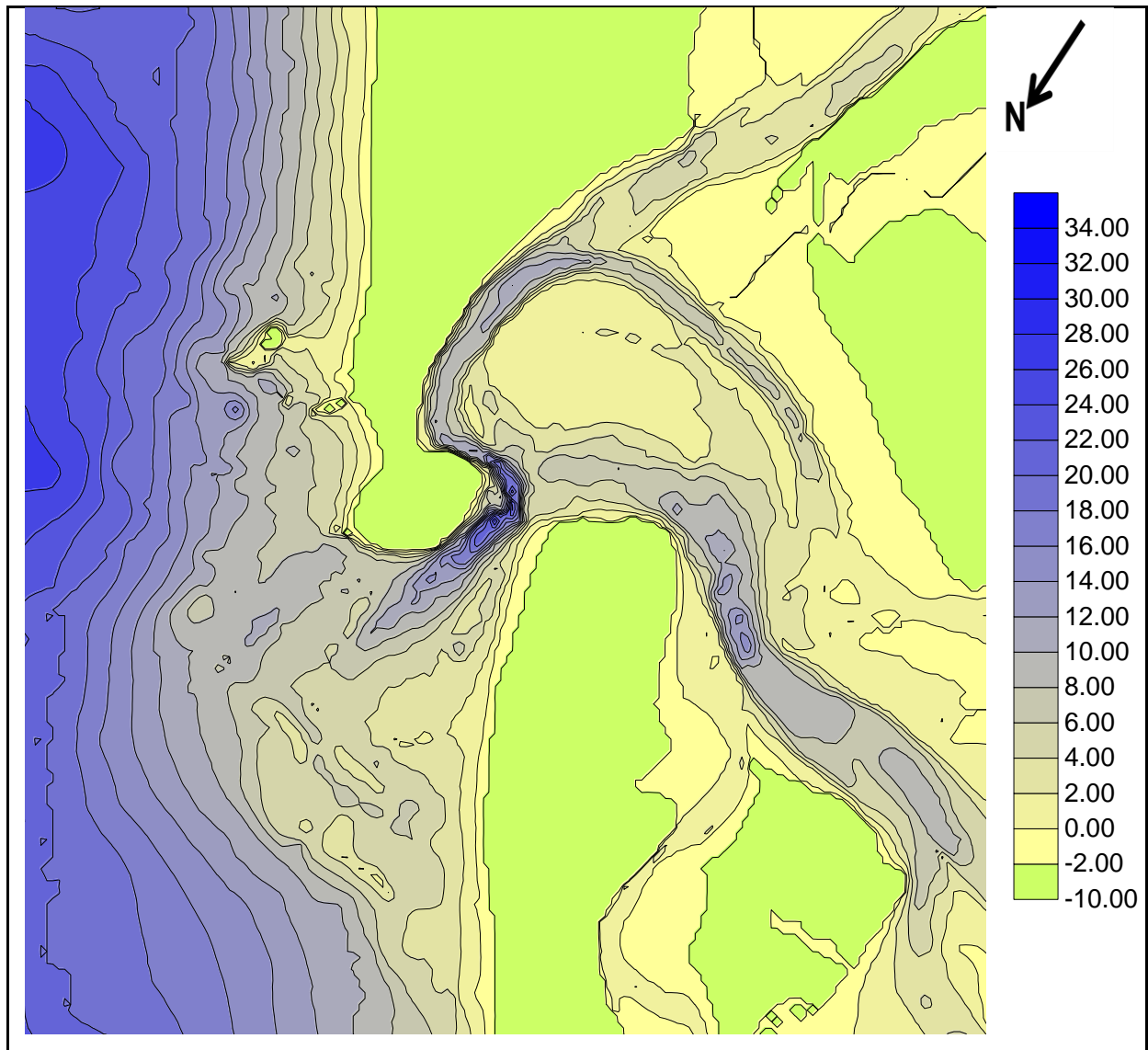


Fig 3.4. 1927 bathymetry of Tauranga Entrance tidal delta system

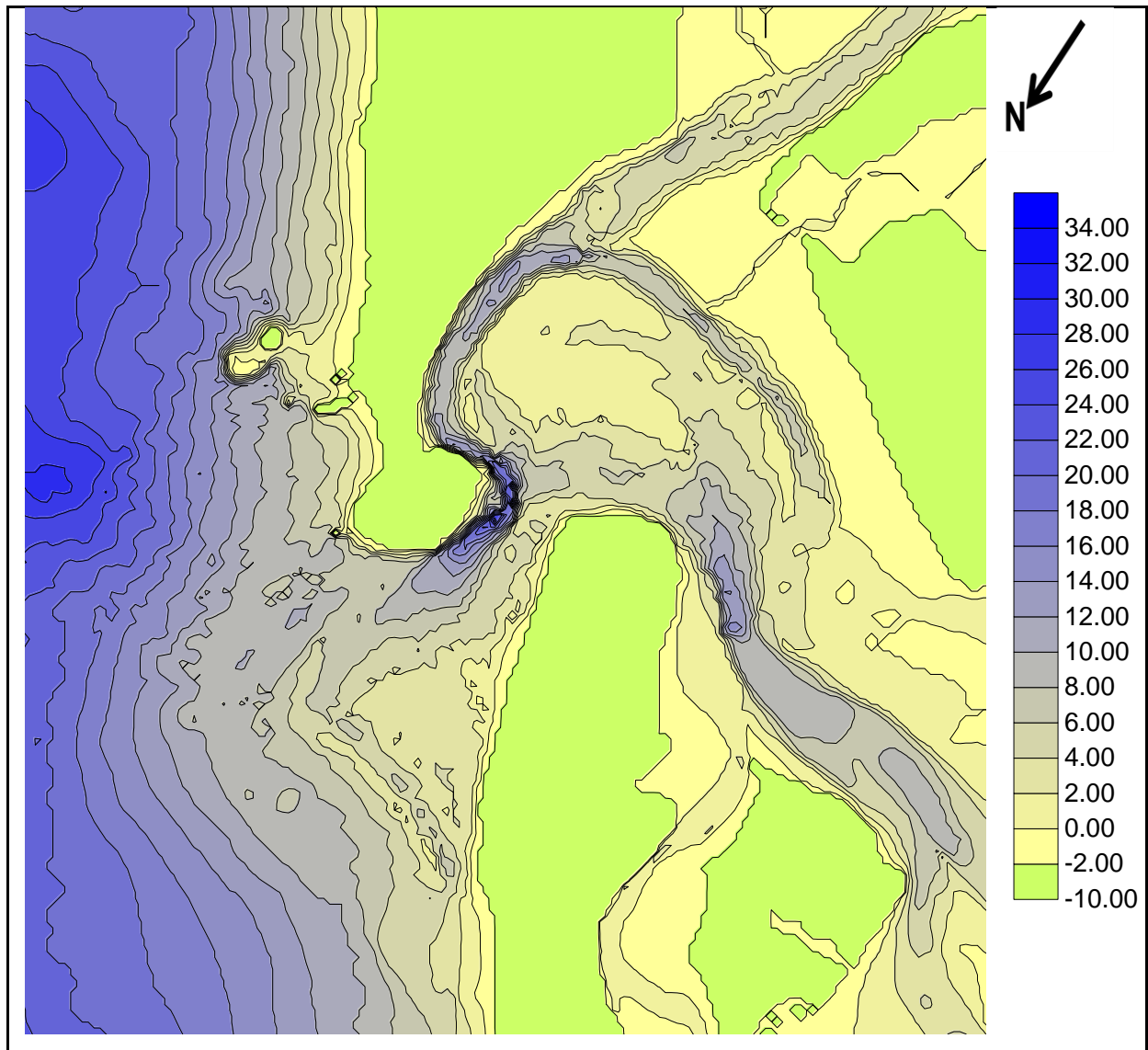


Fig 3.5. 1901 bathymetry of Tauranga Entrance tidal delta system

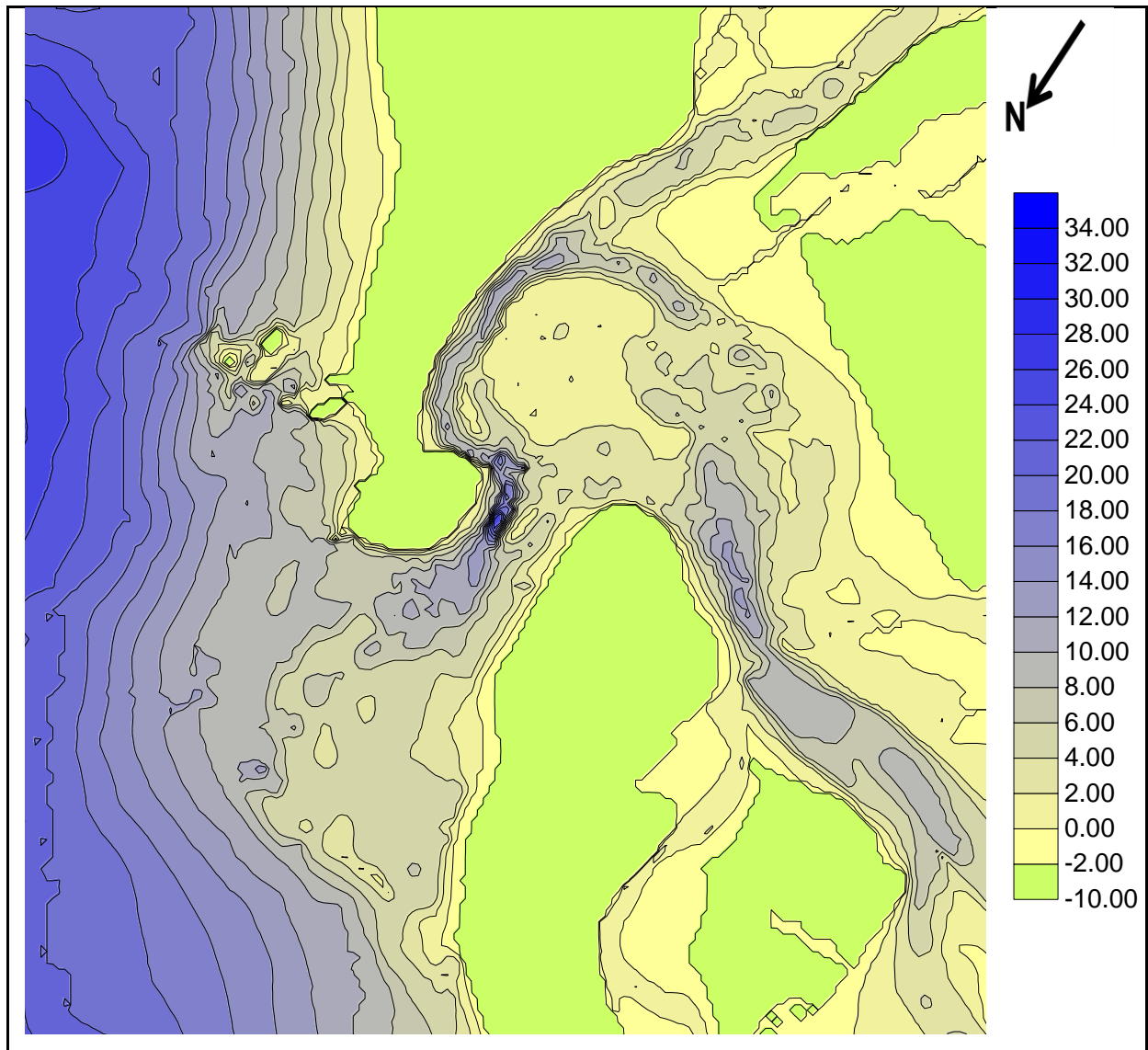


Fig 3.6. 1879 bathymetry of Tauranga Entrance tidal delta system

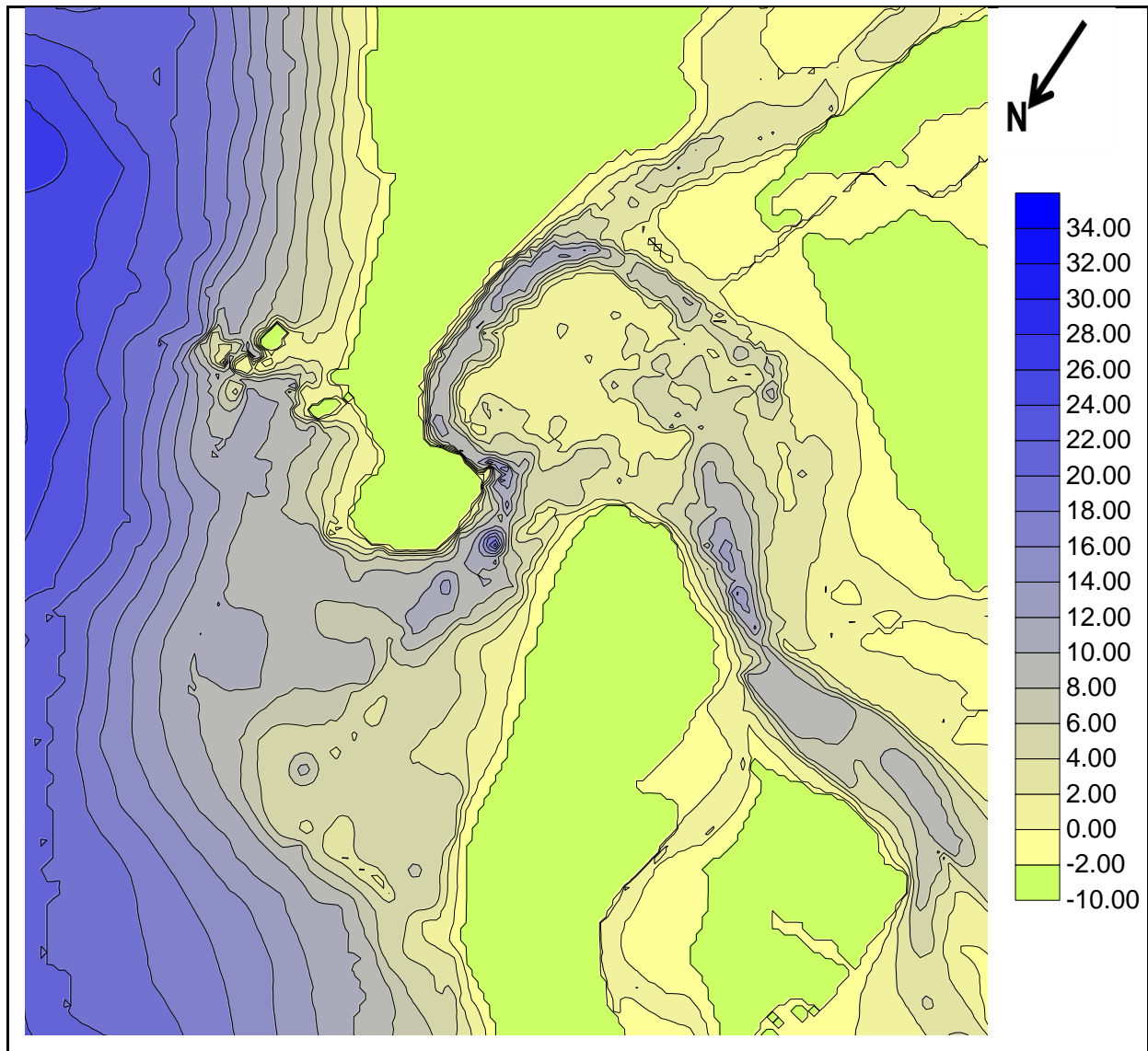


Fig 3.7. 1852 bathymetry of Tauranga Entrance tidal delta system

3.2 BATHYMETRY RESULTS

The following figures show changes in bathymetry, where red indicates areas of increased depths due to erosion scour or dredging while blue indicates areas of accretion. The isolated areas (less than 200 m wide) of erosion and accretion indicated north-east of Moturiki Island (near Mototau Island) are to be interpreted with caution as there is significant variation in the way different hydrographic charts have mapped the rocks in this area, resulting in what falsely looks like significant variation in bathymetry. Change from land to sea is always shown as a change of 10 m even when it is less than that. In the discussion following the major changes identified in the sequence of historical bathymetries are presented.

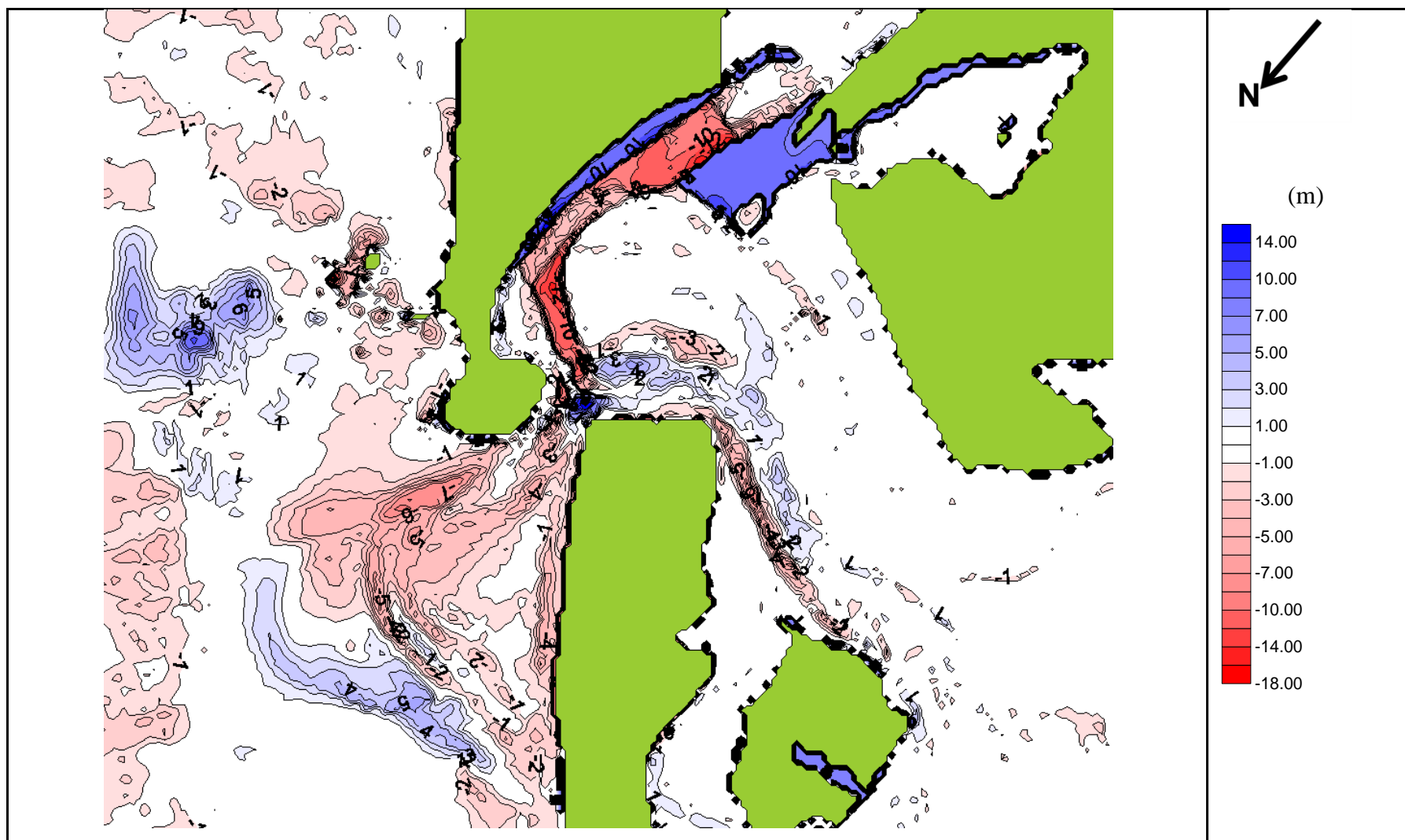


Fig.3.8 :Bathymetric changes between 2006 and 1954. Blue indicates areas of accretion while red indicates areas of erosion. Scale is set to metres.

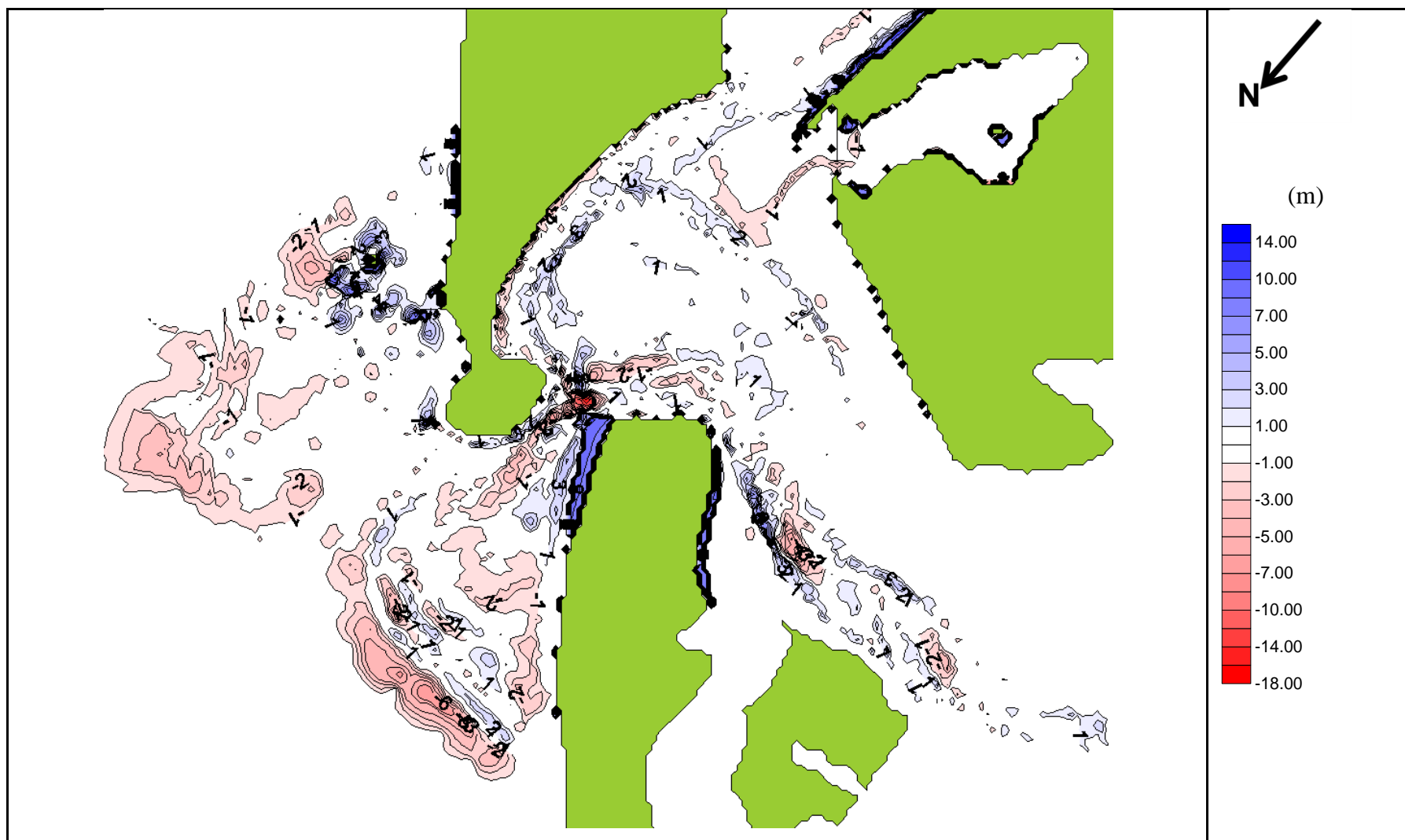


Fig.3.9 :Bathymetric changes between 1954 and 1927. Blue indicates areas of accretion while red indicates areas of erosion. Scale is set to metres.

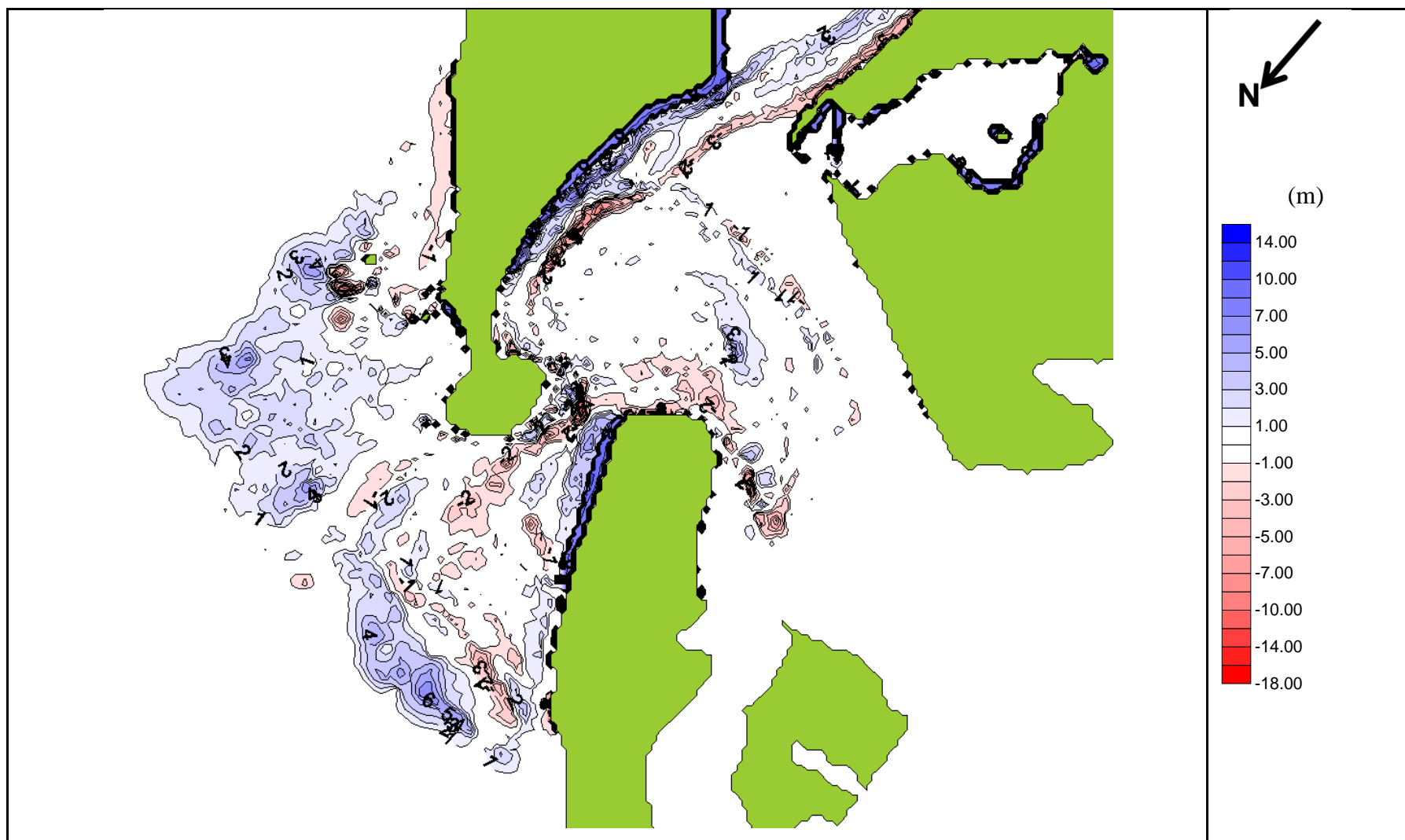


Fig.3.10 :Bathymetric changes between 1927 and 1901. Blue indicates areas of accretion while red indicates areas of erosion. Scale is set to metres.

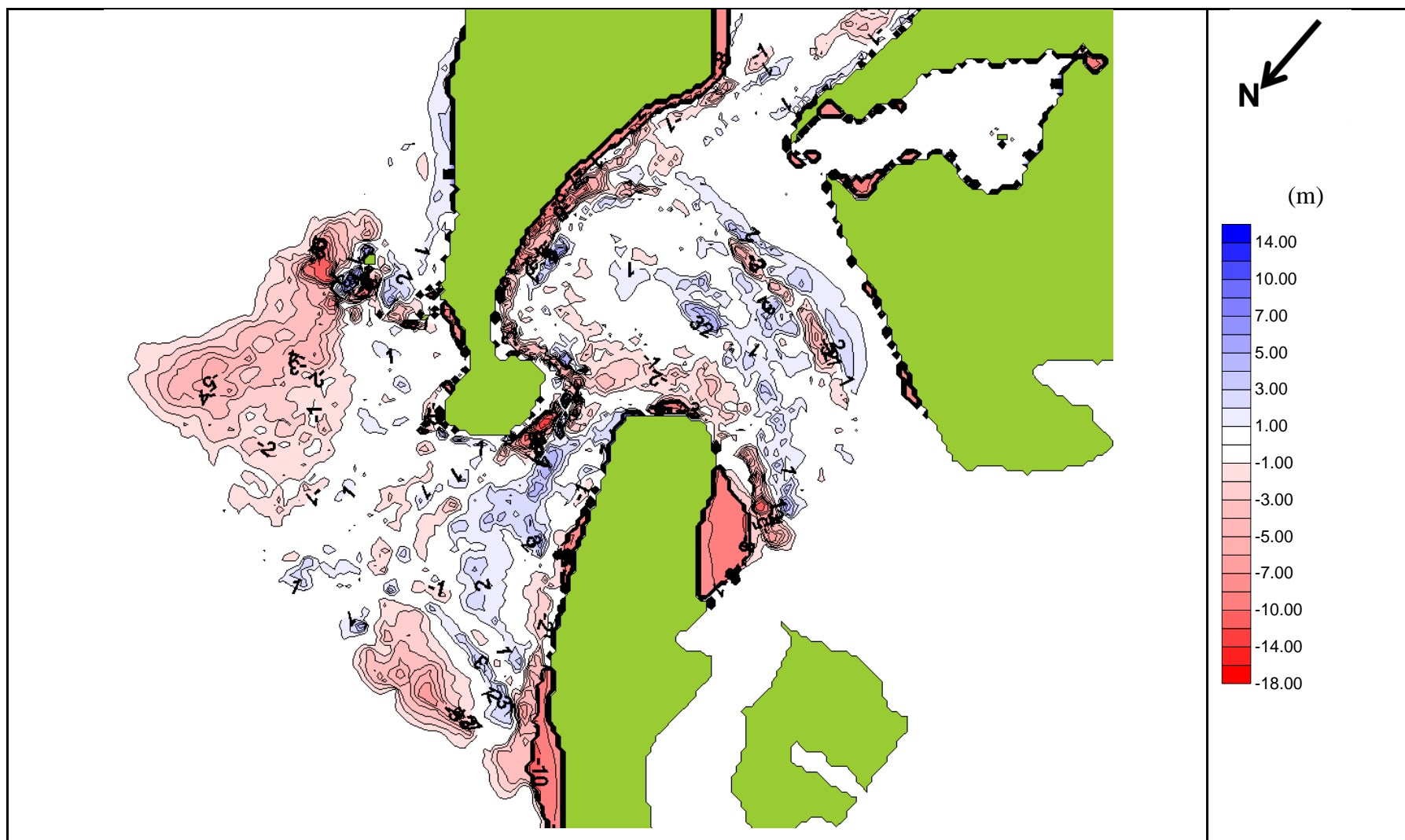


Fig.3.11 :Bathymetric changes between 1901 and 1879. Blue indicates areas of accretion while red indicates areas of erosion. Scale is set to metres.

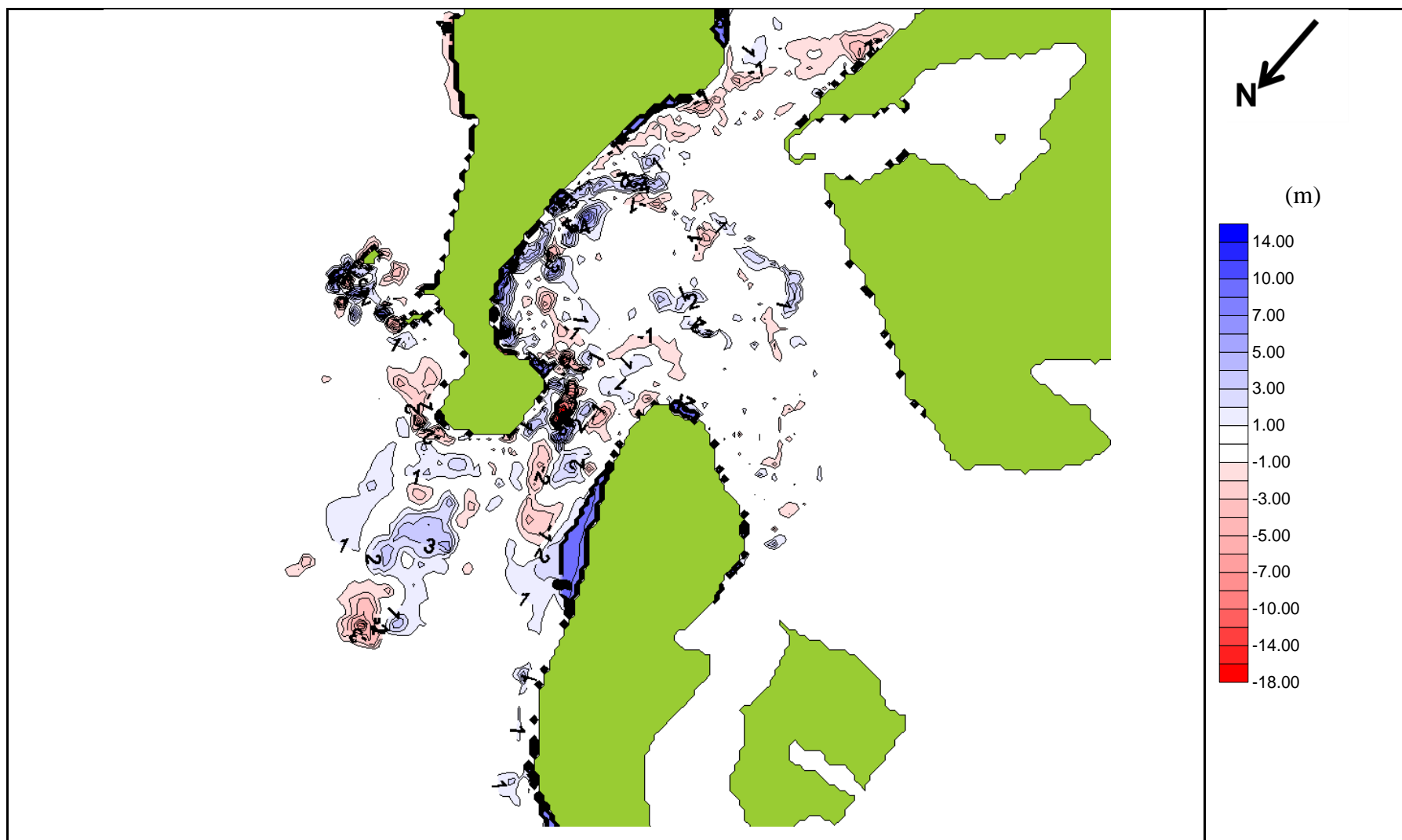


Fig.3.12 :Bathymetric changes between 1879 and 1852. Blue indicates areas of accretion while red indicates areas of erosion. Scale is set to metres.

3.2.1 Changes in bathymetry of Tauranga Harbour 1954 – 2006.

The 1954 bathymetry represents the harbour prior to intervention by dredging, while the 2006 bathymetry is the recent post-dredging situation. Wide spread geomorphic changes are apparent on the ebb tidal delta, while the geomorphic changes on flood tidal delta are primarily limited to the channel surrounding the flood tidal delta.

Between 1954 and 2006 the bathymetry shows the following changes (Fig. 3.8.): The terminal lobe shows shoaling of about 2 – 5 m. Arc shaped features on the swash platform (swash bars) have deepened 3 – 5 m. The Entrance Channel shows deepening of about 7 - 8 m due to dredging. Immediately offshore from Panepane Point there has been shoaling of 12 – 14 m over an area of about 200 – 300 m wide. There is also evidence of shoaling of about 3 - 5 m in the Lower Western Channel, also reported by Dahm (1983). An area on the south-western part of the Centre Bank flood tidal delta, bordering the Lower Western Channel has shoaled about 3 m. There is a long thin band about 150 m wide extending westwards from the southern most part of Matakana Island which indicates shoaling of about 5 m.

Dredging of the Cutter Channel, part of the Maunganui Roads Channel and Stella Passage has resulted in deepening of approximately 10 m. The northern part of the Maunganui Roads Channel has deepened by approximately 4 m due to dredging.

3.2.2 Changes in bathymetry of Tauranga Harbour 1927 - 1954

The ebb tidal delta bathymetry shows considerable changes in geomorphology between 1927 and 1954 on the outer edges near the terminal lobe (Fig. 3.9). On the western side there is scour of up to 6 m, with erosion extending from near the shore to the centre of the ebb tidal delta. Immediately inshore there is a thin line of accretion of up to 2 m, while further inshore there is a similar pattern of accretion and erosion. A large part of the western swash platform and main ebb channel shows erosion of 1 - 2 m. The shore of Matakana Island near Panepane Point on the open ocean side shows marked progradation leading to a reduction in the width of the inlet gorge accompanied by accretion of up to 3 m immediately offshore from this area. A large part of the eastern side of the ETD shows erosion of over 1 m, particularly the outer edges. The centre of the inlet gorge shows an isolated patch of erosion of up to 12 m.

Between 1927 and 1954 the flood tidal delta bathymetry shows changes in geomorphology, primarily in the channels surrounding the FTD, with the shallow central regions showing very little geomorphic change exceeding 1 m. The bathymetry change of Pilot Bay and Maunganui Roads Channel indicates scour of over 1 m on the eastern side of the banks while on the western side there is accretion of 1 - 2 m. This accretion continues around the sides of the FTD into the Otumoetai Channel area. The Lower Western Channel shows erosion of 1 - 2 m near the flood ramp while further up the channel there is a patch of accretion of 1 m near the western edge of Centre Bank. West of Matakana Island the Western Channel bathymetry shows accretion of up to 6 m on the northern edge the channel and erosion of up to 4 m on the southern edge.

3.2.3 Changes in bathymetry of Tauranga Harbour 1901 - 1927

Between 1901 and 1927 widespread changes in bathymetry were apparent on the ebb tidal delta while on the flood tidal delta bathymetric changes were much more limited (Fig. 3.10).

On the eastern ebb tidal delta there is accretion of 1 to 4 m. Accretion on the western side of the ebb tidal delta is less widespread than the east, and is mainly limited to the outer edges near the terminal lobe, where there was accretion up to 6 m. Immediately inshore there is a series of patches of erosion scour of up to 3 m. The main ebb channel shows erosion extending from the inlet gorge to approximately 2 km offshore. The southern tip of the open ocean coast of Matakana Island shows progradation. An area offshore from the southern tip of the open ocean coast of Matakana Island shows shoaling of 3 m.

The centre of the flood tidal delta shows limited bathymetric changes with geomorphic variability primarily limited to surrounding channels. The Lower Western Channel exhibits erosion of about 1 - 2 m extending from the tidal inlet gorge and increasing in extent and depth further up the harbour. The Maunganui Roads Channel bathymetry indicates erosion of about 3 m on the edge of Centre Bank while on the eastern side accretion is present. This pattern of erosion on the western side and accretion on the eastern side of the Maunganui Roads Channel continues into the Stella Passage. Isolated patches of minor (~ 1 m) erosion and accretion are present in the Otumoetai Channel with accretion primarily on the northern side while erosion was primarily on the southern side. The western part of the Centre Bank has eroded 1 – 4 m.

3.2.4. Changes in bathymetry of Tauranga Harbour 1879 - 1901

A bathymetric comparison of 1901 and 1927 shows widespread bathymetric changes over both the ebb and flood tidal delta system (Fig. 3.11).

Between 1879 and 1901 there is widespread accretion of 1 – 6 m east of the Entrance Channel. West of the Entrance Channel near the terminal lobe there is accretion of up to 5 m while closer to the inlet gorge the ebb tidal delta shows erosion of 1 – 4 m. On the eastern side of the inlet gorge there is erosion, which continues through Pilot Bay and down the eastern side of the Maunganui Roads Channel. The flood ramp and Lower Western Channel bathymetries indicated erosion of about 1 – 2 m. The western and central parts of Centre Bank show erosion of about 1 m. The southern part of Centre Bank / northern part of Otumoetai Channel shows a band of erosion while further southern part of the Otumoetai Channel shows accretion of 1 – 2 m.

3.2.5 Changes in bathymetry of Tauranga Harbour 1852 - 1879

A bathymetric comparison of 1852 and 1879 shows widespread bathymetric changes over the ebb and flood tidal delta system (Fig. 3.12).

Near the terminal lobe there is a isolated area of erosion of up to 3 m, while inshore of this feature there has been accretion of up to 3 m between 1852 and 1879. The Matakana Island shoreline on the open ocean side has accreted. West of Mt Maunganui in the Entrance Channel there is an area of erosion of up to 2 m, while the centre of the inlet gorge shows both patches of erosion and accretion exceeding 3 m. The Maunganui Roads Channel shows accretion in a series of isolated spots on the western and eastern sides of up to 4 m interspersed with the occasional patch of erosion of up to 4 m. The flood ramp shows both patches of erosion and accretion of around 1 m. The Western part of the Centre Bank FTD shows both erosion and accretion of around 1 – 2 m.

3.3 VARIATION OF HISTORICAL SEQUENCE RESULTS

The localities for the cross sections were chosen based upon the areas which consistently demonstrated the most change in bird's eye view map of bathymetric change. The localities of the cross section within the harbour, overlain on the 1954 Tauranga Harbour bathymetry is shown in Figure (Fig. 3.13).

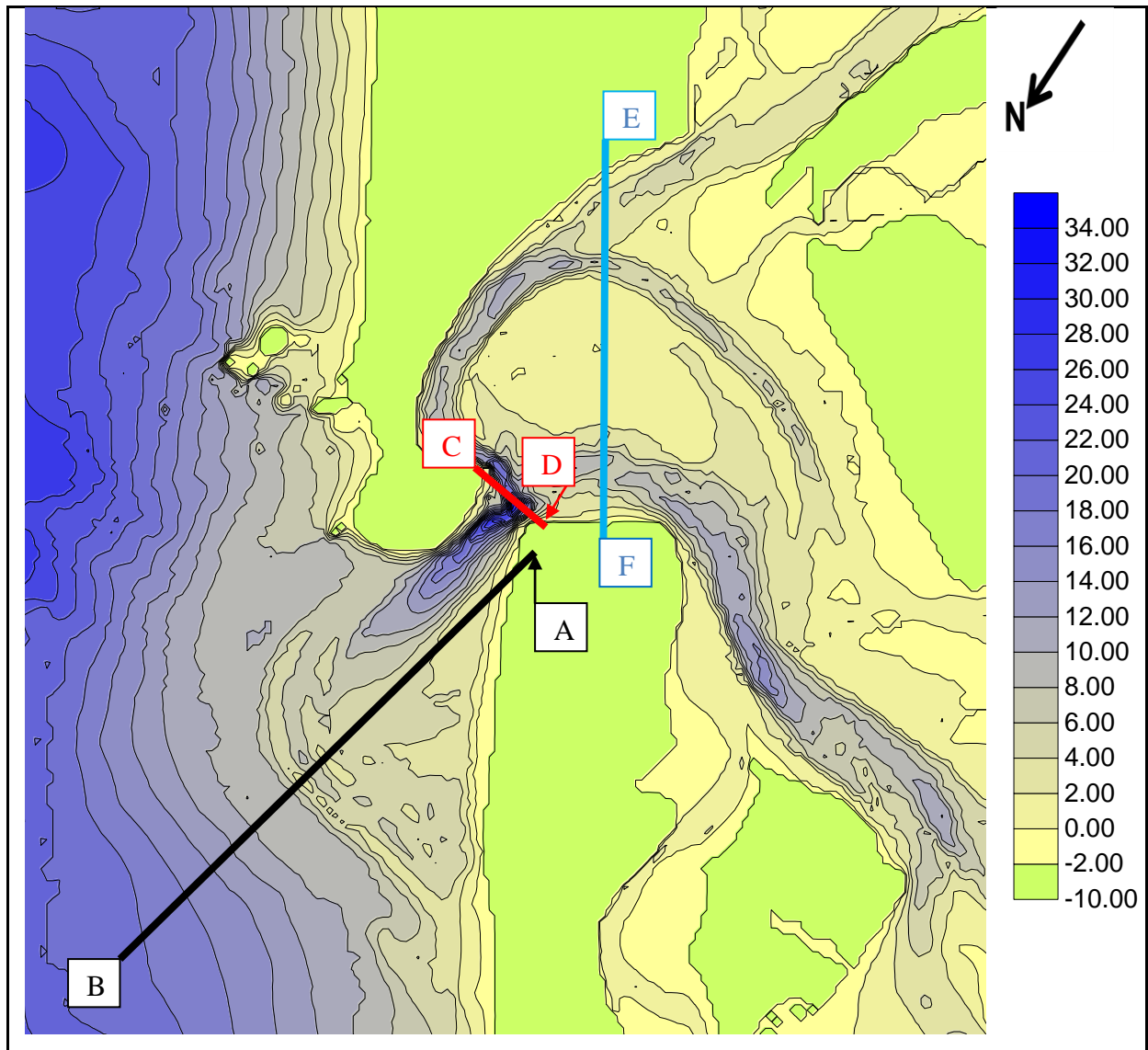


Fig 3.13: Map detailing locations of cross section in tidal delta system, overlaid on the 1954 bathymetry. Black is the ebb tidal delta cross section, red is the tidal inlet gorge cross section and blue is the flood tidal delta cross section

3.3.1. Ebb tidal delta variation in cross section 1852 - 2006



Fig 3.14: Cross sections of Tauranga ebb tidal delta from Matakana Island (A) northwards to the open ocean (B) comparing bathymetries from 1852 – 2006.

The major changes in the cross sections of the ebb tidal delta from Matakana Island near Panepane Point (left side of plot) to down the axis of the ebb tidal delta to the open ocean (right side of plot) between 1852 and 2006 (Fig 3.14.) are as follows:

(i) In 1852 the profile descends to a depth of over 8 m at horizontal distance of nearly 800 m. The profile then rises to a depth of about 3 m at a horizontal distance of about 2500 m from Matakana Island. Two swash bars have a height of 1 and 2 m and each having a horizontal distance of about 200 m .

(ii) In 1879 the profile drops from near CD down to a depth of nearly 8 m at a horizontal distance of about 1200 m. The profile then rises to a depth of over 4 m at a horizontal distance of 2000 m. Further northwards the profile rises to the first swash bar which is over 1 m high with a horizontal distance of 400 m, then a second swash bar which is about 2 m high with a horizontal distance of 400 m. The tidal inlet side of both swash bars is steeper than the open ocean side.

(iii) In 1901 the shoreline (CD) is about 200 m north of the 1852 shoreline. The profile drops to a depth of over 5 m at a horizontal distance of 1100 m. The profile then rises to a depth of about 2.5 m at a horizontal distance of 2300 m. Northwards the profile then drops and rises to form a large swash bar of about 3 m elevation with a horizontal distance of about 300 m.

(iv) In 1927 the shoreline (CD) begins about 1100 m north of the 1852 profile shoreline. The profile drops to 4 m below CD over a horizontal distance of 300 m and then fluctuates around the 4 m depth mark for a horizontal distance of about 1700 m. The profile then drops and rises to form a prominent swash bar feature with an elevation of approximately 1.5 m and a horizontal distance of 300 m. The profile then drops and rises to form the terminal lobe.

(v) The 1954 profile shoreline begins 800 m north of the 1852 profile. The profile drops to about 5 m depth at a horizontal distance of 2000 m. The profile fluctuates around this depth for a horizontal distance of about 700 m. The profile continues northwards dropping then rising to form a swash that has a height of about over 2 m and then an even higher terminal lobe feature which reaches a depth of 3 m before dropping.

(vi) The 2006 profile shoreline begins 600 m northwards of the 1852 profile. From the shoreline (CD), the profile extends northwards dropping to a depth roughly 7 m at a horizontal distance of about 2000 m. From here, it continues northwards at a more or less a constant depth of 7 m for a horizontal distance of 1400 m. Swash bar features of about 1 m

height and 300 wide are present between 3100 and 3700 m on the horizontal distance scale before dropping to a terminal lobe at 4300 m.

3.3.1.1. Summary of geomorphic change of ebb tidal delta.

The major points to note when examining the geomorphic changes in the ebb tidal delta are:

(i) The location of the shoreline on the profiles varies by 800 m on the horizontal distance scale. The horizontal location of the shoreline on the post dredging 2006 profile is neither the highest or the lowest, and is very close to the 1927 profile. This suggests that dredging is not having a significant effect on the shoreline location on this cross section.

(ii) All profiles show some swash bar features. The post dredging 2006 profile shows swash bars that are in a noticeably different location than the swash bars on the pre-dredging profiles (1852 – 1954), being both deeper (at least 2 m) and further offshore (at least 100 m). This suggests that dredging may be affecting the swash bar features.

(iii) The swash platform of the post-dredging 2006 profile is considerably deeper (about 2 m) than the pre-dredging profiles of 1852 to 1954. This suggests that dredging is having an effect on the depth of the swash platform.

3.3.2 Tidal inlet gorge variation in cross section 1852 - 2006

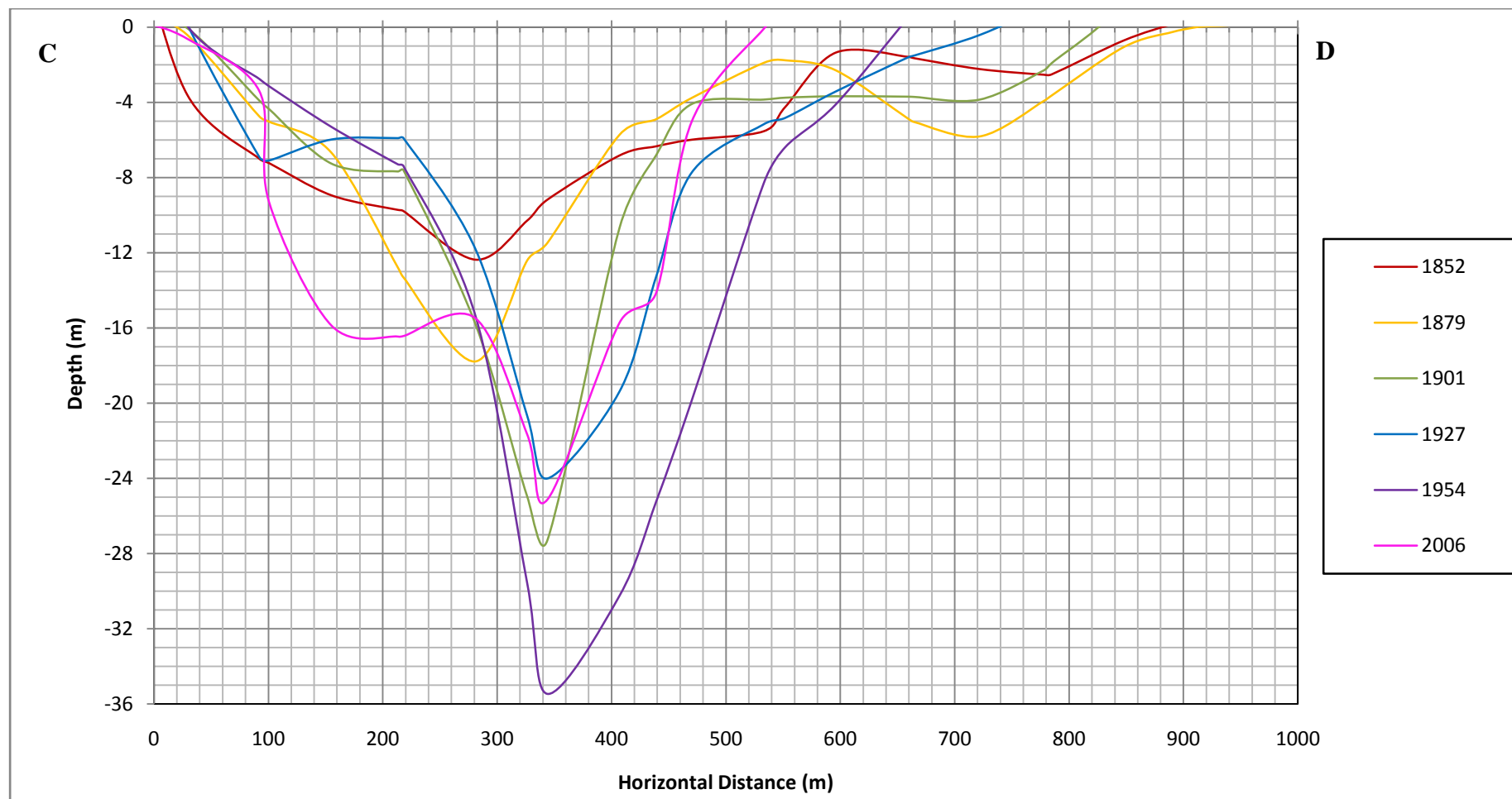


Fig 3.15.: Cross sections of Tauranga tidal inlet gorge from Mt Maunganui (C) to Matakana Island (D) comparing six bathymetries dated 1852, 1879, 1901, 1927, 1954 and 2006. Note the extensive inlet narrowing (by over 360 m) between 1879 and 2006, and channel deepening from ~ 12m in 1852 to ~ 35m in 1954.

The major changes in the cross sections of the tidal inlet gorge between Mt Maunganui (C) and Matakana Island (D), near Panepane Point between 1852 and 2006 (Fig 3.15.) are as follows:

(i) The 1852 profile is one of the widest and the shallowest inlet gorge cross sections being nearly 880 m wide and reaching a maximum depth of just over 12 m at a horizontal distance of 280 m. A channel margin linear bar feature at a horizontal distance of 600 m has a depth of just over 1 m. The deepest part of the channel is very close to the Mt Maunganui side (A).

(ii) The 1879 profile is about as wide as the 1852 profile at about 890 m but reaches a greater maximum depth of nearly 18 m at a horizontal distance of 280 m. A channel margin linear bar feature is shown to rise to a depth of about 2 m at a horizontal distance of 540 m. The profile then drops to a depth of nearly 6 m at a horizontal distance of 720 m.

(iii) The 1901 profile is narrower and deeper than the 1852 and 1879 tidal inlet gorge profiles, being 820 m wide and reaching a maximum depth of over 27 m at a horizontal distance of 340 m. This indicates that the central part of the tidal inlet gorge has moved about 300 m westwards since 1852 and 1879. The channel has a small platform feature on the eastern side, which extends for about 60 m at a depth of just less than 8 m. A more prominent platform is found on the western side, extending horizontally for over 220 m at a depth of just above 4 m.

(iv) The 1927 profile is narrower than the 1852, 1879, and 1901 tidal inlet gorge profiles being about 700 m wide. It reaches a maximum depth of about 24 m at a horizontal distance of 340 m. There is a prominent platform feature on the eastern side being over 100 m wide and ranging in depth between 6 and 7 m.

(v) The 1954 profile is narrower than the 1852, 1879, 1901, and 1927 profiles being about 620 m wide. The profile reaches the greatest maximum depth of all the profiles at over 35 m at a horizontal distance of just over 340 m.

(vi) The 2006 profile is the narrowest of all the tidal inlet gorge profiles being 520 m wide. The profile reaches a maximum depth of over 25 m at a horizontal distance of 340 m. A prominent platform occurs at a depth of about 16 m and has a horizontal width of about 120 m.

3.3.2.1. Summary of geomorphic change of tidal inlet gorge.

The major points to note when examining the geomorphic changes in the tidal inlet gorge are:

(i) The inlet gorge shows a progressive narrowing between 1879 and 2006. The magnitude and direction of natural changes in inlet gorge width prior to dredging (between the bathymetries of 1879, 1901, 1927 and 1954) is consistent with the changes in tidal inlet gorge width occurring post dredging (1954 – 2006) indicating that dredging is having a minimal effect on tidal inlet gorge width.

(ii) The maximum depths of the inlet gorge along this cross section between 1852 and 2006 range between about 12 and 35 m. The post dredging profile of 2006 has a maximum depth of about 25 m and there are two un-dredged profiles (1901 and 1954) which have deeper maximum depths and three un-dredged profiles (1852, 1879, and 1927) which have shallower maximum depths. This indicates that dredging is not having a significant effect on the maximum depth of the inlet gorge.

(iii) Three profiles (1901, 1927, and 2006) have a prominent platform feature on the eastern side of the tidal inlet gorge profile. While the un-dredged profiles of 1901 and 1927 have a prominent profile, the profile of 2006 shows a much deeper profile (~8m deeper) suggesting that dredging may be having an effect on the depth of the tidal inlet gorge eastern platform.

(iii) On the eastern side of the profile near 'A' the cross section in 2006 shows a deepened platform feature at a depth of about 16 m with a length of approximately 120 m. This feature can be linked to the dredging of the Tanea shelf.

3.3.3. Flood tidal delta variation in cross section 1852 - 2006

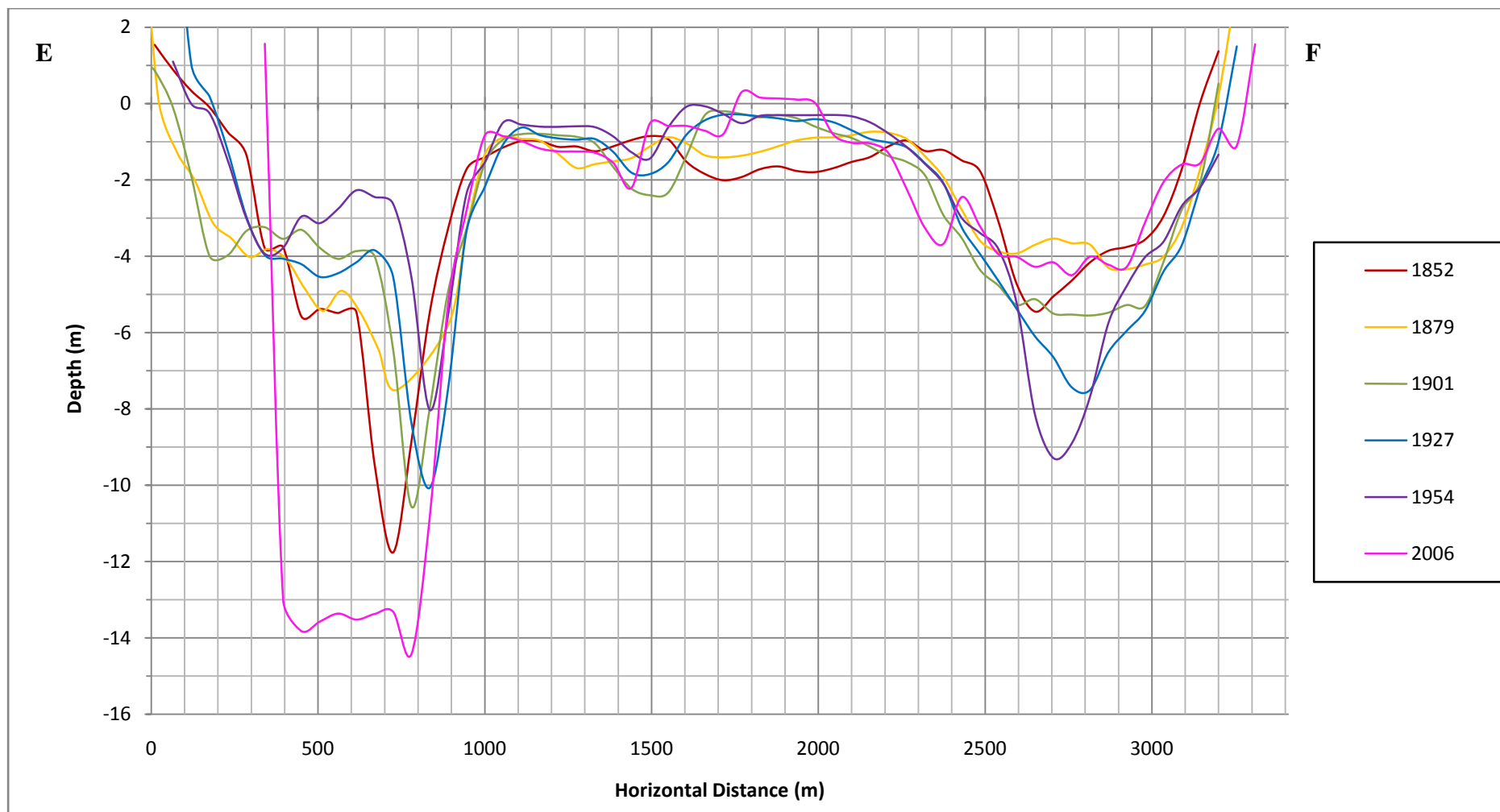


Fig 3.16: Cross sections of Tauranga flood tidal delta from Maunganui Roads Channel (E) to Matakana Island (F) comparing six bathymetries dated 1852, 1879, 1901, 1927, 1954 and 2006.

The major changes in the cross sections of the flood tidal from the southern part of Maunganui Roads Channel (E) to Matakana Island (F) between 1852 and 2006 (Fig 3.16.) are as follows:

(i) In 1852 the Maunganui Roads Channel reaches its greatest depth of nearly 12 m at a horizontal distance of about 700 m from the Maunganui Roads Channel shore. The ebb shield at the western edge of the Maunganui Roads Channel/ eastern edge of the Centre Bank flood tidal delta begins at a horizontal distance of about 1100 m away from the shore. The Centre Bank extends horizontally (towards the Lower Western Channel) for about 1300 m ranging at depths between about 1 to 2 m. The Lower Western Channel reaches a depth of just over 5 m at a horizontal distance of over 2650 m. The Matakana Island shoreline is at a horizontal distance of over 3100 m.

(ii) In 1879 the Maunganui Roads Channel the maximum depth is about 7 m at a horizontal distance of 700 m, indicating that this channel in this location has shoaled about 5 m since 1852. The ebb shield at the eastern side of the Centre Bank begins at a horizontal distance of about 1000 m, similar to 1852. The Centre Bank flood tidal delta extends horizontally towards the Lower Western Channel for about 1300 m, ranging in depths between about 1 to 2 m. The Lower Western Channel is both wider and shallower than it was in 1852 reaching a maximum depth of over 4 m at a horizontal distance of 2800 m.

(iii) The 1901 Maunganui Roads channel has a prominent step like feature beginning at a horizontal distance of just under 200 m from 'E' and ranging between depths of about 3 – 4 m for horizontal distance of about 500 m. The channel then reaches its maximum depth of about 11 m at horizontal distance of just under 800 m. The ebb shield at the eastern side of Centre Bank flood tidal delta, like in 1852 and 1879, begins at about 1000 m. The channel between the ebb shields, which has a maximum depth of over 2 m, is at a horizontal distance of 1500 m. The Centre Bank extends horizontally for about 1300 m, similar to 1879. The depth varies across the Centre Bank flood tidal delta ranging between just under 0 m (chart datum) to just over 2 m. This variation in depth is greater than both the 1852 and 1879 cross sections. The Lower Western Channel reaches a depth of about 5.5 m, similar to 1852, but unlike 1852 the channel continues this

depth for about 400 m. The Matakana shoreline is at a horizontal distance of about 3100 m, similar to 1879 but greater than 1852.

(iv) In 1927 the shoreline on the eastern side begins about 100 m further offshore than the 1879 profile. The 1927 profile shows a similar step like feature as the 1901 profile, and has its maximum depth at a horizontal distance of over 800 m. The ebb shield at the eastern part of the Centre Bank flood tidal delta begins at a horizontal distance of about 1000 m, like all the profiles between 1852 and 1901. The channel between the ebb shields has a maximum depth of less than 2 m at a horizontal distance of about 1500 m. The Centre Bank flood tidal delta extends 1300 m, similar to the 1879 profile, and varies between 0 m (chart datum) and 2 m water depth. The Lower Western Channel reaches a maximum depth of about 8 m at a horizontal distance of 2800 m. The Matakana shoreline is at a horizontal distance of about 3200 m.

(v) In 1954 the profile shows a very prominent step feature before reaching a maximum depth of 8 m at a horizontal distance of about 850 m. From 1852 to 1954, there has been a progressive westwards movement in the location of the maximum depth of the Maunganui Roads Channel. The ebb shield at the eastern part of the entrance channel begins at a horizontal distance of about 1000 m. The channel between the ebb shields has a maximum depth of just over 1 m at a horizontal distance of about 1500 m. The Centre Bank flood tidal delta ranges in depth between 0 m and about 1.5 m and extends horizontally for about 1300 m. The Lower Western Channel has a depth considerably lower than the other profiles reaching a maximum of over 9 m at a horizontal distance of over 2700 m.

(vi) The 2006 profile shows marked changes in bathymetry in the Maunganui Roads Channel with maximum depths reaching over 14 m, and the bottom of the dredged channel being over 400 m wide. Despite the change in the Maunganui Roads Channel the ebb shield at the eastern edge of the Centre Bank flood tidal delta is at a similar location to the other profiles having a horizontal distance of about 1000 m. The channel between the ebb shields has a maximum depth of just over 2 m at a horizontal distance of about 1400 m, which is deeper than the channel between the ebb shields in all the other profiles except for the 1901 profile. The Centre Bank flood tidal delta ranges in depths from over 0 m above sea level, (the highest of all the profiles) to over 2m in water depth, which

is not as deep as the 1901 profile.. The Centre Bank flood tidal delta has a horizontal distance of about 1200 m. The Lower Western Channel has a maximum depth of nearly 5 m, similar to the 1879 profile, at a horizontal distance of about 2750 m.

3.3.3.1. Summary of geomorphic change of flood tidal delta.

The major points to note from examining the geomorphic changes in the flood tidal delta are:

(i) The Maunganui Roads Channel shows a progressive westwards shift of about 100 m in the maximum channel depth between 1852 and 1954. The ebb shield at the eastern edge of the flood tidal delta has also varied by about 100 m.

(ii) The most significant change in the flood tidal delta profiles between 1852 and 1954 is the dredging of the Maunganui Roads Channel which has deepened the channel to over 14 m and widened it to over 400 m.

(iii) The 2006 profile shows that Centre Bank flood tidal delta reaches a height of 0.3 m above CD, slightly above the maximum height of the 1954 flood tidal delta. This increase in the height of the Centre Bank flood tidal delta is consistent with an overall trend of increasing height on the Centre Bank flood tidal delta between 1852 and 1954.

(iv) The 2006 profile for the Lower Western Channel is not significantly different to the other pre-dredging profiles (1852 – 1954) with the 1954 profile being deeper with a maximum depth of over 9 m and the 1879 having a similar maximum depth of more than 4 m. However the shoaling of the Lower Western Channel between 1954 and 2006 is consistent with the dredging of the Maunganui Roads Channel which has increased the tidal flow on the eastern side of the harbour and decreased flow on the western side, thus potentially encouraging deposition leading to shoaling in the Lower Western Channel.

(v) The channel between the ebb shields is apparent at around the horizontal distance of 1500 m from 'E' between 1901 and 2006. Between 1901 and 1954 the channel shows progressive shoaling of about 1 m, while in 2006 the maximum channel depth is similar to that of 1901, being just over 2 m.

In summary a comparison of the flood tidal delta cross sections between 1852 and 2006 suggests that the significant dredging effects are largely limited to

the dredged Maunganui Roads Channel with the changes outside of these area's being consistent with changes that have been occurring in the 150 years prior to dredging.

3.3.4 Summary of geomorphic change of the tidal delta system

The geomorphic investigation of the tidal delta system raises the following important points:

(i) In the tidal inlet gorge between 1852 and 2006 there has been a progressive narrowing of the horizontal distance at 0 m chart datum depth. There has also been considerable variation in the maximum depth of the tidal inlet gorge ranging from a depth of about 12 m in 1852 to about 35 m in 1954. The data suggests that dredging is not having a significant effect on tidal inlet gorge width at CD depth as the changes in the tidal inlet gorge width between 1954 (pre-dredging) and 2006 (post-dredging) are consistent with changes occurring between each of the un-dredged bathymetries (1852 – 1954). A comparison of the tidal inlet gorge maximum depth shows that the pre-dredging bathymetries (1852 – 1954) have both deeper and shallower maximum depths suggesting that dredging is not having a significant effect on tidal inlet gorge maximum depth

(ii) In the flood tidal delta between 1852 and 2006 some of the largest changes can be seen in the Maunganui Roads Channel in post-dredging 2006 profile where the channel has been deepened to over 14 m and widened about 400 m. These changes can be clearly linked with dredging of the Maunganui Roads Channel.

(iii) The Centre Bank flood tidal delta between 1852 and 2006 consistently shows a variation in depth of 1 – 2 m fluctuating around the 1 m depth mark. The highest point on 2006 profile is only marginally higher than the 1954 profile, with the 2006 profile showing a maximum height of 0.3 m above CD while the 1954 profile had a maximum height (minimum depth) of 0.1 m below CD along this profile. This indicates that 2006 Centre Bank profile is not significantly different to the pre-dredging profiles of 1852 to 1954.

(iv) The Lower Western Channel does not display significant variation in maximum depth between the pre-dredging (1852 -1954) and post-dredging profile (2006). The maximum depth of 2006 is similar to that of 1879, both being just

over 4 m. There is no significant difference in the width of the Lower Western Channel between pre-dredging (1852 – 1954) and post dredging profiles (2006) with 2006 profile being slightly less wider than 1901 profile but wider than all the other profiles at 1 m water depth. This suggests that dredging is not having a significant on the Lower Western Channel at the location of the profile.

(v) In the ebb tidal delta the 2006 swash platform is generally 2 m deeper than majority of the other profiles swash platform, also the 2006 swash bars are located further northward.

3.4. DISCUSSION

The geomorphology of Tauranga Harbour tidal inlet delta system also was investigated by the Hydraulics Research Station (1963), Dahm (1983), Barnett (1985), Mathew (1997).

3.4.1 Ebb tidal delta

(i) Mathew (1997) ascertained that the ebb tidal delta generally remained stable between 1989 and 1995 (with significant localised changes), this contrasts with the comparison of the 1954 and 2006 ebb tidal delta cross section profile from this study, as most of the ebb tidal delta shows a general difference in depth of about 2 m between 1954 and 2006. This suggests that changes in the ebb tidal delta occurred outside Mathew's (1997) study period.

(ii) The trend of progressive accumulation of the northern edge of the ebb tidal delta recognised by Barnett (1985) has continued with the 2006 northern edge of the ebb tidal delta further northwards than the 1954 profile.

3.4.2 Tidal inlet

(i) The data from this study confirms the over 300 m decrease in tidal inlet width between 1852 and 1954 noted by the Hydraulics Research Station (1963) and Barnett (1985) and furthermore shows that the general trend of decreasing tidal inlet width is continuing up to 2006.

(ii) The data from this study confirms the narrowing of the tidal inlet gorge between 1852 and 1954 by Barnett (1985)

(iii) A shoreline data analysis conducted by Mathew (1997) near Panepane Point indicated that the shoreline did not undergo significant changes due to the 1991-92 dredging. This is not consistent with the result from this study, which shows a shoreline difference of over 100 m between 1954 and 2006. This suggests that the major changes in the shoreline at this location occurred outside Mathew's monitoring period.

3.4.3 Flood tidal delta

(i) The trend of increasing height of the Centre Bank flood tidal delta between 1852 and 1954 noted by Barnett (1985) is apparent in the examination of the flood tidal delta cross section data. Furthermore, the 2006 cross section data shows this trend of increasing height is continuing.

(ii) The constant instability of the Lower Western Channel, as demonstrated by Barnett (1985), is apparent in the examination of the data from this study, with the maximum channel depths from the profile ranging over 5 m between 1852 and 2006.

(iii) Mathews (1997) recognition that the Lower Western Channel shoaled to less than 5 m below CD between 1982 and 1989 is consistent with the 2006 profile, which also shows shoaling of less than 5 m below CD.

(iv) The shoaling of 0.5 m on the Centre Bank flood tidal delta between 1982 and 1995 addressed by Mathew (1997) is consistent with trend of shoaling between 1954 and 2006 that is apparent in the data from this chapter.

3.5. SUMMARY

This chapter investigated large-scale geomorphic variation of the tidal delta system of Tauranga Harbour between 1852 and 2006 in order to assess the effects of dredging. This is the first study to provide comprehensive plots of historical changes in bathymetry from a birds eye view perspective, as previous studies (Barnett, 1985) only provided limited information such as areas of erosion

and accretion with scale of 1 m and 10 m of erosion and accretion. The scale on the plots from this study provide a *series* of 1m contours illustrating erosion and accretion. This provides significantly more information about the extent and coverage of geomorphic change than previous studies.

Finding from this chapter show that significant large scale geomorphic change as a result of dredging is primarily limited to areas immediately surrounding dredged channels. Outside of the dredged channel areas the geomorphic change in the post dredging bathymetry is either within the limits of natural change or continuing a trend which has been occurring naturally.

4. HYDRODYNAMIC NUMERICAL MODELLING OF HISTORICAL BATHYMETRIES OF TAURANGA HARBOUR

4.0 INTRODUCTION

This chapter investigates the effects of dredging on the channels of the tidal delta system and the current regime of the Tauranga entrance to Tauranga Harbour. Existing conditions (2006) are compared to historical changes in hydrodynamics and current flow patterns prior to dredging. This is achieved through conducting two-dimensional hydrodynamic numerical modelling using the 3DD model, and comparing spatial flow patterns as illustrated by the peak flow velocity vector plots and full tidal cycle residual plots and the difference of vector patterns between models run on various historical bathymetries (from 1852, 1879, 1901, 1927, 1954 and 2006). Dredging was first undertaken at the Tauranga Entrance area in 1968 when the Cutter Channel was dredged (Healy et al., 1998). Therefore the comparison between the 1954 and 2006 model runs takes into account the effects of dredging, while all other model run comparisons are based upon natural changes in bathymetry not affected by dredging.

4.1 METHODS

4.1.1 The hydrodynamic numerical model

The hydrodynamic numerical model used in this study *3DD* employs an explicit finite difference scheme to solve the momentum and continuity equations (Black 2002). Like all hydrodynamic numerical models it solves some form of the Navier-Stokes equations. Specifically the Reynolds average equations are used in this case (Williams, 2006).

4.1.2. Bathymetry

The bathymetries used in the hydrodynamic numerical modelling were also used in the geomorphological comparison investigation - (digitising and gridding processes are described in Chapter 3).

The boundary on the left side of the grid was extended by 20 cells to prevent the current flow of water over the ebb tidal delta interacting with the boundary.

The bathymetry is limited to the southern basin of the Tauranga Harbour, as previous investigations have proven that water bodies in the northern and southern basin are largely separate, with low water exchange between the north and the south (Barnett, 1985).

4.1.3. Boundary Conditions

The tidal boundary file was created using tidal constituents from the Moturiki Island tide gauge, which is located just outside the harbour (Fig. 1.2). The model runs were based on mean spring tide values for 2006 (MHWS 1.86 m , MLWS 0.16 m) (Land Information New Zealand, 2007). The annual average value of mean high and mean low water spring tide varies from year to year on a cycle of approximately 19 years. This variation is in the order of 0.1 – 0.15 m (Land Information New Zealand, 2007). This variability limits the accuracy of this historical hydrodynamic numerical modelling.

River inputs were not used in the model for this study as they were shown to have a negligible effect on hydrodynamics of Tauranga Harbour by the hydrodynamic physical modelling by the Hydraulic Research Station (1963). Wave inputs were not used in the model as it is a tidally dominated inlet (Black, 1984) as shown by the relatively large ebb tidal delta (Davis and Fitzgerald, 2004).

4.1.4. Calibration

The 2006 model was calibrated by Spiers et al. (2009) using an S4 current meter on the model boundary. All the model runs (1852 – 2006) used the same roughness length, horizontal eddy viscosity, horizontal eddy viscosity multiplier, multiplying steps and coastal slip and time steps as the calibrated model run of 2006, but the model runs from 1852 to 1954 were not calibrated. Consequently a qualitative comparison is possible between the years but not a quantitative comparison.

4.2. RESULTS

Hydrodynamic numerical modelling comparing spring tide, mean tide and neap tide modelling of 2006 and 1954 bathymetries was first undertaken demonstrating that in general the current patterns between each tidal situation are similar, with the main difference being a

change in magnitude of current vectors (See Appendix 2). Consequently, all subsequent hydrodynamic numerical modelling in this thesis was based upon the spring tide as this tide has the greatest potential to transport sediment and ultimately determine bathymetric change.

The following results were obtained from the hydrodynamic numerical modelling of a mean spring tide for each bathymetry (2006, 1927, 1901, 1879, and 1852):

- a) a spring tide peak ebb velocity vector plot
- b) a spring tide peak flood velocity vector plot
- c) a difference in spring tide peak ebb velocity vector plot with the preceding bathymetry(2006 – 1954)
- d) a difference in spring tide peak flood velocity vector plot with the preceding bathymetry
- e) a residual distance above threshold plot
- f) a difference in residual distance above threshold plot with the preceding bathymetry.

4.2.1. Points to note regarding interpretation of results.

The spring tide peak velocity vector plots (peak ebb and peak flood) are used to show the current regime at the time of peak tidal current flow for each bathymetry, with red indicating the region with the highest velocities. The difference in spring tide peak velocity vector plots is used to show the changes in current flow that have occurred between each bathymetric survey where the vectors from the earlier bathymetry were subtracted from the vectors from the later bathymetry. In the difference in spring tide peak ebb velocity vector plot, ebb directed vectors indicate an increase in peak ebb velocity between the years, while flood directed vectors indicate a decrease in peak ebb velocity between the years. Conversely, in the difference in spring tide peak flood velocity vector plot, flood directed vectors indicate an increase in peak flood velocity between the years, while ebb directed vectors indicate a decrease in peak flood velocity between the years. Red indicates the area of the greatest velocity change.

The residual distance plots are used to indicate potential net tidally driven generated sediment movement from a mean spring tide. A velocity threshold of 0.3 ms^{-1} was applied to these plots, which represents the sand entrainment velocity threshold (Black, 1983; Black and Healy, 1986; Black et al. 1989). Residual distance vectors are described by Black (1983) as indicating potential net sediment transport after a tidal cycle. In any one place within the

study area, tidal currents can be moving in a variety of different directions and speeds. Consequently sediment transport rates are continually changing based on the changing tidal currents. The *residual velocity* integrated over the tidal cycle accounts for these changes in velocity, and may reflect the net movement of sediment, determining the magnitude of ebb or flood dominance. The *residual distance vectors* (used in this study) are the product of residual velocity and the time that the threshold speed is exceeded. This provides a better descriptor of potential net sediment movement than the residual velocity, as the residual velocity in any one place may be high but with a short duration. The total work on the bed is based upon the time that residual velocity acts (Black, 1983). In this study the greatest residual distance vectors are shown by red.

The difference in residual distance plot represents indicative changes in mean spring tide potential net sediment transport between bathymetries, where the vectors from the earlier bathymetry are subtracted from the vectors from the later bathymetry. This indicates the areas that have undergone a change in net potential tidally driven sediment transport between each bathymetry. Each different type of plot has the same maximum value on the colour scale for each year to aid ready comparison of the data between the years. However, it is important to note that in some cases the actual magnitude of velocity vectors may exceed that shown on the colour scale. Red shows the areas that undergo the greatest change in potential tidally driven sediment transport.

4.3. COMPARISON OF 1954 AND 2006 HYDRODYNAMIC RESULTS

4.3.1. Difference in peak ebb flow conditions 1954 - 2006

A comparison of the spring peak ebb flows of 1954 and 2006 (Fig. 4.2) shows several major differences in the current regime:

(i) The ebb jet is less diffusive and more concentrated in 2006 than in 1954, with a reduction in current velocity vectors near Mt Maunganui. This reduction in velocity vectors is apparent when examining the difference in spring tide peak ebb velocity vector plot, which shows flood orientated vectors indicating a reduction in the ebb current velocity. This reduction in peak ebb current velocity is thought to be due to Entrance Channel deepening and widening due to capital dredging from approximately 8 to 14 m which has increased hydraulic efficiency allowing the jet to flow more directly and diverge less.

(ii) The pathway of currents in Pilot Bay has changed between 1954 and 2006. In 1954 the major tidal stream flowed close to the coast around Pilot Bay while in 2006 the current has a more direct route due to dredging through the Cutter Channel. The reduction in current velocity near the Pilot Bay shore can be seen on Figure 4.3, with flood directed vectors near the shore. The establishment of the Cutter Channel in 1968 (Healy et al., 1998), which previously was a blind flood channel, can be linked with the change in the current pathway increasing the hydraulic efficiency encouraging more water to flow through the Cutter Channel and less through Pilot Bay.

(iii) There has been a reduction in current velocity in the Stella Passage between 1954 and 2006, as shown by flood directed vectors on the plot (Fig. 4.3). This reduction in current velocity is linked with dredging which has deepened the channel from about 5 m to 13 m. The increase in channel cross section has resulted in a reduction in velocity in this area.

(iv) The reduction in current velocity over the upper flood tidal delta and ebb shield between 1954 and 2006 is indicated by the flood directed vectors on Figure 4.3. This is evidently due to deepening of the shipping channels surrounding the flood tidal delta through dredging, which has resulted in a greater discharge through the shipping channels and consequently decreased flow and speeds over the upper flood tidal delta.

(v) A reduction in current velocity near Panepane Point is apparent between 1954 and 2006 as indicated by the flood directed velocity vectors (Fig 4.3). This is thought to be due to a channel deepening and widening due to dredging on the eastern side of the flood tidal delta causing an increase in discharge on the eastern side of the harbour and consequently a reduction in discharge and therefore velocities on the western side of the harbour.

4.3.2 Difference in peak flood flow conditions 1954 - 2006

A comparison of the spring peak flood flows of 1954 and 2006 (Fig. 4.5.) shows several major differences in the current regime:

(i) The reduction in current velocity in the tidal inlet, as indicated by the ebb directed vectors is thought to be possibly due to reduction in the tidal prism.

(ii) The reduction in current velocity close to the Pilot Bay shoreline, as indicated by ebb directed velocity vectors and an increase in current velocity in the Cutter Channel, as indicated by flood directed vectors. This change in current velocity vectors can be linked with the channel deepening through dredging of the Cutter Channel, which has allowed greater discharge through the Cutter Channel and a reduction in currents through Pilot Bay.

(iii) The increase in tidal current velocity through the Otumoetai Channel, as indicated by the flood directed vectors. This is thought to be due to the channel deepening of the Maunganui Roads and Otumoetai Channel which has increased the hydraulic efficiency allowing more water to flow through the Otumoetai Channel at greater speeds.

(iv) The reduction in tidal current velocity on the upper flood tidal delta/ ebb shield region is thought to be due to channel deepening surrounding the flood tidal delta, allowing more water to flow through these channels and consequently less on the upper flood tidal delta, resulting in reduced speeds.

The final major change apparent in the difference in the spring tide peak ebb velocity vector plot 1954 – 2006, is the reduction in tidal current velocity immediately south of Matakana Island, as indicated by the ebb directed velocity vectors.

4.3.3. 2006 Mean Spring Tide Residual Distance Plot

The 2006 mean spring tidal cycle residual distance plot (Fig. 4.6) shows that there is strong ebb dominated residual tidal currents through the main ebb channel, with a decrease in current velocity with increasing distance from the tidal inlet. This is consistent with the bedforms map (Fig.4.6) which shows ebb directed bedforms along the Entrance Channel with wave length decreasing further from the inlet. Flood dominated residual tidal currents are present in the flood marginal channels and the Western side of the Cutter Channel.

This ebb dominated tidal flow of the main ebb channel and the flood dominated flow of the flood marginal channel is consistent with the morphological models of Hayes (1975, 1980), Boothroyd (1985), and Kana (1999). Ebb dominated residual tidal currents are present in Pilot Bay. The flood tidal delta is dominated by flood directed residual tidal currents over the flood ramp half with a sharp change in residual tidal current direction to the east over the ebb shield. South of the ebb shield there is dominant eastwards directed residual tidal currents. These eastwards directed tidal residual currents are strongest north of Sulphur Point. There is a clear convergence of residual tidal current vectors in the north part of Maunganui Roads Channel near the Cutter Channel (indicative of sediment deposition area) this is consistent with the convergence in bedforms shown in the same area by Healy (1985) shown in Fig. 5.16. Interestingly the hydrodynamic numerical model from the same study (Black, 1984) fails to capture this convergence.

The residual tidal currents west of the flood tidal delta are westerly directed and a residual tidal current gyre is present about 800 m west of the southern tip of Matakana Island,

while directly south of Matakana Island there is strong ebb directed currents which converge with the flood directed residual tidal currents near Panepane Point.

4.3.4. Difference in Mean Spring Tide Residual Distance Plot 1954 - 2006

The full spring tidal cycle residual distance vectors indicate potential sediment transport. The major changes in residual vectors between 1954 and 2006 (Fig 4.8) are:

(i) A reduction in flood directed tidal sediment transport on the ebb tidal delta in the western flood marginal flood channel between 1954 and 2006 as indicated by the ebb directed vectors.

(ii) A similar reduction in flood directed tidal sediment transport is evident north/north west of Mt Maunganui.

(iii) On the eastern side of the main ebb channel there has been a reduction in ebb directed tidal sediment transport as shown by the flood directed residual distance vectors.

(iv) An increase in potential ebb directed tidal sediment transport is evident on the outer edge of the main ebb channel near the terminal lobe of the ebb tidal delta, as indicated by the ebb directed vectors of the ETD.

(v) There are also small isolated areas of a reduction in potential tidal sediment transport over the crescent shaped bars on the swash platform of the ETD.

(vi) The greatest difference in potential tidal sediment transport on the tidal delta system between 1954 and 2006 is in the areas surrounding Pilot Bay/ Cutter Channel and Panepane Point. Pilot Bay shows a reduction in ebb directed tidally driven sediment transport, as indicated by flood directed vectors. The eastern part of the Cutter Channel shows an increase in ebb directed tidal sediment transport as shown by ebb directed vectors, while the western part of the Cutter Channel shows an increase in flood dominated sediment transport as indicated by flood directed vectors. Near Panepane Point there has been an increase in flood dominated potential tidal sediment transport on the open ocean side indicated by flood directed vectors, and an increase in ebb dominated tidal sediment transport on the harbour side as shown by the ebb directed vectors.

(vii) On the flood ramp and upper flood tidal delta/ ebb shield there are three distinct areas that show noticeable changes in potential net sediment transport. The first area on the flood ramp, south of Mt Maunganui shows southerly/flood dominated tidal sediment transport in 1954, moving to more south easterly dominated tidal sediment transport in 2006. This is shown in Fig 4.8 as north easterly directed vectors. The second zone in the centre of the flood

tidal delta near the ebb shield shows an increase in flood dominated tidal sediment transport between 1954 and 2006 as shown by the flood directed vectors in Fig 4.8. The third area on the southern part of the flood tidal delta shows an increase in easterly dominated tidal sediment transport between 1954 and 2006 as indicated by the easterly vectors shown in Fig 4.8.

4.4. COMPARISON OF 1927 AND 1954 HYDRODYNAMIC RESULTS

4.4.1. Difference in peak ebb flow conditions 1927 - 1954

The peak ebb tidal current flow between 1927 and 1954 shows limited changes near Panepane Point where there is an isolated area showing a reduction in peak ebb velocity as illustrated by the flood directed vectors (Fig. 4.9.). However, it is important to note that the spatial extent of these changes is small, being approximately 150 m wide and 250 m long.

4.4.2. Difference in peak flood flow conditions 1927 - 1954

The peak flood tidal flow between 1927 and 1954 shows limited changes near Panepane Point (Fig 4.11). On the open ocean side of Panepane Point a small number of ebb directed vectors show a decrease in peak flood tidal current flow, while on the harbour side there is a small number of flood directed vectors indicating an increase in peak flood tidal current flow.

4.4.3. Difference in Mean Spring Tide Residual Distance Plot 1927 - 1954

The key changes in potential net tidally driven sediment transport between 1927 and 1954 (Fig. 4.13) is primarily limited to the areas surrounding Panepane Point, the flood marginal channels and outer edges of the ebb tidal delta as well as the Pilot Bay and Otumoetai Channel areas.

(i) The area surrounding Panepane Point shows the greatest changes for residual distance vectors over the tidal delta system between 1927 and 1954, with a reduction in flood dominated tidal sediment transport on the open ocean side of Panepane Point shown by ebb directed vectors in Fig 4.13. On the harbour side of Panepane Point there is a reduction in ebb dominated tidal sediment transport shown by the flood directed vectors in Fig. 4.13

(ii) The flood marginal channels show an increase in flood dominated potential tidal sediment transport between 1927 and 1954, as shown by the flood directed vectors in Fig. 4.13.

(iii) The outer edges of the western side of the flood tidal delta generally shows an increase in ebb dominated tidal sediment transport, apart from one feature near the terminal lobe which shows a isolated area where there has been a reduction in ebb dominated tidal sediment transport.

(iv) Between 1927 and 1954 Pilot Bay shows a slight reduction in ebb dominated tidal sediment transport near the shore as shown by flood directed vectors (Fig 4.13) and a slight reduction in flood dominated tidal sediment transport further from the shore as shown by ebb directed vectors.

(v) The rest of the flood tidal delta shows very little difference in residual distance vectors, apart from offshore from the Otumoetai channel which shows there has been a slight reduction in westerly/flood dominated tidal sediment transport as shown by the easterly directed vectors in Fig 4.13.

4.5 COMPARISON OF 1901 AND 1927 RESULTS

4.5.1. Difference in peak ebb flow conditions 1901 – 1927

The difference in peak ebb flow conditions plot of 1901 – 1927 shows significant changes in a small area approximately 150 m wide and 500 m long near Panepane Point where there has been a significant reduction in peak ebb tidal current velocity as shown by the flood directed vectors (Fig. 4.15).

The difference in peak ebb flow between 1901 – 1927 is similar to the trends shown in the difference in peak ebb flow between 1927 – 1954 with vectors in each case showing a similar spatial coverage and direction.

4.5.2. Difference in peak flood flow conditions 1901 – 1927

The difference in peak flood conditions of 1901 – 1927 shows a significant reduction in current velocity offshore from Panepane Point, as shown by the ebb directed vectors, while

the landward side shows an increase in current velocity as shown by flood directed vectors (Fig. 4.17).

The difference in peak flood flow between 1901 – 1927 is similar to the trends shown in the difference in peak flood flow between 1927 – 1954 with vectors in each case showing a similar spatial coverage and direction.

4.5.3. Difference in Mean Spring Tide Residual Distance Plot 1901 -1927

A comparison of the mean spring tide residual distance plot 1901 with that of 1927 (Fig. 4.19) suggests that there has been a noticeable change in potential sediment transport near the terminal lobe, Panepane Point and in places in the channels surrounding the flood tidal delta.

(i) Between 1901 and 1927 there has been an increase in potential ebb directed tidal sediment transport near the terminal lobe as shown by the ebb directed vectors.

(ii) Adjacent to Panepane Point in the tidal inlet gorge there has been a reduction in flood dominated tidal sediment transport as shown by the ebb directed vectors. However further towards the centre of the tidal inlet gorge there has been an increase in flood dominated tidal sediment transport as shown by the flood directed vectors. Conversely on the harbour side/south west of Panepane Point there has been a reduction in ebb dominated tidal sediment transport as shown by flood directed vectors.

(iii) The western side of Maunganui Roads Channel shows an increase in ebb dominated tidal sediment transport between 1901 and 1927 as shown by the ebb directed vectors.

(iv) The far western side of Centre Bank shows an increase in easterly dominated tidal sediment transport as shown by easterly directed vectors.

4.6. COMPARISON OF 1879 AND 1901 RESULTS

4.6.1. Difference in peak ebb flow conditions 1879 – 1901

A comparison of peak ebb spring conditions between 1879 and 1901 shows noticeable changes in currents northwest of Mt Maunganui, near Panepane Point, with minor changes over the flood tidal delta (Fig. 4.21).

(i) North west of Mt Maunganui, east of the main ebb channel there has been an increase in peak ebb current velocity, as shown by the ebb directed vectors (Fig. 4.21). Furthermore, there has been an increase in the eddy north of Mt Maunganui, as shown by the pattern of the vectors.

(ii) North of Panepane Point there has been a reduction in mean spring peak ebb current velocity as shown by the flood directed vectors.

(iii) Over the flood ramp there has been a reduction in mean spring peak ebb current velocity as shown by the flood directed vectors.

4.6.2. Difference in peak flood flow conditions 1879 – 1901

The changes in mean spring peak flood current regime between 1879 and 1901 are primarily limited to Panepane Point, Maunganui Roads Channel, with minor changes over the flood tidal delta (Fig 4.23).

(i) There has been a reduction in mean spring peak flood current regime between 1879 and 1901 near Panepane Point and in Maunganui Roads Channel, as shown by ebb directed vectors.

(ii) The northern part of the flood tidal delta, surrounding the flood ramp, also shows a reduction in current velocity albeit to a lesser magnitude than change present near Panepane Point and Maunganui Roads Channel.

4.6.3. Difference in Mean Spring Tide Residual Distance Plot (1879 - 1901)

A comparison of mean spring tide residual distance plots of 1879 and 1901 (Fig. 4.25) indicates that there has been considerable change in potential tidal sediment transport over the ebb and flood tidal delta.

(i) There has been a noticeable reduction in ebb directed tidal sediment transport over the terminal lobe and swash platform between 1879 and 1901 as shown by the flood directed vectors in Fig 4.25.

(ii) On the western side of the main ebb channel there has been an increase in flood directed tidal sediment transport as shown by flood directed vectors.

On the eastern side of the main ebb channel the ebb directed vectors indicate there has been a reduction in flood directed flow through the flood marginal channels.

(iii) The flood directed vectors on the southern side of the Matakana Island indicate that there has been an increase in flood directed tidal sediment transport here.

(iv) There are widespread changes in tidal sediment transport magnitude and direction over the central part of the flood tidal delta. In the southern part of Pilot Bay there has been an increase in ebb directed tidal sediment transport between 1879 and 1901. On the eastern part of the flood tidal delta there has been a reduction in tidal sediment transport in series of isolated spots. In the centre of the flood tidal delta in the upper part of the flood ramp there has been an increase in potential tidal sediment transport, as shown by the flood directed velocity vectors. In the centre of the flood tidal delta, southwest of Matakana Island and north of Sulphur Point there has been a reduction in magnitude and change of direction of tidal sediment transport as shown by the south-westerly directed vectors shown on Fig. 4.25.

(v) In Fig. 4.25 south of the southern tip of Matakana Island there is three distinct units of changing tidal sediment transport which are about 0.5 km wide and over 1 km long. The two southernmost units (in the western part of Otumoetai Channel and west of Centre Bank) show easterly directed vectors indicating that there has been a reduction in the westerly/ebb tidal sediment transport. The northern most unit about 200 m south of Matakana Island shows westerly directed vectors indicating that there has been a reduction in the eastwards ebb tidal sediment transport in this area

4.7. COMPARISON OF 1852 AND 1879 RESULTS

4.7.1. Difference in peak ebb flow conditions 1852 - 1879

A comparison of mean spring peak ebb conditions between 1852 and 1879 (Fig. 4.27) show considerable changes in and just outside of the tidal inlet gorge and in the vicinity of Pilot Bay and Maunganui Roads Channel.

(i) Immediately outside the tidal inlet gorge there has been a slight increase in peak ebb current velocity as shown by ebb directed vectors between 1852 and 1879.

(ii) Within the tidal inlet gorge and in the vicinity of Pilot Bay/Maunganui Roads the changes in current velocity are varied showing both increases and decreases within a short distance of each other.

4.7.2. Difference in peak flood flow conditions 1852 - 1879

A comparison of mean spring peak flood conditions between 1852 and 1879 shows changes in current velocity in the tidal inlet gorge and north of Maunganui Roads Channel (Fig 4.29).

(i) In the tidal inlet gorge the current changes are variable showing both increases and decreases in current velocity within a short distance.

(ii) North of Maunganui Roads Channel shows increases in peak flood currents as shown by the flood directed vectors.

4.7.3. Difference in Mean Spring Tide Residual Distance Plot 1852 – 1879

Changes in potential net tidally driven sediment transport between 1852 and 1879 indicate that there has been a reduction in ebb directed tidal sediment transport in an isolated spot (about 200 m diameter) near the terminal lobe between 1852 and 1879 as shown by the flood directed vectors on Fig 4.31. Most of the main ebb channel shows a similar reduction in potential ebb directed tidal sediment transport. East of the main ebb channel there has been an increase in ebb directed tidal sediment transport as shown by ebb directed vectors on Fig 4.31. Changes in tidal sediment transport on the flood tidal delta varied: generally the flood tidal delta shows a reduction in tidal sediment transport, but there are also isolated exceptions which show an increase in potential tidal sediment transport such as north of Maunganui Roads Channel and west of Centre Bank.

4.8. COMPARISON OF ALL MEAN SPRING TIDE RESIDUAL DISTANCE DIFFERENCE PLOTS.

A comparison of all the mean spring tide residual distance difference plots (1954 – 2007, 1927 – 1954, 1901 – 1927, 1879 – 1901, 1852 – 1879) (Fig. 4.32) indicates that the areas which commonly undergo the most change in tidal sediment transport are:

a) The eastern outer edge of the ebb tidal delta near the terminal lobe, which undergoes change both in isolated spots and in long arcs.

b) The areas surrounding Panepane Point which often shows high difference in potential tidal sediment transport in small areas.

c) The eastern side of the main ebb channel close to the Mt Maunganui

d) The area surrounding Pilot Bay/Cutter Channel and north of Maunganui Roads Channel.

e) The western part of Centre Bank where the Otumoetai Channel and Lower Western Channel meet which shows variation in all of the difference in residual distance plots except for 1852 – 1879.

(Note the lack of changes present in the 1852 – 1879 could be due to the deficiency of accurate bathymetric data in the 1852 chart in this part of harbour).

4.9. COMPARISON WITH HISTORICAL STUDIES

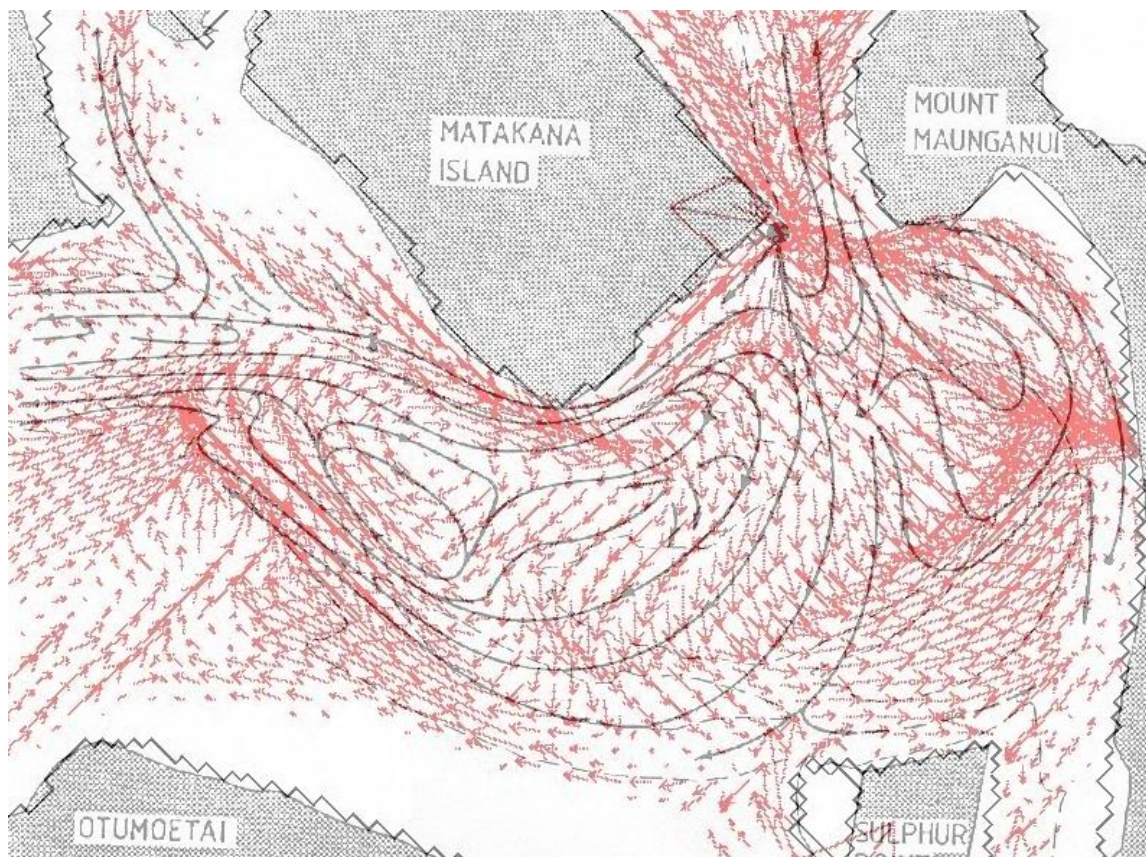


Fig 4.1. Comparison of sediment transport on the Tauranga Harbour flood tidal delta in 2006 and 1984. The 2006 mean spring tide residual distance plot (shown in the red vectors) is overlaid on the 1984 direction of net, total load sediment transport circulation in Tauranga Harbour map (shown in long black arrows) from Black (1984).

A comparison of the Tauranga Harbour flood tidal delta 2006 mean spring tide residual distance plot (shown in the red vectors) with the 1984 direction of net total load sediment transport circulation (shown in long black arrows) (Black, 1984) was undertaken. The 2006 and 1984 data show reasonable similarity in the anti-clockwise sediment transport

loop in north eastern part of the flood tidal delta, but a number of differences are present in the western part of the flood tidal delta system. There is a lack of data in the southeastern part of the tidal delta system in 1984.

(i) The eastern sediment transport loop suggested by Black (1984) is roughly similar to the vectors shown in the 2006 data, with a sharp change from southeasterly sediment transport to northeasterly sediment transport near the ebb shield. The south easterly directed sediment transport in the south of the Cutter Channel and northeasterly sediment transport is captured by both the 1984 and 2006 data. The 1984 data fails to show the strong easterly sediment transport on the south eastern side of the flood tidal delta shown in the 2006 data.

(ii) There is a distinct difference in the direction of vectors in the clockwise sediment circulation loop on the west of the flood tidal delta. The 1984 data suggests south to westerly sediment transport pathway while the 2006 data indicates south to south-easterly potential sediment transport pathway.

(iii) West of the flood tidal delta the 1984 and 2006 data agree in showing north westerly sediment transport. However, the circulating sediment loop that is south west of the southern tip of Matakana Island is represented further north east in the 2006 plot than in the 1984 plot.

(iv) Immediately south of the southern tip of Matakana Island there is a good match in the westerly sediment transport between 1984 and 2006.

(v) South of Panepane Point there is reasonable resemblance in the vectors in the northern part of the clockwise circulating loop, which are directed northerly then easterly then southerly

4.10 Summary

This study conducts two dimensional hydrodynamic numerical modelling using bathymetries from 1852 to 2007 to assess the effects of dredging on hydrodynamics and current regime of the Tauranga Harbour tidal inlet delta system. It is shown that dredging has a noticeable affect on the hydrodynamics and current flow on the tidal delta system.

The effects of dredging are particularly apparent in the Cutter Channel / Pilot Bay region where there has been an increase in flood directed potential net tidal driven sediment transport in the southern part of the Cutter Channel and an increase in ebb directed potential net tidal driven sediment transport in the northern part of the Cutter Channel. This increase in

potential net driven tidal sediment transport is associated with the capital dredging of the Cutter Channel that began in 1968.

Less significant changes in potential net tidal sediment transport associated with dredging can be found in Maunganui Roads Channel and the centre of the flood tidal delta. The Maunganui Roads Channel, shows a reduction in potential net tidal sediment transport associated with channel deepening and the upper flood tidal delta region shows an increase in flood directed potential net tidal sediment transport and a change in net potential sediment transport direction.

Panepane Point shows an increase in flood directed potential net tidal sediment transport on the open ocean side and an increase in ebb directed net tidal sediment transport on the harbour side. The Panepane Point region is historically highly dynamic with ongoing changes in net tidal sediment transport in each of the difference in mean spring tide residual distance plots. A comparison of the 'difference in mean spring tide residual distance vector plots' of 2006 – 1954 and pre-dredging natural 1879 – 1901 shows that the 1879 – 1901 plot shows a similar (possibly higher) potential net sediment transport. This indicates that the changes in net sediment transport due dredging in this area is not significantly different to that which naturally occurs in the un-dredged scenario.

A comparison of the 2006 potential net sediment transport with map of sediment transport by Black (1984) is broadly similar but has a number of noticeable differences such sediment transport direction across the southern flood tidal delta and the location of eddies east of the flood tidal delta.

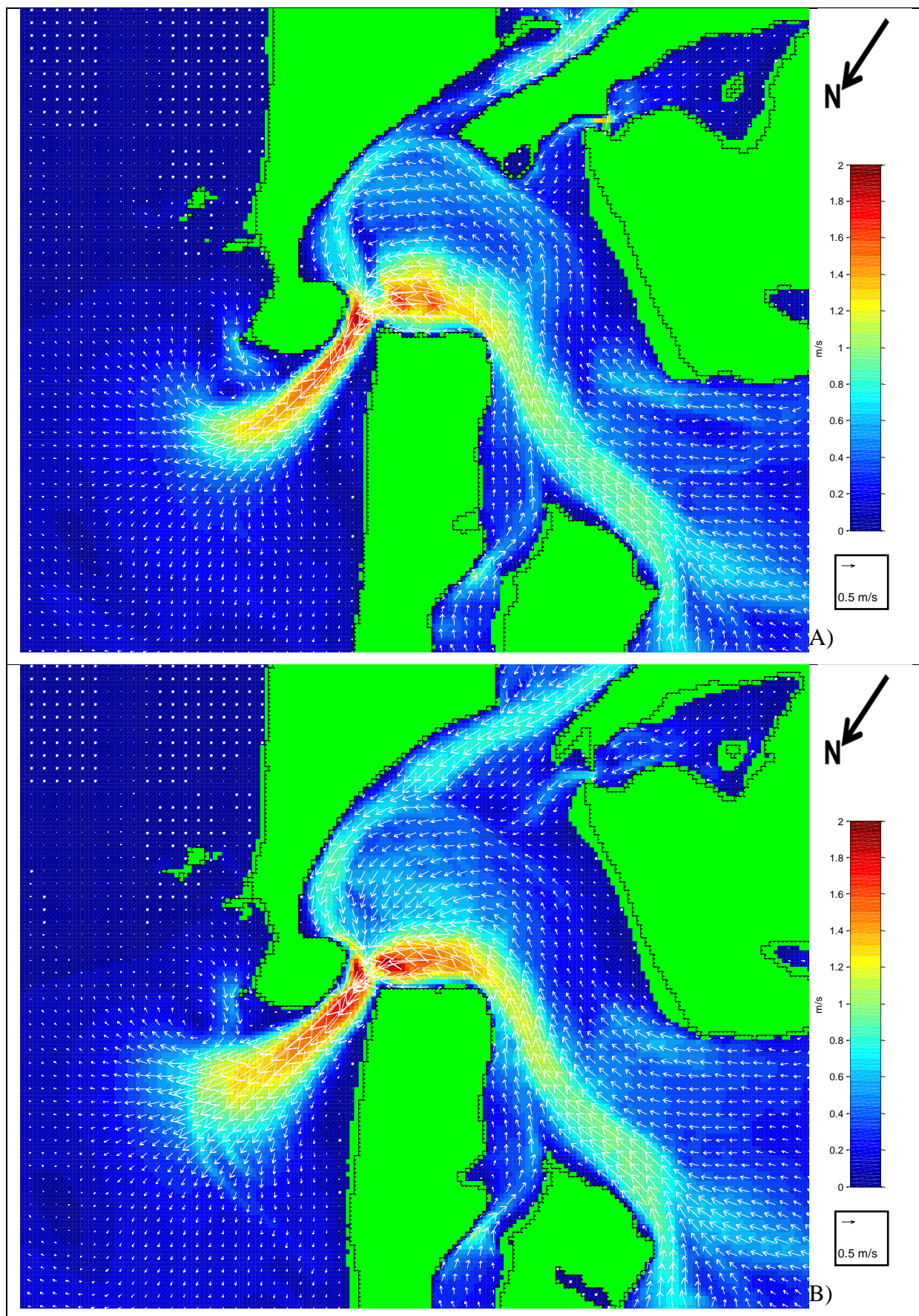


Fig. 4.1: Mean spring tide peak ebb velocity vector plot 2006 (A), and 1954 (B) (Every third vector is displayed, colour scale maximum set at 2 m/s).

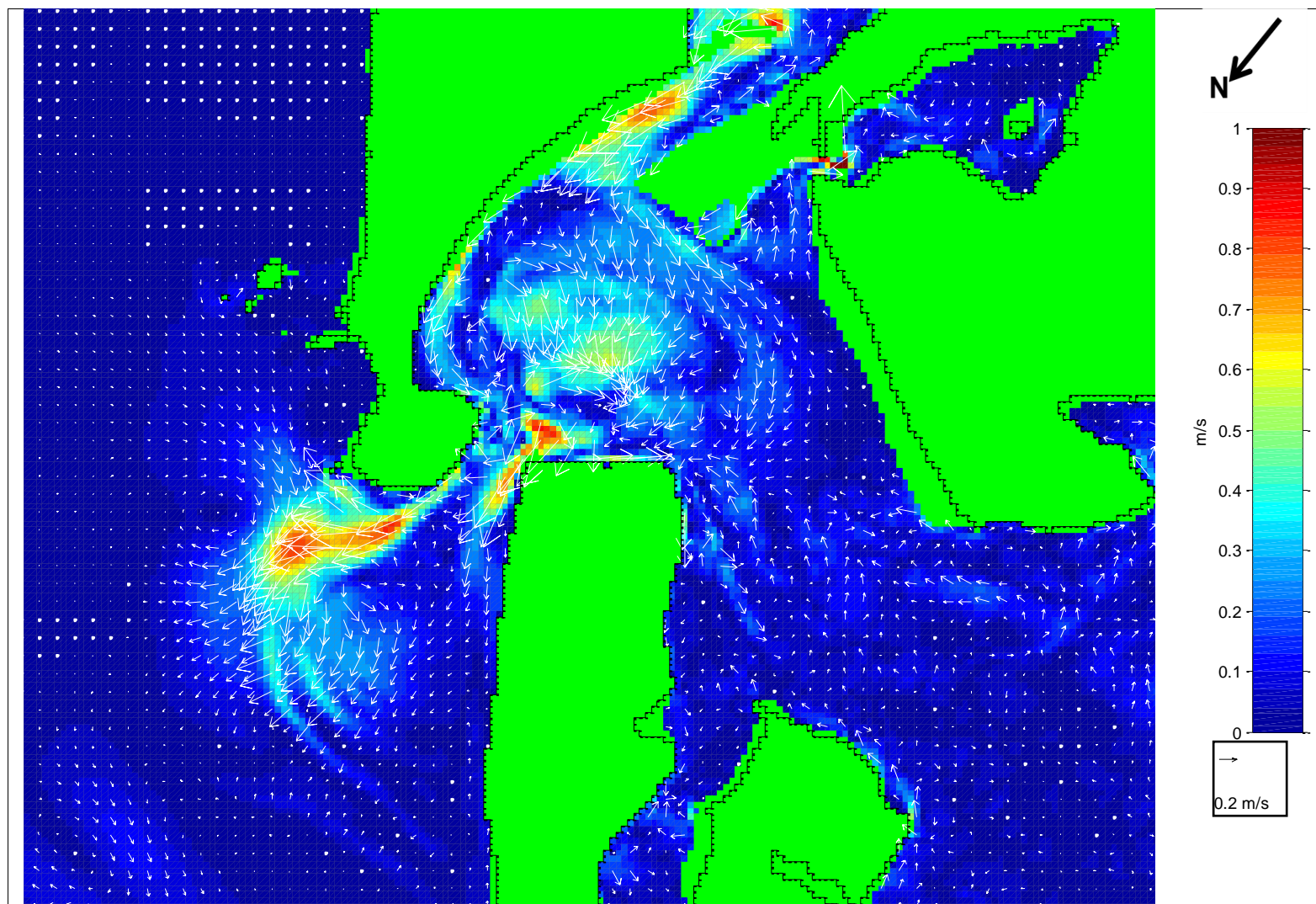


Fig. 4.2: Difference in mean spring tide peak ebb velocity vector plot (2006 – 1954). (Every third vector is displayed, colour scale maximum set at 1m/s).

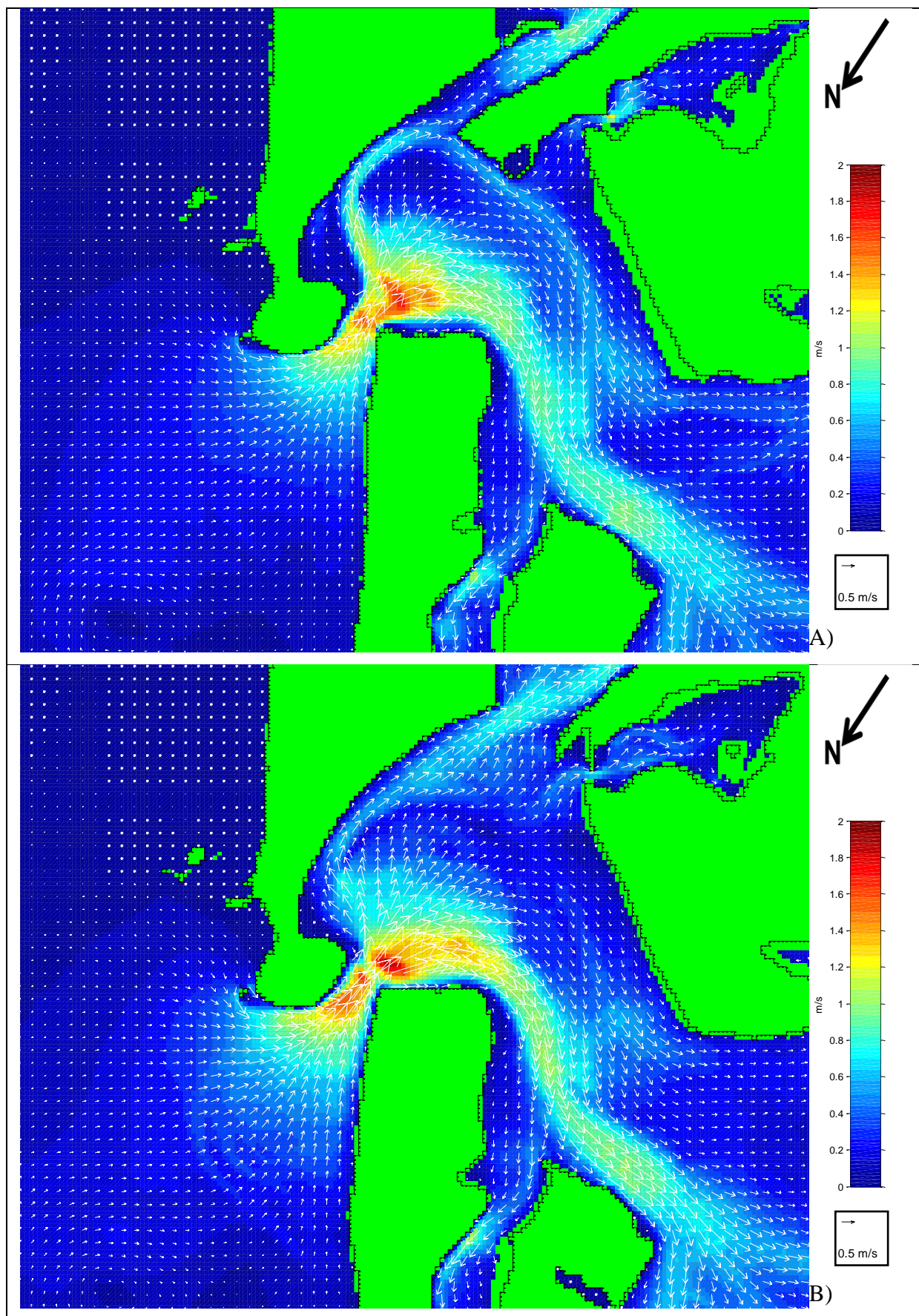


Fig. 4.3: Mean spring tide peak flood velocity vector plot 2006 (A), and 1954 (B) (Every third vector is displayed, colour scale maximum set at 2 m/s).

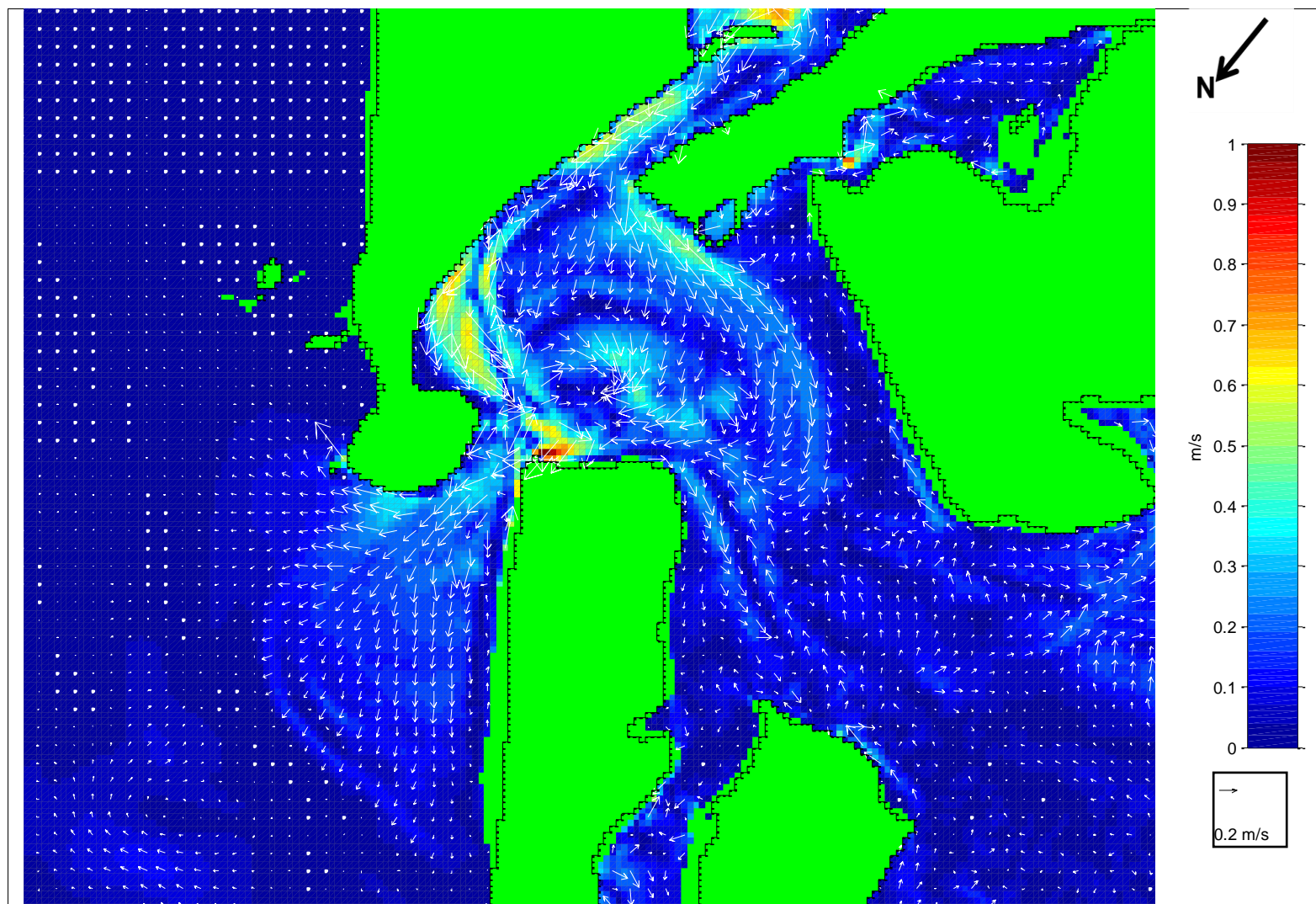


Fig. 4.4: Difference in mean spring tide peak flood velocity vector plot (2006 – 1954). (Every third vector is displayed, colour scale maximum set at 1m/s).

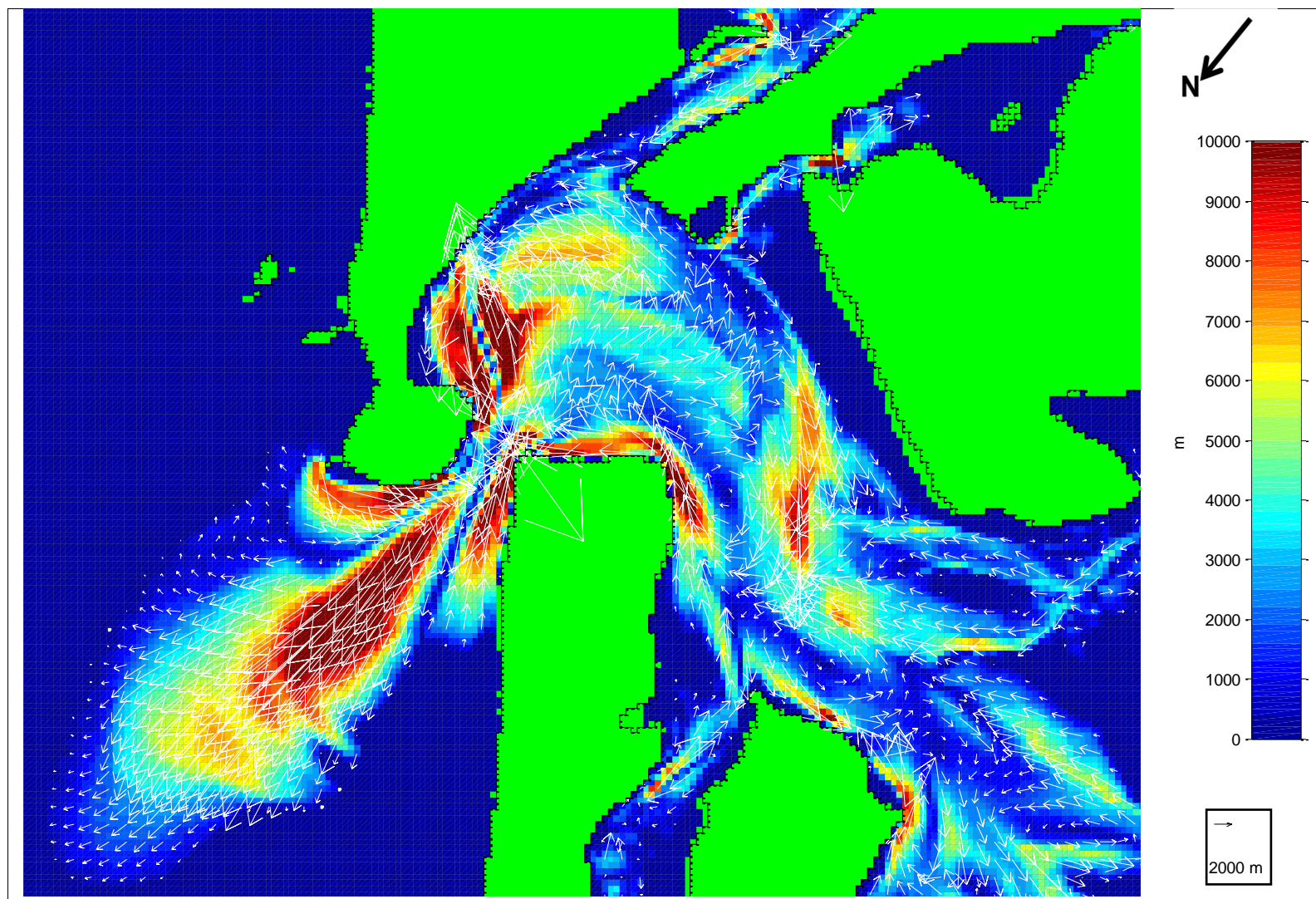


Fig. 4.5: Mean spring tide residual distance vector plot for 2006 (Every third vector is displayed, colour scale maximum set at 10000 m).

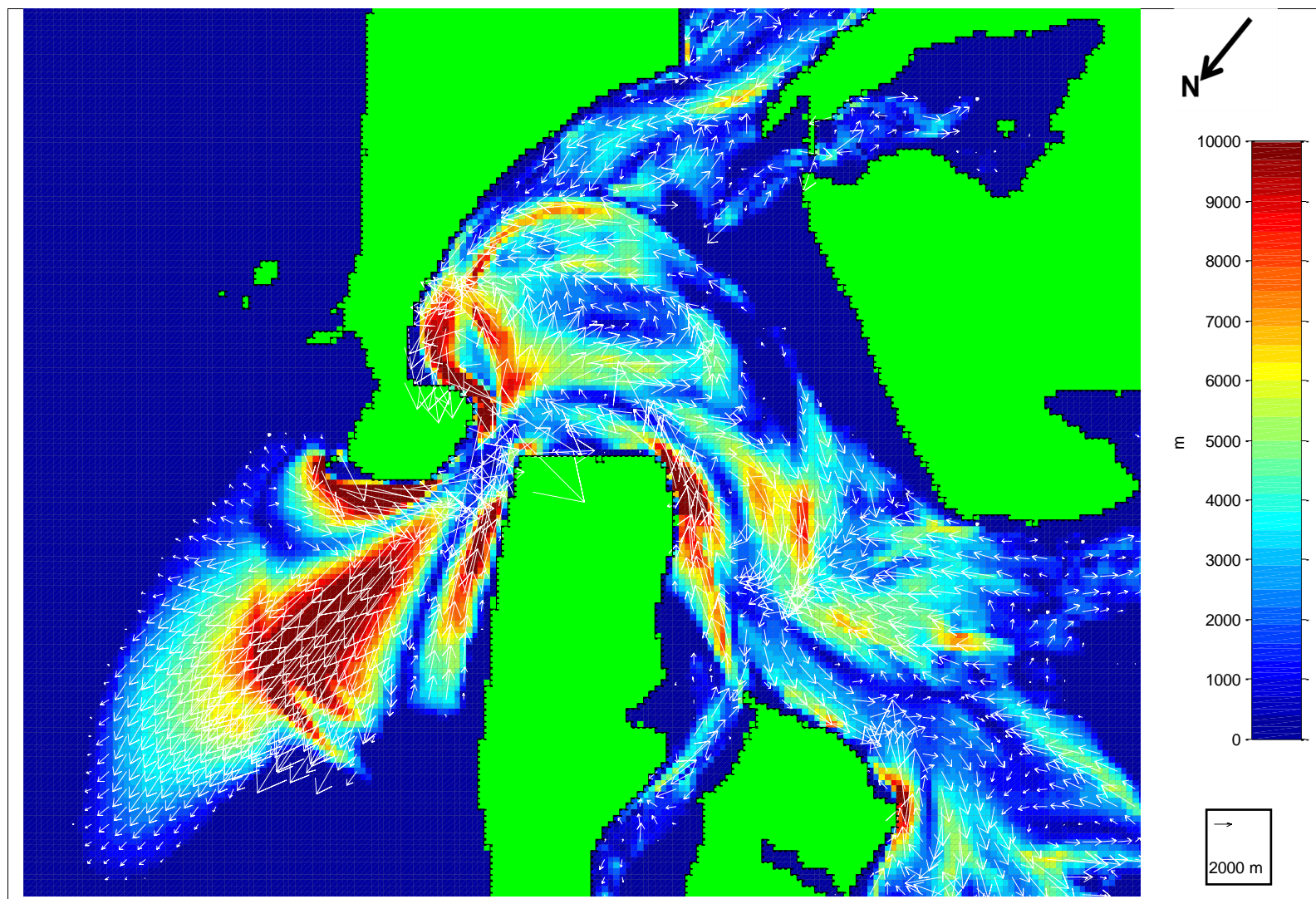


Fig. 4.6: Mean spring tide residual distance vector plot for 1954 (Every third vector is displayed, colour scale maximum set at 1000).

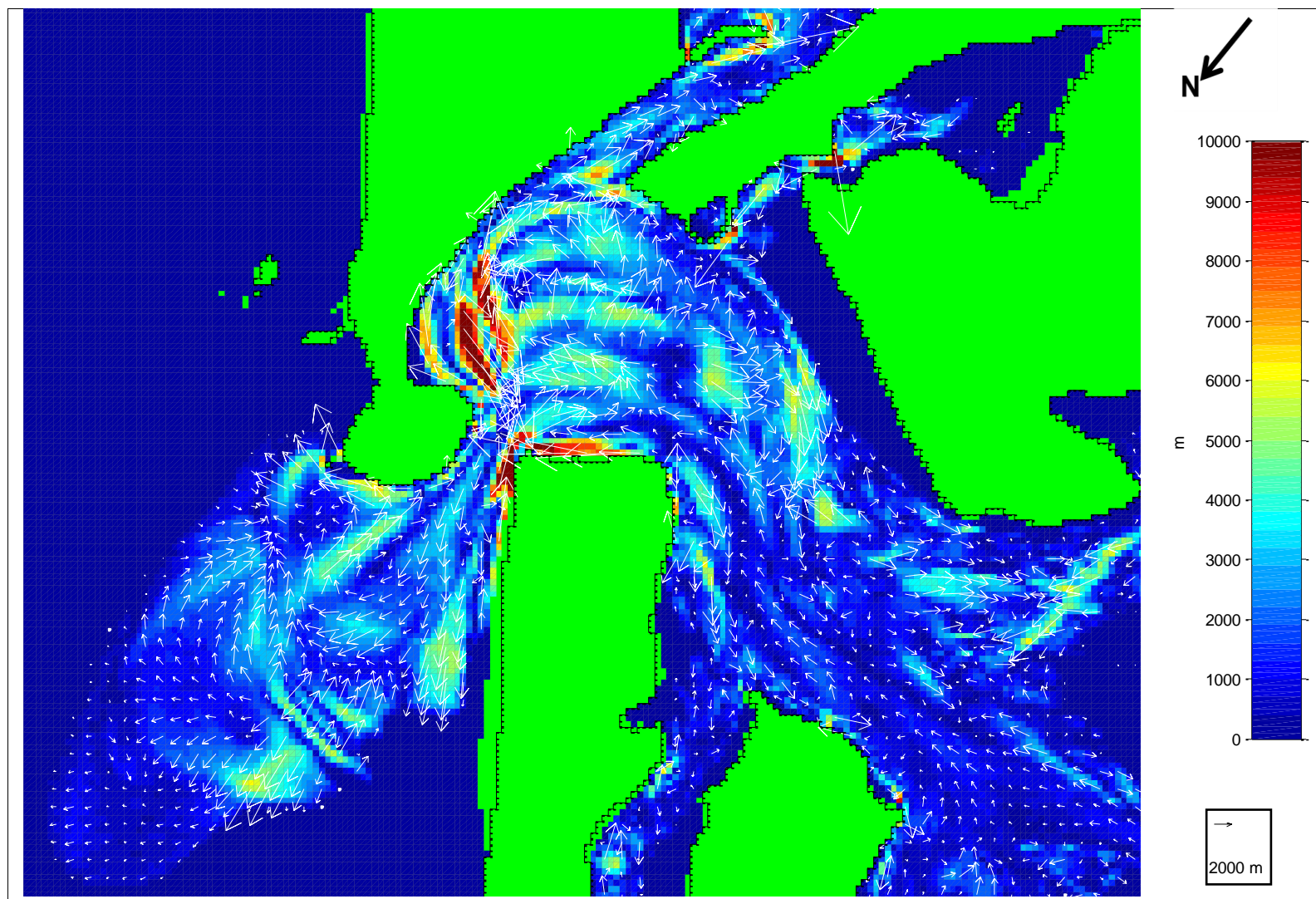


Fig. 4.7: Difference in mean spring tide residual distance vector plot (2006 – 1954) (Every third vector is displayed, colour scale maximum set at 1000).

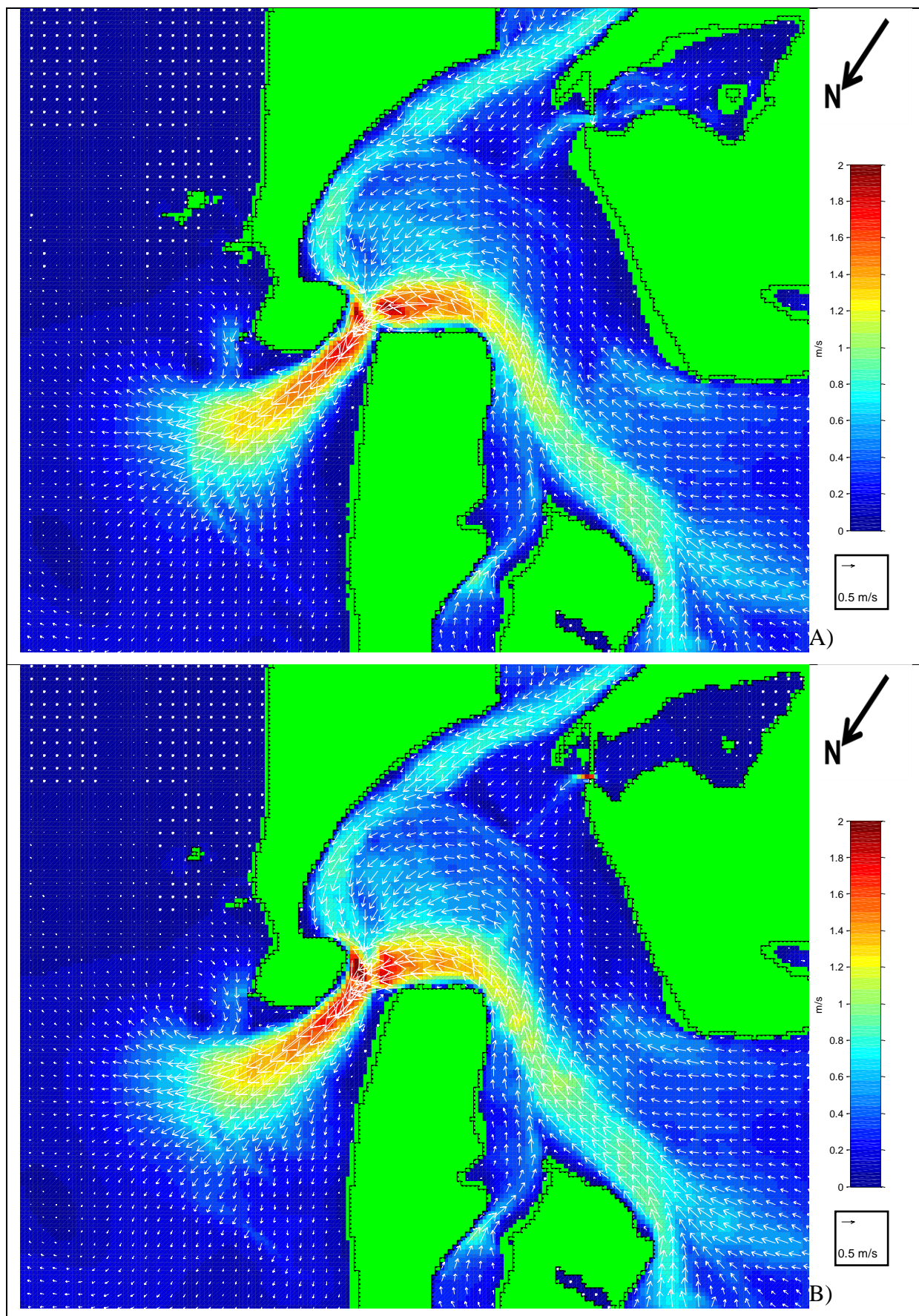


Fig. 4.8: Mean spring tide peak ebb velocity vector plot 1954 (A), and 1927 (B) (Every third vector is displayed, colour scale maximum set at 2 m/s).

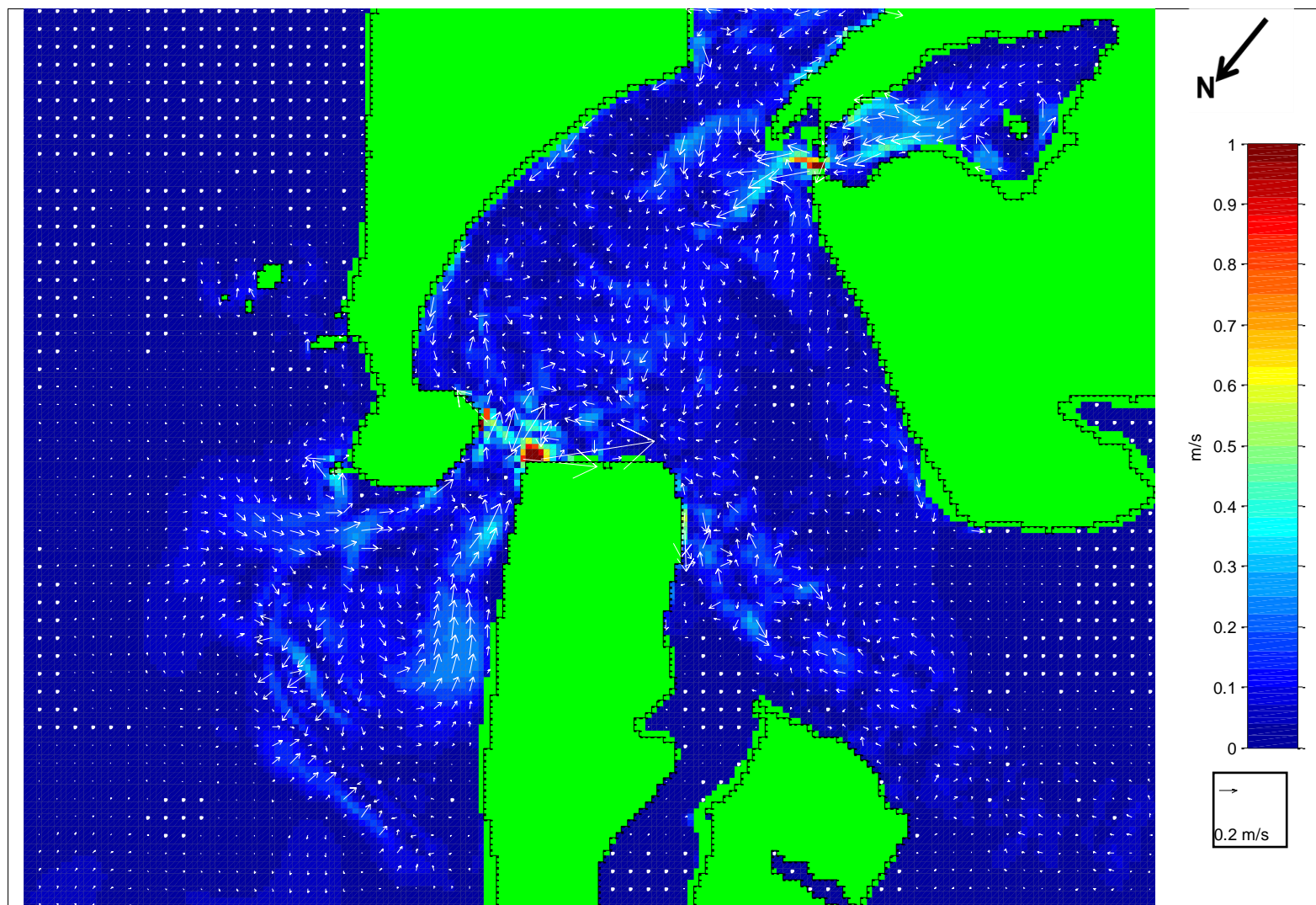


Fig. 4.9: Difference in mean spring tide peak ebb velocity vector plot (1954 - 1927). (Every third vector is displayed, colour scale maximum set at 1m/s).

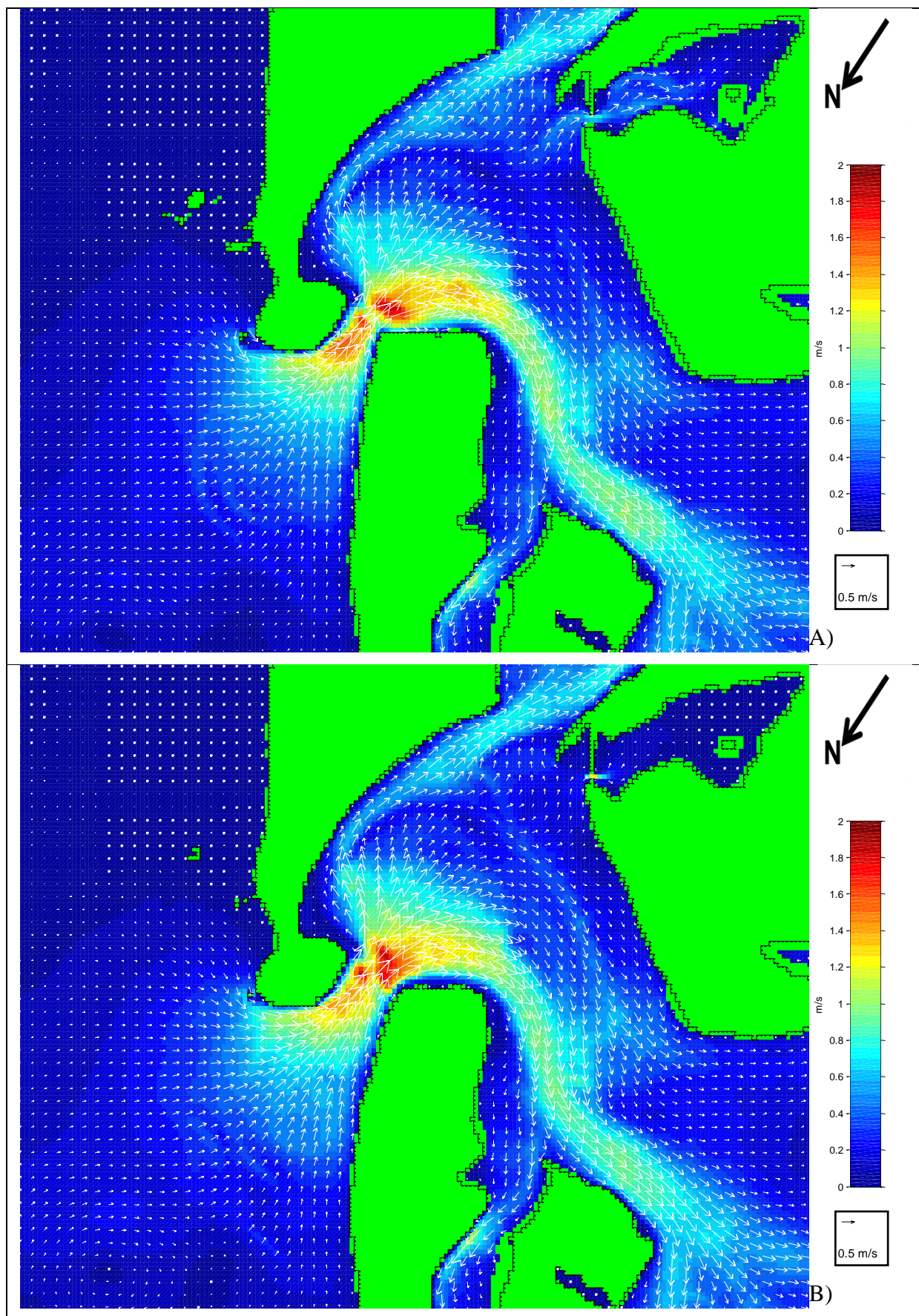


Fig. 4.10: Mean spring tide peak flood velocity vector plot 1954 (A), and 1927 (B) (Every third vector is displayed, colour scale maximum set at 2 m/s).

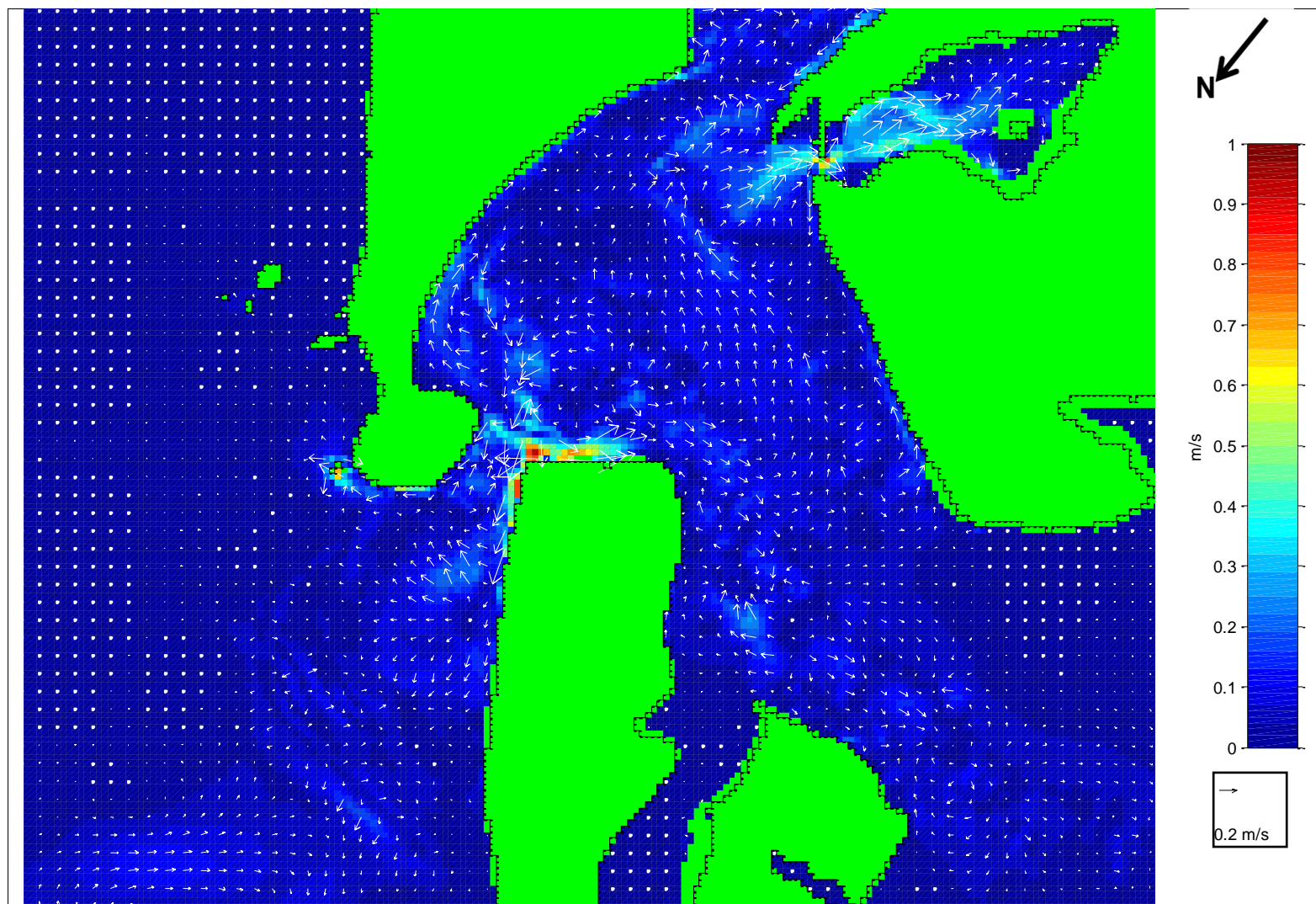


Fig. 4.11: Difference in mean spring tide peak flood velocity vector plot (1954 - 1927). (Every third vector is displayed, colour scale maximum set at 1m/s)

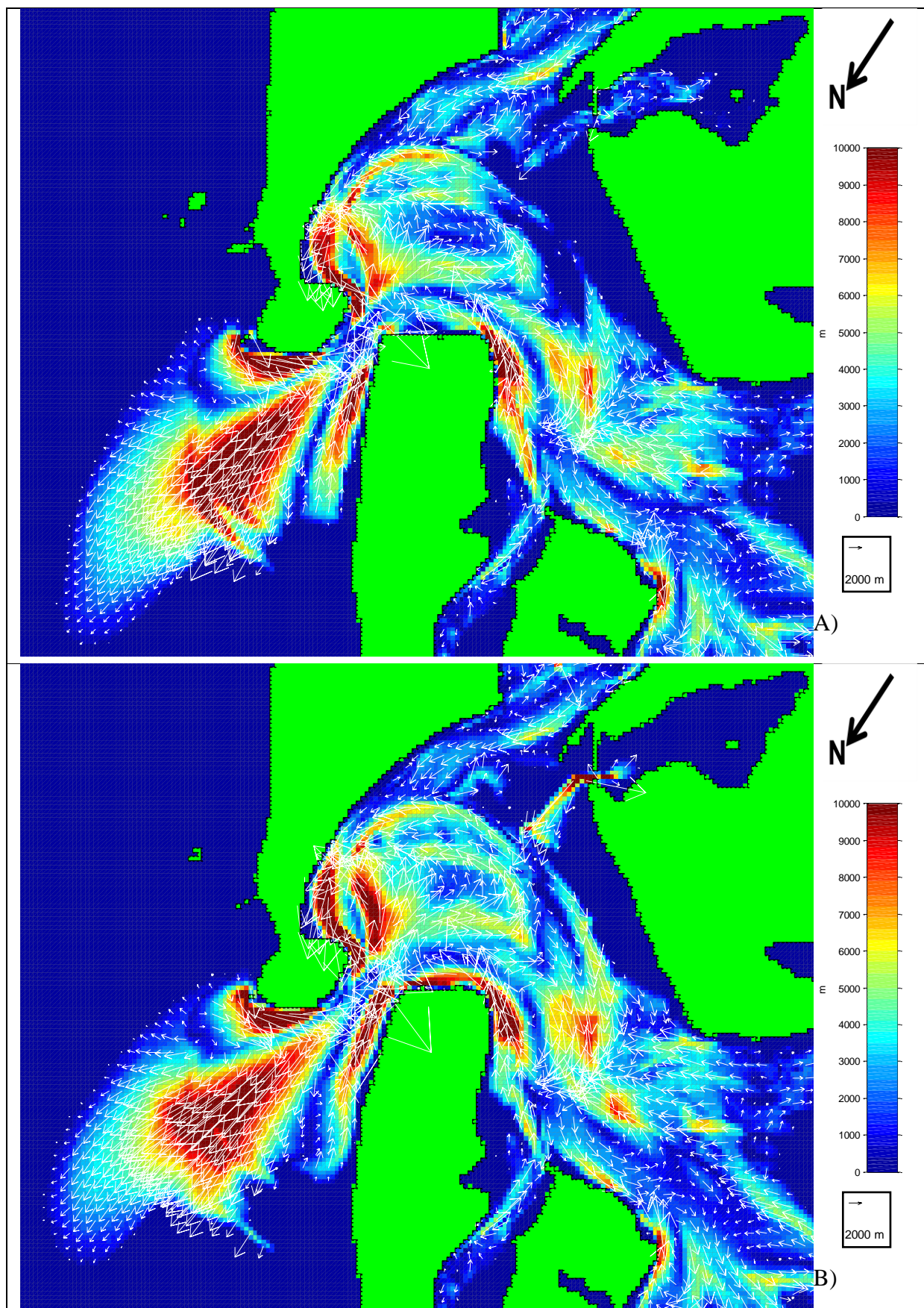


Fig. 4.12: Mean spring tide residual distance vector plot for 1954 (A) and 1927 (B) (Every third vector is displayed, colour scale maximum set at 10000 m)

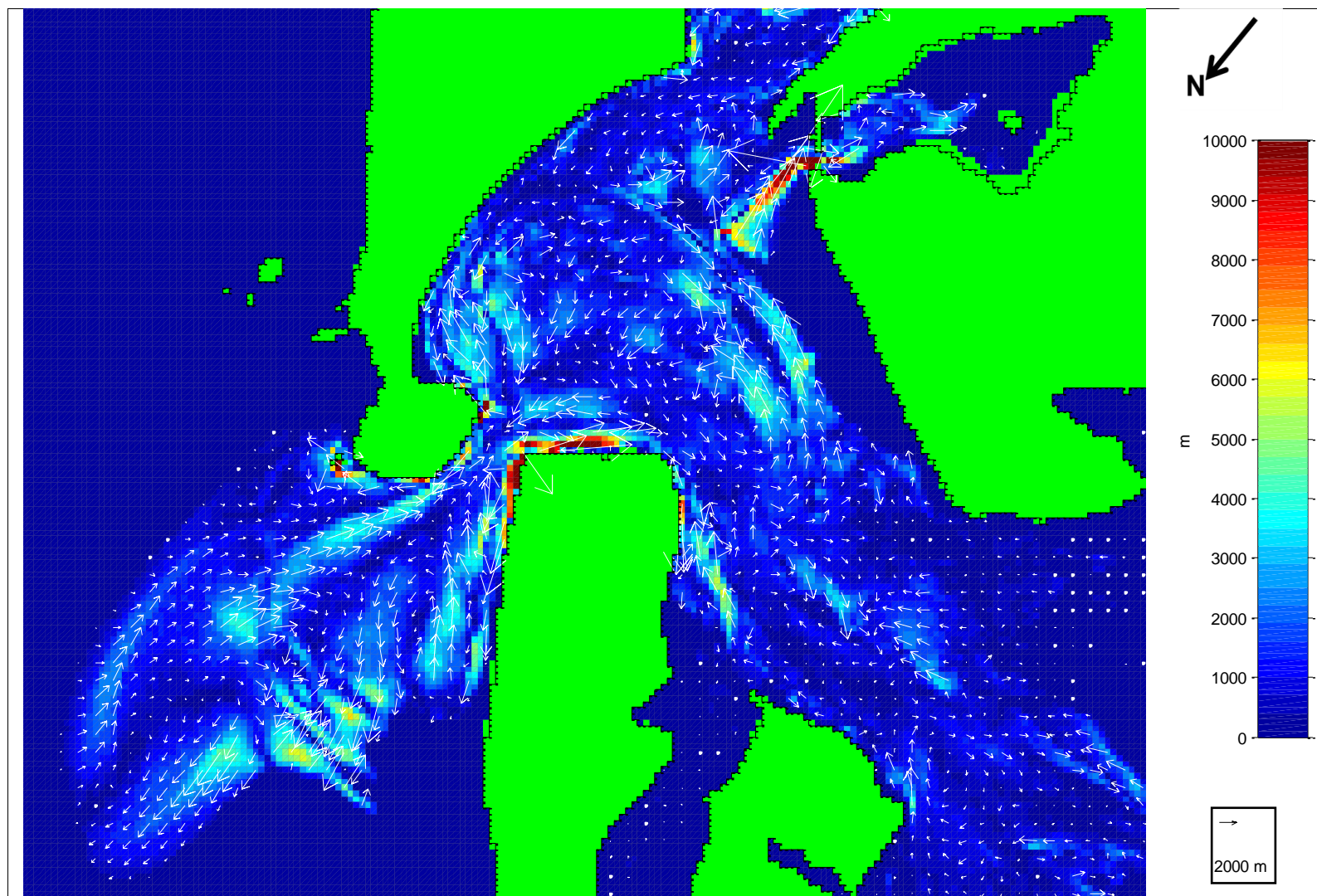


Fig. 4.13: Difference in mean spring tide residual distance vector plot (1954 – 1927) (Every third vector is displayed, colour scale maximum set at 1000).

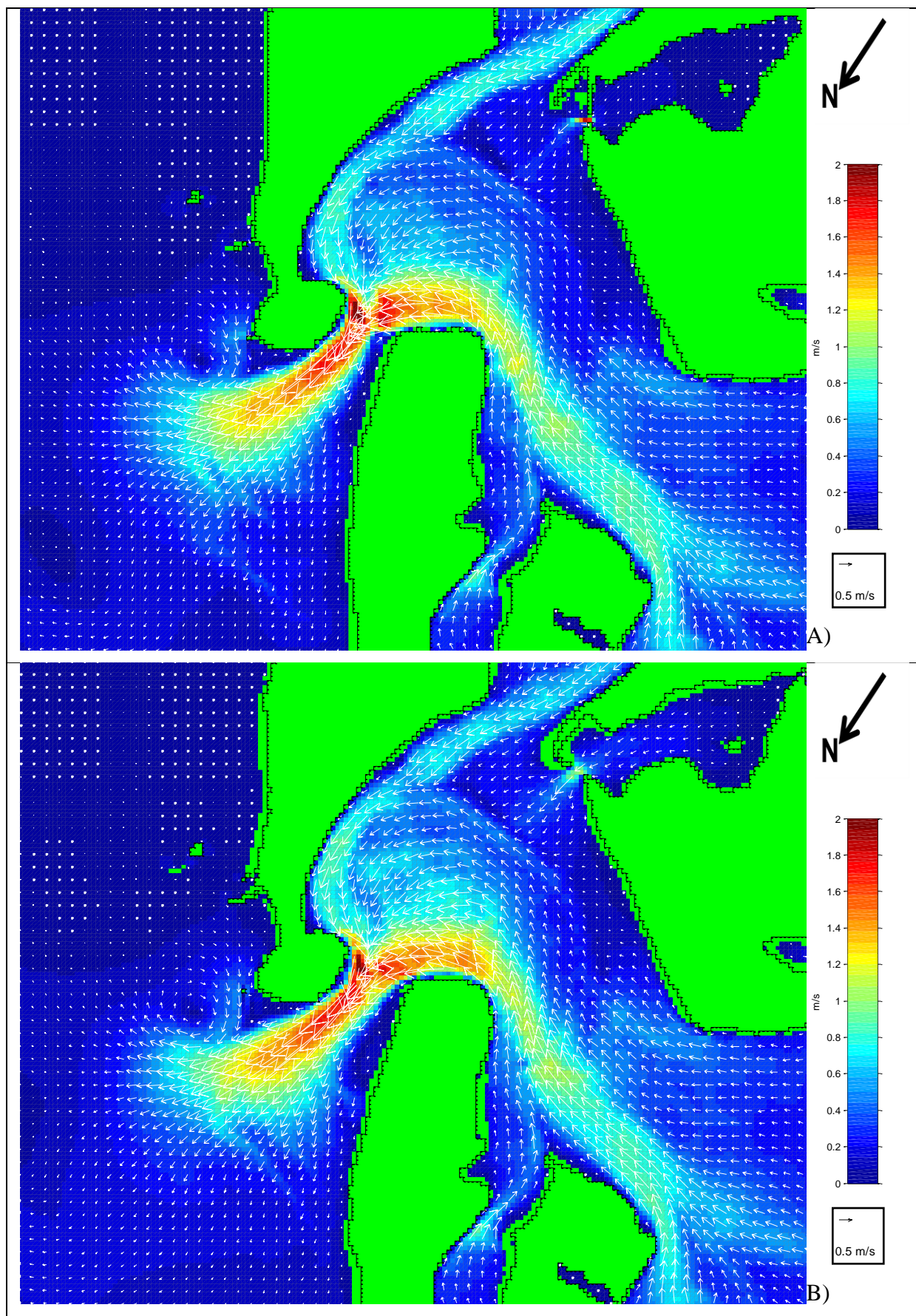


Fig. 4.14: Mean spring tide peak ebb velocity vector plot 1927 (A), and 1901 (B) (Every third vector is displayed, colour scale maximum set at 2 m/s).

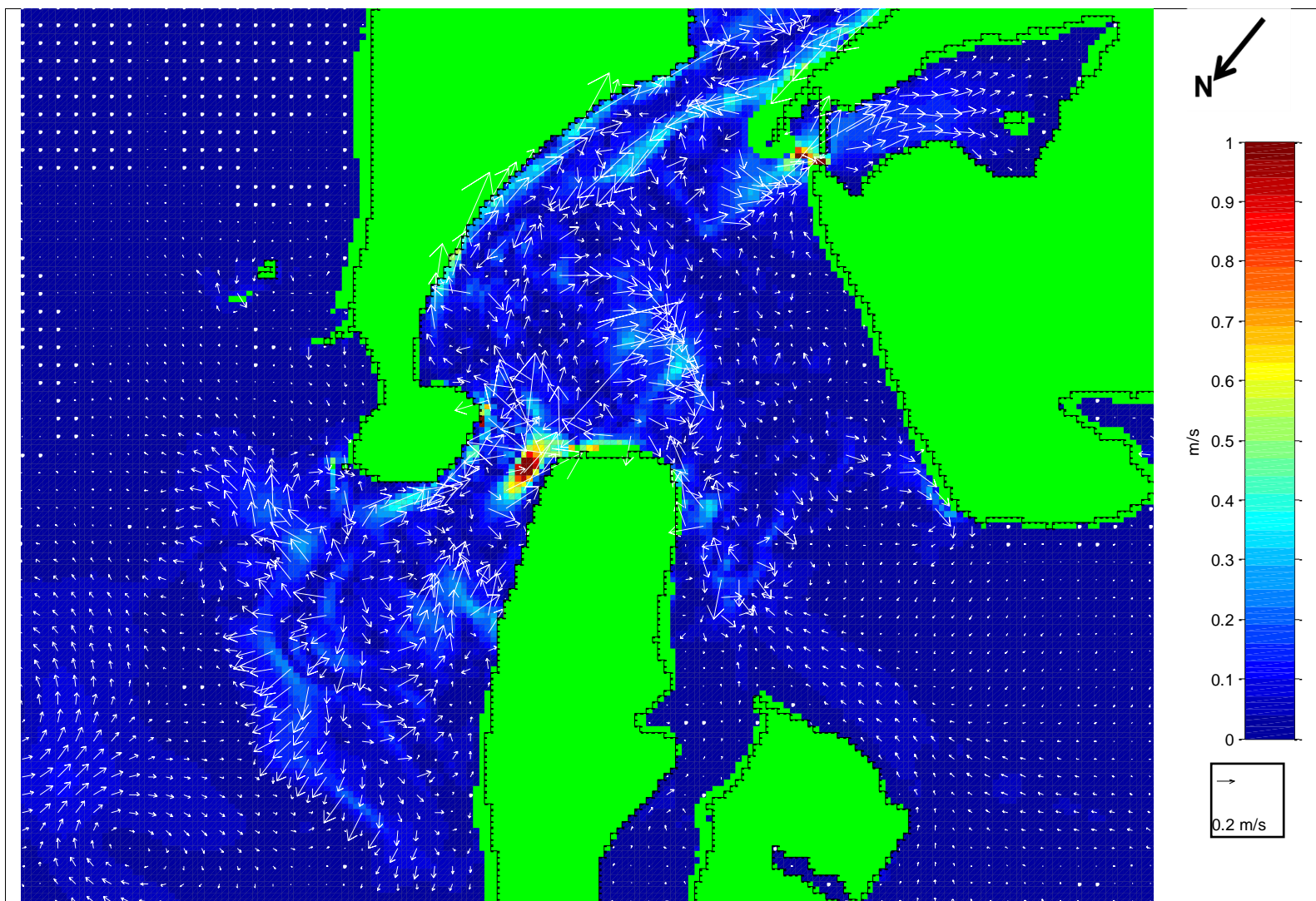


Fig. 4.15: Difference in mean spring tide peak ebb velocity vector plot (1927 - 1901). (Every third vector is displayed, colour scale maximum set at 1m/s)

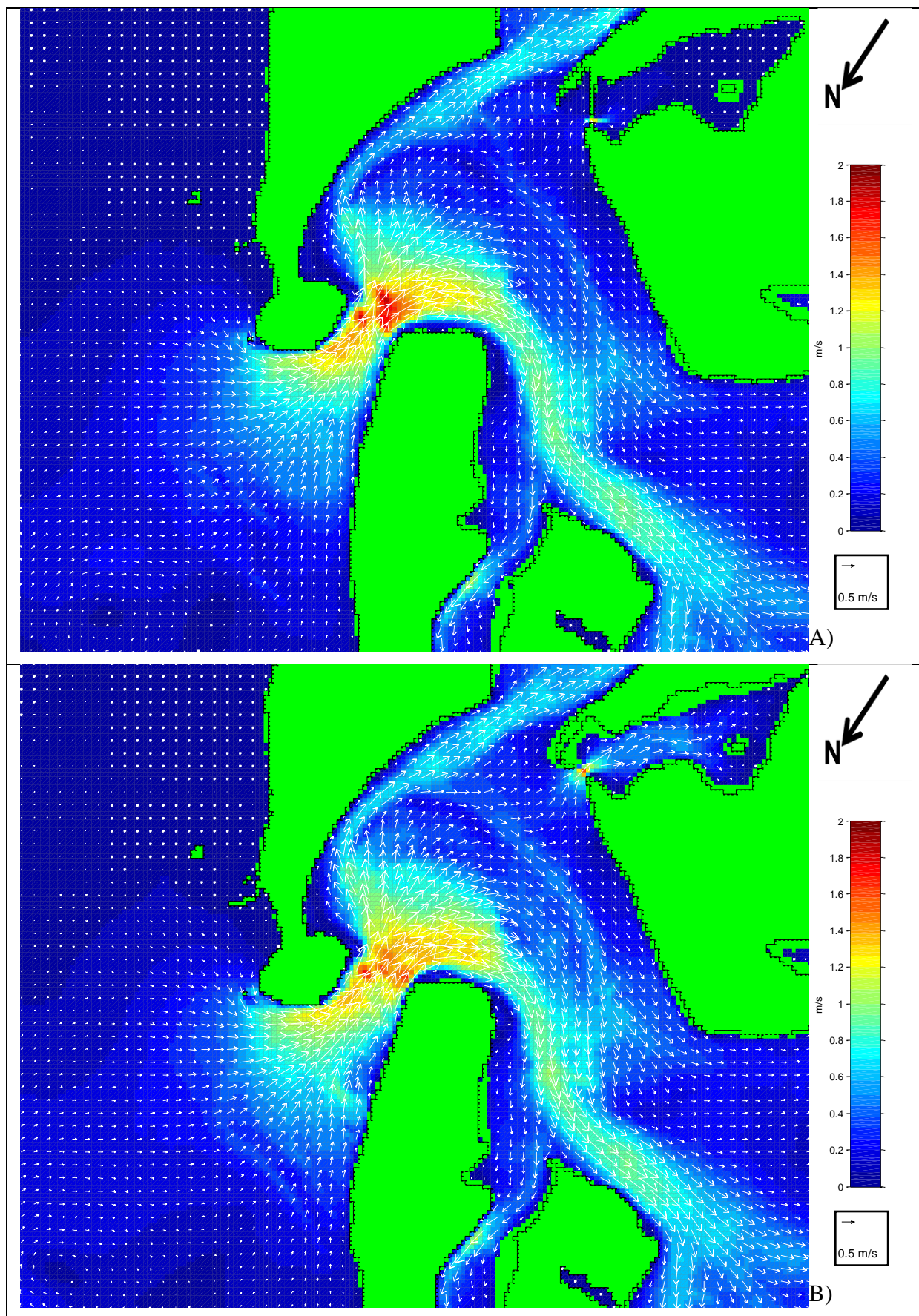


Fig. 4.16: Mean spring tide peak flood velocity vector plot 1927 (A), and 1901 (B) (Every third vector is displayed, colour scale maximum set at 2 m/s).

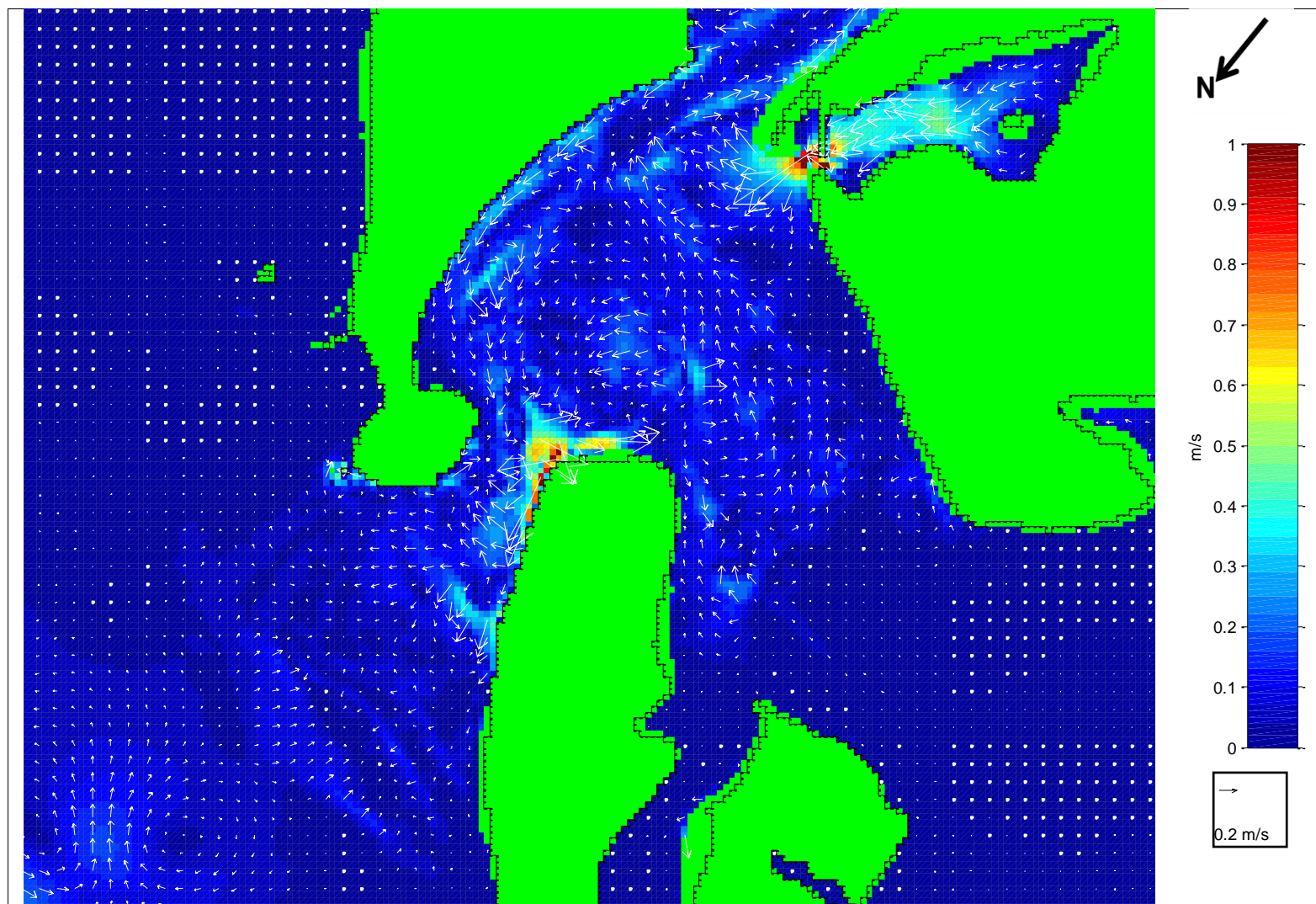


Fig. 4.17: Difference in mean spring tide peak flood velocity vector plot (1927 - 1901). (Every third vector is displayed, colour scale maximum set at 1m/s).

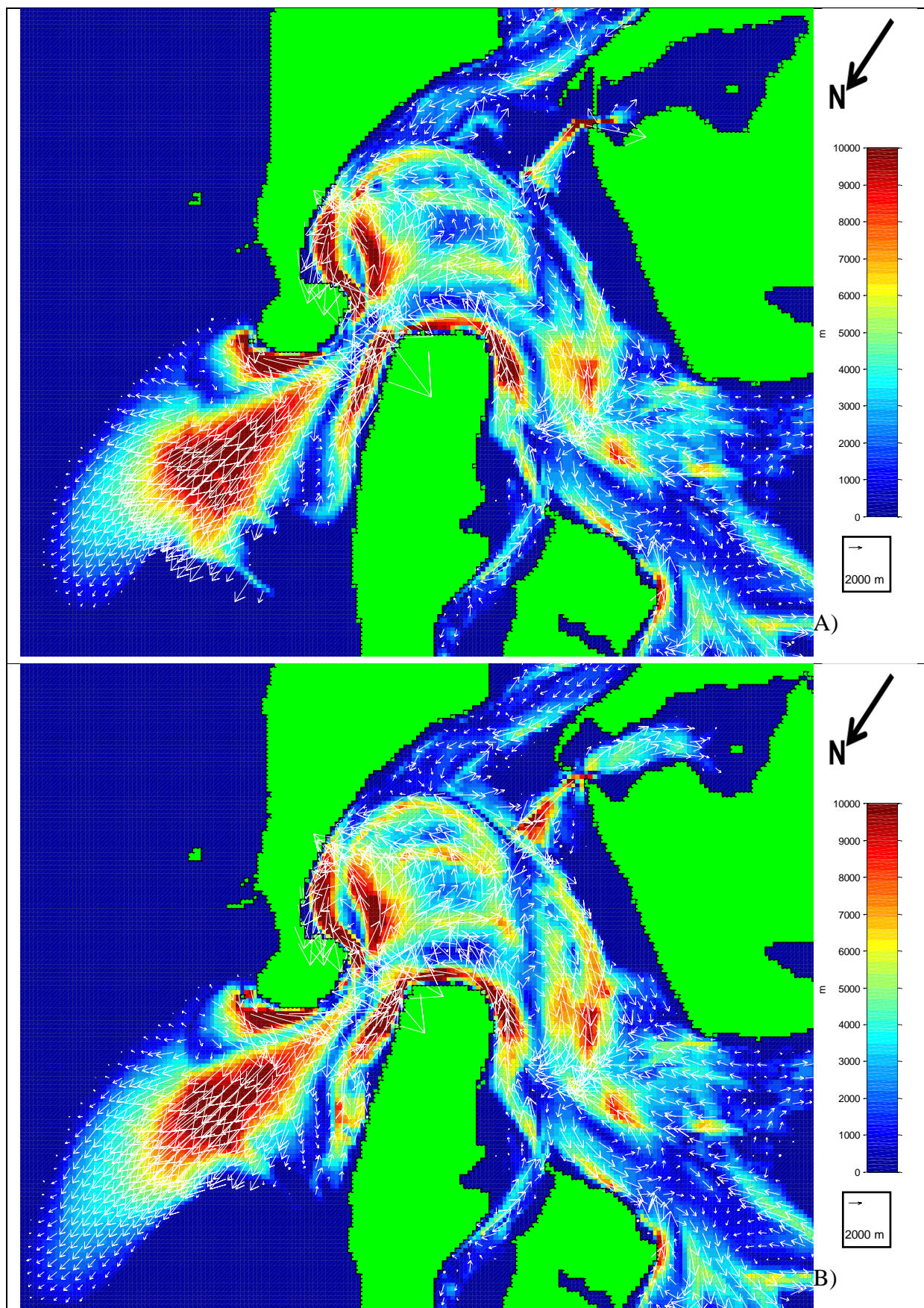


Fig. 4.18: Mean spring tide residual distance vector plot for 1927 (A) and 1901 (B) (Every third vector is displayed, colour scale maximum set at 10000 m).

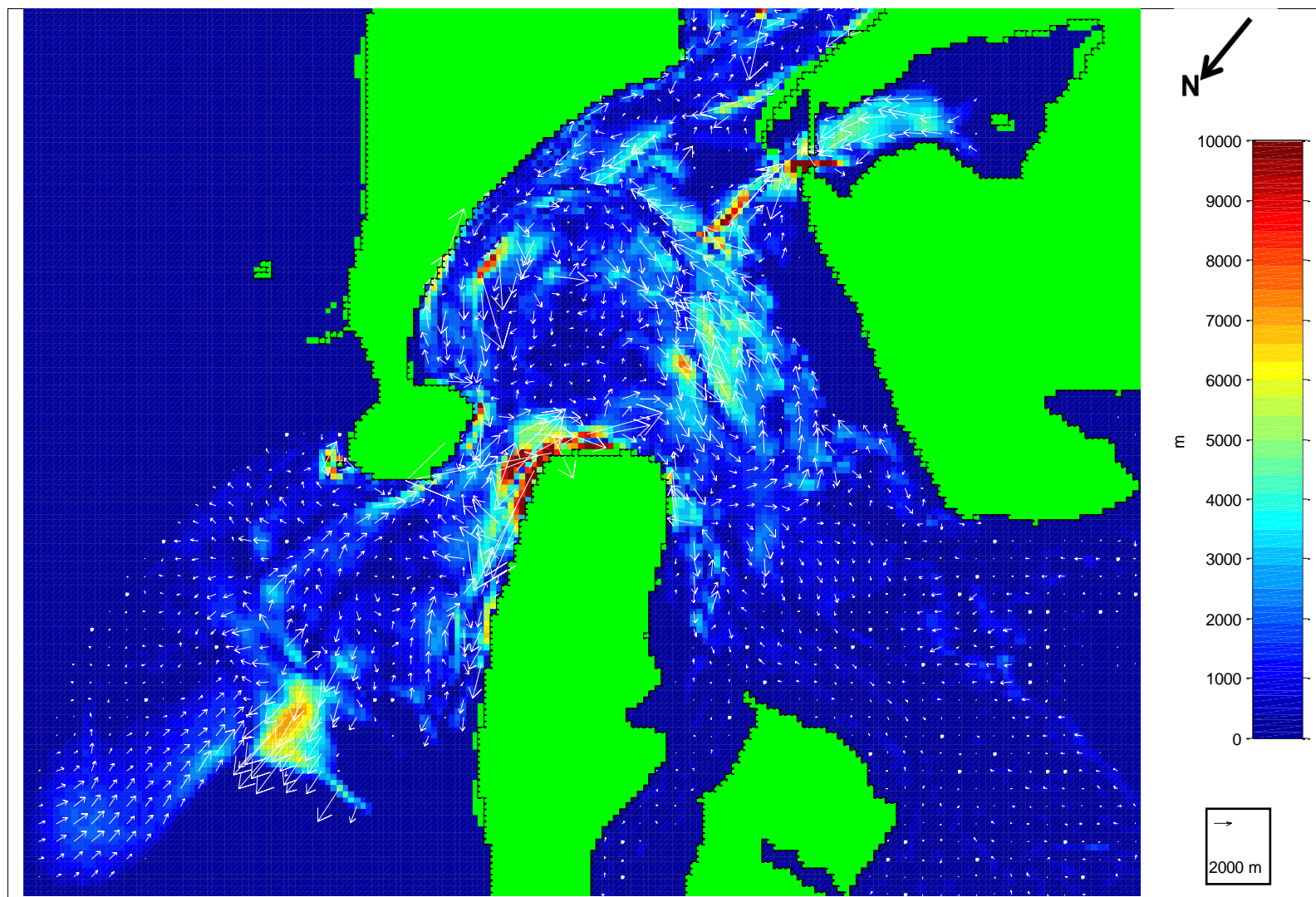


Fig. 4.19: Difference in mean spring tide residual distance vector plot (1927 - 1901) (Every third vector is displayed, colour scale maximum set at 1000).

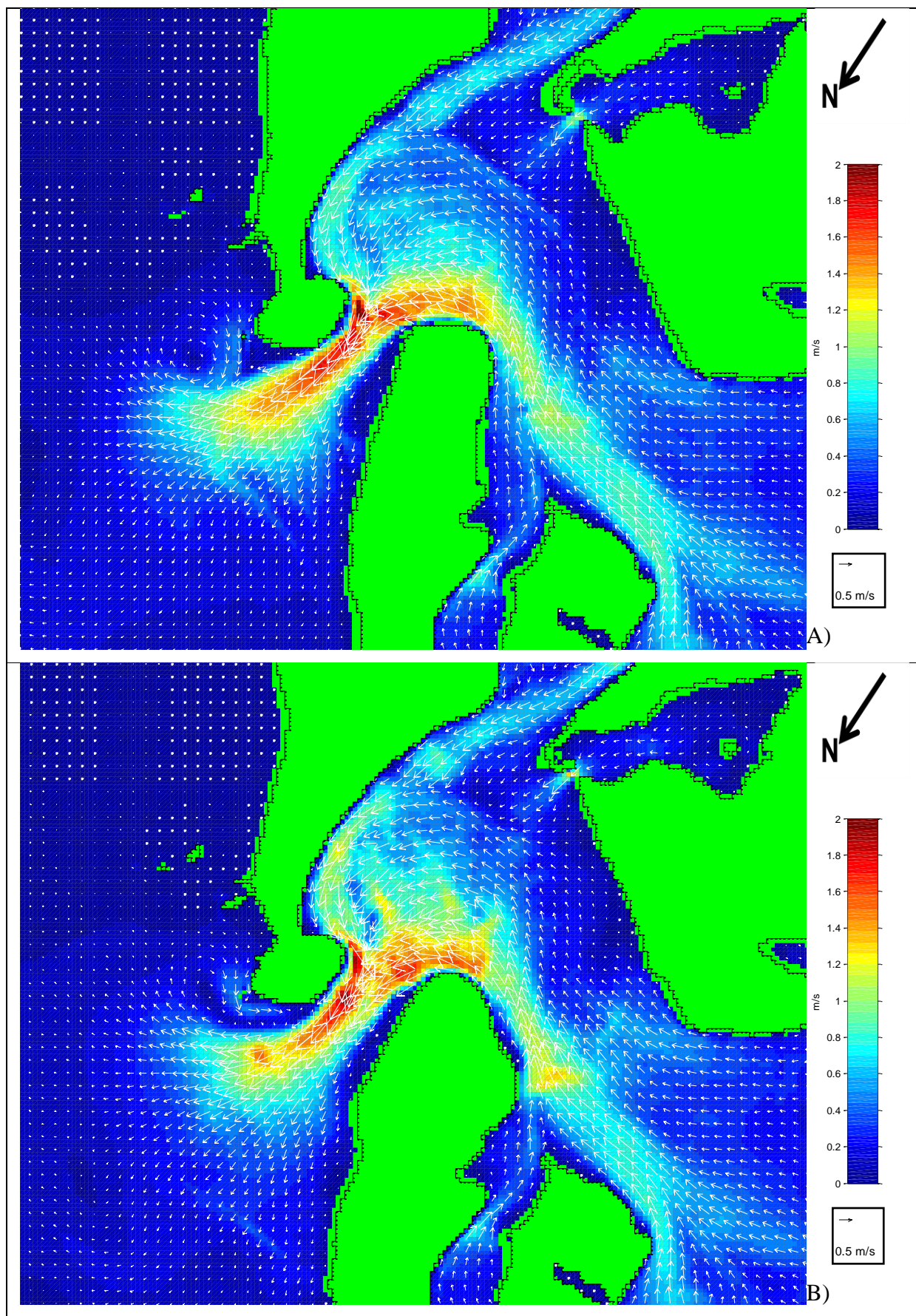


Fig. 4.20: Mean spring tide peak ebb velocity vector plot 1901 (A), and 1879 (B) (Every third vector is displayed, colour scale maximum set at 2 m/s).

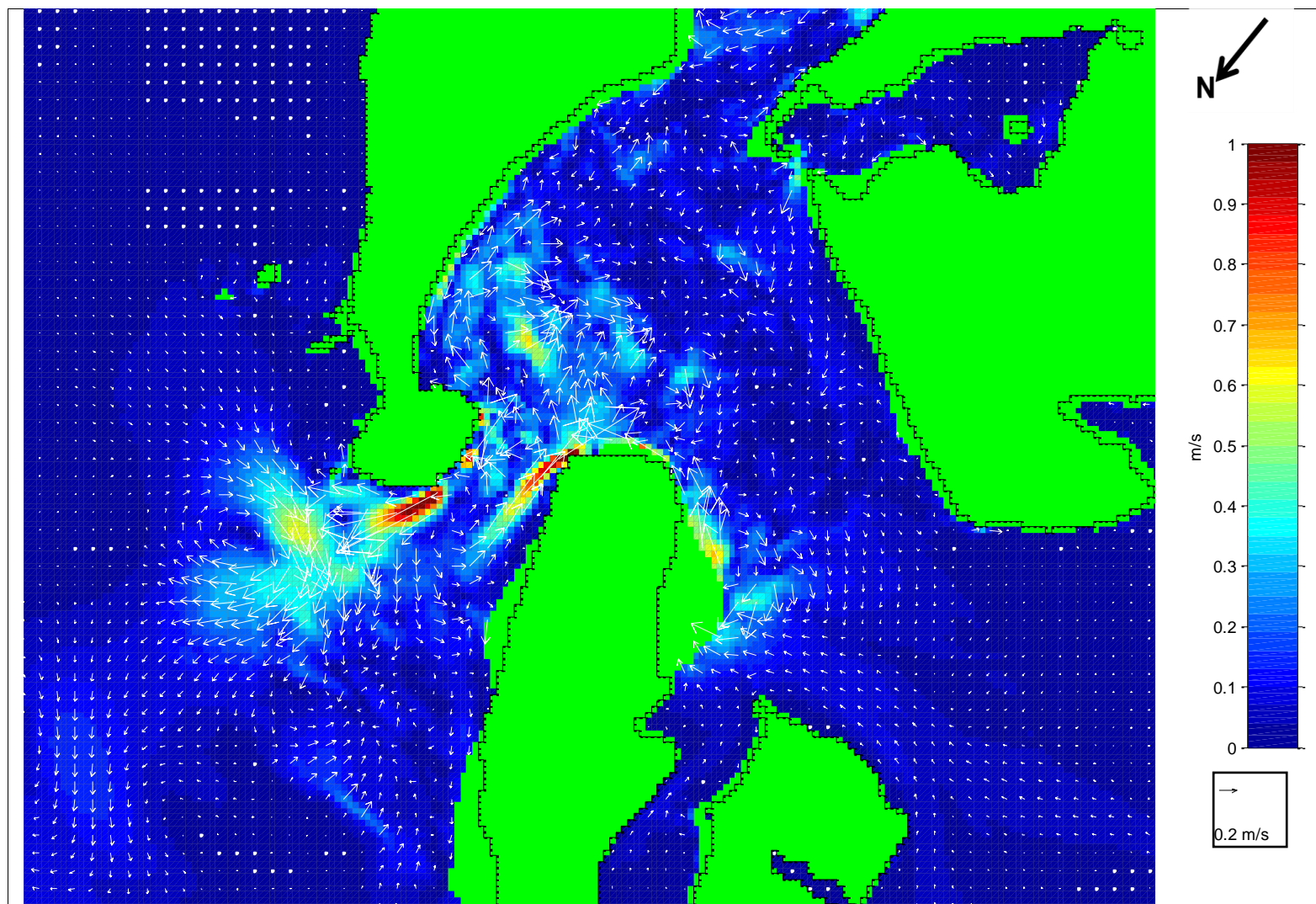


Fig. 4.21: Difference in mean spring tide peak ebb velocity vector plot (1901 - 1879). (Every third vector is displayed, colour scale maximum set at 1m/s)

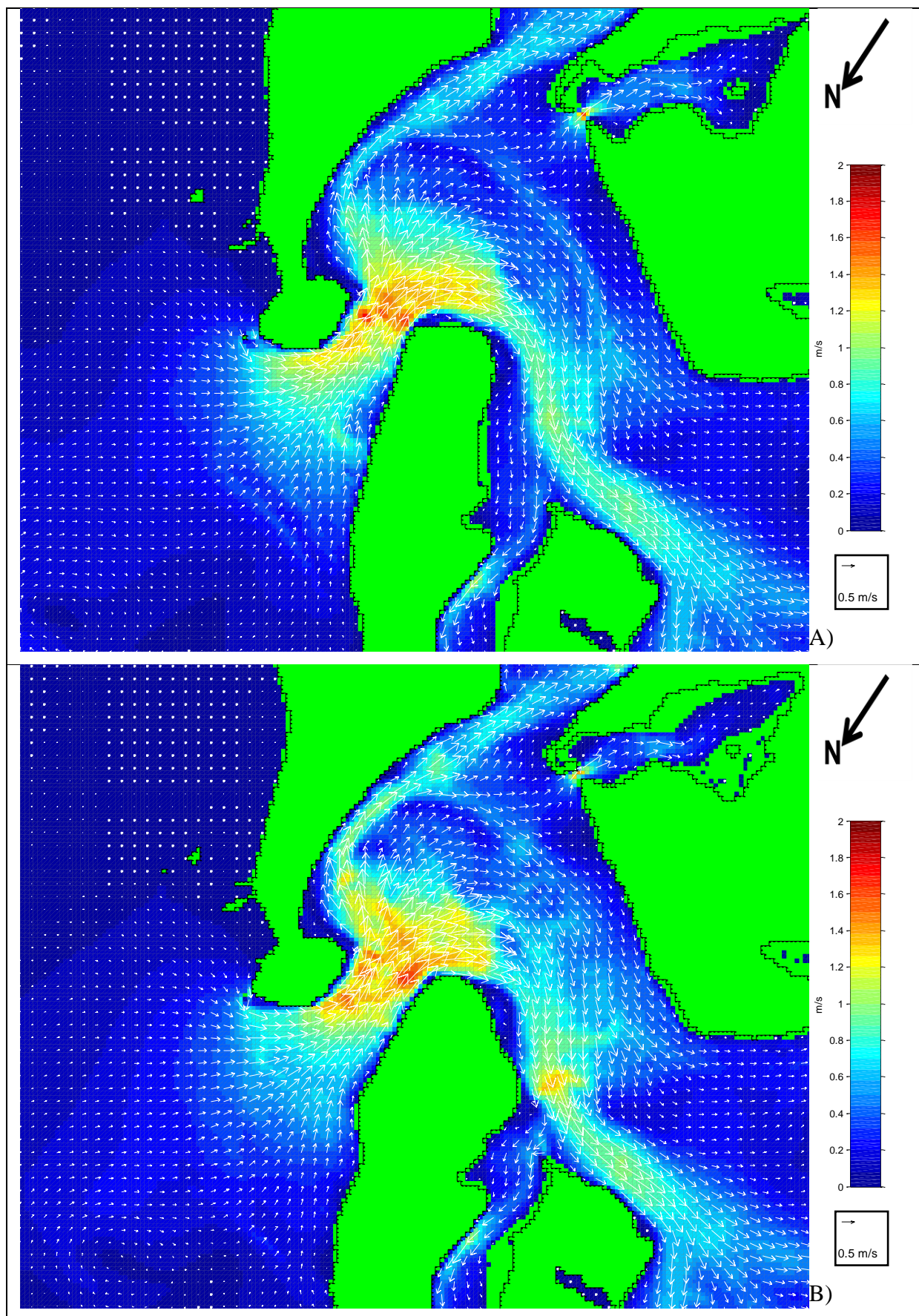


Fig. 4.22: Mean spring tide peak flood velocity vector plot 1901 (A), and 1879 (B) (Every third vector is displayed, colour scale maximum set at 2 m/s).

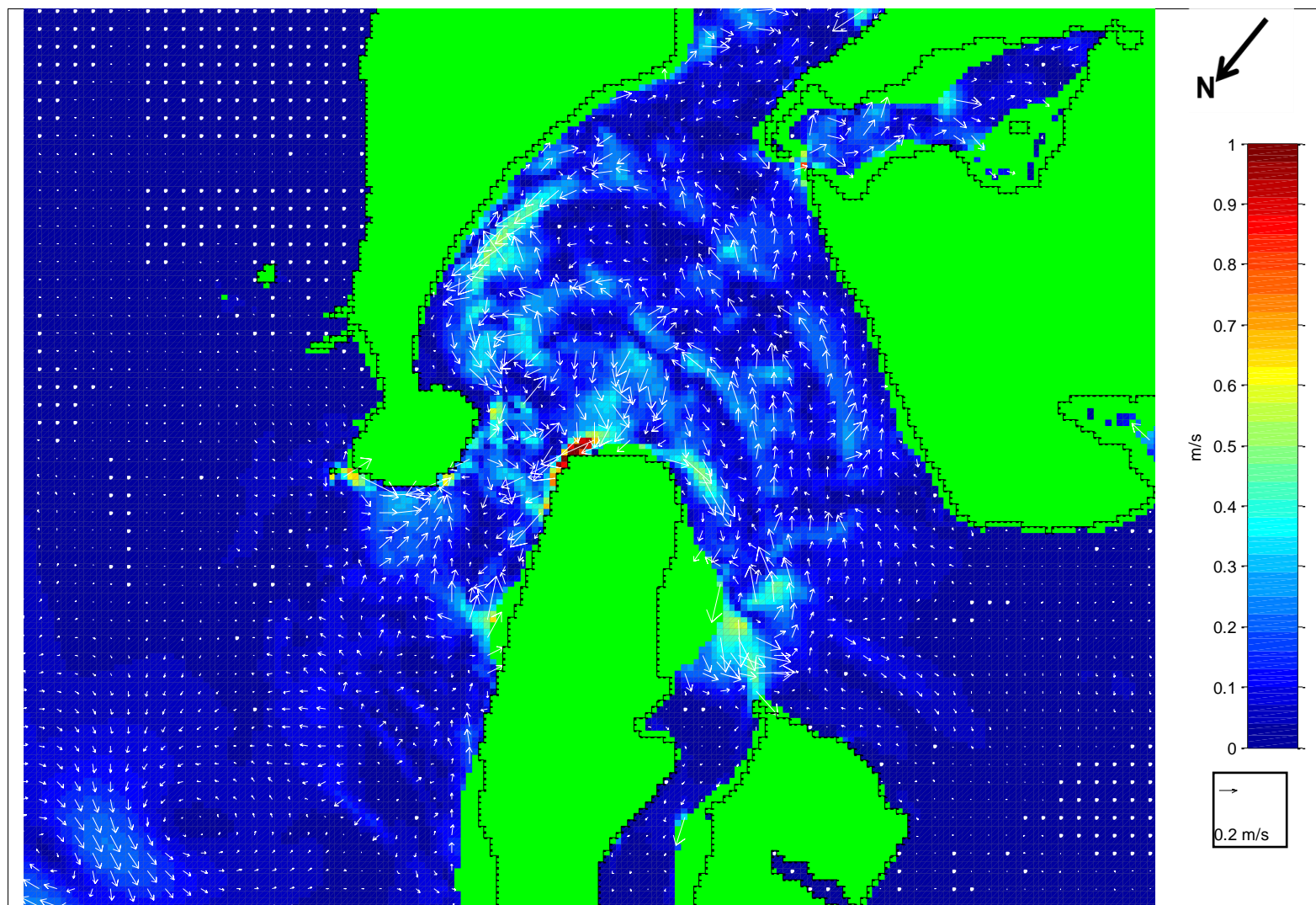


Fig. 4.23: Difference in mean spring tide peak flood velocity vector plot (1901 - 1879). (Every third vector is displayed, colour scale maximum set at 1m/s).

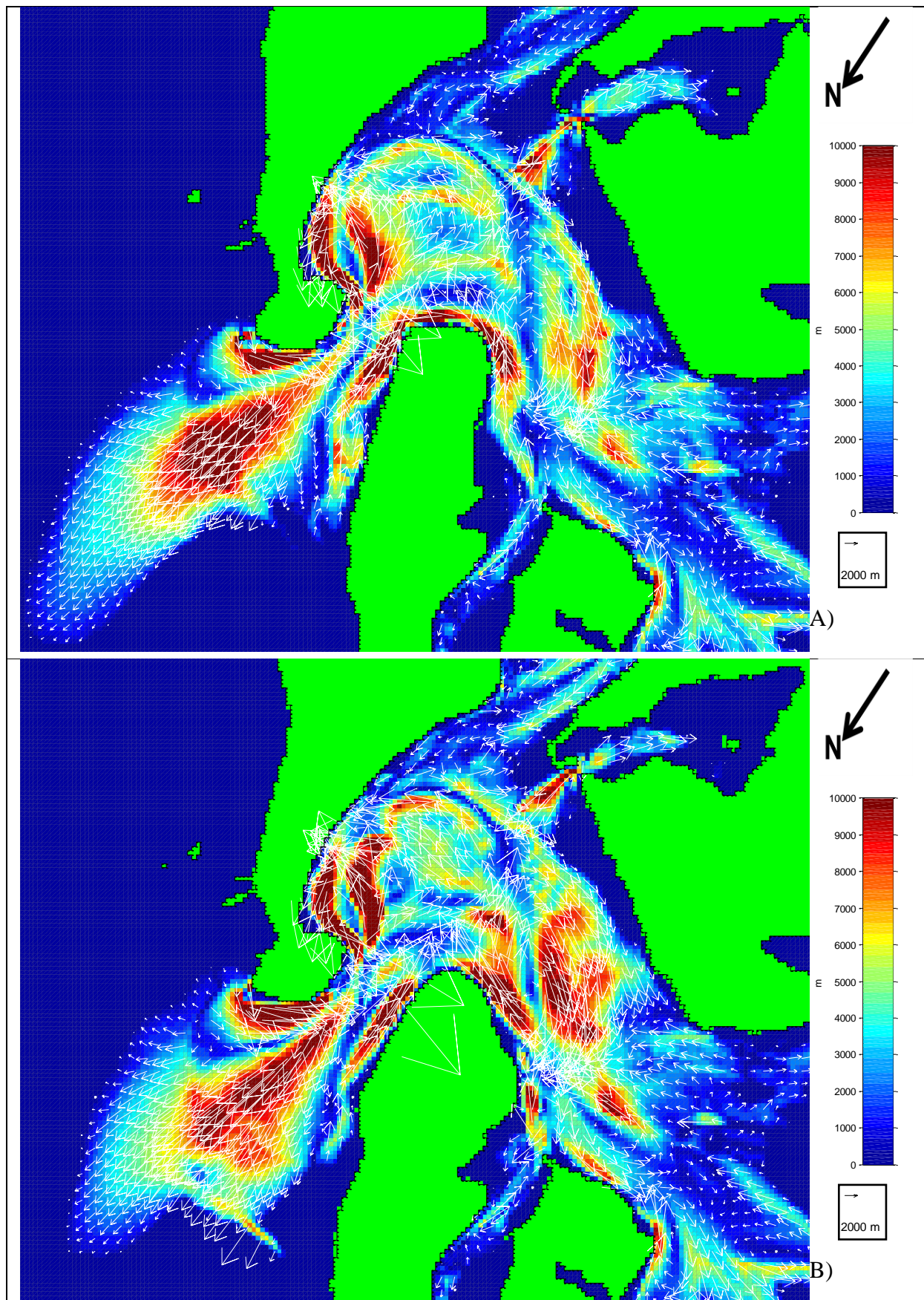


Fig. 4.24: Mean spring tide residual distance vector plot for 1901 (A) and 1879 (B) (Every third vector is displayed, colour scale maximum set at 10000 m).

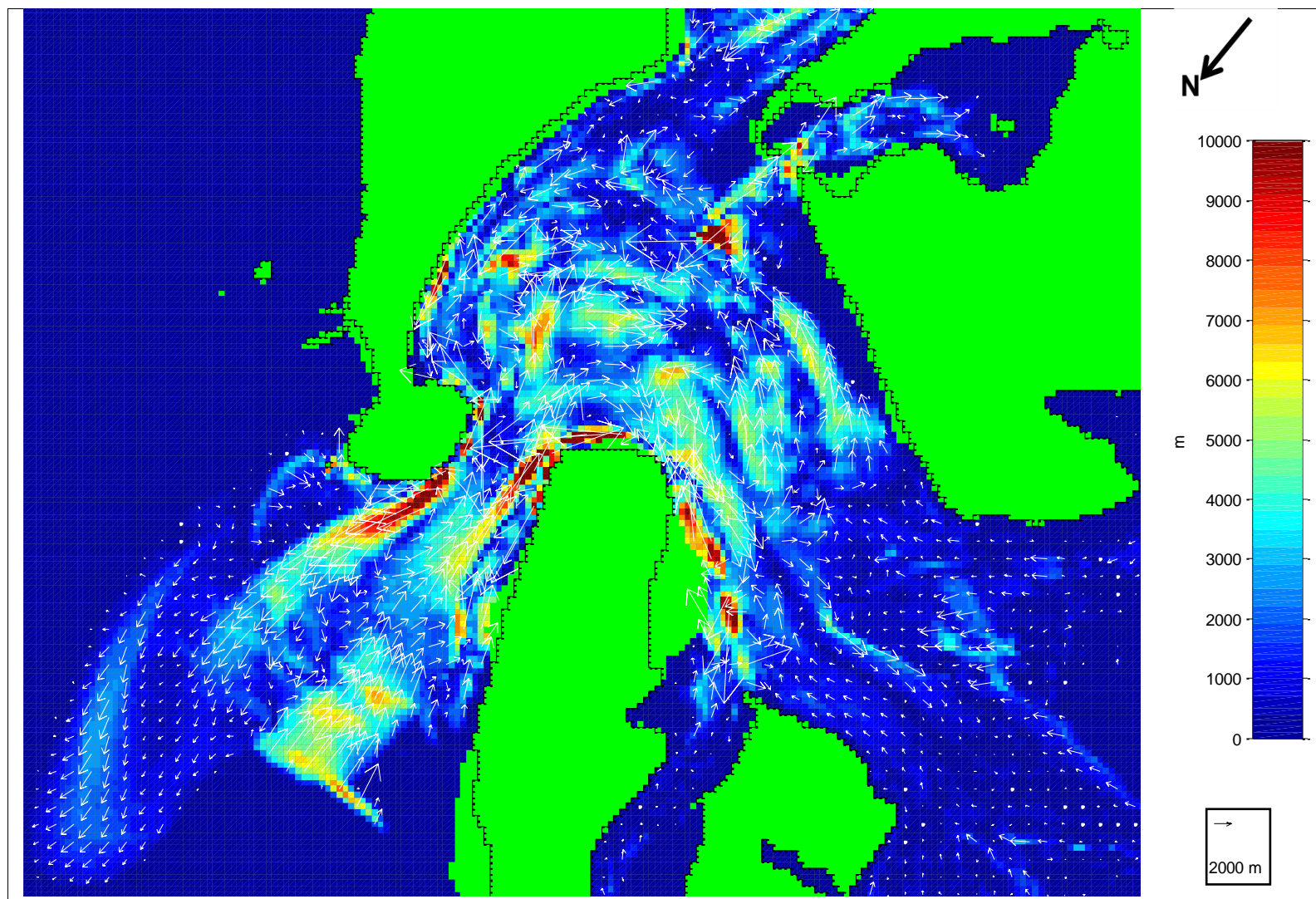


Fig. 4.25: Difference in mean spring tide residual distance vector plot (1879 - 1901) (Every third vector is displayed, colour scale maximum set at 1000).

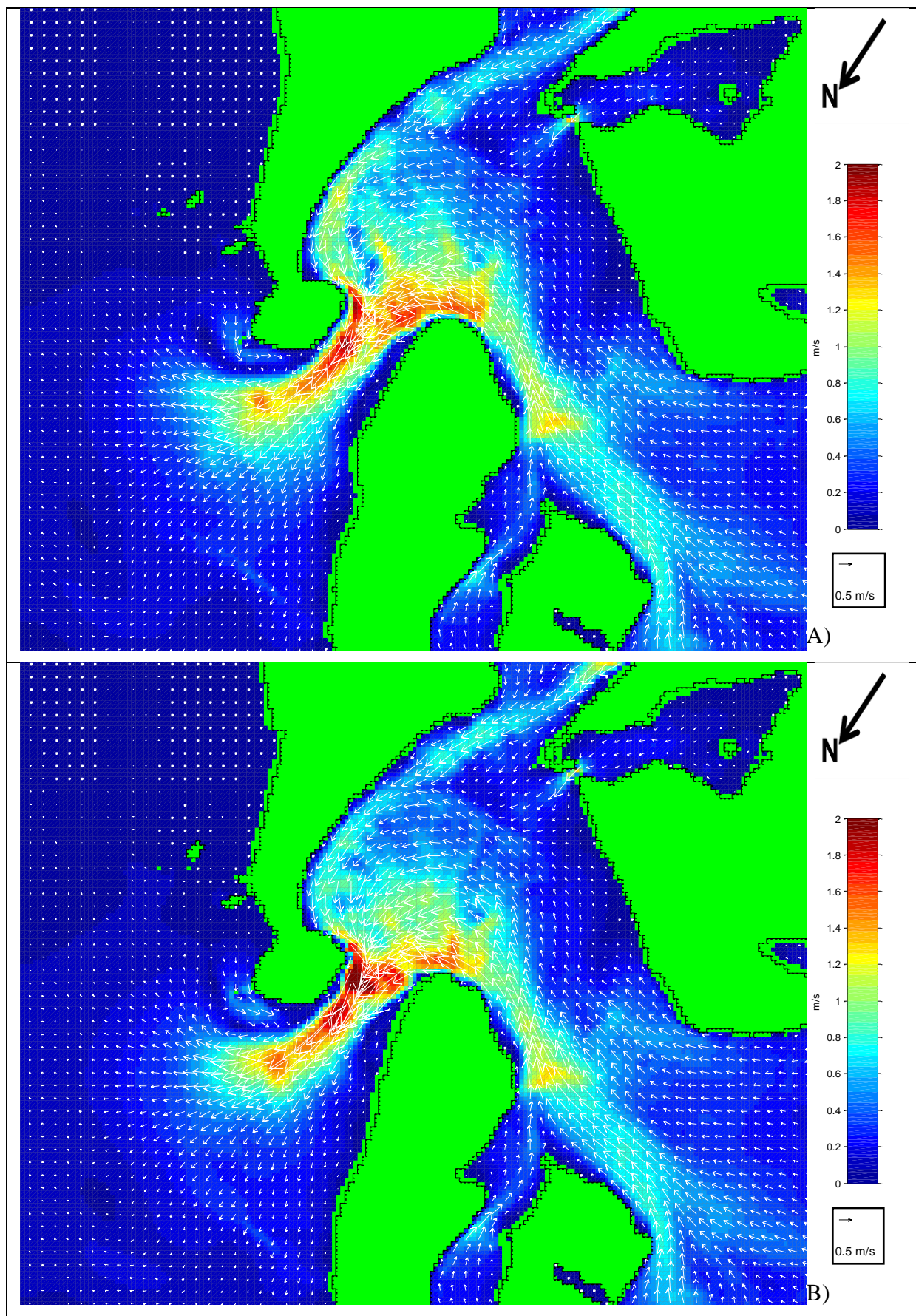


Fig. 4.26: Mean spring tide peak ebb velocity vector plot 1879 (A), and 1852 (B) (Every third vector is displayed, colour scale maximum set at 2 m/s).

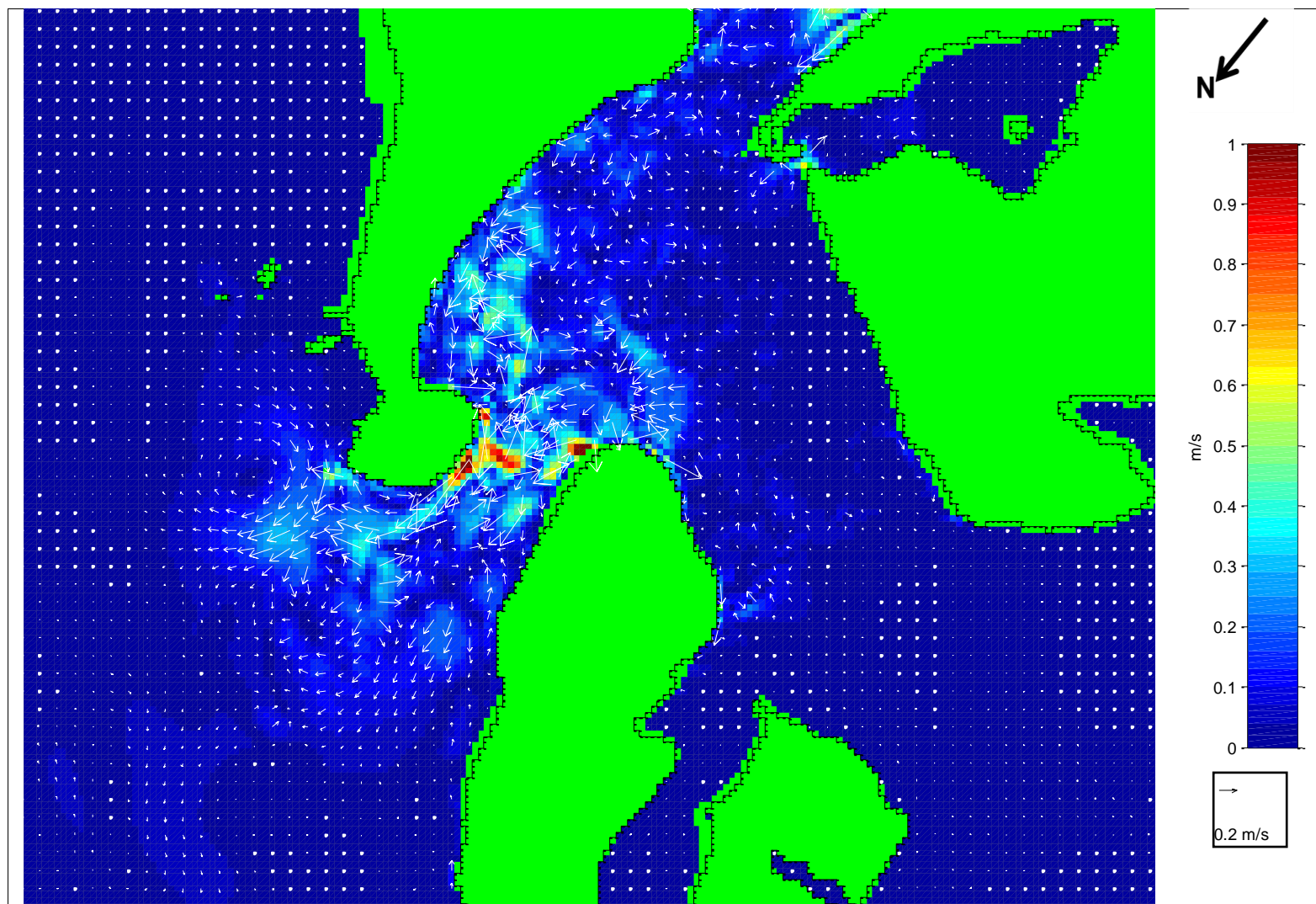


Fig. 4.27: Difference in mean spring tide peak ebb velocity vector plot (1879 - 1852). (Every third vector is displayed, colour scale maximum set at 1 m/s).

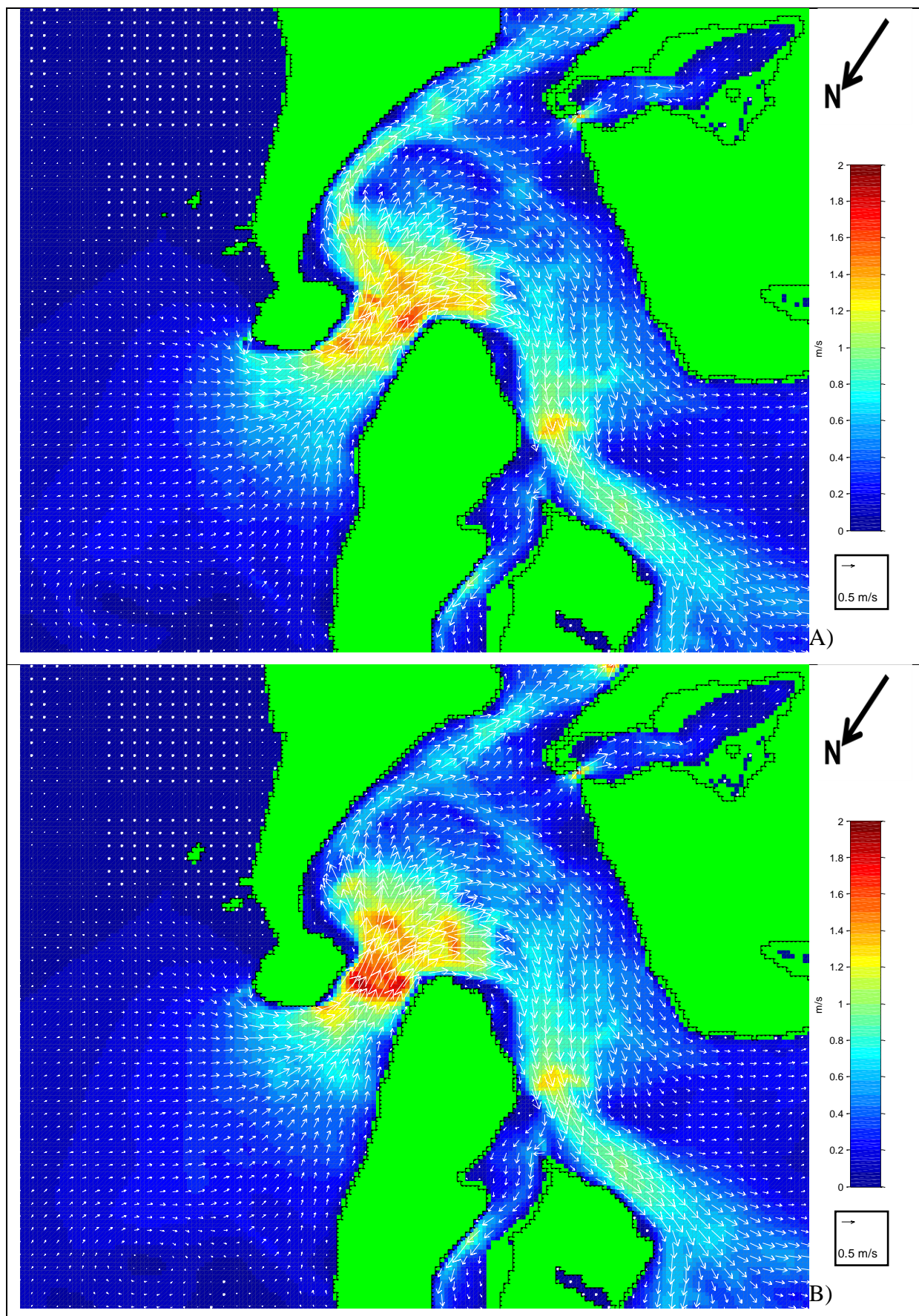


Fig. 4.28: Mean spring tide peak flood velocity vector plot 1879 (A), and 1852 (B) (Every third vector is displayed, colour scale maximum set at 2 m/s).

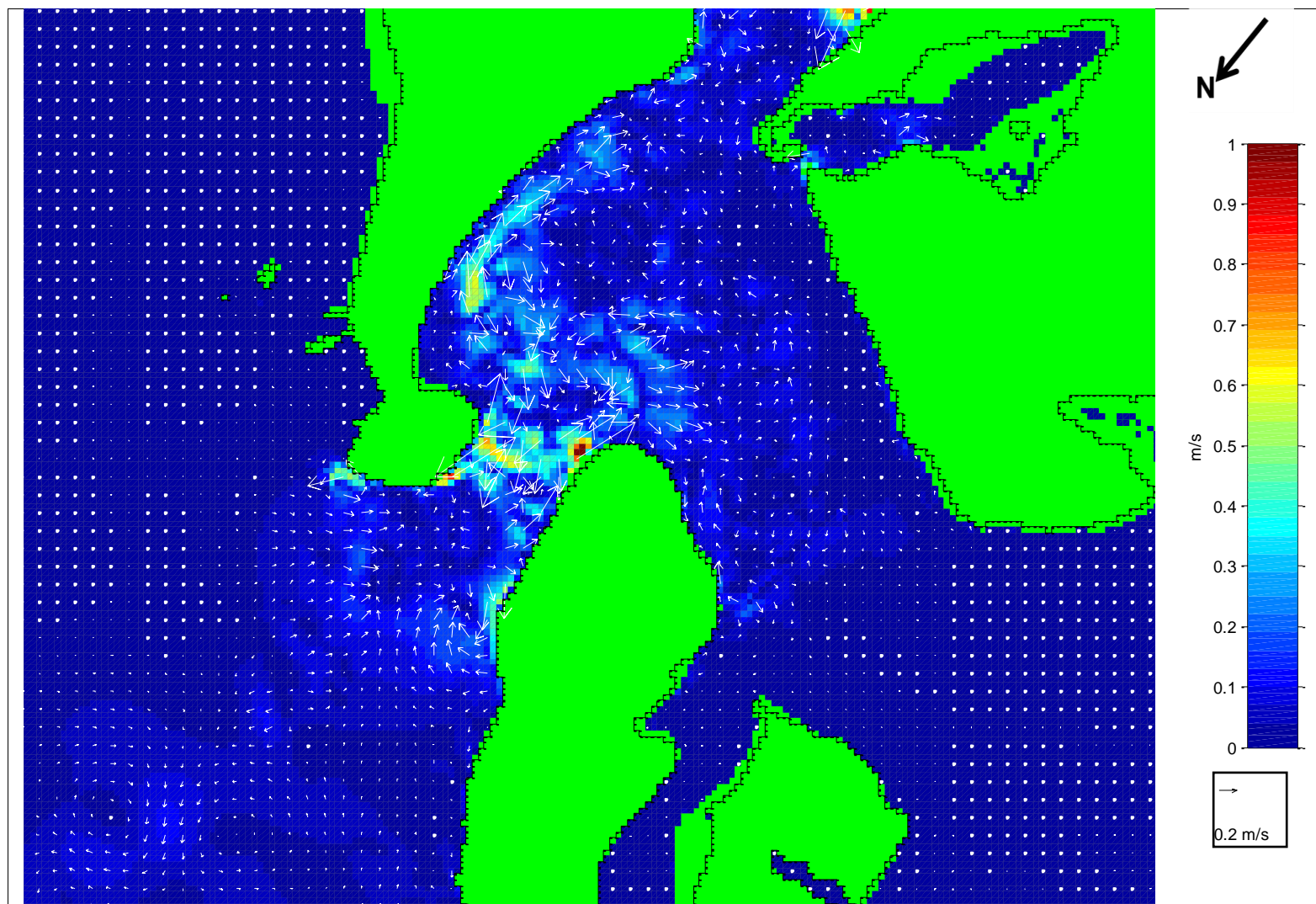


Fig. 4.29: Difference in mean spring tide peak flood velocity vector plot (1879 - 1852). (Every third vector is displayed, colour scale maximum set at 1 m/s).

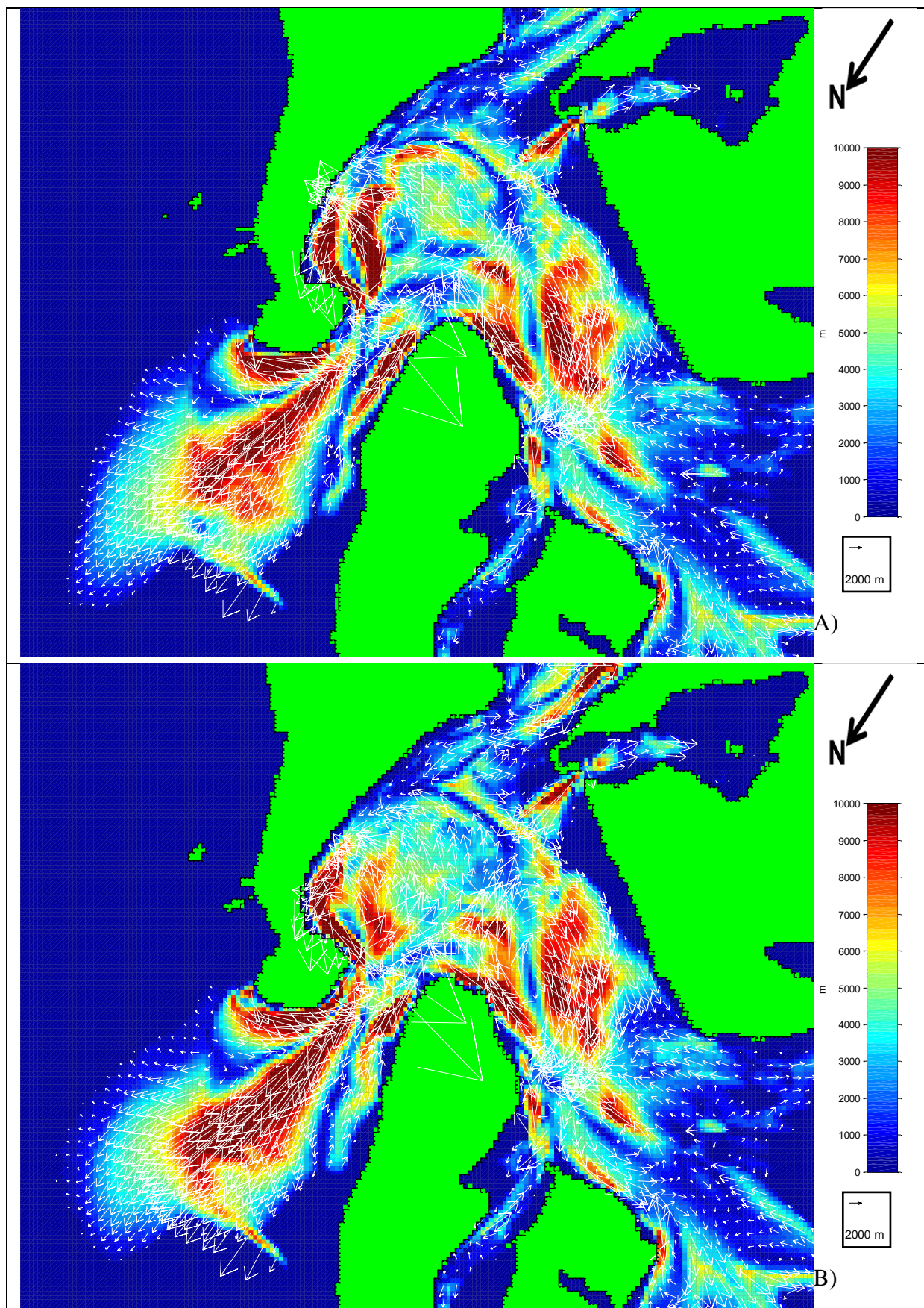


Fig. 4.30: Mean spring tide residual distance vector plot for 1879 (A) and 1852 (B) (Every third vector is displayed, colour scale maximum set at 10000 m).

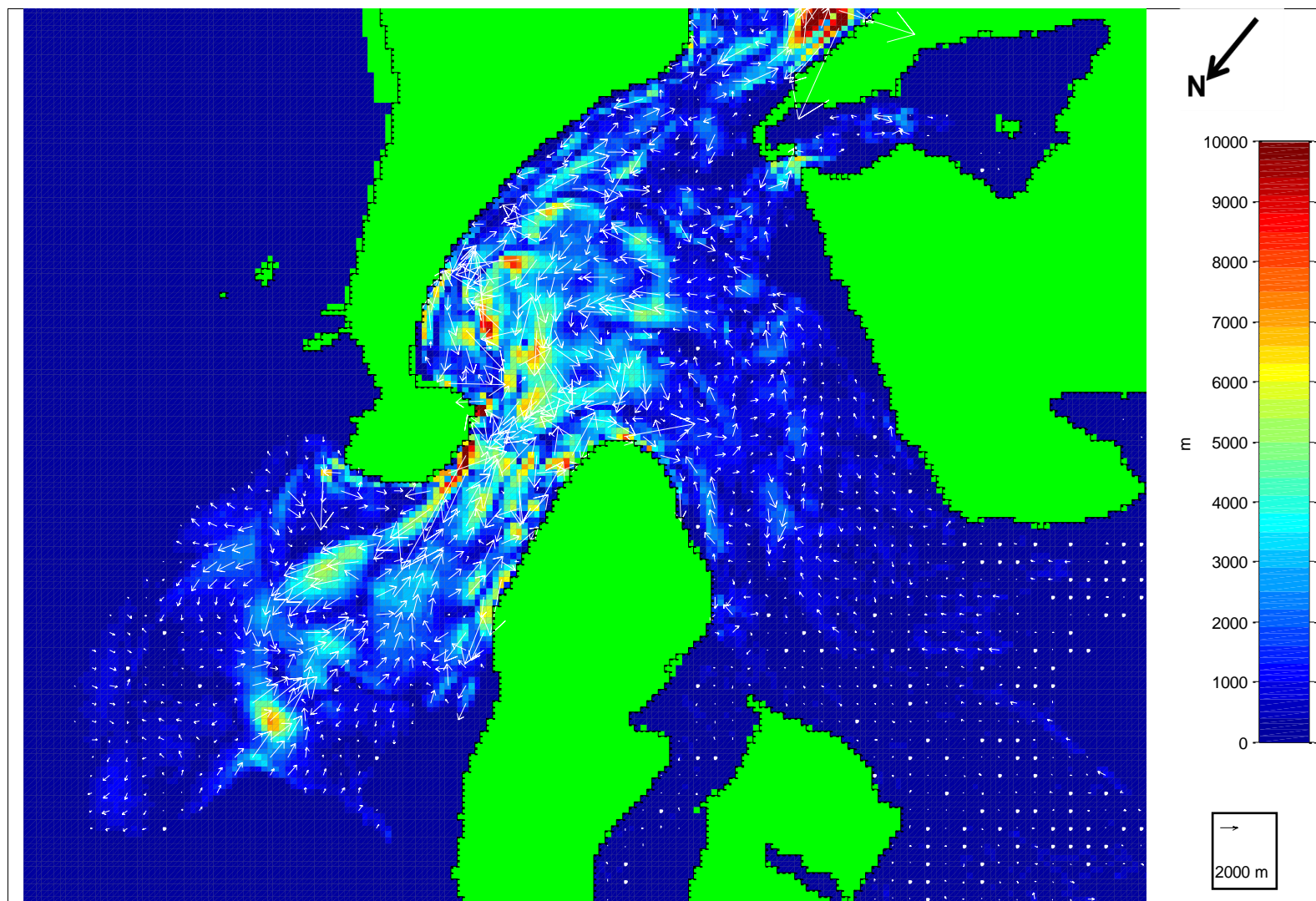


Fig. 4.31: Difference in mean spring tide residual distance vector plot (1879 - 1852) (Every third vector is displayed, colour scale maximum set at 1000

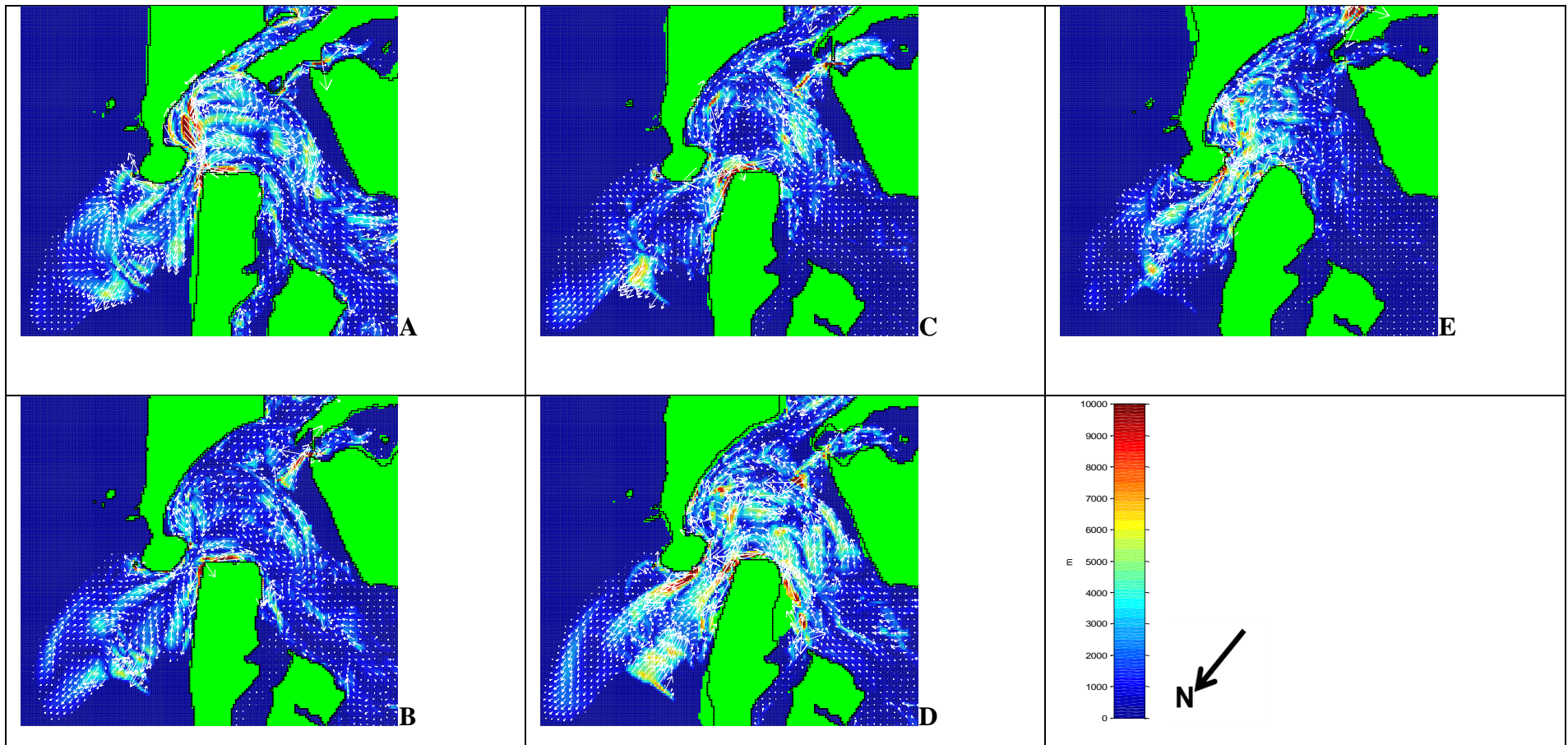


Fig 4.32: Difference in mean spring tide residual distance plots. (A: 2007 – 1954. B:1954 – 1927. C: 1927 – 1901. D: 1901 – 1879. E: 1879 – 1852).

5. CHANGES IN SURFICIAL SEDIMENT, SHELL COVERAGE AND BEDFORMS OF THE TIDAL DELTA SYSTEM.

5.0. INTRODUCTION

The morphology of ebb and flood tidal delta systems is complex with sediment patterns responding to the changing action of high energy waves and currents. (Fitzgerald et al., 2000; Donda et al., 2008). Dredging can significantly affect the evolution of ebb and flood tidal delta systems (Johnson, 1981) and consequently it is important to monitor changes in sedimentation patterns in order to better understand the formation process. Sediment transport pathways can be mapped through the use of sidescan sonar which provides an acoustic image of the seabed, detailing the distribution of surficial sediment, bedforms and large features such as shoals and channels (Lurton, 2002; Morang & Gorman 2005).

Very few studies assessing historical changes in surficial sediments of tidal inlets have been published. Those that are available tend to have a different focus. For example, Lesourd et al. (2003) investigated seasonal variation in the sedimentary regime in a macrotidal estuary over a three year period. Vilas et al. (2005) considered surficial sediment properties of three rias in Spain while Buynevich and Fitzgerald (2003) assessed textural characteristics of bottom sediments from an inlet along a paraglacial coastline. Nitsche et al. (2007) described the distribution of sediment texture in the Hudson River Estuary. Black et al. (1989) investigated sand and shell coverage of a tidal estuary near a future marine terminal. These studies have not considered the changes in surficial sediment over a long term (25 year) period in a dredged tidal inlet delta system, as considered in this study. Therefore, this study may serve as a model for future studies investigating long-term changes in surficial sediments in tidal inlets whilst also providing a basis from which to begin investigating changes in tidal inlet delta ecology, particularly changes in distribution and abundance of benthic organisms that are dependent upon surficial sediment grain size.

Hence, the aim of this chapter is to document changes in the surficial sediment of the ebb and flood tidal delta of the Tauranga entrance to Tauranga Harbour in order to contribute to the understanding to the effect dredging on the changing morphological behaviour.

5.0.1. Sidescan sonar configuration

Sidescan sonar is a device that is used to provide high definition acoustic images of the seafloor. It is primarily used to determine the sediment characteristics of the seabed, surface bedforms, and large features such as shoals and channels. The sidescan sonar measures the time it takes for a transmitted acoustic pulse to reflect off a target and return to the transducer and intensity from which it produces an output known as a sonograph which is analogous to an aerial photograph of the seabed (Morang and Gorman 2005).

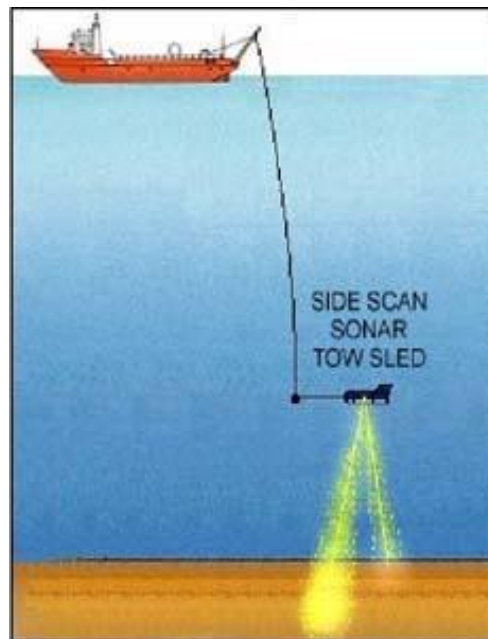


Figure 5.1: Diagram showing the tow fish (or tow sled), electromagnetic cable and the vessel which carries the onboard unit. The outside of the swath covered by the sonar beam is shown in yellow (Source: NOAA, 2002).

The sidescan sonar has three major components (Fig 5.1):

- 1) A “fish” that is towed behind the vessel near the bottom and contains two opposing transducers that transmit and receive the acoustic signal.
- 2) An onboard unit which gathers the data.
- 3) An electromagnetic tow cable that transmits data between the fish and the data acquisition unit (Lurton 2002, Morang et al. 1997).

The transducer is the central part of the sidescan sonar system which transmits and receives the sound. Most transducers contain a piezoelectric crystal; a ceramic material that has the capability of changing shape when a voltage is applied through it. It changes the oscillating electrical energy into mechanical energy, or sound (Mazel 1985) . The sound pulse - controlled by the acoustic properties of the water – travels away from the transducer until it hits the seabed or a target and some of the sound is reflected back to the transducer (Brekhovskikh and Lysanov 2003; Wille, 2005). The transducer then captures the reflected sound energy and converts it back to electrical energy where it is detected by the receiver. This data is then displayed in the form of a sonar image known as a sonograph (Mazel 1985).

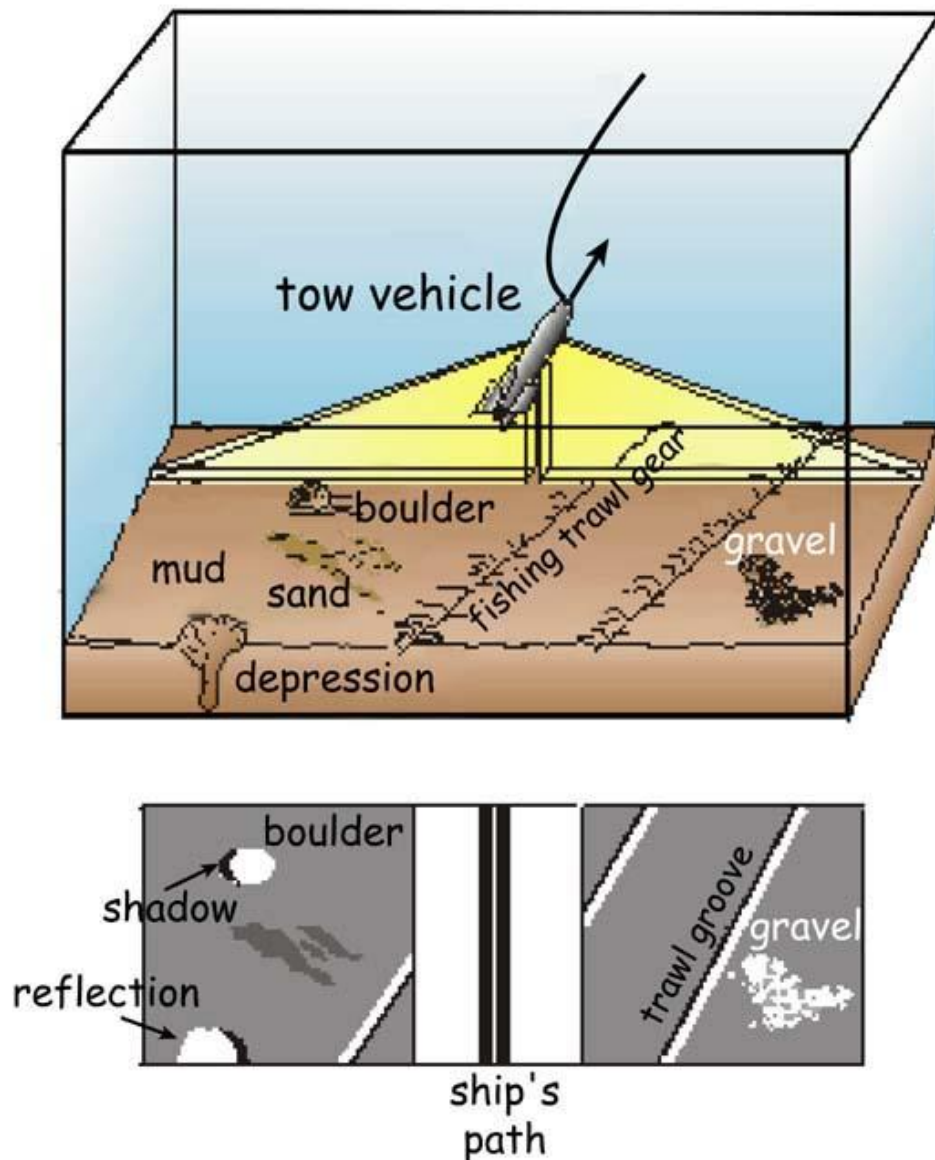


Figure 5.2: Schematic diagram showing the horizontal pulse transmitted by the towfish and the corresponding sonograph image beneath it (Note: In this image high backscatter is shown as light colours and low backscatter is shown as dark colours). (Source: NOAA, 2007).

The transducers in the towfish transmit a high frequency acoustic pulse which is narrow in the horizontal direction (around 1°) at right angles to the tow direction (Fig 5.2). After a short period in time (from a few milliseconds up to one second) the pulse then reflects off the seafloor, and is captured by the transducers which transforms the acoustic energy into electrical energy and transmits the signal to the signal processing unit on the survey boat. The signal processing unit records one pulse at a time, then pieces these pulses together to form a continuous sonograph which is analogous to an aerial photograph (Kenny 2003, Lurton 2002; Morang et al. 1997).

The strength of the backscatter is dependent on the grain size and the roughness of the seabed (Mazel, 1985; Collier and Brown, 2005). Coarse sediments such as bedrock and gravel result in high backscatter due to a high impedance contrast and high surface roughness, which is shown as a dark colour on the sonograph. Fine sediments such as silts and muds result in low backscatter due to low impedance contrast and low surface roughness, which is shown as a light tone on the sonograph. The interpretation of a sonograph is qualitative and must be confirmed with sediment samples in order to provide ground truthing for the survey (Lurton 2002; Morang et al. 1997).

5.1 MATERIALS AND METHODS

5.1.1 Sidescan sonar survey methodology

A sidescan sonar survey was completed over channels surrounding the Mt Maunganui flood tidal delta in Tauranga harbour on the 16th of January 2007, with accompanying ground truthing of 33 grab samples and 36 underwater video camera shots conducted on the 17th of January 2007. The Mt Maunganui ebb tidal delta, dredged channel and adjacent tidal inlet were surveyed by side scan sonar on the 24th of January 2007, with accompanying ground truthing conducted on the 25th of January 2007, taking 67 grab samples and 74 underwater video shots. The sidescan sonar survey used a 500 kHz frequency Klein 595 towfish with a swath width of 150 m. The survey was undertaken on the University of Waikato survey vessel *Tai Rangahau* cruising at an average speed of 2 ms⁻¹, which was slow enough to provide a resolution of at least 0.5 m on the sonograph. Some 22 transect lines parallel to the shore over the ebb tidal delta area were completed ranging in water depths of 3 to 18 m offshore, as well as depths of up to 22 m in the channel. The shore parallel orientation of transect lines enabled better identification of wave formed bedforms, consistent with studies conducted by Harms (1989), Foster (1991) and Spiers (2005). Some 38 transect lines were completed in the channels surrounding the flood tidal delta. The sidescan survey was unable to be undertaken over the shallow ebb shields of the flood tidal delta, as it was too shallow. Consequently, the surficial sediment unit boundaries in this area on the map were inferred. Most of the transect lines were overlapping to help ensure full coverage on the sonograph.

5.1.2. Sonograph Data Post Processing

The onboard system captured the sonograph data using ISIS software. Both an analogue and digital output were produced. Corrections for across and along track, slant range and speed distortions were applied to the digital data using a combination of ISIS SONAR and Delphmap v2.10 software resulting in an along track resolution of about 0.5 m per pixel.

The digital sonograph was then imported into the ArcMap version 9.2 and was overlaid on an aerial photograph of Tauranga Harbour where it was then digitised. The sonograph (Fig. 5.3) was digitised in order to outline areas which share similar surficial sediment properties as indicated by backscatter strength. The sonograph was interpreted at a scale of 1:1000 and was classified into four units which displayed distinctive backscatter imagery which corresponded to a different bottom type (Table 5.1). The sonar mosaic positional accuracy was checked by comparing to structural features such as Sailsbury Wharf, and was found to be approximately 8 m.

5.1.3. Ground Truthing

The groundtruthing for the survey was undertaken from bottom sediment samples using a Van Veen grab sampler and underwater video camera imagery. At each sample point, sediment samples and underwater video footage was taken. The distribution of sample points on the flood tidal delta was based upon a grid structure with a spacing of approximately 300 m. On the ebb tidal delta there was a concentration of sample points near the entrance channel with less densely spaced sample points further away from the entrance channel. This is because previous studies by Healy (1985) and Kruger and Healy (2006) have indicated that this area is particularly dynamic.

Sediment samples were processed in the laboratory using the Rapid Sediment Analyser (RSA) at the University of Waikato - a fall tube system. The RSA measures the settling velocity of the sediment and converts it to the equivalent hydraulic sphere sizes (De Lange et al. 1997). The grain size is measured using phi (Φ) units from the Udden-Wentworth

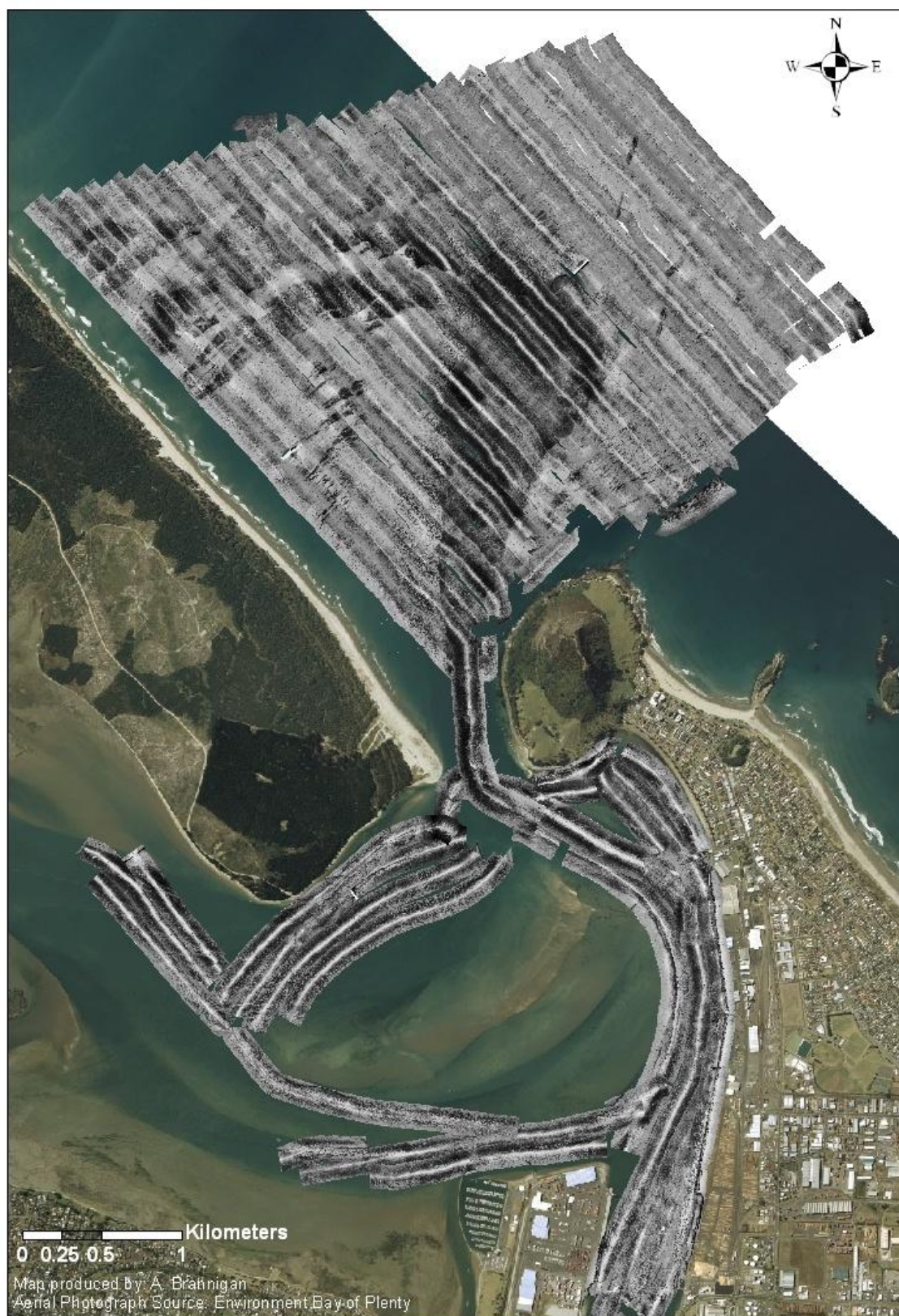



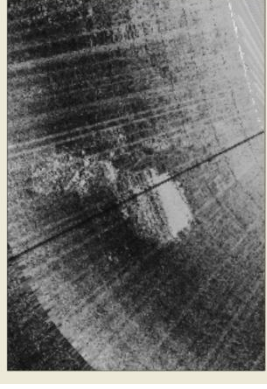


Fig. 5.3: Sidescan sonography output from surveys conducted at the tidal delta system at the Tauranga entrance of Tauranga Harbour in 2007.

Table 5.1: Description of units used for the analysis of surficial sediment on the sonograph.

Unit Name	Image	Description	Location
Fine Sand		Low acoustic return commonly resulting in light grey tone.	Primarily located on swash platform of the ebb tidal delta and channel surrounding tidal flat.
Medium Sand		Moderate acoustic return commonly resulting in moderate grey tone.	Main Ebb channel, and on and around the tidal flat.
Shell Lag		High acoustic return generally resulting in a dark grey image	Main ebb channel and flood tidal delta near the tidal inlet.
Rock		Rough texture with strong shadows.	Limited to tidal inlet gorge and surrounding Mt Maunganui.

scale. The RSA was chosen over grain size measurement devices such as sieves and the Malvern laser sizer as the RSA is based upon the settling velocity and therefore more accurately reflects the behaviour of the sediment in the water. The methodology to analyse the sediment was consistent with that used in Kruger and Healy (2006) in order to aid ready comparison with the data from their study and this. Further details can be found in Appendix 3.

The surficial shell coverage was ascertained through using the underwater video (Fig. 5.4). The footage was analysed through watching the video clip for each sample point once then replaying that same footage again and stopping at a particular frame which was characteristic of the entire (approximately 60 second) clip. That frame was then compared to a Chart for Estimating Mineral Grain Percentage Composition of Rocks and Sediments (Terry and Chillingier, 1955) in order to determine the shell percentage coverage. The measurement of surficial shell coverage is important as at high concentration shells can provide an armouring effect reducing the amount of available sediment that can be entrained as described by Healy (1985). Further details about underwater video imagery can be found in Appendix 3.

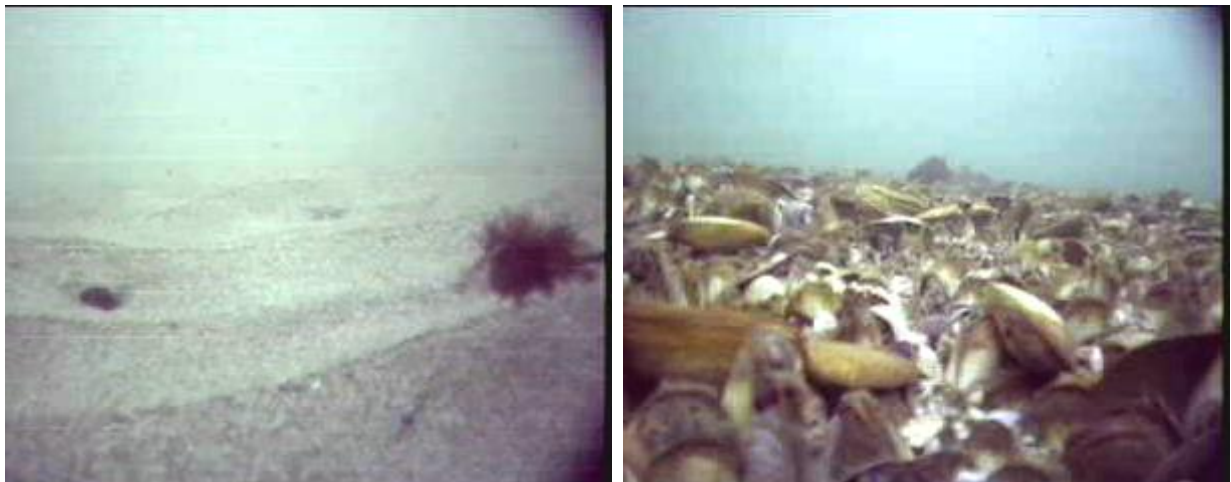


Fig. 5.4. Still images taken from underwater video. The image on the left shows an example of 0% shell coverage while the image on the right shows an example of 100% shell coverage.

5.2 . SURFICIAL SEDIMENT CHARACTERISATION OF THE TIDAL DELTA SYSTEM

5.2.1. Flood Tidal Delta (FTD)

The most conspicuous feature surficial sediment feature on the FTD is the change from high percentage shell coverage over the flood ramp in the north (shown by the black diagonal cross hatch) near the tidal inlet to low shell coverage further southwards on the ebb shield, away from the tidal inlet (shown by the horizontal black lines) (Fig. 5.5). There is also a zone of very fine sand (shown in purple) with no shell in the Stella Passage, the southernmost part of the study area. The middle of the Centre Bank flood tidal delta has a large area of medium sand (shown in brownish orange) with minor shell coverage, flanked east and west by large areas of fine sand (shown in pink) with minor shell coverage. The channels surrounding the FTD are primarily composed of interspersed areas of medium and fine sand with varying levels of shell coverage but with an overall trend of decreasing shell content further from the tidal inlet.

5.2.2. Ebb Tidal Delta (ETD)

The main ebb channel is dominated by medium sand with major shell coverage. Immediately west of the main ebb channel is a zone with medium sand and minor shell coverage (Fig. 5.6). The majority of the remainder of the ETD is covered in fine sand with no shell, apart from on the swash platform. Large rippled medium sand features (approximately 0.25 km long shore x 1 km cross shore) on the swash platform are orientated perpendicular to the shore on the western side of the ebb tidal delta near the terminal lobe. There are also other smaller (approximately 75 m long shore x 250 m cross shore) medium sand features orientated perpendicular to the shore located on both sides of the ebb channel. It is thought that these rippled medium sand features are maintained through wave focussing.

A comparison of the western ETD swash platform 2006 sonograph data with 2006 multibeam bathymetry (where red indicates a shallow area while blue indicates a deeper area) was undertaken over the western swash platform (Fig. 5.7). This indicated that the coarser sand (shown as dark grey) areas were primarily located in the deeper runnels (shown as yellow)

while fine sand (light grey) was primarily located in the shallower areas (red). It is thought that these coarser sand runnel features are maintained through wave focussing.

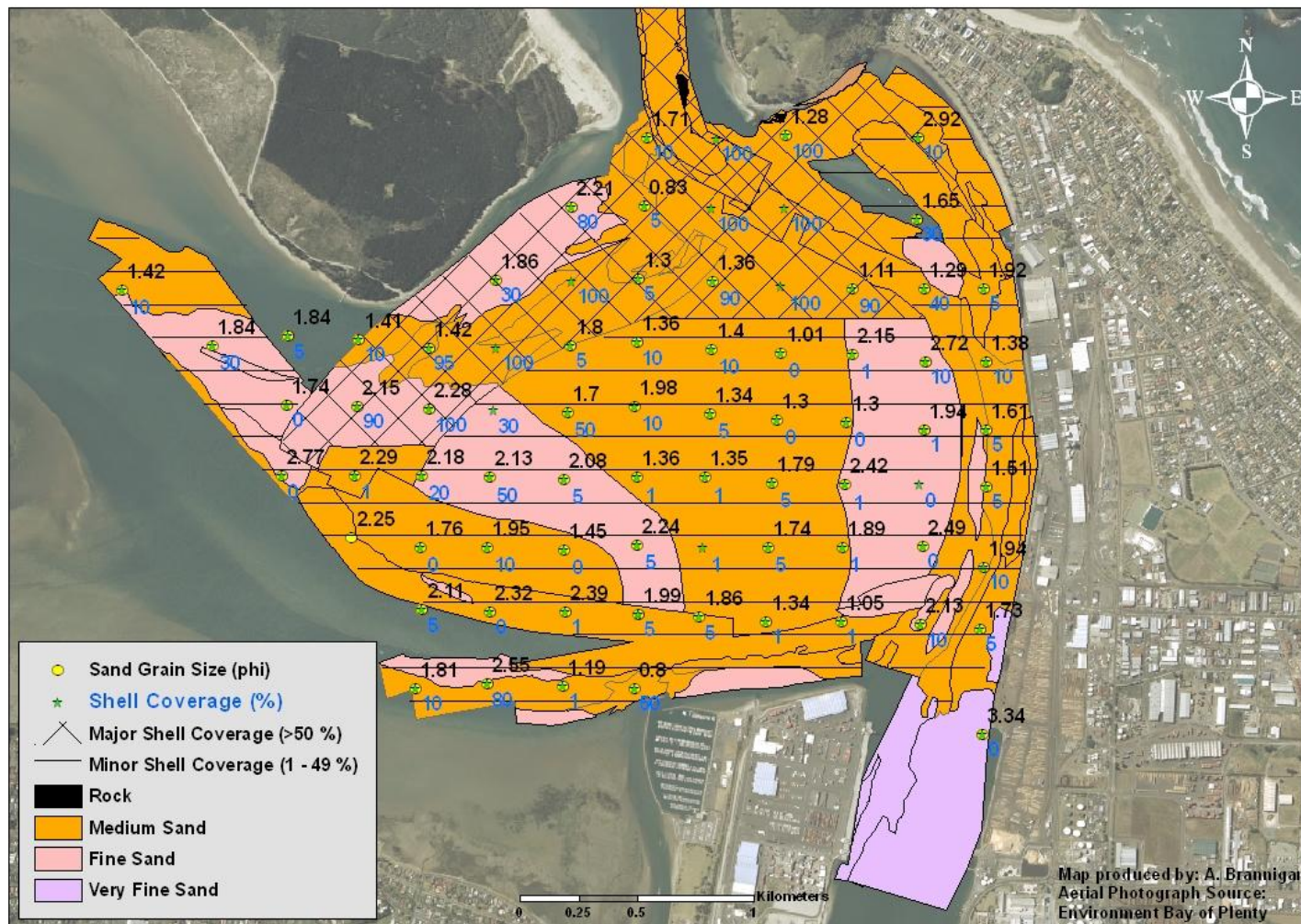


Fig. 5.5: Surficial sediment and shell coverage of the FTD of Tauranga Entrance to Tauranga Harbour in 2007 based on side scan sonar and sediment sampling.

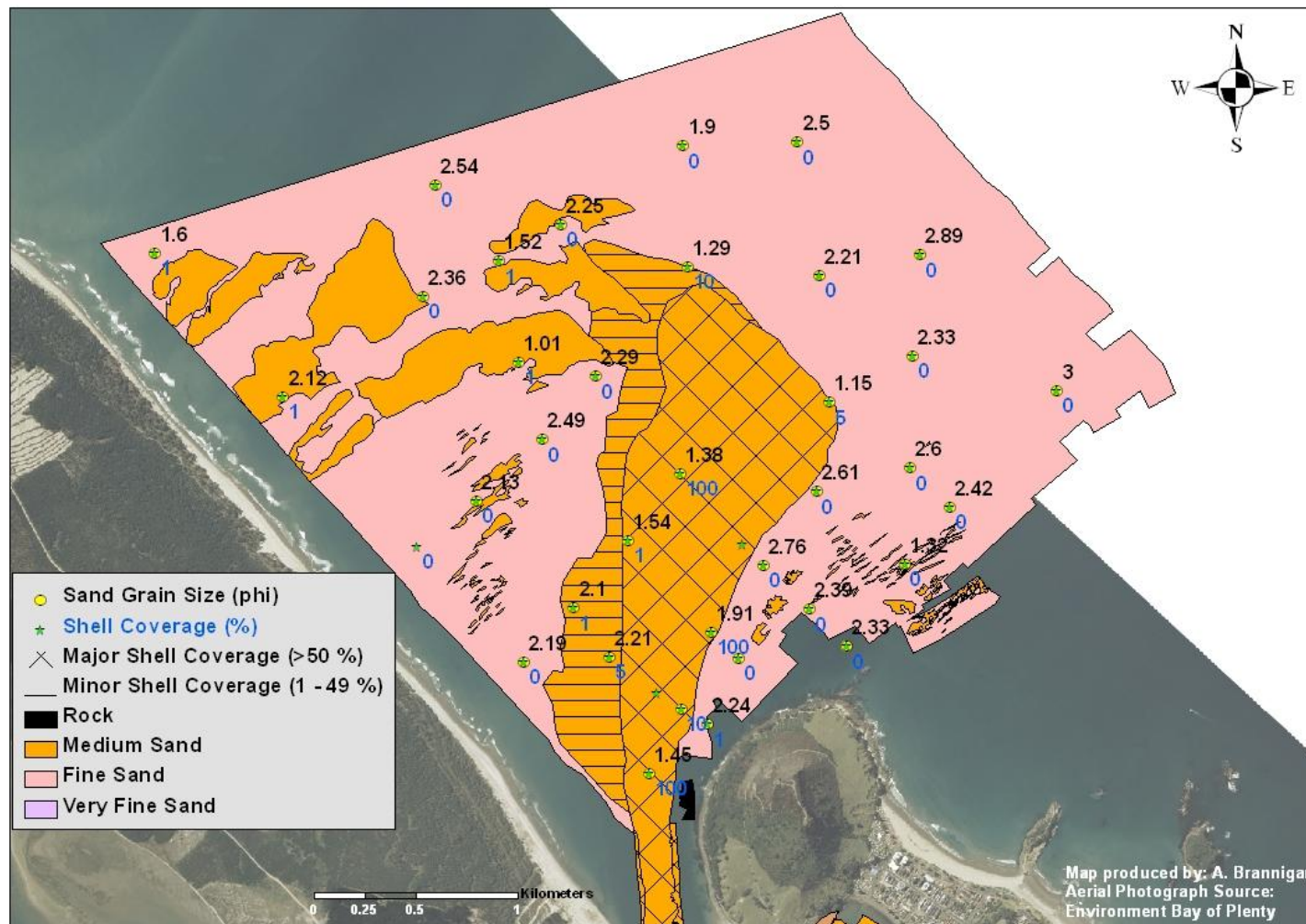


Fig. 5.6: Surficial sediment and shell coverage of the ETD of Tauranga Entrance to Tauranga Harbour in 2007/2007 based on side scan sonar and sediment sampling..

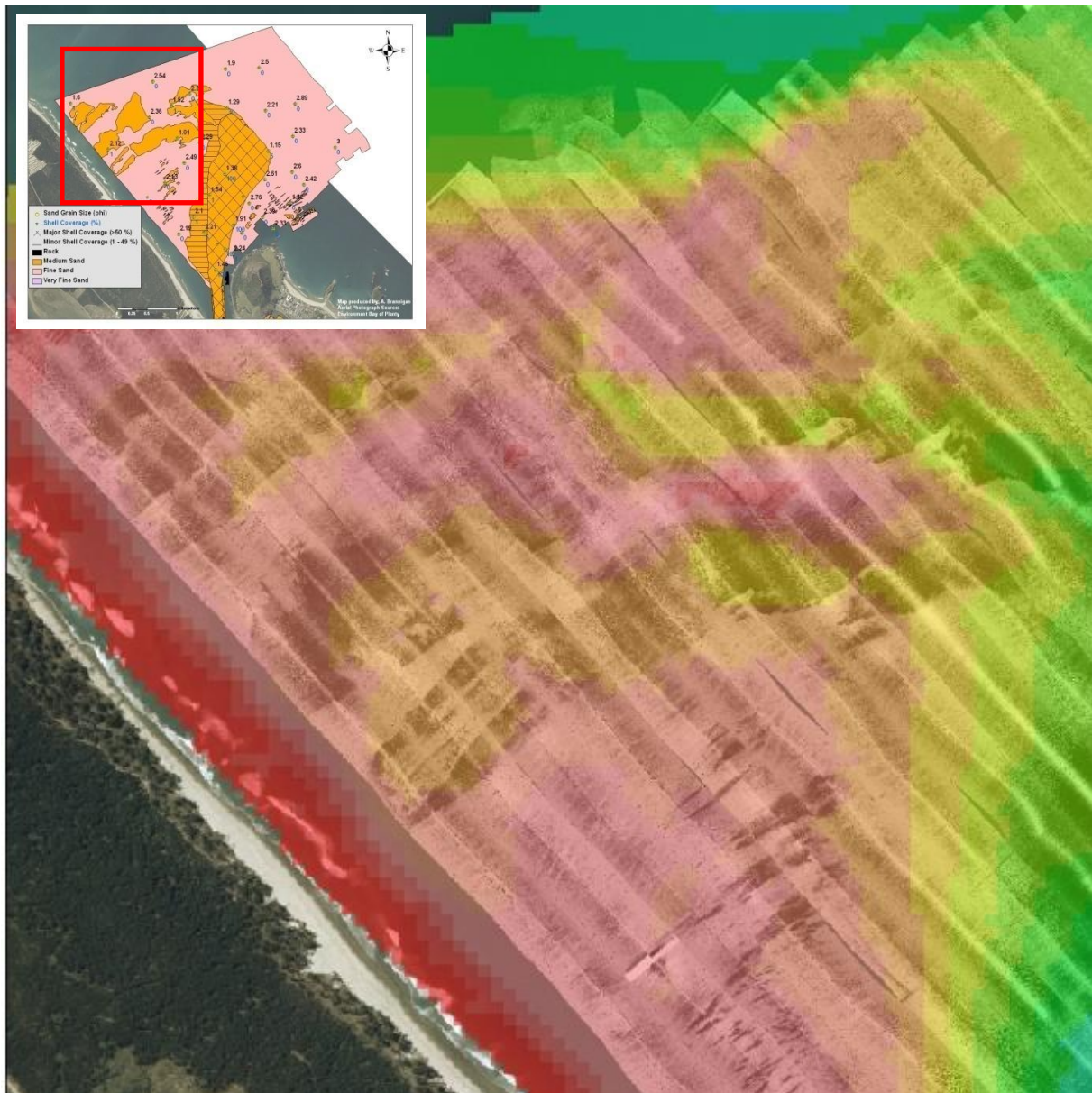


Fig. 5.7. 2006 sidescan sonography overlaid with 2006 multibeam bathymetry in order to show the relationship between depth and grain size on the Tauranga Entrance western ETD. Inset at top left shows location within ETD.

5.3. COMPARISON WITH HISTORICAL SURFICIAL SEDIMENT STUDIES

There have been two historical studies which have focussed on the surficial sediment characteristics of the tidal delta inlet system of Tauranga Harbour: the Tauranga Harbour Study (Healy, 1985) conducted in 1983-1984 which covered both the ETD and FTD and the study conducted in 1999 (Kruger, 1999; Kruger and Healy, 2006) which covered only a limited part of the ETD (Fig. 5.8). Comparisons between the 1998 study and this study were

aided by the similar methodology employed while a comparison with the 1983 Tauranga Harbour Study was limited due to the different sediment facies units used in each study.

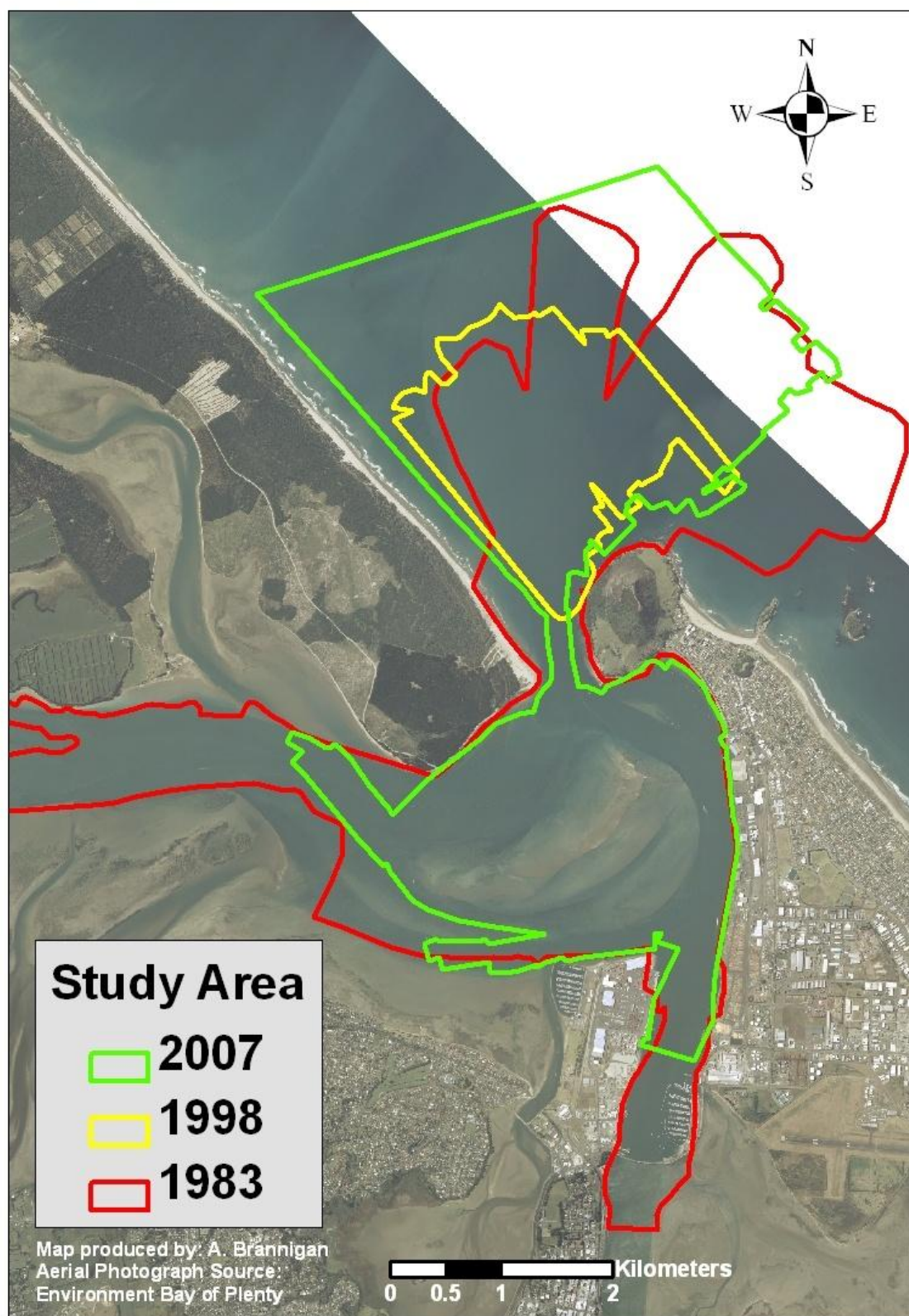


Fig. 5.8: Comparison of extent of area for the present study with the 1983 Tauranga Harbour Study and 1998 study by Kruger of the tidal inlet delta system sedimentation and morphology.

5.3.1. 1983 - 1984 Tauranga Harbour Study

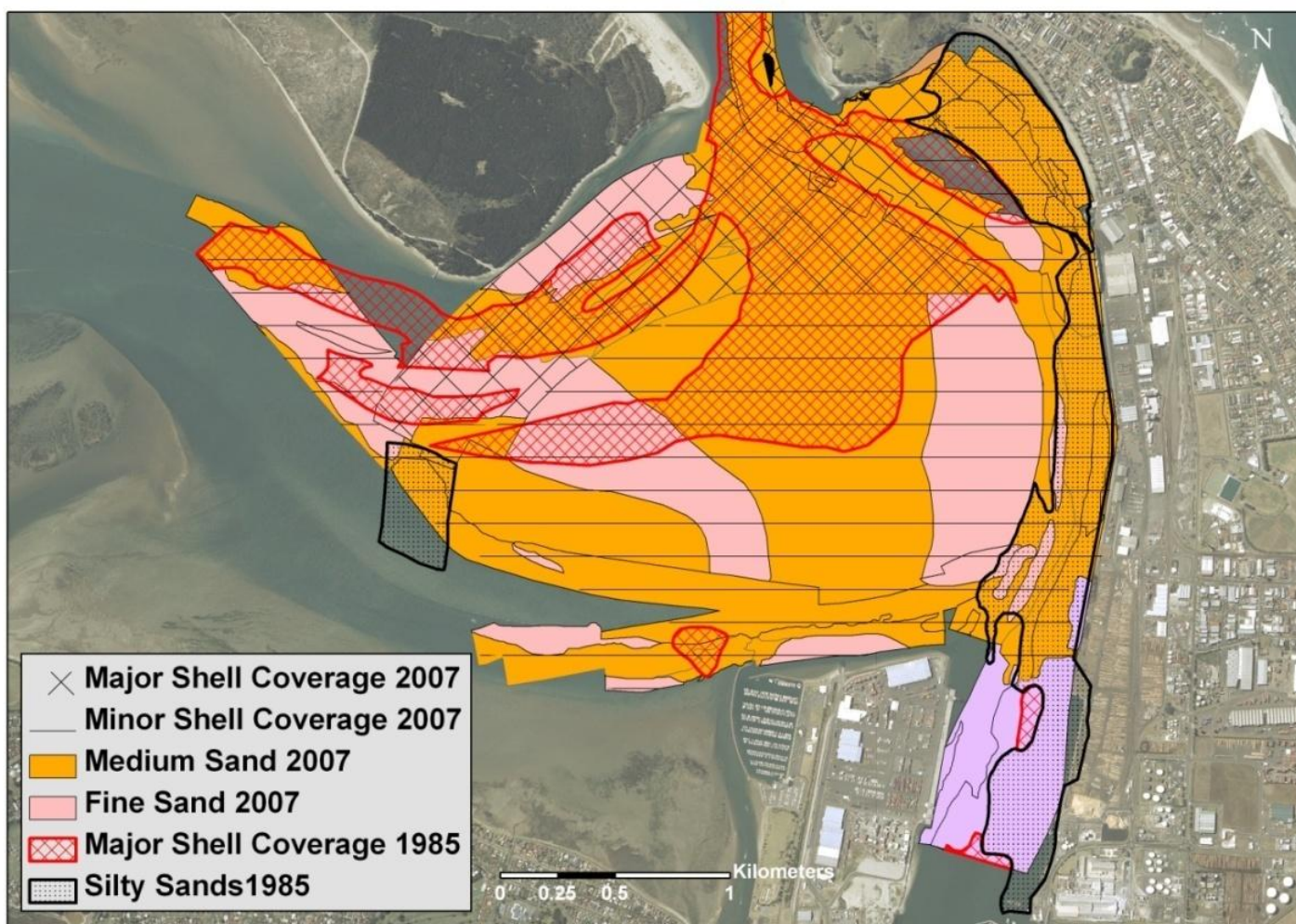


Fig. 5.9: Comparison between 2007 and 1983 surficial sediment on the FTD, with 1983 major shell coverage shown in red hash and 2007 surficial sediment coverage shown in the other colours.

A major difference between the surficial sediment coverage in 1983 and 2007 on the flood tidal delta is the reduction in major shell coverage in 2007 (Fig 5.9). Both 1983 and 2007 show a similar transition of major shell coverage near the tidal inlet, extending down to minor shell coverage further away from the tidal inlet. However, the major shell coverage of 1983 (shown in red diagonal cross hatch) extends much further away from the tidal inlet up to the crest of the northernmost ebb shield. This is in comparison to 2007 where the major shell coverage is primarily limited to the flood ramp and Lower Western Channel with only a small amount of major shell coverage near the northern ebb shield. Furthermore, there is silty sand (shown as a black dotted unit) present in Maunganui Roads Channel east of the FTD in 1983 but in 2007 this has been replaced with fine – medium sands.

The reduction in major shell coverage could potentially in part be a result of dredging of channels surrounding the flood tidal delta causing a reduction in current velocities across the flood ramp / ebb shield area facilitating the deposition of sediment in this area. This is consistent with hydrodynamic numerical modelling data, specifically the difference in mean spring tide flood velocity vector plot (2006 – 1954) which shows a reduction in current velocity in this area.

The change in the Mt Maunganui Roads Channel from silty sand to fine – medium sand could be influenced by maintenance dredging removing fine material leaving a coarser surface.

The key differences between the 1983 and 2007 ETD surficial sediment is the change in the size and position of the shell lag coverage in the main ebb channel (Fig 5.10). The ebb channel major shell coverage in 1983 has a decreased offshore extent and has a more easterly position than the major shell coverage of 2007.

The major trend in comparing the tidal delta system surficial sediment between 1983 and 2007 is the northwards movement of the major shell coverage. The ebb tidal delta shows an increase in major shell coverage between 1983 and 2007, while the flood tidal delta shows a decrease in shell coverage.

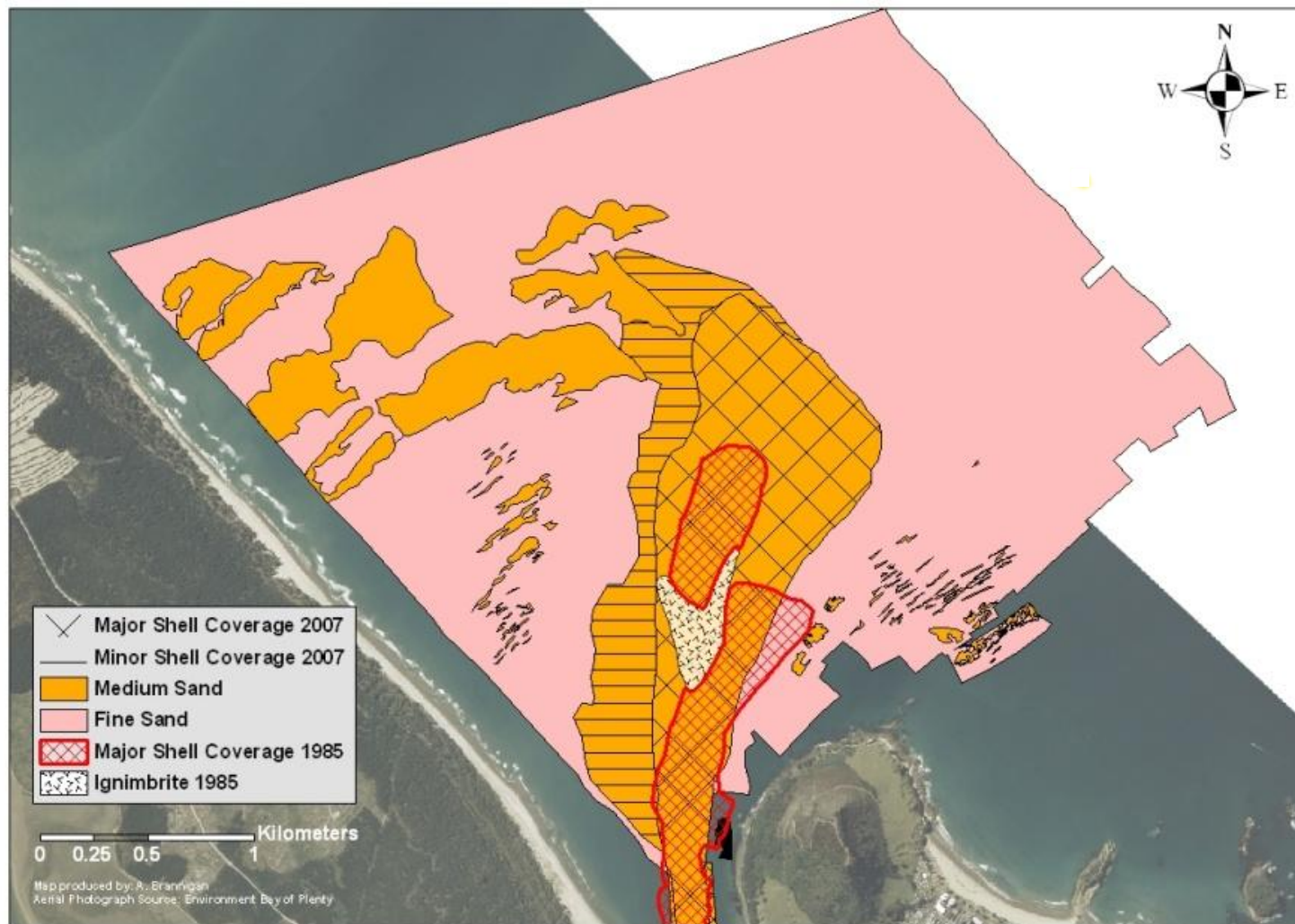


Fig. 5.10: Comparison between 2007 and 1983 surficial sediment on the ETD, with 1983 major shell coverage shown in red hash 1983 ignimbrite shown as a speckled unit and 2007 surficial sediment coverage shown in the other colours.

5.3.2. 1998 Kruger Study

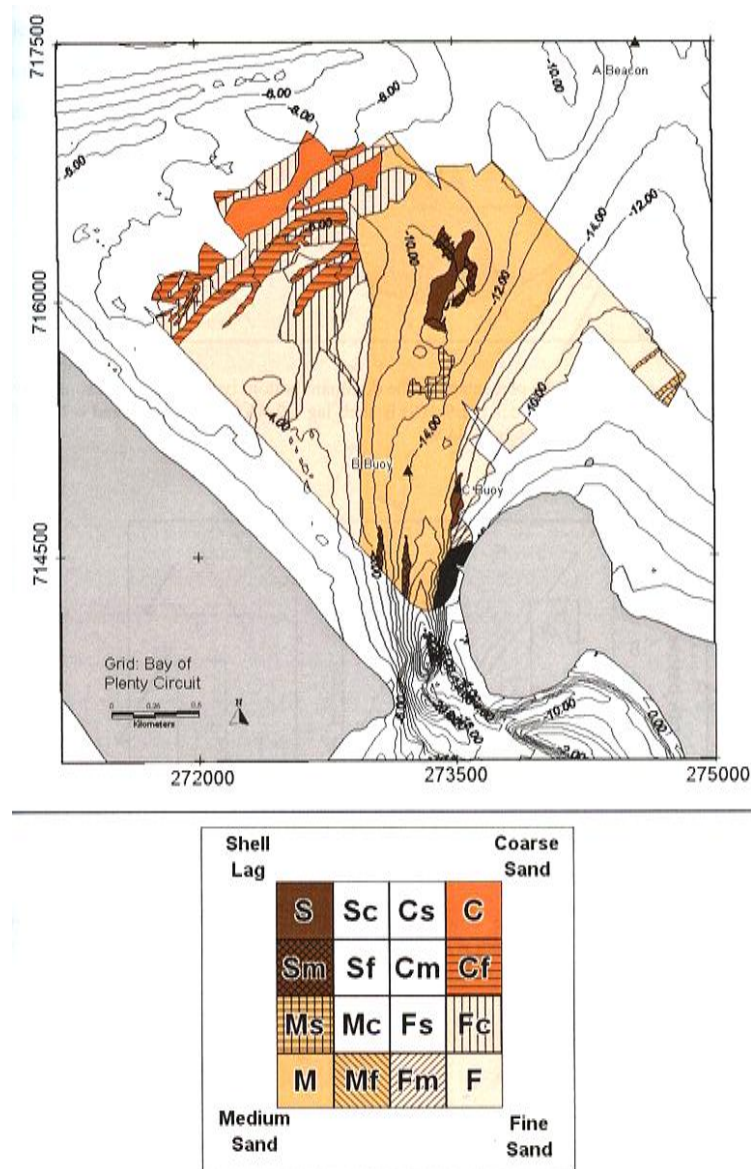


Fig. 5.11: Surficial sediment coverage of ebb tidal delta of Tauranga entrance in 1998 produced by Kruger (1999).

The ebb tidal delta surficial sediment coverage of 1998 has a number of broad similarities with that of 2007, including the location and size of swash platform features and fine sand coverage. The medium sand features on the swash platform present on the 1998 map (Fig. 5.11.) in the north western part of the ebb tidal delta are in approximately the same size and location as the same features in 2007. The fine sand coverage over the swash platform also has approximately the same distribution. The coverage of medium sand in the entrance channel has a similar coverage between 1998 and 2007 while the coverage of shell lag in the entrance channel is significantly smaller in 1998 than that in 2007 and in 1983.

The changes in surficial shell coverage of the entrance channel between 1983 and 2007 at present cannot be adequately explained. Potential reasons may involve the removal of a rocky shelf in the entrance channel in 1992 (between the Tauranga Harbour Study of 1983 and Kruger's study in 1999) which could have changed the direction and magnitude of the ebb jet thus affecting surficial sediment coverage.

5.4. BEDFORMS

Water flowing over sand will form the sand grains into morphological units known as bedforms. The orientation of bedforms (Fig. 5.12) is an indication of flow pathways and sedimentation patterns (Leeder, 1982; Larson et al., 1997). The different types of bedforms are based on the velocity grain size relationship, and are only steady under particular flow conditions (Fig. 13).

Small bedforms such as ripples can often be seen superimposed on larger bedforms such as dunes indicating that there may be considerable variation in the flow field over time. Bedforms can move with the current flow or against the current flow (antidunes), or may remain stable except under particular conditions (Allen, 1985; Larson et al. 1997). An understanding of bedform shape and size is useful as it can help in making quantitative estimates of current strength in ancient and modern sediments due to the sensitivity of bedforms to flow velocity while being somewhat independent of depth (Boothroyd, 1985; Hsu, 1989; Larson et al. 1997). If the flow pattern remains relatively unchanged perpendicular to the flow, and there are no eddies or vortices, the resulting bedform is two dimensional and has a straight crest. However if there is considerable scouring then the bedform reflects this, and the shape produced is three dimensional, eg. three dimensional lunate dunes. Three dimensional bedforms generally occur at higher flow velocities for a given depth and grain size (Kruger, 1999).

The shape and orientation of bedforms can significantly change over a tidal cycle, for example Van Lacker et al. (2004) described that at 'Spratt Sand', the intertidal shoal at Teignmouth (UK), the bedforms rapidly reverse at high water slack and ebb dominated bedforms replace flood dominated bedforms generated during the first part of the flood-ebb cycle. Furthermore, Boothroyd (1985) recognised the same phenomenon with intertidal megaripples.

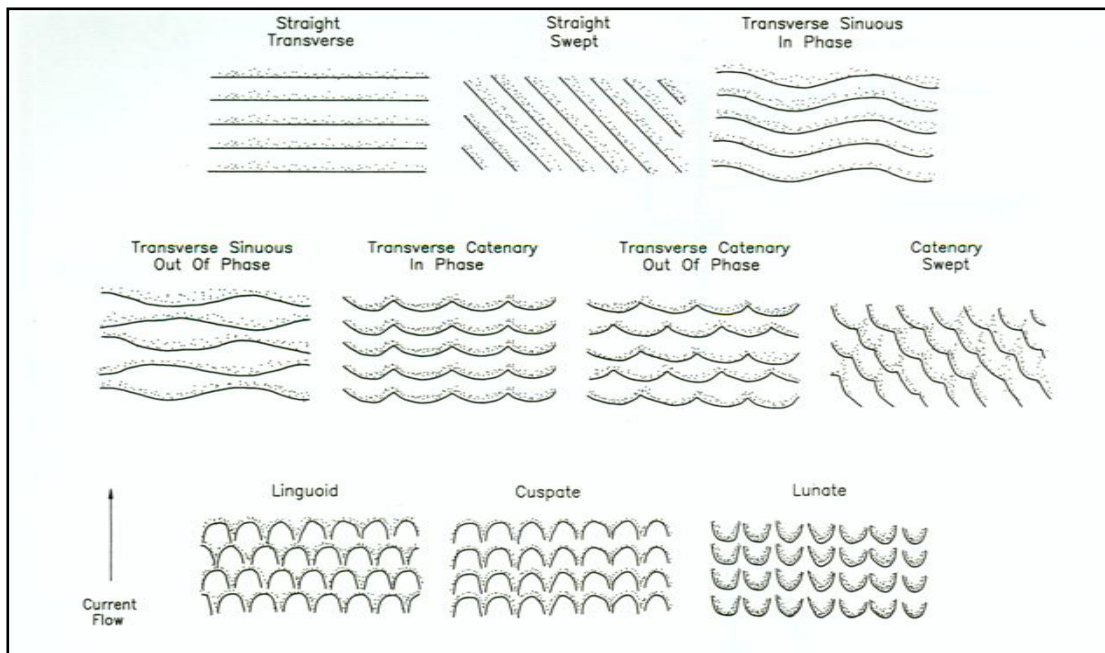


Figure 12. Sediment ripples. Water flow is from bottom to top, and lee sides and spurs are stippled (adapted from Larson et al. 1997; original in Allen, 1968).

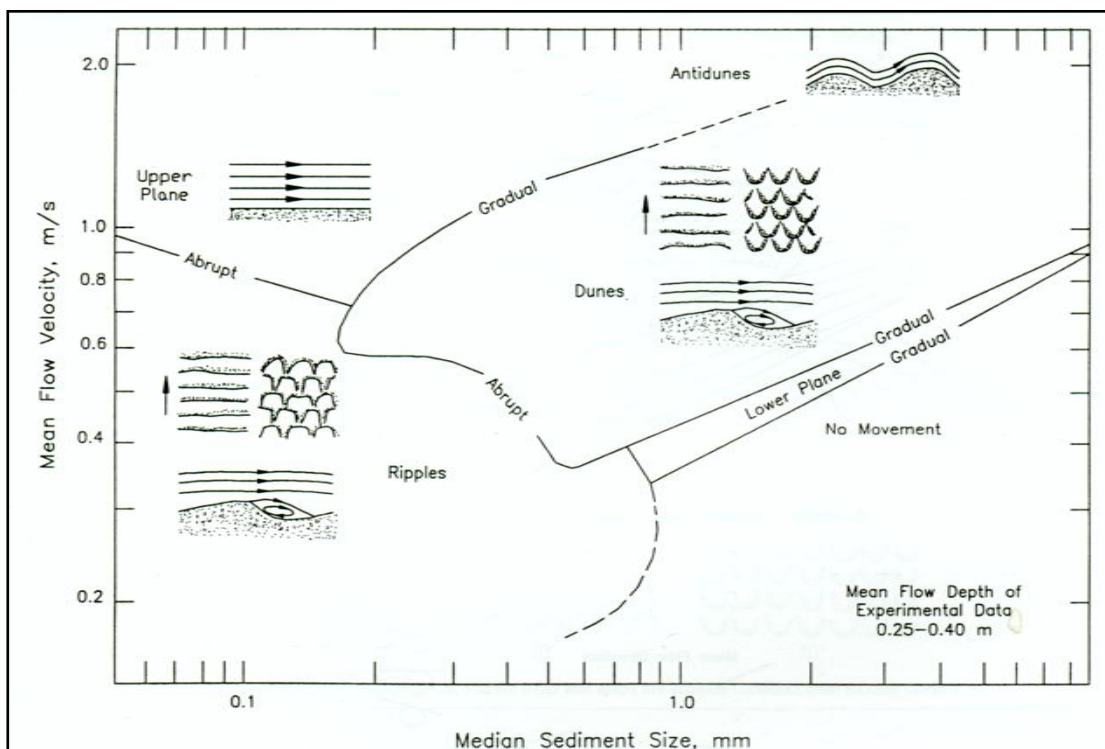


Figure 13. Plot of mean flow velocity against mean grain size, based on laboratory studies, showing stability phases of subaqueous bed forms (Larson et al. 1997; original in Ashley 1990).



Fig 5.14. Bedform map of the Tauranga Entrance tidal delta system for 2006 indicating dominant sediment transport pathways. The green vectors indicate the direction and relative magnitude of sediment movement at various locations around the tidal inlet delta. Bedform data was gathered from the sonograph and aerial photograph.

Given the ability of bedforms to indicate the direction of sediment movement, the bedform data from the sonograph and aerial photographs were used in order to map sediment transport pathways of the tidal delta system of the Tauranga Entrance to Tauranga Harbour.

The Entrance Channel shows northern / north-easterly sediment transport up the main ebb channel. Bedform spacing decreases from ~ 4 m to ~ 2 m with increasing distance from the inlet gorge. This suggests a reduction in northwards sediment transport with increasing distance from the tidal inlet. Offshore from the main ebb channel there are wave generated bedforms orientated perpendicular to the shore with a spacing of 2 m. The main ebb channel has some of the coarsest surficial sediment on the ebb tidal delta meaning that the currents in this location are greater than those areas that show same bedform spacing but with finer sand (Larson et al. 1997).

In the FTD, on the flood ramp, the Lower Western Channel and the Cutter Channel there are diverging bedforms with a spacing of approximately 10 m, this is consistent with the residual distance plot for 2006 which also shows diverging vectors.

The ebb shield shows a comparatively high bedform (13 – 20 m) spacing directed north easterly which is consistent with the 2006 residual distance plot (Fig. 14) which show a sharp north-easterly change in vector direction across the ebb shield.

The bedforms show convergence in the northern part of the Maunganui Roads Channel, which is consistent with the convergence of vectors in the 2006 residual distance plot.

The Otumoetai Channel shows easterly directed bedforms in the eastern part and westerly directed bedforms in the western part – again, this is consistent with vectors of the 2006 residual distance plot.

There is also easterly-directed bedforms about 0.5 km south of the southern tip of Matakana Island.

Overall, the bedform map shows relatively good agreement with the 2006 residual distance plot, with the bedforms on the flood tidal delta being particularly well related to the residual distance plot vector direction and comparative magnitude.

5.5. COMPARISON WITH HISTORICAL BEDFORM STUDIES

5.5.1 1983 Tauranga Harbour Study - Bedforms

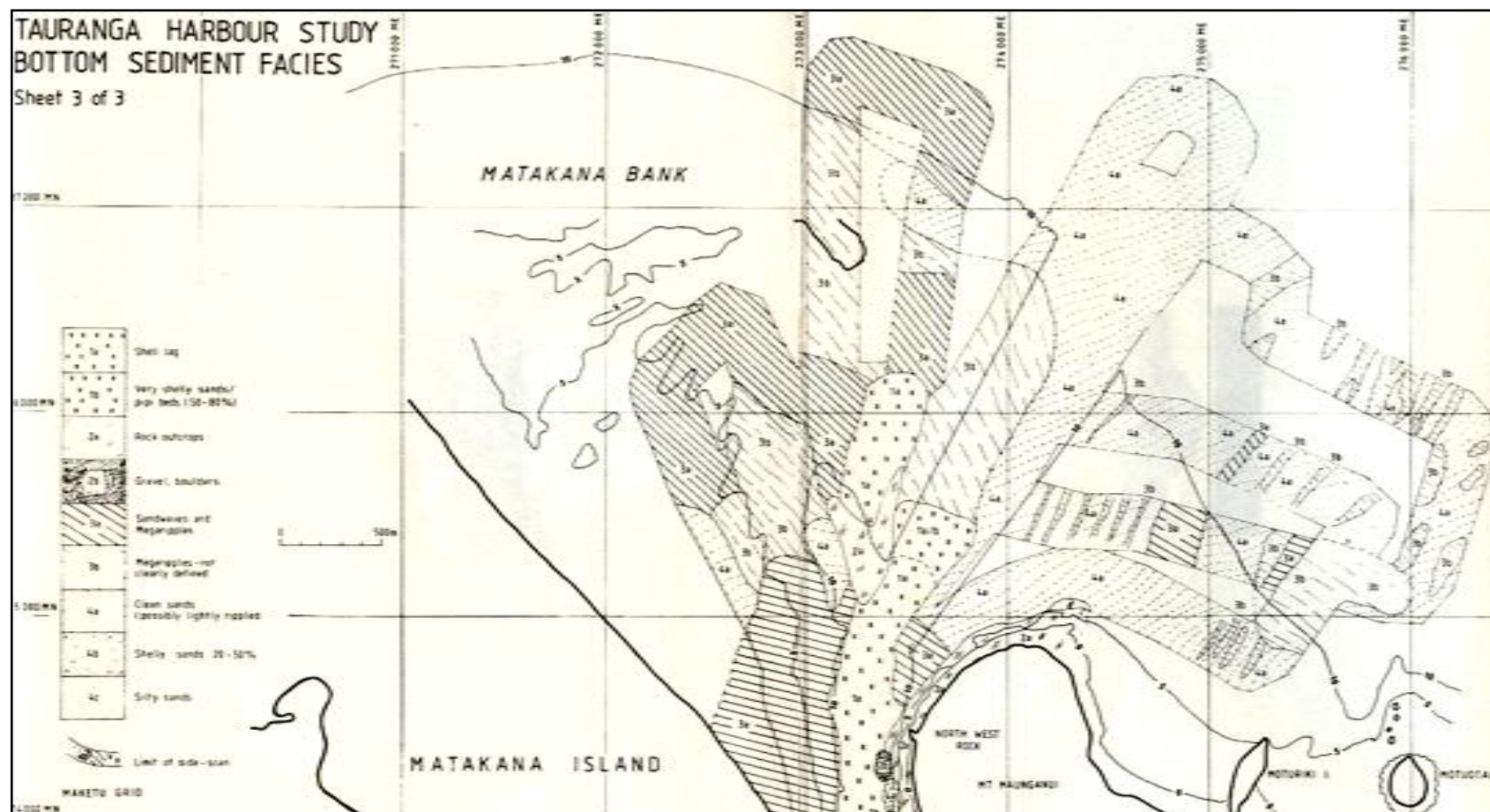


Fig.5.15. Surficial sediment facies of the ETD from the Tauranga Harbour Study (1983 – 1984) (Source: Healy, 1985).

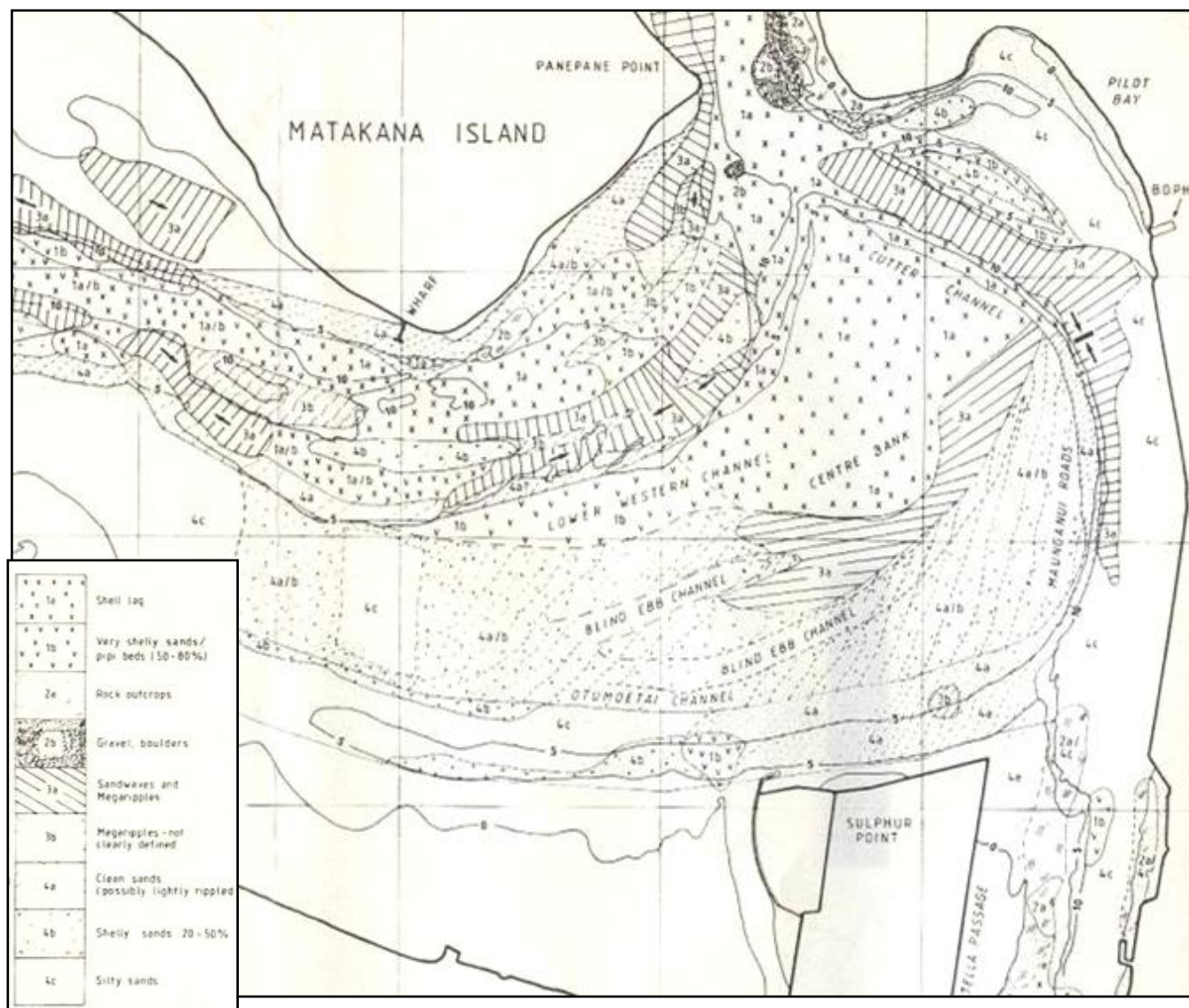


Fig 5.16. Surficial sediment facies of the ETD from the Tauranga Harbour Study (1983 – 1984) (Source: Healy, 1985).

The surficial sediment facies charts of the 1983 Tauranga Harbour Study (Healy, 1985) fail to distinguish between current-formed and wave-formed bedforms, however the wave formed bedforms are limited to the north of the 715000 N grid line on Matakana Bank. Offshore from Mt Maunganui beach (on the open ocean side south-east of Mt Maunganui) there are wave formed megaripples commonly in the form of 'fingers' as noted elsewhere on tidal deltas (Black and Healy, 1983). Similar features are present on the 2007 sonograph north-east of Mt Maunganui.

Large fields of wave formed bedforms are present over the Matakana Bank, while closer to the entrance these bedforms merge with current formed megaripples. Around the tidal gorge and inside the harbour all of the bedforms are current dominated. Sand waves are present only on the Matakana side of the Entrance and are a major sediment transport pathway. Major channel megaripples are found in the Lower Western Channel, in the Cutter Channel and in the side of Maunganui Roads Channel.

In 1983, bedforms converge in the northern part of the Maunganui Roads Channel, and a similar feature is shown in the 2007 sonograph. Furthermore, this point of convergence is consistent with the 2006 mean net spring residual distance plot, which shows a convergence of residual distance vectors, suggesting an area of convergence in potential net tidal sediment transport.

Well formed, obliquely orientated channel marginal sand waves are present on the shallowest part of the Centre Bank from the ebb shield. Healy (1985) interprets the position and alignment of the bedforms as being a sedimentation zone in dynamic balance between the currents decelerating off the lagged flood ramp, and the ebb flow sweeping across the Centre Bank from the Otumoetai and Stella Passage Channels.

5.5.2. 1998 Kruger Study - Bedforms

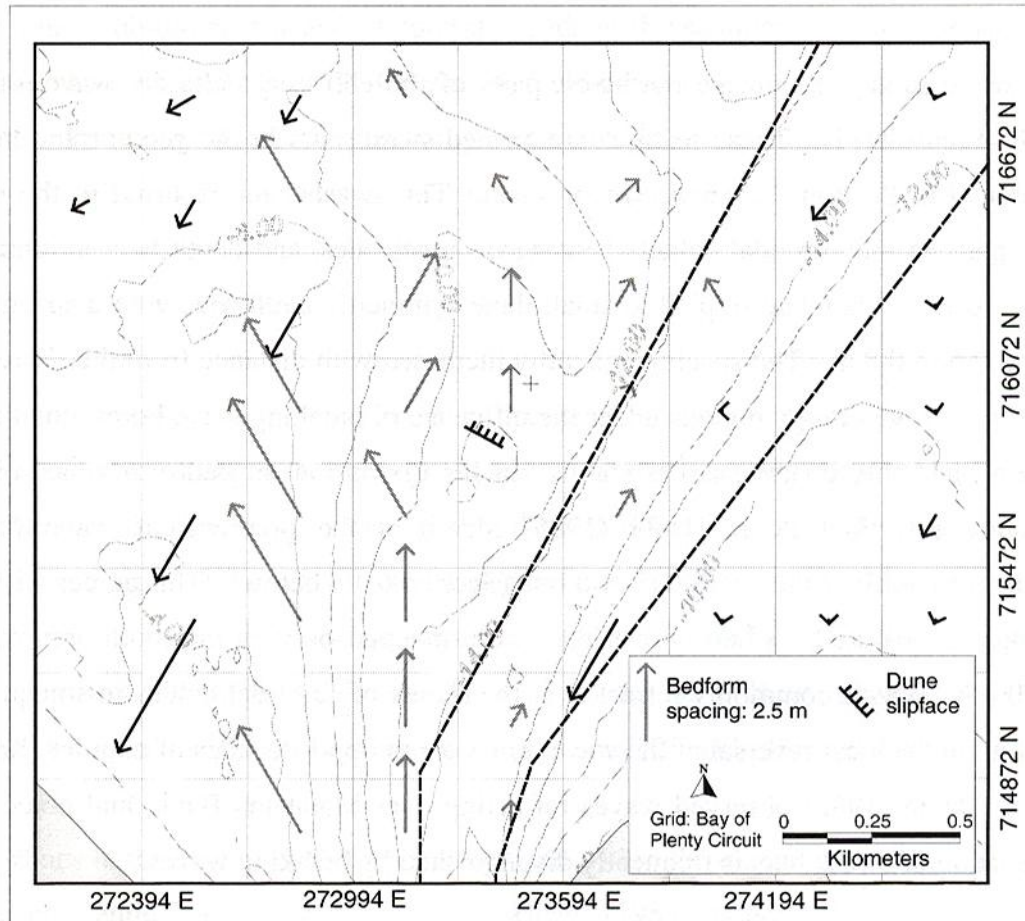


Fig.5.17. Bedform spacing and orientation map. Grey vectors represent direction of motion of tide induced bedforms, and black vectors represent bedform movement due to wave action (Source: Kruger, 1999).

The bedform map of ebb tidal delta by Kruger (1999) shows north directed bedforms with a spacing of 2.5 m in the main ebb channel directly north of the tidal inlet, bedform spacing decreases with increasing distance from the tidal inlet. Bedforms with a similar direction and spacing are also present in 2006.

West of the main ebb channel on the swash platform the bedforms are north-westerly directed with a bedform spacing of 4.5 m, again with the spacing decreasing with increasing distance from the tidal inlet. The 2006 bedform map fails to capture these bedforms.

Wave forced bedforms on the eastern swash platform and outer part of the western swash platform are minor (less than 1.2 m), while the wave forced

bedforms on the inner part of western swash platform are stronger (2 – 4.5 m). The 2006 bedform shows a bedforms of similar bedforms and spacing.

In general the spacing and direction of bedforms over the ebb tidal delta are similar between 2006 and 1998 with only minor differences.

5.6. CONCLUSIONS

The investigation into surficial sediment of tidal delta system of the Tauranga Entrance raises the following major points:

(i) The 2007 surficial sediment coverage of the ETD has a main ebb channel dominated by medium sand and major shell coverage, wave formed medium rippled sand features present in the runnels between the swash bar while the majority of the rest of the tidal delta is covered in fine sand with little to no shell

(ii) Between 1983 and 2006 the ebb tidal delta shows considerable changes in surficial sediment coverage. In 1983 the major shell coverage extended about 1 km north of Mt Maunganui, in 1998 there is only a minimal amount of major shell coverage in the main ebb channel while in 2006 the major shell coverage extends about 700 m further northwards than it did in 1983. This suggests considerable changes in sediment transport.

(iii) The 2007 surficial sediment coverage of the flood tidal delta is dominated by major shell coverage on the flood ramp and the Lower Western Channel. The channels surrounding the flood tidal delta and the ebb shield have interspersed zones of medium and fine sand with primarily minor shell coverage.

(iv) The flood tidal delta shows significant changes in major shell coverage between 1983 and 2006. In 1983 the major shell coverage almost borders the entire crest of the northern ebb shield, while in 2006 there has been a noticeable reduction in major shell coverage with it being limited to the Lower Western Channel and the flood ramp. This suggests a reduction in near bottom currents on the central flood tidal delta and ebb shields between 1983 and 2006.

(v) The ETD has ebb dominated bedforms along the length of the main ebb channel, which is consistent with 2006 mean spring tide residual distance

plot, the rest of the ebb tidal delta shows wave directed bedforms. The FTD shows bedforms diverging over the flood ramp, then undergoing a significant change in direction over the ebb shield. There also is convergence of bedforms in the northern part of the Maunganui Roads Channel. All these FTD bedform observations are consistent with the 2006 mean spring tide residual distance plot. The convergence of bedforms in the northern part of Maunganui Roads Channel is shown in the Tauranga Harbour Study surficial sediment facies map (Healy, 1985). The 2006 bedform map good agreement with the majority of the 1998 bedform map by Kruger (1999). Overall the comparison of the bedforms map between 1983 and 2006 shows that the bedform distribution remains relatively consistent.

6. CONCLUSIONS AND SUMMARY

6.0 INTRODUCTION

The general aims of this thesis are to:

- i) Analyse historical changes to inlet delta system geomorphology using historical hydrographic charts.
- ii) Conduct hydrodynamic numerical modelling using historical bathymetries to access changes in peak spring flow and potential net tidal sediment transport
- iii) Analyse historical changes in surficial sediment and bedforms

6.1 TIDAL INLET DELTA SYSTEM GEOMORPHOLOGY

Key findings of the geomorphic study are:

- Between 1852 and 2006 the most significant changes in tidal inlet delta system geomorphology occur between 1954 and 2006 (Fig. 3.8.) where the shipping channels have deepened up to 12 m, widespread erosion of over 1 m is present on the ebb tidal delta, with the Entrance Channel showing deepening due to dredging of 7 m. The terminal lobe shows extensive shoaling of 4 – 5 m associated with locational extension northwards. The Lower Western Channel demonstrated accretion of up to 4 m in the same time period.
- The tidal inlet gorge shows a progressive narrowing from 1879 to 2006 of about 900 m. The magnitude of narrowing between 1954 (pre-dredging) and 2006 (post dredging) (55 m) is slightly larger than the magnitude of narrowing evident in each of the historical pre-dredging bathymetries from 1852, 1879, 1901, 1927, and 1954.
- The flood tidal delta cross section profile shows shoaling of the ebb shields of 0.3 m above CD in the post dredging conditions of 2006. However the difference in elevations between 1954 and 2006 is only marginal at 0.4 m.

- The reduction in maximum depth (from ~ 9 m below CD to ~ 4 m below CD) in the Lower Western Channel between 1954 and 2006 is the greatest change evident in the Lower Western Channel when comparing the sequence of historical bathymetries. This suggests that dredging of the shipping channel through the originally blind Cutter Channel may have induced shoaling in the Lower Western Channel. However it is important to note that the maximum depth of the 2006 profile is close to the maximum depth of the 1879 profile, indicating that the 2006 profile is not outside the boundaries of natural change evident in historical bathymetries.

6.2 TIDAL INLET DELTA SYSTEM HYDRODYNAMICS

Major findings from the hydrodynamic investigation are:

- There are obvious changes in potential net tidal sediment transport in the tidal delta system between 1954 and 2006 that can be related to dredging, particularly of the Cutter Channel and Maunganui Roads Channel. Analysis of the pattern of full tidal cycle residuals suggest the northern side of the Cutter Channel demonstrates increased ebb dominated potential net tidal sediment transport, while the southern side of the Cutter Channel shows increased flood dominated potential net tidal sediment transport. This change in net tidal sediment transport evidently occurs in response to the capital dredging of the Cutter Channel, which formerly was a blind flood channel.
- Panepane Point shows noticeable changes in potential net tidal sediment transport with both large increases and decreases present in all the difference in residual distance vector plots between 1852 and 2006, indicating that it is a highly dynamic region.

6.3. SURFICIAL SEDIMENT PATTERNS OF THE TIDAL DELTA SYSTEM

- This study provides the most comprehensive map of surficial sediment and shell coverage to date for 2007 conditions, showing that on the ETD the main ebb channel is dominated by medium sand and major shell coverage ($> 50\%$), medium sand wave generated bedforms in the runnels between swash bars, and fine sand with low shell over the remainder of the ETD. The flood tidal delta is shown to have major shell coverage in the Lower Western Channel and surrounding the flood ramp, while the majority of the remainder of the FTD is covered in minor shell coverage ($< 50\%$). Interspersed areas of medium and fine sand are found in the FTD channels.
- A comparison of surficial sediment maps of 1983 from the Tauranga Harbour Study with those of the present study shows that there has been an overall northwards extension of major shell coverage on the sea floor, with a reduction in major shell coverage on the FTD and an increase in major shell coverage on the ETD. This change of surficial shell coverage should be associated with increase in scour on the ETD and a decrease in current velocity on the higher elevations of the FTD. However the difference in spring tide residual distance vector plots from 1954 – 2007 does not support the surficial sediment findings as it show a decrease in residual distance vectors on the appropriate place on the ETD and a increase in residual distance vectors on the appropriate place on the FTD. However, the residual distance plot relates to the time period being 1954 – 2006, not the time period 1983 to 2006.
- The 2007 bedform map is consistent with the 2006 mean spring tide residual distance plot showing a sharp change in the direction of bedform orientation over the FTD ebb shield from southwards directed to north-easterly directed bedforms. The ebb dominated main ebb channel with decreasing bedform spacing is also consistent with the 2006 mean spring tide residual distance plot, of decreasing velocity with increasing distance from the inlet.

- A comparison of historical bedform maps of 1983 (Healy, 1985) and 1998 (Kruger, 1999) shows reasonable agreement with the finding of the 2007 bedform map, particularly the point of bedform convergence on the Cutter Channel / northern Maunganui Roads Channel and ebb directed bedforms of the main ebb channel. This indicates little change in sedimentation pattern at this location since 1983.

6.4 IMPLICATIONS FOR PORT OF TAURANGA LTD.

The contemporary shipping channel configuration has affected the hydraulic efficiency of the channel systems leading to changed tidal flow patterns. This has evidently induced some change on the FTD due to a greater easterly ebb flow component, but the morphological changes have been of similar magnitude to natural changes before the commencement of dredging. So although the deepening of shipping channels has caused hydraulic change, the FTD has remained largely a dynamic equilibrium feature with morphological change since the dredging consistent with changes noticed in the historical bathymetries from 1852.

6.5 SUGGESTIONS FOR FUTURE RESEARCH

Future research could be undertaken using wave forcing in the hydrodynamic numerical model which is likely to provide a more thorough understanding of the ebb tidal delta system. Undertaking a sediment transport model will provide additional information about the sediment transport pathways in the inlet delta system. The existing surficial sediment map from this study could be used to provide accurate information about bottom roughness in the hydrodynamic numerical model. A smaller grid cell size for hydrodynamic numerical modelling will provide greater resolution so that finer scale hydrodynamic features can be recognised. Analysis of additional cross sections could be conducted at other places within the harbour to further assess geomorphic change.

REFERENCES

- Allen, J.R.L., 1985. Principles of Physical Sedimentology. George Allen & Unwin, North Sydney, Australia. 272p.
- Barnett, A.G., 1985. Tauranga Harbour Study, part I overview, part III hydrodynamics, Ministry of Works and Development.
- Black, K. 1983. Sediment Transport and Tidal Inlet Hydraulics. PhD Thesis, University of Waikato, pp. 82-83.
- Black, K., 1984. Sediment Transport. Tauranga Harbour Study, Part IV Text, Figures and Tables. University of Waikato, Hamilton. 159 p.
- Black, K.P., 2002. The 3DD Computational Marine and Freshwater Laboratory Model 3DD Description and Users Guide. pp. 19 – 29.
- Black, K.P., Healy, T.R. 1983. Side-scan Sonar Survey. Northland Forestry Port Investigation. Northland Harbour Board. 88p.
- Black, K.P., Healy, T.R., 1986. The sediment threshold over tidally induced megaripples. *Marine Geology*. 69, 219 – 234.
- Black, K.P., Healy, T.R., Hunter, M.G., 1989. Sediment dynamics in the lower section of mixed sand and shell lagged tidal estuary, New Zealand. *Journal of Coastal Research*. 5(3) 503 – 521.
- Boothroyd, J.C., 1985. Tidal inlets and tidal deltas. In: Davis Jr, R.A. (Ed.), *Coastal Sedimentary Environments*. Springer-Verlag, New York, 450p.
- Brekhovskikh, L. M. & Lysanov, Y. P., 2003, *Fundamentals of Ocean Acoustics*, Springer, New York, U.S.A . pp. 1 -116.
- Buynevich, I.V., Fitzgerald, D.M., 2003. Textural and compositional characterization of recent sediments along a paraglacial estuarine coastline, Maine, USA. *Estuarine Coastal Shelf Science*, 56, 139 - 153.
- Collier, J.S. and Brown, C.J., 2005. Correlation of sidescan backscatter with grain size distribution of surficial seabed sediments. *Marine Geology*, 214, 431 - 449.
- Dahm, J., 1983. The geomorphic development, bathymetric stability and sediment dynamics of Tauranga Harbour. MSc. Thesis, University of Waikato, 230p.
- Davies-Colley, R., 1976. Sediment dynamics of Tauranga Harbour and the Tauranga Inlet. MSc. Thesis, University of Waikato, NZ, 148p.
- Davies-Colley, R., Healy, T., 1978^a. Sediment transport near the Tauranga Entrance to Tauranga Harbour. *New Zealand Journal of Marine and Freshwater Research*, 12(3), 237-243.

- Davies-Colley, R. Healy, T., 1978^b. Sediment and hydrodynamics of the Tauranga Entrance to Tauranga Harbour. *New Zealand Journal of Marine and Freshwater Research*, 12 (3), 225 -236.
- Davis Jr, R., Fitzgerald, D.M., 2004. Beaches and Coasts. Blackwell Publishing, Oxford, UK. 216p.
- De Lange, W.P., 1988. Wave climate and sediment transport within Tauranga Harbour, in the vicinity of Pilot Bay. Ph.D. Thesis, University of Waikato, 96 p.
- De Lange, W.P., 1991. Wave climate for No.1 Reach, Port of Tauranga, Tauranga Harbour, Report to Port of Tauranga Ltd., Hamilton, New Zealand; Department of Earth Sciences, University of Waikato, 18p.
- De Lange, W.P., Healy, T.R., Darlan, Y., 1997. Reproducibility of sieve and settling tube textural determinations for sand sized beach sediment. *Journal of Coastal Research*, 13, 73 - 80.
- Donda. F., Brancolini, G., Tosi, L., Kovacevic, V., Baradello, L., Gacic, M., Rizzetto, F., 2008. The ebb-tidal delta of the Venice Lagoon, Italy. *The Holocene*, 18, 267-278.
- Fitzgerald, D. M., Kraus, N.C., Hands, E.B., 2000. Natural mechanisms of sediment bypassing at tidal inlets. Technical report ERDC/CHL CHETN-IV-30. US Army Corps of Engineers, Vicksburg. 10p.
- Foster, G., 1991. Beach nourishment from a nearshore dredge spoil dump at Mount Maunganui Beach. MSc. Thesis, Department of Earth Science, University of Waikato. 142p.
- Harms, C., 1989. Dredge spoil dispersion from an inner shelf dump-mound. M(Phil) thesis, Department of Earth Science, University of Waikato. 177p.
- Hayes, M.O., 1975. Morphology of sand accumulations in estuaries: an introduction to the symposium. In: Cronin, L.E. (Eds.), *Estuarine Research*, Volume II, Geology and Engineering. Academic Press, New York, NY, 3 - 22.
- Hayes, M.O., 1980. General morphology and sediment patterns in tidal inlets. *Sedimentary Geology*, 26(1/3), 139-156.
- Healy, T.R., 1985. Tauranga Harbour Study, Parts II and V, Field Data Collection Programme and Morphological Study. University of Waikato, Hamilton. 25p.
- Healy, T. R., Cole, R. and De Lange, W., 1996. Geomorphology and ecology of New Zealand shallow estuaries and shorelines. In: Nordstrom K.F. And Roman, C. T. (Eds.), *Estuarine Shores: Evolution, Environments and Human Alterations*. Wiley & Sons. London, UK. pp. 115 -154.
- Healy, T.R., McCabe, B. and Thompson, G., 1991. Port of Tauranga channel deepening and widening programme, 1991 – 1992 Environmental Impact Assessment Report, 122p.

- Healy, T., Thompson, G., Mathew, J., Pilditch, C., and Tian, F., 1998. Assessment of environmental effects for Port of Tauranga Ltd. Maintenance dredging and disposal. University of Waikato, Hamilton, New Zealand. 170p.
- Hicks, M.D, Hume, T.R., 1996. Morphology and size of ebb tidal deltas at natural inlets on open-sea and pocket-bay coasts, North Island, New Zealand. *Journal of Coastal Research*, 12(1), 47 - 63.
- Hsu, K.J., 1989. Physical Principles of Sedimentology. Springer-Verlag, Berlin, Germany, 233p.
- Hume, T. M. and Herdendorf, C. E., 1992. Factors controlling tidal inlet characteristics of low drift coasts. *Journal of Coastal Research*, 8(2), 355 - 375.
- Hume, T. M., Herdendorf, C. E., 1998. A Geomorphic Classification of Estuaries and its Application to Coastal Resource Management - A New Zealand Example. *Ocean and Shoreline Management*, 11, 249 - 274.
- Hydraulics Research Station., 1963. Tauranga Harbour Investigation. Report on First Stage. Report No. 201. Hydraulics Research Station, Wallingford, England. 69p.
- Hydraulics Research Station., 1968. Tauranga Harbour Investigation. Report on the second stage. Report No. EX 395. Hydraulics Research Station, Wallingford, England. 92p.
- Johnston, S.A., 1981. Estuarine dredge and fill activities: a review of impacts. *Environmental Management*, 5, 427 - 440.
- Kana, T.W., Hayter, E.J., and Work, P.A., 1999. Mesoscale sediment transport at Southeastern U.S. Tidal Inlets: conceptual model applicable to mixed energy settings. *Journal of Coastal Research*, 15(2), 303 - 313.
- Kenny, A.J., 2003. An overview of seabed-mapping technologies in the context of marine habitat classification, *ICES Journal of Marine Science*, 60(2), 411p.
- Kruger, J., 1999. Sedimentation at the Entrance Channel of Tauranga Harbour, New Zealand. MSc. Thesis, University of Waikato, NZ, 169p.
- Kruger, J. and Healy, T.R., 2006. Mapping the morphology of a dredged ebb tidal delta, Tauranga Harbour, New Zealand. *Journal of Coastal Research*, 22 (3), 720-727.
- Land Information New Zealand, 2006. New Zealand Nautical Almanac 2006/07.
- Larson, R.; Morang, A., and Gorman, L., 1997. Monitoring the coastal environment; part II: sediment sampling and geotechnical methods, *Journal of Coastal Research*, 13(2), 308 - 330.
- Leeder, M.R., 1982. *Sedimentology Processes and Products*. George Allen and Unwin, Sydney, Australia, 344p.

- Lesourd, S., Lesueur, P., Brun-Cottan, J.C., Garnaud, S., Poupinet, N., 2003. Seasonal variations in the characteristics of superficial sediments in a macrotidal estuary (the Seine inlet, France). *Estuarine Coastal Shelf Science*, 58, 3 - 16.
- Lurton, X., 2002. *An Introduction to Underwater Acoustics*. Chichester: Praxis Publishing Ltd, New York, U.S.A. 9p.
- Mackay, G.H., Latimer, G.J., Smith, K.R., 1995. Wave climate of the western Bay of Plenty, New Zealand, 1991 – 1993. *New Zealand Journal of Marine and Freshwater Research*, 29, 311 - 327.
- Mathew, J., 1997. Morphologic changes of tidal deltas and an inner shelf dump ground from large scale dredging and dumping, Tauranga, New Zealand. Ph.D. Thesis, 328p.
- Mazel, C., 1985. Side-scan sonar training manual. Klein Associates, Salem, New Hampshire, pp. 3-14.
- Medina, R., Marino-Tapia, I., Osorio, A., Davidson, M., Martin, F.L., 2007. Management of dynamic navigational channels using video techniques. *Coastal Engineering*, 54, 523-537.
- Morang, A., Gorman, L. 2005. Monitoring Coastal Geomorphology. In: M. Schwartz (Ed.), *Encyclopedia of Coastal Science*, Springer, Dordrecht, pp. 663 - 673.
- Morang, A.; Larson, R. and Gorman, L., 1997. Monitoring the coastal environment; part III: Geophysical and research methods. *Journal of Coastal Research*, 13(4), 1064 - 1085.
- Nitsche, F.O., Ryan, W.B.F., Carbotte, S.M., Bell, R.E., Slagle, A., Bertinado, C., Flood, R., Kenna, T., McHugh, C., 2007. Regional patterns and local variations of sediment distribution in the Hudson River Estuary. *Estuarine Coastal Shelf Science*, 71, 259 - 277.
- Rea, D., and Graham, B., 1998. Port of Tauranga Economic Impact Study. Hamilton: University of Waikato. 4p.
- Siegle, E., Huntley, D.A., Davidson, M.A., 2004. Physical controls on the dynamics of inlet sandbar systems. *Ocean Dynamics*, 54, 360–373.
- Siegle, E., Huntley, D.A., Davidson, M.A. 2007. Coupling video imaging and numerical modelling for the study of inlet morphodynamics. *Marine Geology*, 236, 143 – 163.
- Spiers, K., 2005. Continued beach renourishment from dredge spoil disposal. MSc. Thesis, University of Waikato. 241p.
- Spiers, K.C., Healy, T.R., Winter, C., 2009. Ebb-jet dynamics and transient eddy formation at Tauranga Harbour: implications for Entrance Channel shoaling. *J. Coast. Res.*, 25(1), 234 – 247.

- Terry, R.D. and Chillinger, G.V., 1955. Summary of “Concerning some additional aids in studying sedimentary formations”. *Journal of Sedimentary Petrology*, 25, 229 - 234.
- Van Lancker, V., Lanckneus, J., Hearn, S., Hoekstra, P., Levoy, F., Miles, J., Moerkerke, G., Monfort, O., and Whitehouse, R., 2004. Coastal and nearshore morphology, bedforms and sediment transport pathways at Teignmouth (UK). *Continental Shelf Research*, 24(1), 1171 - 1202.
- Vilas, F., Bernabeu, A.M., Mendez, G., 2005. Sediment distribution pattern in the Rias Baixas (NW Spain): main facies and hydrodynamic dependence. *Journal of Marine Systems*. 54, 261 - 276.
- Wille, P., 2005. *Sound images of the ocean in research and monitoring*. Springer, Berlin, Germany. pp. 21 – 39.
- Williams, B., 2006. Hydrobiological Modelling. Processes, numerical models and applications. University of Newcastle, NSW, Australia, 688p.

APPENDIX 1: HYDROGRAPHIC CHART ACCURACY

The following provides a guide to accuracy of the historic original hydrographic charts

Horizontal Scale (1852 – 1954)

The horizontal positions would have been fixed by sextant:

0.5mm X scale (accounting for accuracy in plotting on the chart) + 5m (accounting for sextant accuracy)

For eg:

So if the scale is 1: 8000 then:

$$0.5 \times 8000 = 4000\text{mm} = 4\text{m} + 5\text{m} = 9\text{m}.$$

Chart Scale

1954 1:9000 Horizontal Scale 1954: $(0.5 \times 9000\text{mm}) + 5\text{m} = 9.5\text{ m}$

1927 1:6336 Horizontal Scale 1927: $(0.5 \times 6336\text{mm}) + 5\text{m} = 8.2\text{ m}$

1901 1:8003 Horizontal Scale 1901: $(0.5 \times 8003\text{mm}) + 5\text{m} = 9.0\text{m}$

1879 1:9130 Horizontal Scale 1879: $(0.5 \times 9130\text{mm}) + 5\text{m} = 9.6\text{ m}$

1852 1:9130 Horizontal Scale 1852: $(0.5 \times 9130\text{mm}) + 5\text{m} = 9.6\text{ m}$

Vertical Scale for 1954 (Navy Surveys after the WW2 used echosounders)

1 foot (30cm) estimated accuracy of echosounder + 20 cm accounting for the tide = 50cm.

Vertical Scale for 1901 to 1927 (Leadline soundings)

15 cm (accounting for leadline and heave of the boat) + 20cm accounting for the tide = 35 cm

Vertical Scale for 1852 to 1879

15 cm (accounting for leadline and heave of the boat) + 20cm (accounting for the tide) and 20cm accounting for the lack of tidal datum.
= 55cm.

Data from Scott Preskett

APPENDIX 2: COMPARISON OF SPRING, NEAP AND MEAN TIDES

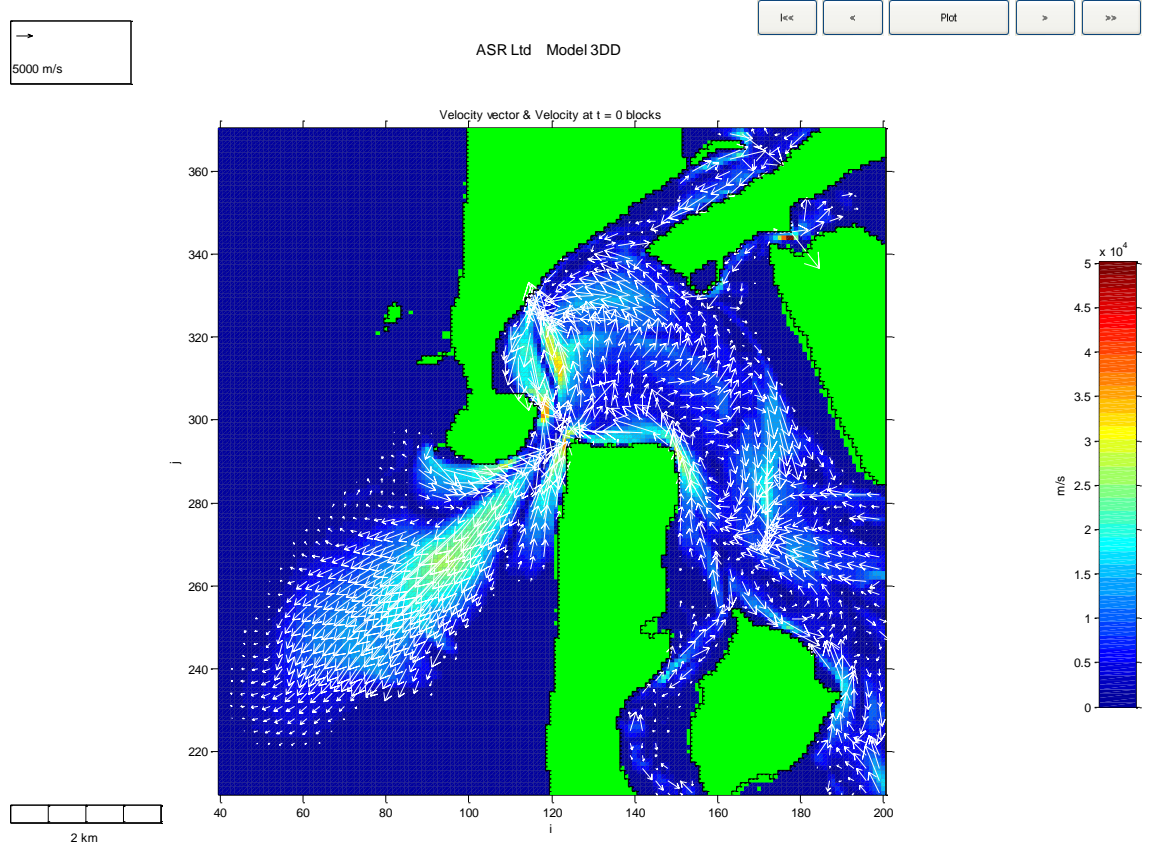


Fig. A.1: Spring tide residual distance vector plot above a threshold of 0.3 ms^{-1} for 2006.

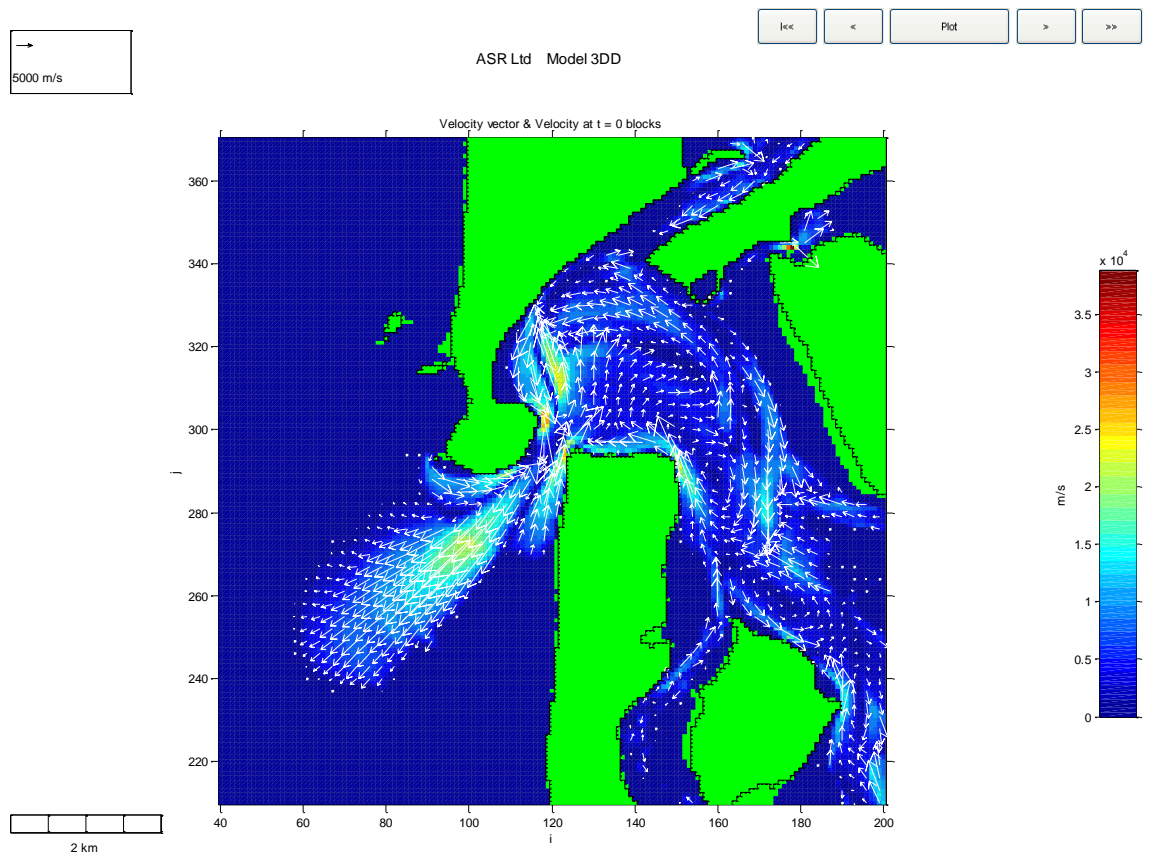


Fig. A.2: Neap tide residual distance vector plot above a threshold of 0.3 ms^{-1} for 2006.

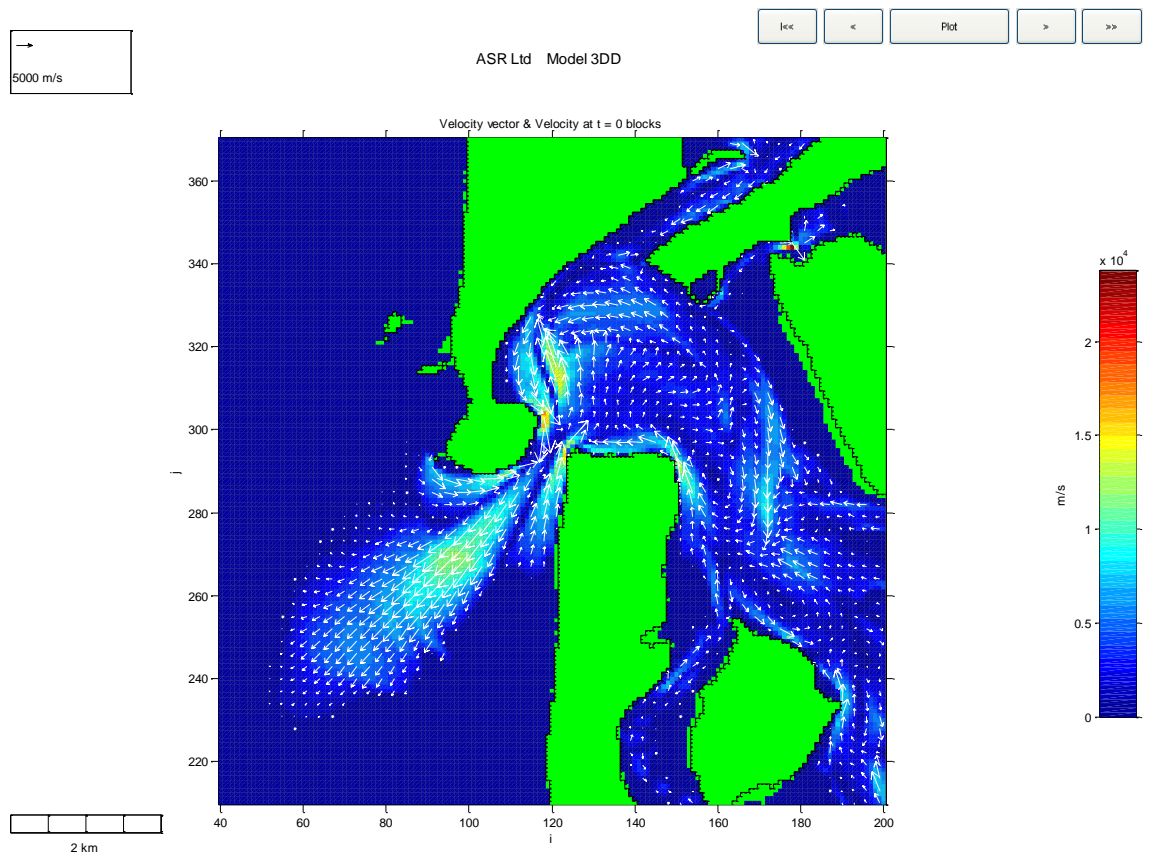


Fig. A.3: Mean tide residual distance vector plot above a threshold of 0.3 ms^{-1} for 2006.

APPENDIX 3: SEDIMENT SAMPLE AND SHELL COVERAGE SPECIFICATIONS

East	North	Mz	% Shell cover	Name	% Content < 4Φ	% Content between 4Φ and -2Φ	% Content > - 2Φ
2789565	6395275	1.9	0	EA2	0	100	0
2788968	6394887	2.25	0	EA4	0	100	0
2788663	6394710	1.52	1	EA5	0	100	0
2788295	6394538	2.36	0	EA6	0	100	0
2787609	6394043	2.12	1	EA8	0	100	0
2790123	6395294	2.5	0	EB1	0	100	0
2789590	6394684	1.29	10	EB3	0	100	0
2789139	6394144	2.29	0	EB5	0	100	0
2788879	6393833	2.49	0	EB6	0	100	0
2788555	6393535	2.13	0	EB7	0	100	0
2788263	6393306	-	0	EB8	-	-	-
2790231	6394640	2.21	0	EC2	0	100	0
2789552	6393668	1.38	100	EC5	64	36	0
2789298	6393338	1.54	1	EC6	0	100	0
2789031	6393008	2.1	1	EC7	7	93	0
2788784	6392741	2.19	0	EC8	2	98	0
2790727	6394741	2.89	0	ED1	0	100	0
2790282	6394017	1.15	5	ED3	8	92	0
2789857	6393319	-	90	ED5	-	-	-
2789438	6392589	-	100	ED7	0	100	0
2790689	6394246	2.33	0	EE2	0	100	0
2790219	6393579	2.61	0	EE4	4	96	0
2789958	6393217	2.76	0	EE5	0	100	0
2789704	6392887	1.91	100	EE6	72	28	0
2789558	6392512	2.15	10	EE7	2	98	0
2789400	6392195	1.45	100	EE8	0	100	0
2789838	6392760	2.34	0	EEF6	0	100	0
2790676	6393694	2.6	0	EF3	0	100	0
2790187	6393001	2.39	0	EF5	0	100	0
2789685	6392436	2.24	1	EF7	0	100	0
2791393	6394075	3	0	EG1	0	100	0
2790873	6393503	2.42	0	EG3	0	0	0
2790650	6393224	1.32	0	EG4	25	75	0
2790365	6392817	2.33	0	EG5	6	94	0
2788352	6395084	2.54	0	EX5	0	100	0
2786980	6394748	1.6	1	EX8	0	100	0
2788764	6394214	1.01	1	EZ2	19	81	0
2789207	6392765	2.21	5	EZ5	11	89	0

2787850	6390346	1.84	5	FA4	4	96	0
2787844	6390054	1.74	0	FA5	5	95	0
2787825	6389749	2.77	0	FA6	3	97	0
2788155	6390333	1.41	10	FB4	39	61	0
2788149	6390047	2.15	90	FB5	28	72	0
2788136	6389749	2.29	1	FB6	3	97	0
2788123	6389489	2.25	-	FB7	30	70	0
2788453	6390295	1.42	95	FC4	64	36	0
2788453	6390035	2.28	100	FC5	46	53	0
2788422	6389749	2.18	20	FC6	13	87	0
2788415	6389444	1.76	0	FC7	0	100	0
2788422	6389177	2.11	5	FC8	16	84	0
2788396	6388841	1.81	10	FC9	20	80	0
2788739	6390587	1.86	30	FD3	49	51	0
2788739	6390295	-	100	FD4	0	100	0
2788726	6390028	-	30	FD5	-	-	-
2788714	6389743	2.13	50	FD6	20	80	0
2788701	6389444	1.95	10	FD7	0	100	0
2788714	6389171	2.32	0	FD8	13	87	0
2788701	6388860	2.55	80	FD9	31	66	3
2789063	6390898	2.21	80	FE2	0	100	0
2789063	6390581	-	100	FE3	10	90	0
2789057	6390308	1.8	-	FE4	14	86	0
2789044	6390022	1.7	50	FE5	28	72	0
2789031	6389736	2.08	5	FE6	14	83	3
2789031	6389431	1.45	0	FE7	1	99	0
2789038	6389171	2.39	1	FE8	36	64	0
2789025	6388854	1.19	1	FE9	50	50	0
2789387	6391197	1.71	10	FF1	2	98	0
2789374	6390905	0.83	5	FF2	18	82	0
2789349	6390593	1.3	5	FF3	1	99	0
2789342	6390320	1.36	10	FF4	38	62	0
2789330	6390047	1.98	10	FF5	20	80	0
2789342	6389743	1.36	1	FF6	14	86	0
2789342	6389457	2.24	5	FF7	19	80	1
2789349	6389158	1.99	5	FF8	0	100	0
2789330	6388841	0.8	50	FF9	0	100	0
2789679	6391190	-	100	FG1	-	-	-
2789660	6390892	-	100	FG2	-	-	-
2789666	6390581	1.36	90	FG3	69	31	0
2789660	6390289	1.4	10	FG4	43	57	0
2789654	6390016	1.34	5	FG5	26	74	0
2789634	6389743	1.35	1	FG6	5	95	1
2789622	6389444	-	1	FG7	0	100	0
2789609	6389146	1.86	5	FG8	32	68	1
2789977	6391203	1.28	100	FH1	30	70	0

2789971	6390892	-	100	FH2	0	100	0
2789958	6390562	-	100	FH3	0	100	0
2789958	6390276	1.01	0	FH4	54	46	0
2789939	6389990	1.3	0	FH5	1	99	0
2789920	6389717	1.79	5	FH6	20	80	0
2789901	6389444	1.74	5	FH7	6	93	0
2789895	6389127	1.34	1	FH8	2	98	0
2790263	6390549	1.11	90	FI3	33	66	0
2790263	6390270	2.15	1	FI4	28	71	0
2790238	6389978	1.3	0	FI5	0	100	0
2790231	6389711	2.42	1	FI6	35	65	0
2790219	6389444	1.89	1	FI7	12	88	0
2790212	6389127	1.05	1	FI8	19	81	0
2790543	6391197	2.92	10	FJ1	10	90	0
2790536	6390847	1.65	30	FJ2	55	45	0
2790568	6390549	1.29	40	FJ3	66	34	0
2790574	6390238	2.72	10	FJ4	49	49	1
2790568	6389946	1.94	1	FJ5	44	56	0
2790549	6389711	-	0	FJ6	-	-	-
2790562	6389450	2.49	0	FJ7	7	93	0
2790555	6389114	2.13	10	FJ8	12	88	0
2790822	6390549	1.92	5	FK3	0	100	0
2790835	6390238	1.38	10	FK4	18	82	0
2790835	6389946	1.61	5	FK5	2	98	0
2790835	6389704	1.51	5	FK6	9	91	0
2790822	6389362	1.94	10	FK7	4	96	0
2790809	6389095	1.73	5	FK8	5	95	0
2790820	6388645	3.34	0	FK9	0	95	5
2787527	6390307	1.84	30	FM1	31	69	0
2787144	6390542	1.42	10	FM2	36	64	0